Metabolomic Analysis, Isolation, Characterization and Synthesis of

Bioactive Compounds from *Hypericum* species (Hypericaceae)

Dissertation

zur Erlangung des Doktorgrades der Naturwissenschaften

(Dr. rer. nat.)

der

Naturwissenschaftlichen Fakultät II

Chemie, Physik und Mathematik

der Martin-Luther-Universität

Halle-Wittenberg

vorgelegt von

Herrn M.Sc. Serge Alain Fobofou Tanemossu

geb. am 09.10.1986 in Nkongsamba, Kamerun

The work presented in this thesis was designed by Prof. Dr. Ludger A. Wessjohann, Dr. Katrin Franke, and myself and performed by me (M.Sc. S. A. Fobofou) at the Department of Bioorganic Chemistry of the Leibniz Institute of Plant Biochemistry (IPB) in cooperation with the Martin-Luther University Halle-Wittenberg.

Supervisor: Prof. Dr. Ludger A. Wessjohann

"This dissertation is submitted as a cumulative thesis according to the guidelines provided by the PhD-program of the Martin-Luther University Halle-Wittenberg. The thesis comprises seven peer-reviewed and original research papers (five already published and two in preparation), which cover the majority of first author's research work during the course of his PhD."

Serge Alain Fobofou T.

"*Gedruck mit Unterstützung des Deutschen Akademischen Austauschdienstes*"

1. Gutachter: Prof. Dr. Ludger Wessjohann

2. Gutachter: Prof. Dr. Ludger Beerhues

Tag der Verteidigung: 14. Dezember 2016

The Lord is my strength and my shield; my heart trusted in Him and I am helped (Psalm 28:7).

"Many times a day I realize how much my outer and inner life is built upon the labors of people, both living and dead, and how earnestly I must exert myself in order to give in return how much I have received."

Albert Einstein

To the Almighty God,
my family and friends

Table of contents

Acknowledgements

and for editing my manuscripts for common English language mistakes during their summer internships at the IPB. I also wish to acknowledge all my former lecturers at the University of Dschang (Cameroon), especially my former M.Sc. supervisors Profs. Dres. Pierre Tane and Wabo Kamdem Hippolyte for their teaching and mentorship. I am grateful to the DAAD committee members, referees and staff, especially to my fellowship advisor Ms. Christine Butter (now called Mrs. Eschweiler), who made me get to Germany and constantly provided the support I needed.

In addition, I also wish to thank the people without whom I could not have been what I am. Special acknowledgements go to my late mother Mrs. Madeleine Tsasse for her steadfast and unconditional love, prayers, support, and encouragement. Whenever I doubted, she had been there to say with a trustful heart: "You will arrive in Jesus's name." I am also grateful to my father Mr. Tanemossu, sisters, and brothers for their constant love, supports, patience, prayers, and encouragement. Especial thanks go to my elder brother Dr. Sylvain V.T. Sob for his great advices. I am profoundly thankful to all my fellow Christians, especially to Apostle Simon P. Bayama E. and wife for their great spiritual support and life changing teaching in heart, so that I may know the mystery of God's love and mercy, namely, Christ, in whom are hidden all the treasures of life, success, peace of heart, wisdom, and knowledge, etc. Especial thanks go to my friends, brothers and sisters in Christ of the Evangeliumsgemeinde in Halle-Germany for their prayers.

Finally, financial support from the DAAD for a doctoral grant and two RISE fellowships is highly appreciated. I am grateful to the IPB for supporting the lab costs and travel to conferences. I acknowledge the Lindau Nobel Laureate and Falling Walls Foundations which, through their respective fellowships, gave me the unique opportunities to present my ideas and PhD thesis results at their respective meetings and also to learn about cutting-edge science, share, and meet with some of the brightest and most esteemed minds on the planet.

List of abbreviations

[α]	Specific rotation	**LC**	Liquid chromatography
AIDS	Acquired immune deficiency syndrome	**LC-MS**	Liquid chromatography/mass spectrometry
bs	Broad signal	*m*	Multiplet
CC	Column chromatography	**MIC**	Minimum inhibitory concentration
CCID$_{50}$	(50%) Cell Culture Infective Dose	**m.p.**	Melting point
CD	Circular dichroism	**MS**	Mass spectrometry
CFU	Colony-forming unit	**MS^{n}**	Tandem mass spectrometry
CoA	Coenzyme A	**MVDA**	Multivariate data analysis
COSY	Correlated spectroscopy	*m/z*	Mass-to-charge-ratio
d	Doublet	**NMR**	Nuclear magnetic resonance
dd	Doublet of doublet	**NOESY**	Nuclear Overhauser effect spectroscopy
ddd	Doublet of doublet of doublet	**NNRTI**	Non-nucleoside/nucleotide reverse transcriptase inhibitor
DEPT	Distortionless enhancement by polarization transfer	**NRTI**	Nucleoside/nucleotide reverse transcriptase inhibitor
DFT	Density functional theory	**PCA**	Principal component analysis
DMAPP	Dimethylallyl pyrophosphate	**PAL**	Phenylalanine ammonia lyase
DMSO	Dimethylsulfoxide	**PI**	Protease inhibitor
DMSO-d6	Deuterated dimethylsulfoxide	**PMS**	Phenazine methosulfate
DSM	Deutsche Sammlung von Mikroorganismen	**ppm**	Parts per million
EDDA	Ethylenediamine diacetate	**rel. int.**	Relative intensity
EIMS	Electron impact mass spectrum	**ROESY**	Rotational frame Overhauser effect spectroscopy
ESIMS	Electron spray ionization mass spectrum	**RPMI**	Roswell Park Memorial Institute
FTICR	Fourier transform ion cyclotron resonance	*s*	Singlet
GC	Gas chromatography	*t*	Triplet
GPP	Geranyl pyrophosphate	**TAL**	Tyrosine ammonia lyase
HCA	Hierarchical cluster analysis	**TLC**	Thin layer chromatography
HIV	Human immunodeficiency virus	**TMS**	Tetramethylsilane
HMBC	Heteronuclear multiple bond connectivity	**TSA**	Tryptic soy agar
HMDSO	Hexamethyldisiloxane	**UPLC**	Ultra performance liquid chromatography
HPLC	High pressure liquid chromatography	**UV**	Ultraviolet
HR-FTMS	High resolution Fourier transform mass spectrum		
HSQC	Heteronuclear single quantum coherence		
IR	Infrared		
J	Coupling constant		

1. General introduction

1.1. Introduction and objectives

Drug discovery from natural products started about 200 years ago when a 21-year-old German pharmacist's apprentice named Friedrich Sertürner isolated the first pharmacologically active pure compound from a plant: morphine from opium produced by seed pods cut from the poppy, *Papaver somniferum* L. (Hamilton and Baskett, 2000). Since then, plants, microorganisms, and animals have been excellent sources of complex chemical structures with a wide variety of biological activities and potential applications in chemistry, medicine, and biology (Chibale *et al*., 2012). Natural products represent an opportunity to develop new therapies, as they have been evolutionary selected to play a targeted role in organisms (Li and Vederas, 2009). Up to 1990, about 80% of drugs were either natural products or analogs inspired by them (Li and Vederas, 2009). Antibiotics (e.g. penicillin, tetracycline, and erythromycin), antiparasitics (e.g. avermectin and analogs), antimalarials (e.g. quinine and artemisinin), lipid control agents (e.g. lovastatin and analogs), immunosuppressants for organ transplants (e.g. cyclosporine and rapamycins), and anticancer drugs (e.g. taxol and doxorubicin) revolutionized medicine. Life expectancy in much of the world lengthened from about 40 years early in the 20th century to more than 77 years today (Li and Vederas, 2009). In addition, the award of half of the 2015 Nobel Prize in Physiology or Medicine jointly to William C. Campbell and Satoshi Ōmura for discovering avermectin, with the other half being awarded to Tu Youyou for discovering artemisinin, highlights the global acceptance of the impact of natural products on our society as these discoveries have saved millions of lives. Despite this successful history of drug discovery from nature, the interest of pharmaceutical companies in natural products research dropped in the past decades (for the reasons, see introduction of Chapter 2). Nevertheless, it is estimated that from 1981 to 2010 more than 60% of all the approved therapeutic agents were natural products or derivatives or inspired by natural products (Newman and Cragg, 2012); and approximately 25% of the drugs prescribed worldwide come from plants (Zhang *et al*., 2013). Even more interesting, it is estimated (WHO Fact sheet No. 134) that about 75% of the world population rely on plants and plant products as their major source of medicine.

Despite the progress made in medicine and related sciences, it is rated that infectious diseases annually kill about 14 million people worldwide, mostly in the developing countries. In developed countries, incidents of epidemics due to drug resistant microorganisms and the emergence of hitherto unknown diseases caused by microbes pose enormous public health threats (Fonkwo, 2008). Many frequently used drugs are expensive or not readily available and a major setback to

their continuous usage is the development of resistance. There is thus a need for new drugs that will be able to act for longer periods before resistance sets in (McGaw *et al.*, 2000).

Historically, plants have provided a source of inspiration for novel drug compounds, as plant derived medicines have made large contributions to human health and well-being. They play two major roles in the development of new drugs: they may become the basis for the development of a medicine acting as a natural blueprint for the development of new drugs or a phytomedicine to be used for the treatment of diseases (Iwu *et al.*, 1999). There are several examples of pure compounds from plants (e.g. taxol from *Taxus brevifolia* Nutt.) or standardized medicinal plant extracts (e.g. Bronchipret® made of *Thymus* extract by the pharmaceutical company Bionorica®) prescribed in modern medicine. The sequence for development of pharmaceuticals usually begins with the identification of lead molecules from complex matrices and requires a multidisciplinary collaboration of (ethno)-botanists, chemists, microbiologists, pharmacologists, toxicologists, and more recently chemioinformaticians for the quantitative structure-activity relationship (QSAR), computer assisted drug design (CDD), *in silico* screening (e.g. of natural products library), and also for rapid analysis of bioactive crude extracts (metabolomics).

As part of our ongoing effort to discover potential lead compounds from plants, plants of the family Hypericaceae were selected for investigation based on their rich chemistry and history of providing active compounds utilized as commercial drugs, e.g. derived from their ethno-medicinal uses, and influenced by the chemical (chemotaxonomic) significance since many species remain uninvestigated both chemically and pharmacologically. The aim of this work was to compare the metabolic profiles of different *Hypericum* species, isolate and characterize the chemical constituents of selected (prioritized) *Hypericum* species by both chromatographic and spectroscopic means, and evaluate their biological activities. In this thesis, after an introduction including a general overview and a literature survey (Chapter 1), the results of the research work will be presented in chapters along with descriptions of the experimental procedures. Motivated by our high interest in the rapid detection of novel bioactive compounds from complex matrices (bioactive extracts) and to avoid re-isolation of known compounds (replication), we applied metabolomics (Chapter 2) for the prioritization of *Hypericum* extracts for new compounds discovery. Some of the prioritized *Hypericum* extracts were chemically investigated (Chapters 3-6) to afford new natural products whose isolation, structural elucidation including some syntheses and CD spectra calculations and biological activities are herein reported. Owing to our interest in investigating other chemically unexplored members of the Hypericaceae family, this work also describes the chemistry of *Psorospermum densipunctatum* Engl. for the first time (Chapter 7).

1.2. The family Hypericaceae Juss.

Hypericaceae Juss. is a family of plants comprising 9 genera and 540 species with a nearly worldwide distribution (Stevens, 2007). The taxonomic description of the Hypericaceae family has long been discussed. It was treated as subfamily Hypericoideae Engl. within Clusiaceae Lind. (Guttiferae Juss.) (Nürk and Blattner, 2010). However, the recent classification of flowering plants splits Clusiaceae into three families, one of which (Hypericaceae) matches the former Hypericoideae (AGP, 2009).

Hypericaceae are evergreen herbs, shrubs or rarely trees or climbers, with resinous juice (Hutchinson and Dalziel, 1954). Leaves are simple, opposite or verticillate and often alternate, entire, or glandular with secretory cavities containing oil or resin. Stipules are absent. They are rarely coriaceous and usually marked with translucent or black dots (glands). Flowers are usually yellow or white. The most common genera within the Hypericaceae include *Hypericum* L.*, Psorospermum* Baker*, Vismia* Vand.*,* and *Triadenum* Raf. (Hutchinson and Dalziel, 1954; Stevens, 2007). Approximately 80% of the diversity within the family is in the genus *Hypericum.*

1.3. The genus *Hypericum* L.

Hypericum L. (St. John's worts) is a genus of flowering plants which comprises about 450 species with a nearly worldwide distribution with a centre of diversity in temperate regions of Eurasia (Fig. 1.1). *Hypericum* is absent in tropical lowlands, deserts, and polar regions (Crockett and Robson, 2011). In the tropics and warm temperate area *Hypericum* is almost always confined to highland habitats and mountains (e.g. Mount Cameroon, Mount Bamboutos, and the Andes). All members of the family may be referred to as St. John's wort, though they are often simply called *Hypericum* (Nürk and Blattner, 2010), and some authors limit St. John's wort specifically to *Hypericum perforatum* L. only.

1.3.1. Botany and taxonomy of the genus *Hypericum*

The botany and taxonomy of the genus *Hypericum* were intensively reviewed based on its morphology (Crockett and Robson, 2011). *Hypericum* species vary from annual, hardy, or perennial herbaceous plants 5-10 cm tall to shrubs and small trees up to 12 m tall. They are typically recognized by their leaves which are opposite, simple and entire, elliptic to ovate or lanceolate, lacking stipule. The flowers are yellow with petals and several stamens in 3 or 5 fascicles, style free, and have pale and sometimes reddish to black glandular secretions (glands). The fruit, unlike those of some other members of Hypericaceae, is a dehiscent capsule which splits to release the numerous small seeds;

in some species, it is fleshy or berry-like. They contain small cylindrical light brown to black seeds (Hutchinson and Dalziel, 1954; Crockett and Robson, 2011).
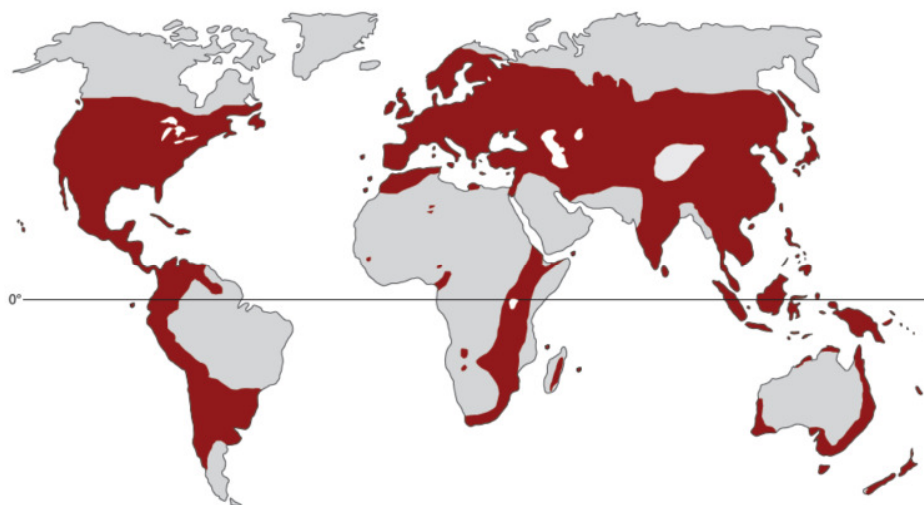
Fig. 1.1. Distribution of *Hypericum* (modified from Robson 1977; Nürk, 2011; Nürk *et al*., 2013)

The systematic position and taxonomy of *Hypericum* are shown in Scheme 1.1. Several examples of *Hypericum* species investigated in this thesis with five petals and elliptic or lanceolate leaves are depicted in Fig. 1.2. The interested reader is encouraged to check the literature for more detailed and specific aspects on the taxonomy, morphology, phylogenic and phylogenetic analyses, and distribution of *Hypericum* (Robson 1977; Crockett and Robson, 2011; Nürk and Blattner, 2010; Nürk, 2011; Nürk *et al*., 2013, Stevens, 2007; Hutchinson and Dalziel, 1954).

Class ⟶ *Magnoliopsida*

Subclass ⟶ *Rosidae*

Order ⟶ *Malpighiales*

Family ⟶ Hypericaceae Juss.

Genus ⟶ *Hypericum* L.

Scheme 1.1. Taxonomy of *Hypericum* L. (Kadeheit *et al*., 2014).

Fig. 1.2. Pictures of selected *Hypericum* species investigated in this thesis.

1.3.2. Medicinal uses, secondary metabolites, and biological activities of *Hypericum*

The most well known and investigated *Hypericum* species, *H. perforatum* L. (common St. John's wort), was described in Hippocrates's manuscript (ancient Greece) to be active against evil spirits (the name depression was not used in ancient times). Nowadays, *H. perforatum* extract is prescribed (licensed) in Europe and North America against mild to moderate depression and anxiety (Woelk, 2000). In Germany, St. John's wort is the leading treatment for depression, outselling synthetic drugs (e.g. fluoxetine, Prozac®). In 2004, sales valued more than € 70 million in Germany alone. The flowering tops of *H. perforatum* are also prepared as a decoction or infusion and taken internally for sedative or tonic purposes, or applied externally as a poultice or prepared

as an oil-infusion to treat sciatica, neuralgia and speed wound-healing (Crockett and Robson, 2011). The secondary metabolites (Fig. 1.3) with biological activity reported from *H. perforatum* include naphthodianthrones (0.05-0.15%, e.g. hypericin and pseudohypericin), phloroglucinols (up to 5%, e.g. hyperforin and adhyperforin), tannins and proanthocyanidins (6-15%), and flavonoids (2-5%, e.g. quercetin, rutin, hyperoside and kaempferol). Other constituents include phenolic acids, coumarins, xanthones, vitamins A and C, terpenes, sterols, and volatile oils (Crockett and Robson, 2011; Nathan, 2001; Farag and Wessjohann, 2012). Most of these compound classes have been also reported from other *Hypericum* species. *Hypericum* extracts and compounds exhibit broad biological activities including antibacterial, cytotoxic, antimalarial, anti-inflammatory, and antiviral effects among others (Zofou *et al.*, 2011; Xu *et al.*, 2015; Tanaka and Takaishi, 2006; Don *et al.,* 2004). *Hypericum* species other than *H. perforatum* have also been ethno-medicinally used throughout the world. In Cameroon, *Hypericum* is a multipurpose plant used against epilepsy, skin infections, tumors, and viral and microbial diseases. The stem bark of *H. lanceolatum* Lam. is usually boiled in water and administered either as a steam bath or orally for the treatment of malaria and other fevers. The roots are also known for their activity against intestinal worms and dysentery, and they are combined with *Mangifera indica* L. (Mango tree) leaves, boiled and administered as a drink to the afflicted. In the Lebialem Division (South West Region), decoction of fresh leaves is taken orally to "treat nerves" (Zofou *et al.*, 2011). In China, *H. monogynum* L. is used for the treatment of hepatitis, acute laryngopharyngitis, conjunctivitis, and snake bites (Xu *et al.*, 2015). In Japan, *H. chinense* is used as a folk medicine for the treatment of sterility (Tanaka and Takaishi, 2006). Because acylphloroglucinols and coumarins constitute most of the new and chemically intriguing compounds described in this thesis, the next part of this chapter is dedicated to them.
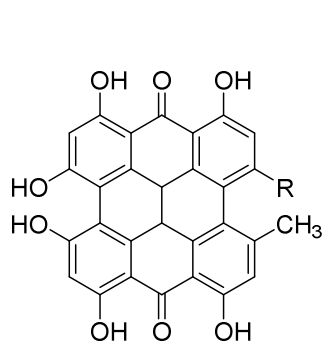
Hypericin   R = CH$_3$
Pseudohypericin R = CH$_2$OH
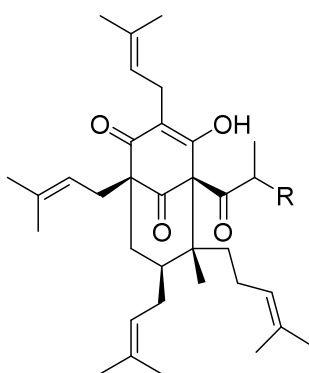
Hyperforin   R = CH$_3$
Adhyperforin   R = CH$_2$CH$_3$
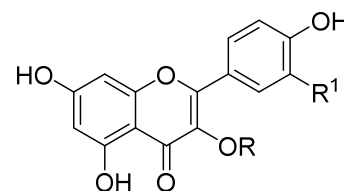
Quercetin   R = H   R^1 = OH
Hyperoside R = β–Gal   R^1 = OH
Kaempferol R = H   R^1 = H

Fig. 1.3. Some of the most known bioactive compounds from the genus *Hypericum*.

1.3.2.1. Acylphloroglucinols

The genus *Hypericum* is a great source of acylphloroglucinol (acylated 1,3,5-trihydroxybenzene) derivatives. Acylphloroglucinols from *Hypericum* species have broad biological activity profiles including antidepressive (e.g. hyperforin), antibacterial, antitumor, antiproliferative, and antiangiogenic activities (Xu *et al*., 2015). With their diverse biological activities and fascinating structural architectures, these compounds have attracted great attention in bioorganic, synthetic, and medicinal chemistry.

The acyl chain of phloroglucinols from *Hypericum* is mostly formed from an isobutyryl, 2-methylbutyryl, or benzoyl moiety. Acylphloroglucinols are biosynthetized (Fig. 1.4) following a polyketide pathway from the condensation of three molecules of malonyl-CoA and a coenzyme A-activated acid (isobutyryl-, 2-methylbutyryl-, or benzoyl-CoA) catalyzed by chalcone synthase, chalcone synthase like-enzyme (e.g. valerophenone synthase), or benzophenone synthase to give a linear tetraketide intermediate, which is subsequently cyclized into acylphloroglucinol via intramolecular Claisen condensation (Zuurbier *et al*., 1998; Klundt *et al*., 2009). These products are the intermediates of natural xanthones and prenylated acylphloroglucinols. For instance, the benzophloroglucinol intermediate is susceptible to regioselective oxidative phenol coupling reactions catalyzed by cytochrome P450 enzymes to give xanthone (Klundt *et al*., 2009). Acylphloroglucinol intermediates are susceptible to sequential prenylation or geranylation catalyzed by prenyl transferase (DMAPP-PTase) or geranyl transferase (GPP-PTase). The often several-fold prenylated or geranylated acylphloroglucinol intermediates undergo intramolecular cyclization and oxidation processes or electrophilic attack of a further DMAPP (hyperforin-like compound biosynthesis) on the 2′/3′ double bond of a pre-implanted geranyl/prenyl chain to afford bi-, tri-, polycyclic polyprenylated acylphlogucinols and complex cage compounds (Xu *et al*., 2015 Adam *et al.,* 2002). The biosynthesis of acylphloroglucinols is depicted in Fig. 1.4.

Acylphloroglucinols were isolated from several other families of plants including Myrtaceae (e.g. *Eucalyptus apodophylla* Blakely & Jacobs), Cannabinaceae (e.g. *Humulus lupus* L.), and Clusiaceae (*Clusia nemorosa* G. Mey.) (Ferreira *et al*., 2015; Farag *et al*., 2014). Reviews on bioactive phloroglucinols from natural origin (plants, marine, and micro-organisms) were reported along with their synthetic aspects (Singh and Bharate, 2006; Singh *et al*., 2010).
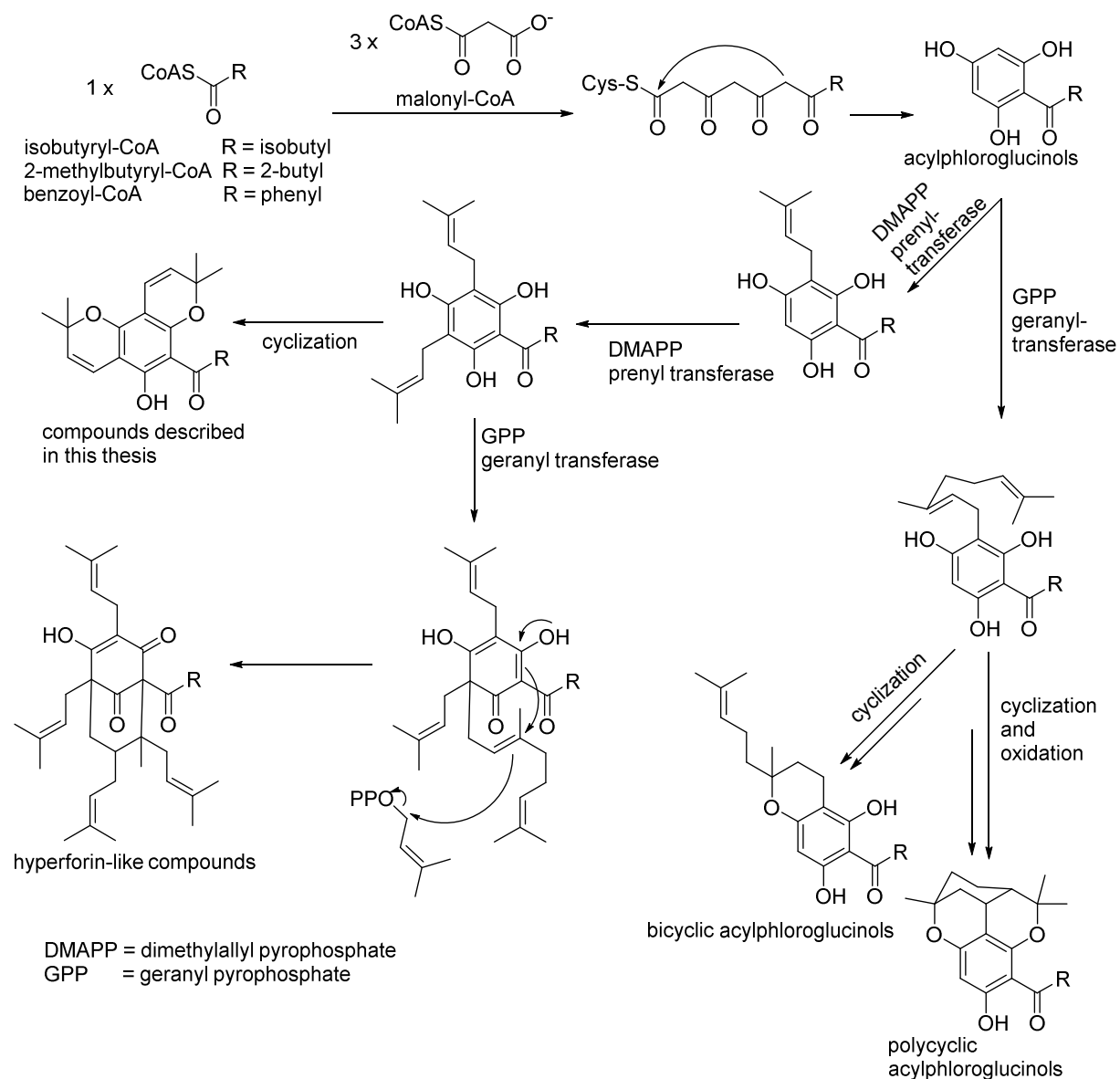
Fig. 1.4. Biosynthesis of acylphloroglucinol derivatives (Zuurbier *et al*., 1998; Klundt *et al*., 2009; Adam *et al.,* 2002).

1.3.2.2. Coumarins

Coumarin (2*H*-1-benzopyran-2-one) derivatives are phenylpropanoids made of fused benzene and α-pyrone ring. More than 1300 coumarins of natural origin (plants, bacteria, and fungi) have been reported. They can be classified as simple coumarins, furanocoumarins (linear and angular types), pyranocoumarins (linear and angular types), phenyl coumarins, prenylated coumarins, and biscoumarins. They possess antibacterial, antiviral, anticoagulant, anticonvulsant, antioxidant, anti-allergic, anticancer, neuroprotective, antitubercular, and anti-inflammatory activities (Venugopala *et al*., 2012; Musa *et al*., 2008). For example, some coumarins isolated from tropical Malaysian plants of the genus *Calophyllum* L. (Calophyllaceae) were identified as HIV-1-specific non-nucleoside inhibitors among which (+)-calanolide A and inophyllum B (Fig. 1.5) are the most

potent (Flavin *et al.,* 1996). Coumarins also occur in Moraceae, Urticaceae, Brassicaceae, Fabaceae, Apiaceae, Rutaceae, and Leguminosae, among others (Venugopala *et al*., 2013; Farag *et al.*, 2013).

Coumarins have rarely been reported from the genus *Hypericum*, while biscoumarins have never been reported (except in this study). Coumarins and biscoumarins have been isolated from *H. keniense* Mildbr. and *H. riparium* A. Chev. (Ang'edu *et al.,* 1999), both plants belong to the tropical African *Hypericum* section *Campylosporus* (Spach) R. Keller. Biscoumarins have been isolated from plants (e.g. *Urtica dentata* Hand.) and fungi (e.g. kotanin from *Aspergillus* species) (Fig. 1.5). Naturally occurring biscoumarins are biosynthetically built up by oxidative homocoupling of coumarins including umbelliferone, siderin, esculetin, scopoletin, and iso-scopoletin (Fig. 1.5). This "dimerization" gives rise to both constitutionally symmetric and unsymmetric products (Bringmann *et al.,* 2011). The biosynthesis of coumarin derivatives has been discussed using both plants and microorganisms as models. They are produced by hydroxylation and lactonization of cinnamic acid or *p*-coumaric acid or their ester derivatives. Phenylalanine and tyrosine can be converted into cinanmic acid and *p*-coumaric acid by phenylalanine (or tyrosine) ammonia lyase (PAL) or (TAL), respectively (Yang *et al.,* 2015).
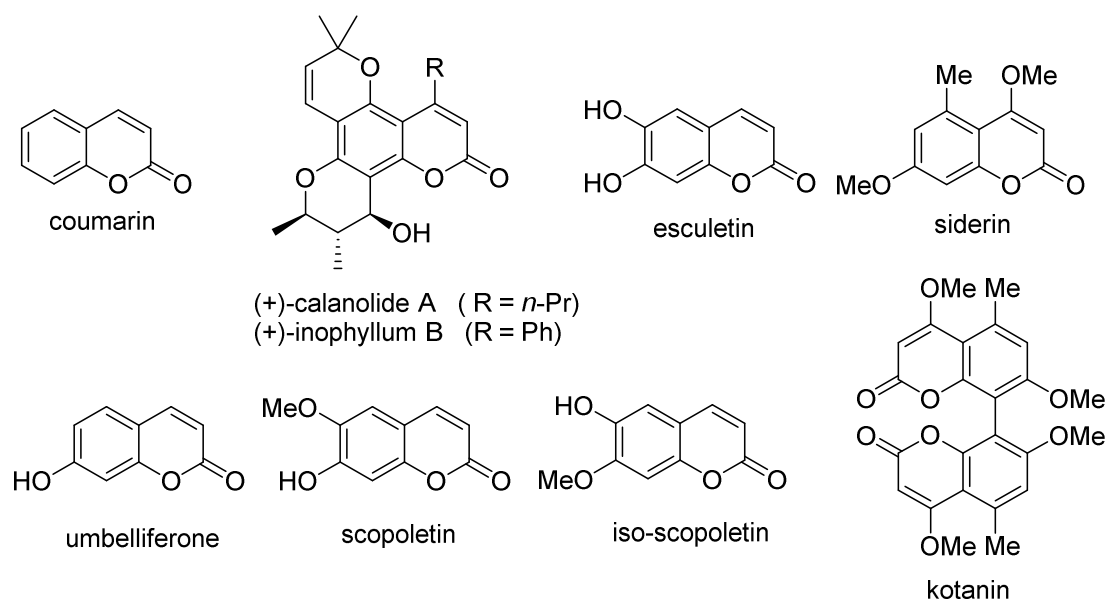
Fig. 1.5. Some naturally occurring coumarin derivatives.

The biosynthetic pathway from cinnamic acid to coumarin was elucidated in *Arabidopsis thaliana*. The hydroxylation at C-6´ of cinnamoyl-CoA by a 2-oxoglutarate-dependent dioxygenase (feruloyl CoA 6´-hydroxylase [F6´ H], also known as *p*-coumaroyl CoA

2′-hydroxylase [C2′ H]), is a key step for the biosynthesis of coumarin (Fig. 1.6). Similarly, umbelliferone, esculetin, and scopoletin are formed from *p*-coumaric acid, caffeic acid, and ferulic acid, respectively, by a combination of *p*-cinnamic acid: CoA ligase (4CL) and F6′ H (Yang *et al.,* 2015).

PAL = phenylalanine ammonia lyase
TAL = tyrosine ammonia lyase
4 CL = *p*-cinnamic acid:CoA ligase
F6'H = feruloyl CoA 6'-hydroxylase
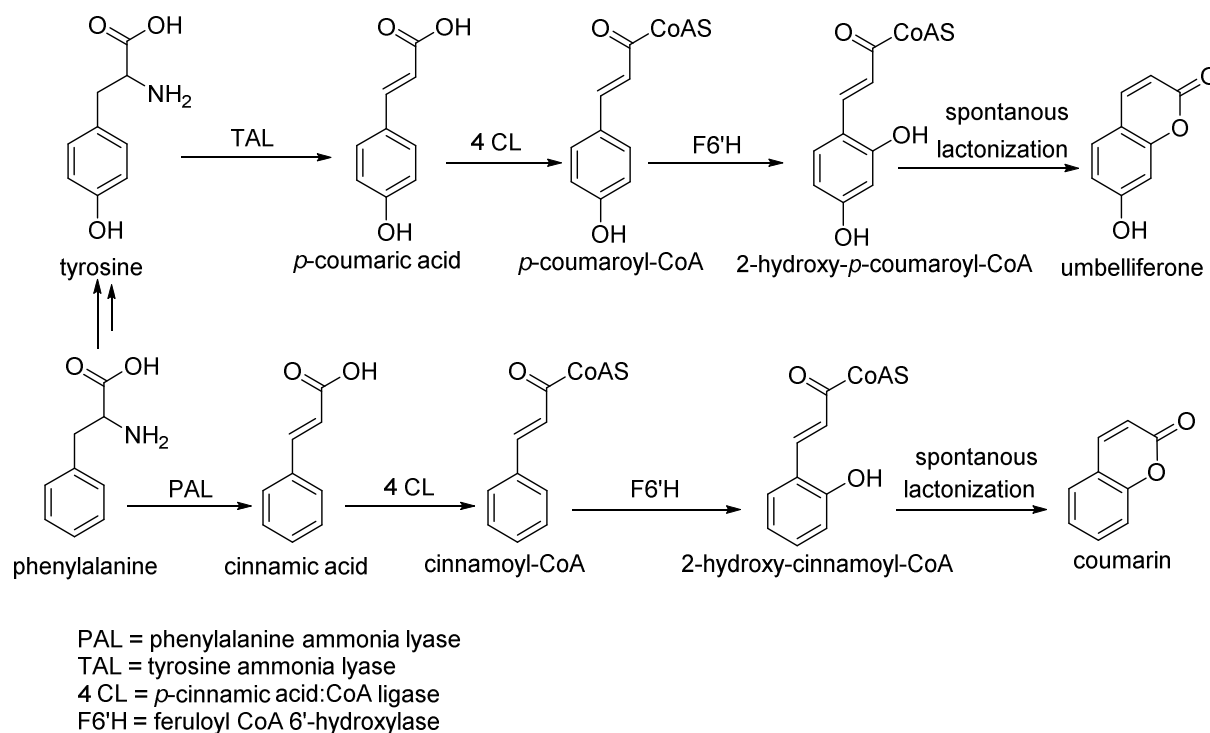
Fig. 1.6. Biosynthetic pathway of coumarins starting with phenylalanine (adapted from Yang *et al*., 2015).

1.4. Metabolomics and multivariate data analysis

As of the year 2000, a new discipline of system biology called metabolomics has rapidly emerged and attracted attention with increasing yearly number of publications (2 publications in 2000 to 2,065 in 2014, results from PubMed search with key word "metabolomics"). The term metabolomics from metabolites is an analogy to proteomics from proteins and genomics from genes. Ultimately, metabolomics should be connected to proteomics and genomics information to acquire new biological knowledge from functional genomics (e.g. the function of a gene or protein). Metabolomics aims at analyzing qualitatively and quantitatively all the metabolites in a given system at a given time (e.g. plant, marine and microorganism, tissue, cell, etc.). This is a quite ambitious goal, which in a strict sense is impossible to meet, because to date no single method or combination of analytical technologies is sensitive, selective, or comprehensive enough to measure "all" the metabolites (Kim *et al.*, 2010; Lammerhofer and Weckwerth, 2013). To get a

better understanding of the complexity of investigated matrices, more than 3,000 metabolites have been reported just from a part of tobacco leaves, and moreover, they have different concentrations (micromolar up to picomolar), chemical classes (molecular weight), solubility, stability, and polarity (Kim *et al.*, 2010). A more realistic definition of metabolomics is the analysis of all the metabolites in a given organism under certain conditions and all the metabolomic works refer either to metabolite fingerprinting or metabolite profiling. In biological studies metabolite fingerprinting is sometimes followed by metabolite profiling. The former is the high throughput qualitative analysis of biological samples, for example, two different genotypes or treatments (e.g. wild type/mutant, disease/healthy or stressed/non-stressed), to discover differences between them. The latter is the identification and quantification of a specific and often limited number of metabolites because of their role in understanding biological processes (Wolfender *et al.*, 2015; Lammerhofer and Weckwerth, 2013; Kim *et al.*, 2010). Metabolomics has been classified as targeted or untargeted, though targeted metabolomics in *sensu strictu* is not metabolomics but just targeted analytics. Targeted analyses focus on a predefined group of metabolites with most cases requiring identification and quantification of as many metabolites as possible within the group. In comparison, untargeted approaches are more holistic and focus on the detection of as many metabolites as possible ("all one can measure") without necessarily a specific knowledge of these metabolites (Lammerhofer and Weckwerth, 2013). A metabolomic analysis consists of different steps namely experimental design, sample preparation, sample analysis, data pre-processing and analysis (multivariate data analysis or chemometrics), compounds identification, and experimental validation (Chapter 2). Metabolomics has been applied in plant sciences for the quality control of herbal medicines, chemotaxonomy, bioactivity screening, developmental changes, and characterizing genetically modified crops (Wolfender *et al.*, 2015; Lammerhofer and Weckwerth, 2013).

There are several platforms (HPLC and TLC-UV, CE-MS, GC-MS, LC-MS, MS^n, and NMR) for metabolomics; each has its strong and weak points. Among these techniques, mass spectrometry (especially LC-MS) and NMR are currently considered to be the most suitable and used approaches (Wolfender *et al.*, 2015; Verpoorte *et al.*, 2008). Mass spectrometry is mostly hyphenated to separation methods like gas chromatography (GC) or liquid chromatography (LC). The hyphenation makes data become multidimensional (e.g. three-dimensional with retention time properties, mass-to-charge ratio, and intensity, or even four-dimensional if MS/MS is added). This helps for higher resolution and improves the detection, identification, and quantification of compounds (Lammerhofer and Weckwerth, 2013). GC-MS shows high sensitivity, resolution, and a reproducible fragmentation pattern of molecules. Commercial databases are available for

compound identification. However, a disadvantage of GC-MS is the limited range of polarity and molecular weights of metabolites that can be measured, and secondary metabolites need to be derivatized to become more volatile. Non-volatile compounds, for examples glycosides, cannot be analyzed by GC-MS (Wolfender *et al*., 2015; Verpoorte *et al*., 2008). The wide range of molecular weights and polarity, sensitivity, and the exact molecular weight are definitely the strong points of LC-MS or LC-HRMS in metabolomics. Furthermore, tandem MS^n techniques allow for partial structure determination of metabolites. However, such fragmentation processes strongly depend on the spectrometer and experimental conditions used. This creates the complications in spectral libraries and the storage of data. Another problem is the possibility of ion suppression effects and low ionization, which affect the quantification of metabolites (Lammerhofer and Weckwerth, 2013). An absolute quantification is only possible with calibration curves of individual compounds; this is unrealistic if calibration curves of hundreds of metabolites are needed (Wolfender *et al*., 2015; Verpoorte *et al*., 2008).

Absolute quantification, easy sample preparation, short time measurement (for ^{1}H NMR), compounds identification, and uniformity are some of the strong points of NMR techniques. Absolute quantification is feasible because signal intensity (in ^{1}H NMR) is dependent only on molar concentration of the compound (Kim *et al*., 2010). An NMR spectrum is a physical characteristic of a compound and is therefore highly reproducible, meaning the data are unbiased. The non-selectiveness also makes NMR an appropriate tool for profiling. A major problem is the low sensitivity and resolution, though both can be improved with high field instruments (e.g. 1000 MHz) and cryoprobes (Wolfender *et al*., 2015; Verpoorte *et al*., 2008). Although different in the technology applied, all platforms of metabolomics produce a huge amount of data. In order to be meaningful, these data need to be processed and statistically analyzed (Chapter 2) using multivariate data analysis such as PCA, PLS, or OPLS in order to acquire scientific information.

Principal component analysis (PCA) is the most common and basic point for all multivariate data analysis. The starting point for PCA is a matrix of data with *N* rows (observations: analyzed samples, etc.) and *K* columns (variables: LC-MS and NMR signals, etc.). PCA is a clustering method for data visualization and simplification without any prior knowledge of the samples (Eriksson *et al*., 2001). PCA is thus an unsupervised and unbiased method. It uses mathematical models to reduce the dimensionality of a multivariate data set by data decomposition. This method generates scores and loading vectors and can be represented in graphical forms known as *score plot* and *loading plot* (Chapter 2). The score plot can be employed to identify the differences or

similarities among the samples, easily detecting outliers. The loading plot helps to identify signals (metabolites) responsible for differences between clusters (Lammerhofer and Weckwerth, 2013).

The partial least squares to latent structure (PLS) based method is a regression extension of the PCA and the basis for supervised multivariate data analysis in which a prior knowledge of the data is mandatory (Lammerhofer and Weckwerth, 2013). The model focuses on variables of interest. In the PLS, the data matrices are divided into two or more groups of variables. The orthogonal partial least squares (OPLS) is a modification of PLS in which the projection is rotated in such way that the first component PC1 shows the between class difference. These methods use some preselected groups of variables and are sometimes more efficient in separating samples than the PCA. Similar to PCA, score and loading plots are also used to visualize the respective score and loading vectors (Eriksson *et al.*, 2001).

References

Adam, P., Arigoni, D., Bacher, A., Eisenreich, W., **2002**. Biosynthesis of hyperforin in *Hypericum perforatum. J. Med. Chem.* 45, 4786-4793.

AGP (Angiosperm Phylogeny Group), **2009**. An update of the Angiosperm Phylogeny Group classification for the orders and families of flowering plants: APG III. *Bot. J. Linn. Soc*. 161, 105-121.

Ang'edu, C. A., Schmidt, J., Porzel, A., Gitu, P., Midiwo, J. O., Adam, G., **1999.** Coumarins from *Hypericum keniense* (Guttiferae). *Pharmazie* 54, 235-236.

Bringmann, G., Gulder, T., Gulder, T.A.M., Breuning, M., **2011**. Atroposelective total synthesis of axially chiral biaryl natural products. *Chem. Rev.* 111, 563-639.

Chibale, K., Coleman, M.D., Masimirembwa, C., **2012**. Drug discovery in Africa. Springer-Verlag, Berlin Heidelberg (Germany).

Crockett, S.L., Robson, N.K.B., **2011**. Taxonomy and chemotaxonomy of the genus *Hypericum. Med. Aromat. Plant Sci. Biotechnol.* 5, 1-13.

Don, M.-J., Huang, Y.-J., Huang, R.-L., Lin, Y.-L., **2004**. New phenolic principles from *Hypericum sampsonii*. *Chem. Pharm. Bull.* 57, 866-869.

Eriksson, L., Johansson, E., Kettaneh-Wold, N., Wold, S., **2001**. Multi-and megavariate data analysis: Principles and applications. Umetrics Academy (Sweden).

Farag, M.A., Wessjohann, L.A., **2012**. Metabolome classification of commercial *Hypericum perforatum* (St. John's wort) preparations via UPLC-qTOF-MS and chemometrics. *Planta Med.* 78, 488-496.

Farag, M.A., Weigend, M., Luebert, F., Brokamp, G., Wessjohann, L.A., **2013**. Phytochemical, phylogenetic, and anti-inflammatory evaluation of 43 *Urtica* accessions (stinging nettle) based on UPLC–Q-TOF-MS metabolomic profiles. *Phytochemistry* 96, 170–183.

Farag, M.A., Mahrous, E.A., Lübken, T., Porzel, A., Wessjohann, L., **2014**. Classification of commercial cultivars of *Humulus lupulus* L. (hop) by chemometric pixel analysis of two dimensional nuclear magnetic resonance spectra. *Metabolomics* 10, 21-32.

Ferreira, R.O., da Silva, T.M.S., de Carvalho, M.G., **2015**. New polyprenylated phloroglucinol and other compounds isolated from the fruits of *Clusia nemorosa* (Clusiaceae). *Molecules* 20, 14326-14333.

Flavin, M.T., Rizzo, J.D., Khilevich, A., Kucherenko, A., Sheinkman, A.K., Vilaychack, V., Lin, L., Chen, W., Greenwood, E.M., Pengsuparp, T., Pezzuto, J.M., Hughes, S.H., Flavin, T.M., Cibulski, M., Boulanger, W.A., Shone, R.L. Xu, Z.-Q., **1996**. Synthesis, chromatographic resolution, and anti-human immunodeficiency virus activity of (+)-canalonide A and its enantiomers. *J. Med. Chem.* 39, 1303-1313.

Fonkwo, P.N., **2008**. Pricing infectious disease: The economic and health implications of infectious diseases. *EMBO Rep.* 9, 13-17.

Hamilton, G.R., Baskett, T.F., **2000**. In the arms of Morpheus: the development of morphine for postoperative pain relief. *Can. J. Anaesth.* 47, 367-374.

Hutchinson, J., Dalziel, J.M., **1954**. Flora of West Tropical Africa. Ed. Keay, R.W., Crown Agents for Overseas Governments and Administrations, Millbanks, London S.W.1 (U.K.).

Iwu, M.W., Ducan, A.R., Okunji, C.O., **1999**. New antimicrobials of plant origin. Ed. Janick, J., Perspectives on new crops and new uses, ASHS press, Alexandria, VA (USA).

Kadereit, J.W., Körner, C., Kost, B., Sonnewald, U., **2014**. Strasburger Lehrbuch der Pflanzenwissenschaften, 37. Auflage. Springer Spektrum, Berlin Heidelberg (Germany).

Kim, H.K., Choi, Y.H., Verpoorte, R., **2010**. NMR-based metabolomic analysis of plants. *Nat. Protoc.* 5, 536-549.

Klundt, T., Bocola, M., Beuerle, T., Liu, B., Beerhues, L., **2009**. A single amino acid substitution converts benzophenone synthase into phenylpyrone synthase. *J. Biol. Chem.* 284, 30957-30964.

Lammerhofer, M., Weckwerth, W., **2013**. Metabolomics in practice: Successful strategies to generate and analyze metabolic data. Wiley VCH, Weinheim (Germany).

Li, J. W.-H., Vederas, J.C., **2009**. Drug discovery and natural products: End of an era or endless frontier? *Science* 325, 161-165.

McGaw, L.J., Jäger, A.K., Staden, J.V., **2000**. Antimalarial, anthelmintic and anti-amoebic activity in South African medicinal plants. *J. Ethnopharmacol.* 72, 247-263.

Musa, M.A., Cooperwood, J.S., Khan, M.O.F., **2008**. A review of coumarin derivatives pharmacotherapy of breast cancer. *Curr. Med. Chem.* 15, 2664-2679.

Nathan, P.J., **2001**. *Hypericum perforatum* (St. John's wort): a non-selective reuptake inhibitor? A review of the recent advances in its pharmacology. *J. Psychopharmacol.* 15, 47-54.

Newman, D.J., Cragg, G.M., **2012**. Natural products as sources of new drugs over the 30 years from 1981 to 2010. *J. Nat. Prod.* 75, 311-335.

Nürk, N.M., Blattner, F.R., **2010**. Cladistic analysis of morphological characters in *Hypericum* (Hypericaceae). *Taxon* 59, 1495-1507.

Nürk, N.M., **2011**. Phylogenetic analyses in St. John's wort (*Hypericum*). Inferring character evolution and historical biogeography. PhD thesis, Free University Berlin.

Nürk, N.M., Madrinan, S., Carine, M.A., Chase, M.W., Blattner, F.R., **2013**. Molecular phylogenetics and morphological evolution of St. John's wort (*Hypericum*; Hypericaceae). *Mol. Phylogenet. Evol.* 66, 1-16.

Robson N.K.B., **1977**. Studies in the genus *Hypericum* L. (Guttiferae): 1. Infrageneric classification. *Bulletin of the British Museum (Natural History), Botany* 5, 291–355.

Stevens, P.F., **2007**. The families and genera of vascular plants. Ed. Kubitzki, K., Hypericaceae, Springer, Berlin Heidelberg (Germany).

Singh, I. P., Bharate, S.B., **2006**. Phloroglucinol compounds of natural origin. *Nat. Prod. Rep.* 23, 558–591.

Singh, I.P., Sidana, J., Bharate, S.B., Foley, W.J., **2010**. Phloroglucinol compounds of natural origin: Synthetic aspects. *Nat. Prod. Rep.* 27, 393–416.

Tanaka, N., Takaishi, Y., **2006**. Xanthones from *Hypericum chinese*. *Phytochemistry* 67, 2146-2151.

Venugopala, K.N., Rashmi, V., Odhav, B., **2013**. Review on natural coumarin lead compounds for their pharmacological activity. *BioMed Res. Int.* DOI: 10.1155/2013/963248.

Verpoorte, R., Choi, Y.H., Mustafa, N.R., Kim, H.K., **2008**. Metabolomics: back to basics. *Phytochem. Rev*. 7, 525-537.

Woelk, H., **2000**. Comparision of St. John's wort and imipramine for treating depression: randomized crontolled trial. *BMJ* 321, 536-539.

Wolfender, J.-L., Marti, G., Thomas, A., Bertrand, A., **2015**. Current approaches and challenges for metabolite profiling of complex natural extracts. *J. Chromatogr. A* 1382, 136-164.

Xu, W.-J., Zhu, M.-D., Wang, X.-B., Yang, M.-H., Luo, J., Kong, L.-Y., **2015**. Hypermongones A-J, rare methylated polycyclic prenylated acylphloroglucinols from the flowers of *Hypericum monogynum. J. Nat. Prod.* 78, 1093-1100.

Yang, S.-M., Shim, G.Y., Kim, B.-G., Ahn, J.-H., **2015**. Biological synthesis of coumarins in *Escherichia coli. Micro. Cell. Fact.* 14, 65. DOI: 10.1186/s12934-015-0248-y.

Zhang, A., Sun, H., Wang, X., **2013**. Recent advances in natural products from plants for treatment of liver diseases. *Eur. J. Med. Chem.* 63, 570-577.

Zofou, D., Kowa, T.K., Wabo, H.K., Ngemanya, M.N., Tane, P., Titanji, V.P.K., **2011**. *Hypericum lanceolatum* (Hypericaceae) as a potential source of new anti-malarial agents: a bioassay-guided fractionantion of the stem bark. *Malar. J.* 10, 167. DOI: 10.1186/1475-2875-10-167.

Zuurbier, K.W.M., Fung, S.-Y., Scheffer, J.J.C., Verpoorte, R., **1998**. In-vitro prenylation of aromatic intermediates in the biosynthesis of bitter acids in *Humulus lupulus. Phytochemistry* 49, 2315-2322.

Chapter 2

NMR and LC-MS based metabolome analyses of plant extracts for natural product class mapping and prioritization in new natural product discovery: the example of St. John's wort (*Hypericum*)

Graphical abstract*
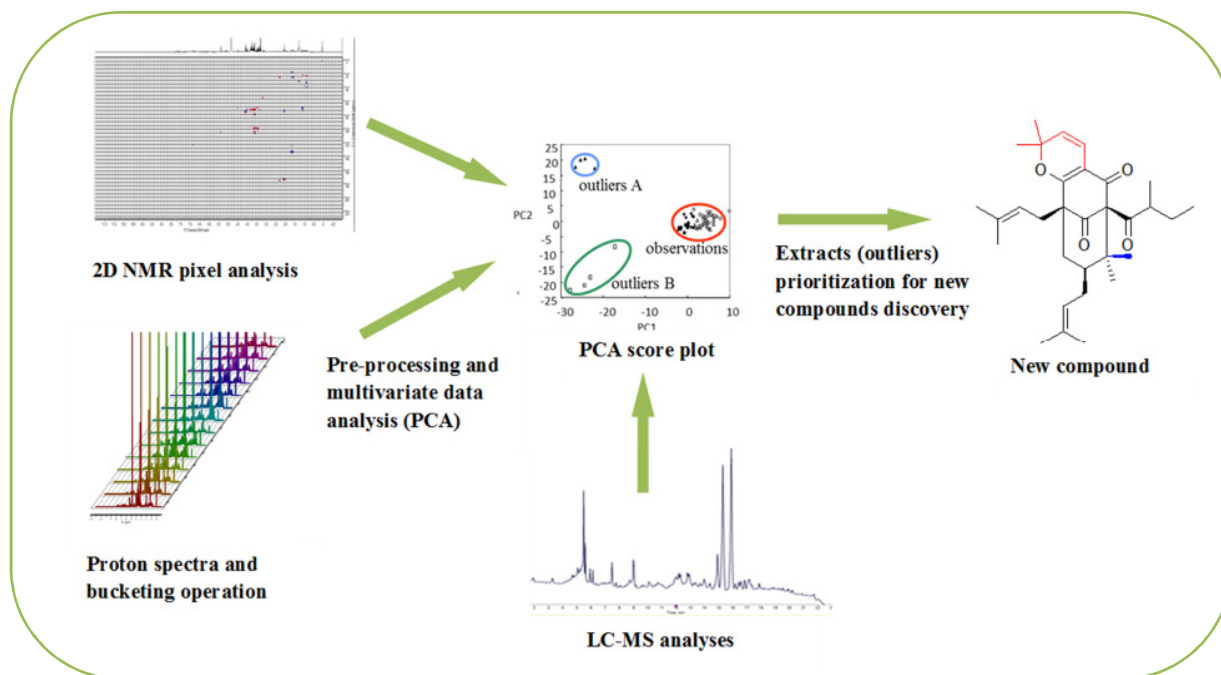
Highlights

- Rapid and easy metabolomic profiles based approaches for extract prioritization

- New natural products discovery from prioritized extracts among 17 *Hypericum* species

- Simple methods for detecting new bioactive compounds and avoiding replication

- Applications of ^{1}H NMR, 2D NMR, and LC-MS metabolomics in natural products

- Metabolite fingerprinting of 17 different *Hypericum* species

Abstract

Natural products are important sources of biologically active compounds. They have made substantial contributions to human health and well-being. However, the challenges that hinder the rapid discovery of new bioactive natural products are many, with the greatest obstacles being replication and the time required for isolation and characterization of secondary metabolites from complex mixtures. Methods for selecting the most suitable plant extracts for drug discovery rely on literature searches, bioactivity results, or ethno-botanical knowledge, and fail to take into account the structural novelty of secondary metabolites. This chapter describes metabolomic approaches for extract prioritization to aid natural product discovery based on three independent analytical methods: ^{1}H NMR, 2D NMR pixel analysis, and LC-MS. The data are evaluated by multivariate analysis, especially principal component analysis (PCA). As a proof of concept, we applied ^{1}H NMR/PCA, ^{1}H-^{13}C HMBC/PCA, and UPLC-TOF-MS/PCA to segregate extracts from 17 different *Hypericum* species (including the popular St. John's wort, *H. perforatum*), and to select those that will with high propability lead to novel natural products. The separation and purification of compounds identified as peaks from prioritized extracts afforded several novel natural products. A correlation between the metabolite profiles and biological activity of investigated *Hypericum* species is discussed in this first report on combining chromatography, spectroscopy and multivariate data analysis for plant extracts priorization in novel natural products discovery.

Key words: 2D NMR metabolomics, ^{1}H NMR and LC-MS metabolomics, multivariate data analysis, *Hypericum*, dereplication.

2.1. Introduction

Despite the success of nature in providing unique chemical entities, the interest of pharmaceutical companies in natural products research programs has significantly decreased in the last three decades (Newman and Cragg, 2012; Newman, 2008). This was a result of the perceived disadvantages of natural products (difficulties in access and supply, complexities of natural product chemistry and the time-consuming work involved, increasing legal problems and concerns about intellectual property rights) and the expectations associated with using combinatorial chemistry as the future source of a massive number of novel compounds and drug leads (new chemical entities) (Newman, 2008; Harvey, 2008). However, these expectations were shown to be overrated. For this and other reasons, the number of active compounds that reached the market in the last three decades significantly decreased. It is, however, noteworthy that the output of newly launched drugs has dropped during a period of declining interest in natural products (Newman and Cragg, 2012; Cragg and Newman, 2013; Yuliana *et al*., 2011). Common synthetic libraries from combinatorial chemistry often show much less chemical diversity, functionality or chirality than natural product libraries, but most of all they lack the evolutionary pre-selection of biological functionality including important characteristics for drug-like properties which give them the competitive edge (Wessjohann *et al*., 2005; Yuliana *et al*., 2011). However, combinatorial chemistry is a powerful tool for structure optimization once an active lead compound has been identified.

It is estimated that less than 10% of the world's biodiversity has been investigated for biological activity (Dias *et al*., 2012). About only 6% of the approximately 300,000 plant species has been systematically investigated pharmacologically and only 15% chemically (Newman, 2008; Dias *et al*., 2012). One obstacle is the lack of efficient and high-throughput techniques able to identify chemical novelty from complex mixtures (extracts) and avoid replication/rediscovery of known compounds, making phytochemistry a laborious, expensive, and time-consuming work (Raskin *et al*., 2002). There is a need for new strategies to improve the efficiency of natural products research. We imagined that techniques which can rapidly discriminate (bioactive) extracts, before time-consuming isolations, and show the signals of chemical entities making differences among them can help to find needles in the haystack and avoid redundant compounds in drug discovery programs. Such new chemical entities can then be rapidly isolated guided by their specific physicochemical characteristics (e.g. MS or NMR signals, or retention times). Since metabolomic studies and metabolome fingerprints ideally cover all metabolites reasonably accessible by physicochemical (analytical) separation and detection methods, metabolome analyses and

evaluation techniques can help to choose the best plant extracts for compound discovery. Compared to, e.g. a random or ethno-botanically based selection, the distinction is based on structural and physicochemical properties extracted from the mixture without prior separation of a compound. Some researchers have already made efforts towards the prioritization of natural products extracts. Hou *et al*. (2012) reported the metabolic profiles of microbial strains using LC-MS coupled to multivariate data analysis for discovering new chemical compounds. Macintyte *et al*. (2014) correlated LC-MS profiles with bio-assays results to prioritize marine microbial strains for drug discovery efforts. Samat *et al*. (2014) applied a metabolomic tools based on PCA on LC-MS profiles of photocytotoxic extracts to identify two photosensitizers, and the Wessjohann's group correlated plant and fungal extract LC-MS data with bioactivities (Degenhardt *et al*., 2014; Wessjohann, 2014).

In our continuing investigation of secondary metabolites from plants of the Hypericaceae family (Fobofou *et al.,* 2016a, b; Fobofou *et al*., 2014; Fobofou *et al*., 2015a, b; Farag and Wessjohann, 2012; Porzel *et al*., 2014), in the present study we apply untargeted metabolomics by multiplex analytical approaches (LC-MS, 1D NMR, 2D NMR) interpreted by multivariate data analysis or chemometrics to prioritize the best plant extracts (without prior knowledge of their chemical constituents) for discovering new compounds. We hypothesized that, in the multivariate data analysis, extracts clustering together contain similar or the same secondary metabolites, while outliers are those extracts with chemically different metabolites, and by this means can identify extracts with unique chemistry without having to separate all the metabolites. Compounds from prioritized extracts can be rapidly isolated guided by their MS or NMR profiles since the loading plots will directly tell which peaks are responsible for the distinct behavior. Unlike other studies that focus on LC-MS of known matrices and compare different extracts from the same plant species, the present study considers less or uninvestigated plant species, more complex matrices, extracts from different plant species, and different analytical approaches including two dimensional NMR evaluated by chemometric methods, and thereby this demonstrates the power of LC-MS and NMR based metabolomic methods for high-throughput natural product research.

2.2. Results and discussion

It is estimated that the chemistry of more than 60% of the *Hypericum* species remains unknown (Crockett and Robson, 2011). Despite this, most of the metabolic profiling studies carried out on *Hypericum* species intended to compare *H. perforatum* obtained from different origins based on the identification and quantification of reference and known compounds (e.g. hyperforins, hypericins, flavonoids, etc.) (Farag and Wessjohann, 2012; Huck *et al*., 2006; Maggi *et al*., 2004;

Tolonen *et al.*, 2003). In this study, we segregated methanolic leaf extracts from 17 different *Hypericum* species obtained from the United States, Europe, and Cameroon (for details see experimental section). We hypothesized that species that cluster in the same group (e.g. group of *H. perforatum*) after statistical analysis contain similar or the same metabolites, which may differ for example in the concentration of these compounds, while outliers likely contain chemical novelty or unprecedented compounds classes from the genus *Hypericum*. NMR metabolomic profiles were measured without any chromatographic separation while hyphenated techniques (LC-TOF-MS) were used for mass spectrometry (MS). Multivariate data analysis (e.g. PCA) allows to discriminate extracts within the large sets of data obtained and to have a clear visualization on differing groups. The separation and purification of compounds from prioritized extracts then should significanty enhance the chance to find and eventually to localize/identify novel natural products. Since analyses such as PCA are based on finding maximum similarities, it also give the maximum non-similarities. However, since in PCA individual data are statistically "mixed" when downgrading the dimensionality, the indication of something distinct is statistical, i.e. the probability of finding new compounds in a sample showing such distinction will be significantly higher than picking an average, despite the remaining statistical risk that in single cases this may not be true.

2.2.1. ^{1}H NMR and 2D NMR pixel analysis based extracts prioritization

NMR is a powerful technique and can holistically give information on all the metabolites present in the extract (Kim *et al.*, 2010). It has advantages over other analytical approaches because it is unbiased, stable over time, highly reproducible, does not require prior chromatographic separation, has easy sample preparation, can be applied for various chemical classes, and spectra can be recorded in a relatively short time; however, the major disadvantage is its low sensitivity. The basic requirement for ^{1}H NMR to detect a given metabolite is the presence of protons in the structure (which is the case for all organic natural products), enabling ^{1}H NMR to detect compounds that cannot be detected by mass spectrometry (MS) in the case of low ionization (Kim *et al.*, 2010). The identification of known compounds in the ^{1}H NMR spectrum of extracts is possible by comparison of signals with those in the literature or of reference compounds measured under the same conditions, in exceptional cases it can also be done *de-novo*, if the spin system of a new metabolite can be separated, e.g. by multidimensional techniques (Porzel *et al.*, 2014).

Three separate sample replicates from the dried leaves of 17 *Hypericum species* (e.g. 1A, 1B, 1C for *H. perforatum*. See Table 2.1), extracted and prepared as described in the experimental

section, were submitted for ^{1}H NMR and ^{1}H-^{13}C HMBC analysis. HMBC spectra were acquired on the proton channel, compensating partially the low sensitivities typical of ^{13}C NMR. The presence of a large number of signals (or cross peaks) with different intensities hurdle a visual comparison of the extracts. Thus, we used chemometrics for a holistic and semi-automated comparison between the samples. The three replicates aimed at verifying the reproducibly of our manipulations and measurements. The obtained spectra were processed using ACD/Lab software with a macro and submitted for statistical analysis using the R programming language. The PC1 and PC2 plots allow for discrimination between *Hypericum* species while the loading plots reveal discriminating signals.

2.2.1.1. ^{1}H NMR metabolomics based method

The results of the 51 (17 × 3 replicates) ^{1}H NMR spectra of *Hypericum* crude extracts after processing and principal component analysis (PCA) are depicted in Figure 2.1A. A 22-components model was computed and PC1 and PC2 explain 65% of the variation, with PC1 (44%) being the dominant factor for the classification of the groups. The clustering of the three replicates highlights the precision of the method. Discriminating proton NMR signals are presented in the loading plots (Figures 2.1B and 2.1C). The 17 *Hypericum* species are separated by the PC1 into two main groups; the first onto the negative co-ordinates (scores) values is formed by group A containing 12 species including *H. perforatum* that cluster very well, and the second onto the positive scores of group B/group C containing 5 *Hypericum* species which are rather spread. PC2 counts for 21% of the variation and separates group C from group B, with the latter, however, being rather inhomogeneous in itself. The PCA is a map of the 17 *Hypericum* species. Species chemically close to each other have similar properties (profiles), whereas those far from each other are dissimilar with respect to metabolites profiles. Extracts of Group A (*H. perforatum, H. kouytchense, H. polyphyllum, H. androsaenum, H. tetrapterum, H. inodorum, H. undulatum, H. frondosum, H. patulum, H. buckleyi, H. pulchrum,* and *H. calycinum*) are clustered together, thus representing a group of *Hypericum* extracts with some similarity in their metabolites profiles. Because *H. perforatum* (control) belongs to group A, it can be assumed that extracts of other group A members chemically are not so far from *H. perforatum* profiles. Outliers (extracts of groups B and C) are discriminated from those of group A, with *H. hircinum* (11A, B, C), *H. olympicum* (13A, B, C), *H. lanceolatum* (15A, B, C), *H. roeperianum* (16A, B, C), and *H. peplidifolium* (17A, B, C) appearing to be the discriminated species according to ^{1}H NMR-PCA. This suggests that it might be worthwhile to look more closely into the chemical composition of *Hypericum* species in groups

B and C if one is interested in compounds distinct from those commonly known from the *H. perforatum* cluster. Before doing so, it is advisable to have a closer look at what causes the biggest

Table 2.1. Origin and abbreviation of *Hypericum* species used in this study.

Hypericum species	Label (three replicates)	Origin
H. perforatum L.	1A, 1B, 1C	Staudengärtnerei Gaißmayer GmbH and Co. KG (Illertissen, Germany).
H. kouytchense A. Lev.	2A, 2B, 2C	N.L. Chrestensen Erfurter Samen- und Pflanzenzucht GmbH (Erfurt, Germany)
H. polyphyllum Boiss. & Balansa	3A, 3B, 3C	Staudengärtnerei Gaißmayer GmbH and Co. KG (Illertissen, Germany).
H. androsaenum L.	4A, 4B, 4C	Jelitto Staudensamen GmbH (Schwarmstedt, Germany)
H. tetrapterum Fr.	5A, 5B, 5C	Prime Factory GmbH and Co. KG (Hennstedt, Germany)
H. inodorum Mill.	6A, 6B, 6C	N.L. Chrestensen Erfurter Samen- und Pflanzenzucht GmbH (Erfurt, Germany)
H. undulatum Schousb. ex Willd.	7A, 7B, 7C	N.L. Chrestensen Erfurter Samen- und Pflanzenzucht GmbH (Erfurt, Germany)
H. patulum Thunb.	8A, 8B, 8C	Frankfurt Botanical Garden (Frankfurt, Germany)
H. buckleyi M. A. Curtis	9A, 9B, 9C	Frankfurt Botanical Garden (Frankfurt, Germany)
H. pulchrum L.	10A, 10B, 10C	Frankfurt Botanical Garden (Frankfurt, Germany)
H. hircinum L.	11A, 11B, 11C	Frankfurt Botanical Garden (Frankfurt, Germany)
H. calycinum L.	12A, 12B, 12C	Frankfurt Botanical Garden (Frankfurt, Germany)
H. olympicum L.	13A, 13B, 13C	Frankfurt Botanical Garden (Frankfurt, Germany)
H. frondosum Michx.	14A, 14B, 14C	Middle Tennessee State University (MTSU) Garden. Identified by Prof. Jeffrey Walck (MTSU, Murfreesboro, USA)
H. lanceolatum Lam.	15A, 15B, 15C	Collected at Mount Bamboutos (Mbouda, Cameroon) and identified at the Cameroon National Herbarium where a voucher specimen (No 32356/HNC) is deposited
H. roeperianum Schimp. ex A. Rich.	16A, 16B, 16C	Collected at Mount Bamboutos (Mbouda, Cameroon) and identified at the Cameroon National Herbarium (No 33796/HNC).
H. peplidifolium A. Rich.	17A, 17B, 17C	Collected at Mount Bamboutos (Mbouda, Cameroon) and identified at the Cameroon National Herbarium (No 26774/SFR/Cam)

differences between the two main groups, i.e. to gain a more detailed NMR overview on the general chemistry of *H. perforatum* extract. The high resolution ^{1}H NMR (Figure 2.2) of *H. perforatum* extract can be divided into four main regions: the first (8.0-5.5 ppm) are signals due to aromatic protons of quercetin conjugates (flavonoids) and chlorogenic acid, the second (5.5-4.6 ppm) are signals due to prenyl side chain of phloroglucinols and anomeric protons of sugar units, the third (4.6-3.2 ppm) are signals of sugar units, and the fourth (3.2-0.5 ppm) can be attributed to

aliphatic protons of fatty acids and phloroglucinols including the prenyl groups (i.e. allylic methyl groups). These observations from the ^{1}H NMR spectrum of *H. perforatum* are in agreement with
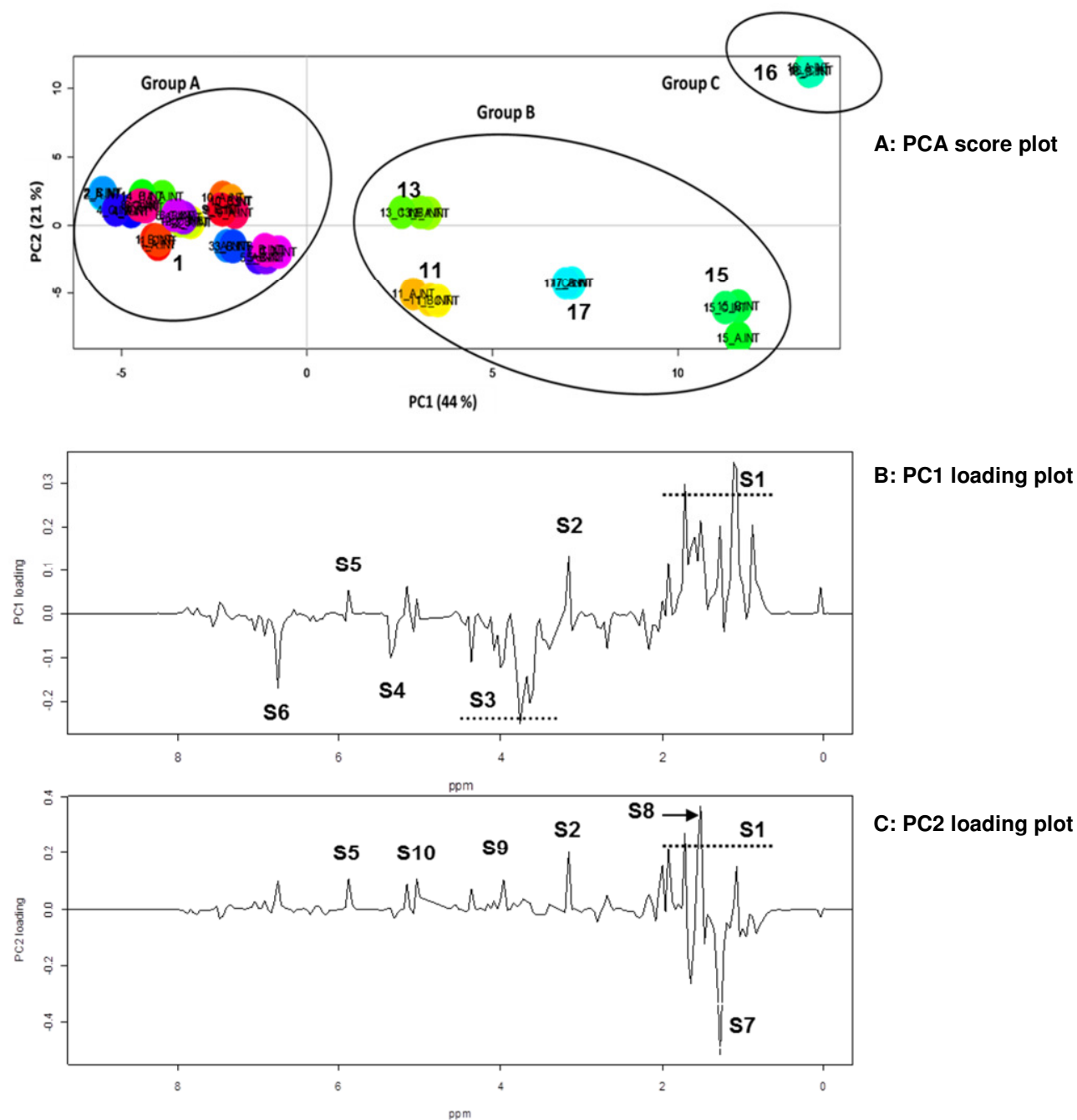
Figure 2.1. A. ^{1}H NMR principal component analyses of 17 *Hypericum* species. For numbers = species, see Table 2.1. Letters represent technical replicates. Oval groupings are for discussion purposes only, as variation within such a group maybe larger than between individual members of different groups (e.g. 13/16 vs. 13/5). **B.** PCA loading plot of the first principal component showing the main variables. **C.** PC2 loading plot and contributing protons signals: **S1** (signals of aliphatic protons of terpene (prenyl/geranyl) and acyl moieties of acylphloroglucinols), **S2** (methylene (CH$_2$) signals of prenyl/geranyl side chains), **S3** (protons of sugar moieties of glycosylated flavonoids), **S4** (anomeric protons of sugars), **S5** (aromatic protons of di-substituted 1,3,5-trihydroxybenzene), **S6** (signals of flavonoid aglycones), **S7** (methyls of acyl moieties), **S8** (methyl groups of prenyls/geranyls), **S9** (methine protons of acyl moieties), and **S10** (olefinic protons of prenyls/geranyls).

those reported in the literature (Porzel *et al*., 2014; Bilia *et al*., 2001; Rasmussen *et al*., 2006; Schmidt *et al*., 2008).

The PCA loading plots (Figures 2.1B and 2.1C) reveal information on variables responsible for the discrimination patterns observed on the PCA score plots. The PC1 loading plot (Figure 2.1B) shows that acylphloroglucinol derivatives are highly abundant in the extracts located in the positive PC1 region (groups B/C) while glycosylated flavonoids play the major role for the discrimination (negative PC1) of group A from the others. The PC2 loading (Figure 2.1C) exhibits signals which contribute to the separation between group C (positive PC2) and group B (negative PC2). Though *Hypericums* of both groups are rich in acylphloroglucinols, geranyl/prenyl and benzene protons dominate the positive PC2 (group C, *H. roeperianum*). From this finding one can hypothesize that extracts from *Hypericum* species clustering in groups B/C maybe more likely to contain new phloroglucinol derivatives that are structurally different from those reported from *H. perforatum*, i.e. hyperforins (**2.1-2.2**), and are less promising for flavonoids. Extracts of groups B/C are therefore prioritized for new compounds discovery, with *H. roeperianum* and *H. lanceolatum* being the most discriminated outliers.
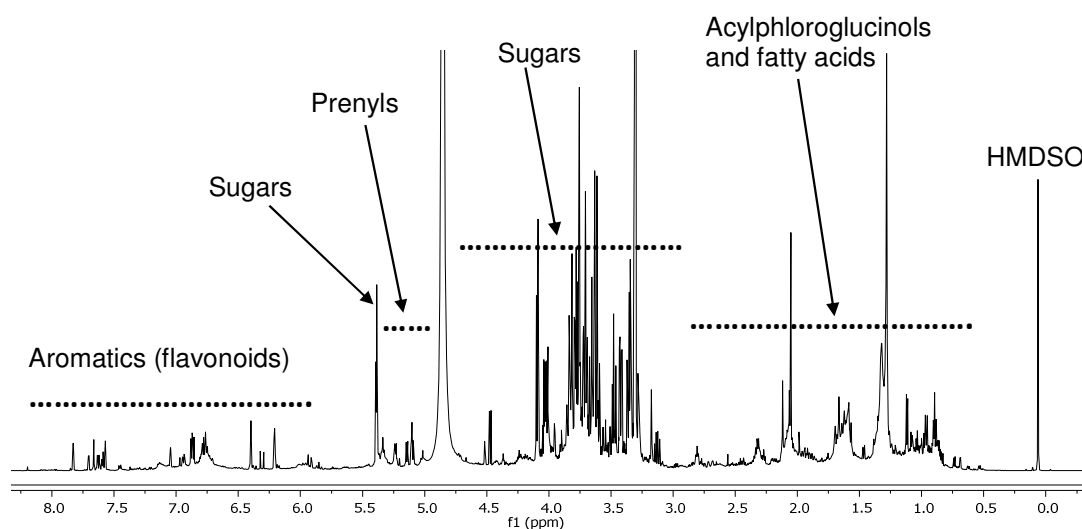
Figure 2.2. ^{1}H NMR (CD$_3$OD, 600 MHz) spectrum of *H. perforatum* extract. HMDSO = Hexamethyldisiloxane.

2.2.1.2. 2D NMR metabolomics based method

Alhough the ^{1}H NMR-PCA in this case already appears to be a sufficient and powerful tool for comparing and prioritizing *Hypericum* species based on their proton signatures, one of the major problems of one dimensional methods is the loss of information due to proton signals overlapping in the ^{1}H NMR spectra. The introduction of a second dimension (here: ^{13}C signals in HMBC) can

help to distinguish between overlapping signals through long range ^{1}H-^{13}C correlation (Mahrous *et al.*, 2015). This additional chemical/structural information generated in a 2D NMR fingerprint represents each metabolite by sets of ^{1}H and ^{13}C peaks, separating extracts based on both their ^{1}H and ^{13}C NMR profiles. In the ^{1}H NMR based metabolomics, spectra were divided into hundred regions (buckets) of chemical shifts that were integrated for multivariate data analysis (Kim *et al.*, 2010), whereas in the 2D NMR (^{1}H-^{13}C HMBC), HMBC spectra were divided into thousands of squares of fixed size (2D-buckets = pixels) to generate a "pixel map". The integration volume associated with each square was automatically computed to create a large data set that was subsequently analyzed using the same chemometric methods well established for one-dimensional spectra. Our group (Farag *et al.*, 2014) successfully applied this pixel analysis approach for the classification of commercial cultivars of *Humulus lupulus* L. (hops). In order to demonstrate the power of 2D NMR metabolomics for extracts prioritization for new compounds discovery, ^{1}H-^{13}C HMBC spectra (17 × 3 sample replicates) of 17 *Hypericum* species were recorded, processed using ACD/Lab software, and analyzed using chemometric tools with R-scripts.

PCA was applied to have a clear visualization on the different outliers (prioritized extracts). The results of the 51 spectra (17 × 3 replicates) after processing and multivariate data analyses are depicted in Figure 2.3A. Again, extraction and 2D NMR-measurements are highly constant with samples A, B, C always clustering together. PC1 (44%) and PC2 (13%) account for 57% of the variation among the *Hypericum* species, with PC1 (44%) being the dominant principal component for the classification of the groups. The PCA score plot (Figure 2.3A) displays the separation of the 17 *Hypericum* species into two main areas with one cluster (in group 1) and related groups 1 and 3, vs. a more distinct group 2. The latter consists of *H. olympicum* (13), *H. buckleyi* (9), and *H. frondosum* (14) which have the highest PC1 score values. PC2 could separate extracts on the negative PC1 values, where *H. roeperianum* (16), *H. peplidifolium* (17), and *H. lanceolatum* (15) are located at the highest positive PC2 values. *H. kouytchense* (2) has the most negative PC2 value.

Several *Hypericum* species including *H. perforatum* (control) cluster with similar PC1/PC2 values (see cluster in group 1). The discriminated *Hypericum* species (groups 2 and 3 and some in group 1) are those that potentially contain new natural products or at least compounds structurally different from those occurring in *H. perforatum*. These scoring results correlate to those previously obtained from ^{1}H NMR-PCA, because the 2D NMR-PCA successfully discriminates extracts that were already discriminated by the ^{1}H NMR-PCA. However, some differences are observed between the two methods in separating *Hypericum* extracts. Some species (e.g. *H. buckleyi*, 9) which were not separated by the ^{1}H NMR-PCA, appear separated after 2D NMR-PCA analyses.

A: PCA score plot

B: PC1 loading plot

C: PC2 loading plot

Figure 2.3. A. 2D NMR (HMBC) pixels principal component analyses of 17 *Hypericum* species. For numbers = species see Table 1.1. Letters represent technical replicates. Oval groupings are for discussion purposes only, as variation within such a group maybe larger than between individual members of different groups. **B.** PC1 loading plot and contributing signals. H-values are proton chemical shifts. C-values are carbon chemical shifts. **C.** PC2 loading plot and contributing signals.

This, as expected, highlights the power of HMBC to discriminate/resolve overlapping proton signals through long range ^{1}H-^{13}C coupling and distinguish extracts with similar proton profiles but different carbon signatures. There are also a few samples that appear less segregated (e.g. *H. lanceolatum*, 15), and most interesting are samples that discriminate in both methods and promise optimum distinction considering both ^{1}H and ^{13}C signals (e.g. *H. roeperianum*, 16).

In order to explain the most discriminating ^{1}H/^{13}C signals among the *Hypericum* species, we analyzed the PCA loading plots (Figure 2.3B and 2.3C). Cross peaks (colored in green on Figure 2.3B) that correspond to the allylic coupling of the prenyl/geranyl side chains, i.e. δ ^{1}H/^{13}C of 1.40/126.0, 1.40/131.5, 1.40/137.0, 1.50/21.3, 1.50/137.0, and 1.50/131.5, contribute positively to the PC1. Signals that give negative PC1 values can be assigned to allylic coupling of prenyls of hyperforin derivatives (δ ^{1}H/^{13}C of 2.31/26.8, 2.31/175.5, 1.60/26.8, 1.60/126.0, 1.60/137.0) (Bilia *et al*., 2001), and coupling of sugar moieties (δ ^{1}H/^{13}C 3.64/70.9, 3.64/98.4, 3.64/103.9, and 4.04/70.1) of quercetin conjugates (Schmidt *et al*., 2008).

The PC2 contributes only 13% of the variation among *Hypericum* extracts but, nevertheless, could clearly segregate some extracts (Figure 2.3A). The HMBC cross peaks that contribute negatively to the PC2 values (see loading plot in Figure 2.3C) can be assigned to signals of chlorogenic acid (δ ^{1}H/^{13}C 6.79/148.0) (Bilia *et al*., 2001; Schmidt *et al*., 2008), and sugars of quercetin conjugates (δ ^{1}H/^{13}C 2.21/70.9, 3.64/70.9, 3.64/76.4, 3.64/81.9, 3.64/98.4, 3.64/103.9, 3.74/76.4) (Bilia *et al*., 2001; Schmidt *et al*., 2008). HMBC correlations that account for the positive PC2 values correspond to coupling of acyl moieties (δ ^{1}H/^{13}C 1.09/214.1, 1.09/21.3, and 1.09/43.3), prenyl chains (δ ^{1}H/^{13}C 1.60/126.0, 1.60/131.5, 1.70/126.0, and 1.70/137.0), and characteristic cross peaks (δ ^{1}H/^{13}C 3.23/126.0, 3.23/164.5) of allylic protons of prenyl chains of *C*-prenylated acylphloroglucinol cores (Porzel *et al*., 2014; Drewes and van Vuuren., 2008). It can be retained from this analysis that the PCA separated *Hypericum* extracts with respect to their content of glycosylated phenolics, chlorogenic acid, and prenylated acylphloroglucinols. These results are in agreement with the ^{1}H NMR based method. Extracts with the lowest PC1/PC2 values are rich in glycosylated phenolics and chlorogenic acid (e.g. extract 2 and cluster in group 1) while those with the highest PC1/PC2 values are rich in prenylated phloroglucinols (e.g. 13 and 16). Without any chromatographic separation and prior to any (time consuming) isolation, it is thus possible to map the chemistry of 17 *Hypericum* species with respect to major natural product classes and typical moieties of these (e.g. prenyl side chains). Extracts in groups 2 and 3 (Figure 2.3A) are the outliers that can be prioritized for new compounds discovery, with *H. roeperianum*

(16) and *H. olympicum* (13) being the most discriminated ones. These outliers according to the 2D NMR overview should most likely contain new acylphloroglucinol derivatives.

2.2.2. LC-MS metabolomics based extracts prioritization

LC-MS technology has played the major role in metabolomic field because of its high resolution and sensitivity and widespread availability as well as the higher abundance of LC-MS devices and trained operators in comparison to NMR instruments and operators (Lammerhofer and Weckwerth, 2013). With the availability of open-source and online data mining platforms (e.g. XCMS online and MetaboAnalysts) or MS manufacturers' software (e.g. MarkerView for AB Sciex instruments), it no longer requires bioinformatics skills to perform classical (e.g. control versus test groups) LC-MS metabolomics on non-large data sets (Lammerhofer and Weckwerth, 2013; Tautenhanh *et al.*, 2012).

In effort to investigate plant extracts in a holistic, high-throughput, and untargeted manner to find bioactive and new natural products among redundant compounds, LC-MS metabolomics is an indispensable method for the prioritization of plant extracts for new compounds discovery, if the focus shall include also less abundant compounds not visible in NMR (<< 1% of extract dry weight or in overlap regions). Following the samples preparation process (See Experimental Section), LC-MS data were acquired, and PCA was used to explore the variability among the *Hypericum* species (Farag and Wessjohann, 2012; Porzel *et al.*, 2014). LC-MS data acquired in negative ionization modes of 51 extracts (17 *Hypericum* species × 3 sample replicates) were exported to Excel by employing MarkerView software. This software applies noise filtering, baseline correction, peak picking, peak integration, and alignment. Multivariate data analysis was performed on scaled and normalized MS-data using the program SIMCA-P.

The PC1 plotted against PC2 scores (Figure 2.4A) displays three main areas. The three technical replicates cluster together; which demonstrates the precision of our extraction, solid phase extraction (SPE), and UPLC-MS measurements. Five outliers can be observed on the PCA scores plot (in areas 1 and 2), of which two are displayed on the positive PC2 (area 2: *H. olympicum* (13A/B/C) and *H. polyphyllum* (3A/B/C)) while three appear on the negative PC1 values (area 1: *H. peplidifolium* (17A/B/C), *H. lanceoatum* (15A/B/C), and *H. roeperianum* (16A/B/C)). The remaining 12 *Hypericum* species (including *H. perforatum* (control)) cluster together in area 3 at similar PC1/PC2 values; they are not very separated based on the PCA scores plot. *H. olympicum* and *H. polyphyllum* are the most separated along the PC2 scores, whereas *H. peplidifolium* and *H. lanceolatum* are the most discriminated along PC1. *Hypericum* extracts from areas 1 and 2 (Figure

2.4A) are those outliers that should be prioritized for new compounds discovery based on MS data, a result that largely conforms to the analyses of the two NMR techniques described previously for that purpose.
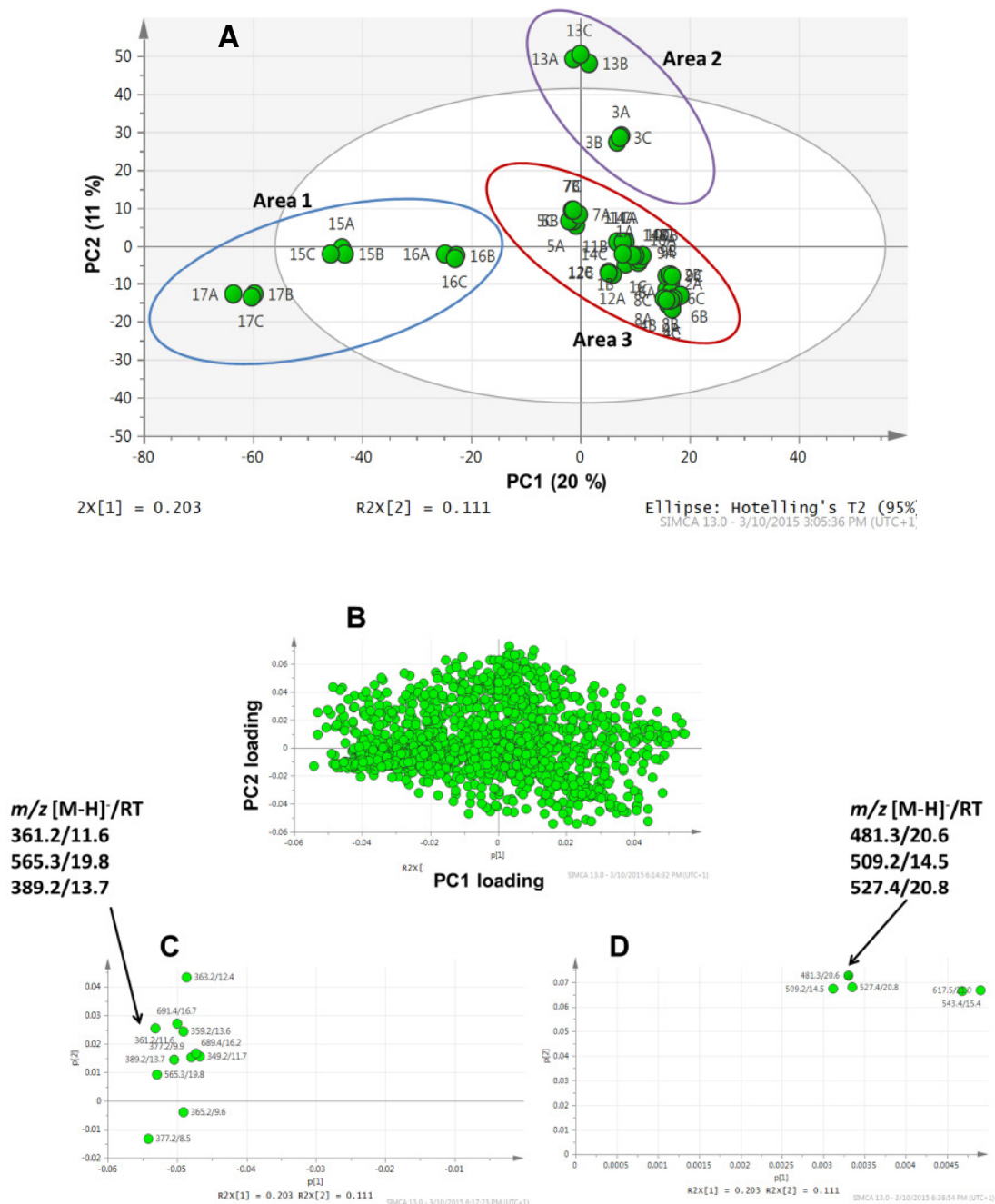
Figures 2.4. A. PCA of 17 *Hypericum* species analyzed by UPLC-qTOF-MS. For numbers = species see Table 2.1. Letters represent technical replicates. Oval groupings are areas for discussion purposes only, as variation within such a group maybe larger than between individual members of different groups. **B.** full PC1/PC2 loading plots. **C.** Zoomed PC1/PC2 loading plots revealing the most discriminatory signals ([M-H]⁻/RT: 361.2/11.6; 565.3/19.8; 389.2/13.3) along the negative PC1. **D.** Zoomed PC1/PC2 loading plots revealing the most discriminatory signals ([M-H]⁻/RT: 481.3/20.6; 509.2/14.5; 527.4/20.8) along the positive PC2.

The separation observed on the PCA scores plots (Figure 2.4A) can be explained using the PCA loading plots (Figure 2.4B-D) which reveal the most discriminatory MS signals, *m/z*-RT 361.2/11.6 on the negative PC1 and *m/z*-RT 481.3/20.6 on the positive PC2. Further discriminatory signals include *m/z*-RT 565.3/19.8 and 389.2/13.7 for the discrimination on the negative PC1 and *m/z*-RT 509.2/14.5 and 527.4/20.8 for the segregation on the positive PC2. Trend plots reveal the distribution of these ions over all analyzed extracts. For example (Figures 2.5-2.8), the ion *m/z* 527.4 occurs only in *H. olympicum* (13A/B/C) and *H. polyphyllum* (3A/B/C). It can also be seen (Figures 2.5-2.8) that the ion *m/z* 361.2 is highly abundant in extracts 15, 16, and 17, and absent in several extracts including *H. perforatum* (1A/B/C). The compound with *m/z* 361.2 (**2.3**) was later isolated from *H. peplidifolium* and characterized to be petiolin-J (**2.3**). As a final example, the ion *m/z* 481.2 is present in extracts 3 and 13 and is also absent in *H. perforatum*.
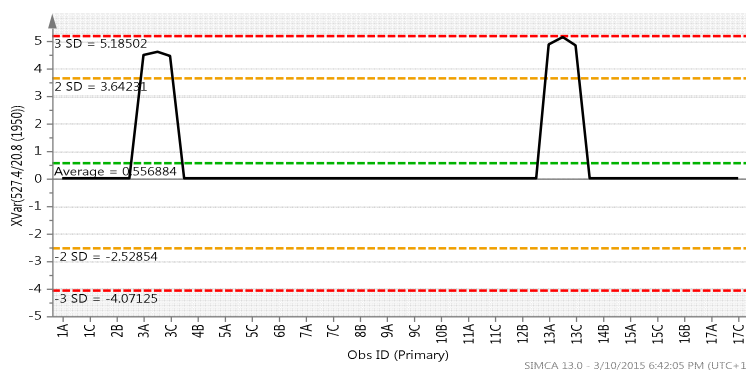
Figure 2.5. Trend plot for *m/z* 527.4 [M-H]⁻. The plot shows the distribution of the ion m/z 527.4 [M-H]⁻ over all the *Hypericum* extracts. This ion is present only in *H. polyphyllum* and *H. olympicum.*
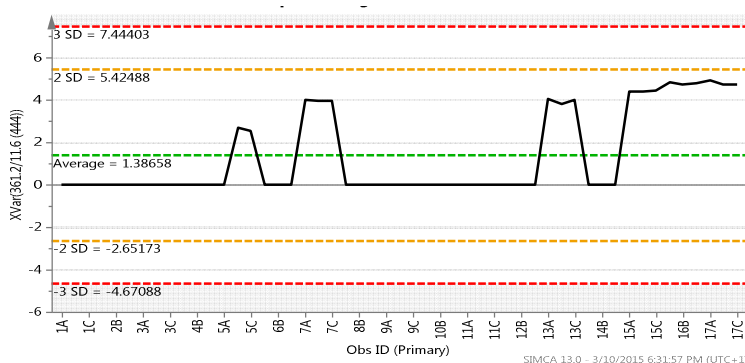
Figure 2.6. Trend plot for *m/z* 361.2 [M-H]⁻ (petiolin J). The plot shows the distribution of the ion at *m/z* 361.2 [M-H]⁻ over all the *Hypericum* extracts. The ion is highly abundant in extracts 15, 16, and 17.
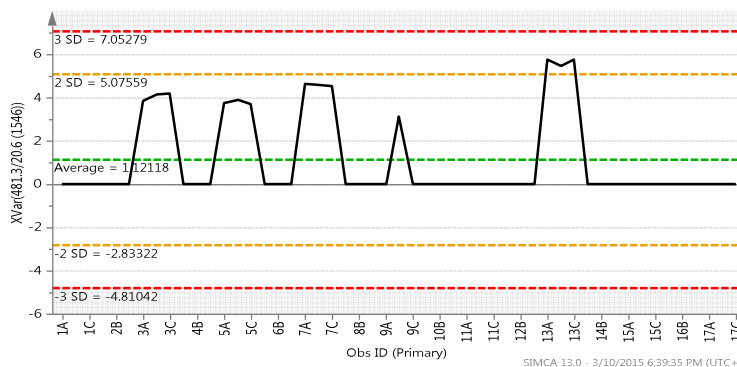
Figure 2.7. Trend plot for *m/z* 481.3 [M-H]⁻. The plot shows the distribution of the ion at *m/z* 481.3 [M-H]⁻ over all the *Hypericum* extracts.
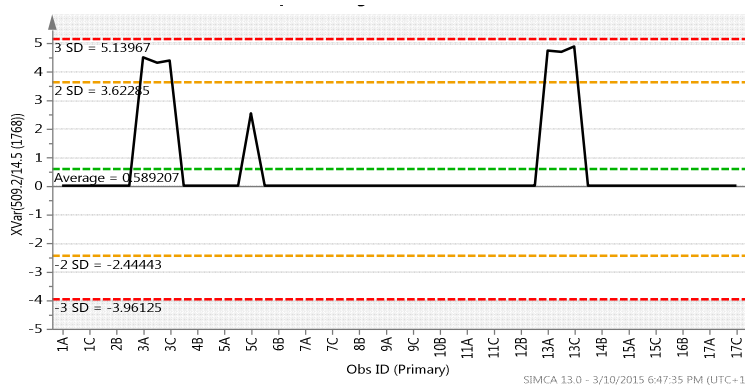
Figure 2.8. Trend plot for *m/z* 509.2 [M-H]⁻. The plot shows the distribution of the ion at *m/z* 509.2 [M-H]⁻ over all the *Hypericum* extracts.

Though petiolin-J is not a new compound, it was only recently reported as a new antimicrobial constituent of the Japanese *H. pseudopetiolatum* var. *kiusianum* (Tanaka *et al*., 2010). It is important to note that petiolin-J (**2.3**) is a prenylated acylphloroglucinol possessing a methyl group on the trioxygenated benzene nucleus of chromane. This chemical feature makes petiolin-J unique or at least very different, for example, from those phloroglucinols (**2.1-2.2**) abundant in St. John's wort. The isolation and characterization of chemical constituents from *H. polyphyllum* is still in progress in our lab. However, the compound with *m/z* 481.2 was already isolated and identified to be hyperpolyphyllirin (**2.4**) previously characterized by Porzel *et al*. (2014) from the crude extract of *H. polyphyllum*, also having a methyl in the core phloroglucinal moiety. The constitution of hyperpolyphyllirin likely is the correct form of the never well characterized adhyperfirin. Compound **2.4** (*m/z* 481.2), a deprenylated methylhyperforin, in a later publication was independently named hyperibine J (**2.4**) by Mitsopoulou *et al*. (2015) as a natural product also to be found in the Greek *H. triquetrifolium*. The uniqueness of the polycyclic polyprenylated acylphloroglucinol (PPAP) hyperpolyphyllirin (syn. hyperibine J, **2.4**) is that it possesses a methyl substituent instead of a prenyl side chain (like hyperforin) at C-1.

A comparative visual inspection of NMR-PCA and LC-MS-PCA results shows that almost the same extracts are prioritized (discriminated) by all of these methods, except that the 2D NMR-PCA displays a higher number of outliers than other methods.

2.2.3. Biological activity and phytochemical investigation

2.2.3.1. Biological activity

In order to establish whether there is a correlation between the biological activity and the metabolite profiles, we evaluated the cytotoxicity against PC-3 and HT-29 cancer cell lines and anti-HIV-1 activity of the leaf extract of each of the 17 *Hypericum* species. The anti-HIV activity (using MT-4 cells infected with HIV_{IIIB}) was measured in parallel with the cytotoxicity against uninfected MT-4 cells. The results of our assays (Table 2.2) clearly show that there is a correlation between the metabolite profiles and cytotoxicity against PC-3, HT-29, and MT-4. Indeed, extracts clustering together on the PCA plot show similar biological activity profiles. For instance, considering the NMR-PCA analyses (Figures 2.1A and 2.3A) and the results in Table 2.2, one easily observes that *H. perforatum* (1) and species of the same cluster/group (e.g. *H. kouytchense* (2), *H. androsaenum* (4), *H. tetrapterum* (5), etc.) exhibit similar activity with moderate to no cytotoxicity (growth inhibition of less than 30% or $CC_{50} > 45$ µg/ml). The discriminated *Hypericum* species, as shown on the three independent PCA score plots, exhibit higher and more significant cytotoxic activity (growth inhibition of more than 30% or $CC_{50} < 45$ µg/ml). Furthermore, the most discriminated *Hypericum* species (e.g. *H. hircinum* (11), *H. olympicum* (13), *H. lanceolatum* (15) *H. roeperianum* (16), and *H. peplidifolium* (17)) exhibit the highest cytotoxic effects. Because the most segregated *Hypericum* species (e.g. *H. roeperianum*, etc.) have a higher content of prenylated compounds/acylphloroglucinols and aromatics (see discussion on PCA loading plots above) and are poorer in glycosylated flavonoids than *H. perforatum* and the other species of its cluster/group, these cytotoxicity studies suggest that some prenylated acylphloroglucinols are likely responsible for the cytotoxic activity of *Hypericum* species. Assuming in a first approximation the absence of synergistic or uncovered trace compound effects of the chemical constitutents of the prioritized *Hypericum* species, the isolation of cytotoxic prenylated acylphloroglucinols from the discriminated phenotypes would not rely on serendipity. Cytotoxicty has previously been reported for some prenylated acylphloroglucinols from the genus *Hypericum* (Wang *et al.*, 2012; Xu *et al.*, 2010). No significant anti-HIV activity was observed for the extracts from the leaves of the 17 *Hypericum* species, as they all failed to protect MT-4 cells infected with HIV_{IIIB} ($CC_{50} > EC_{50}$). However, the stem bark of *H. roeperianum* shows significant

anti-HIV-1 activity (Table 2.2), which, to our knowledge, has never been reported for the genus

Hypericum.

Table 2.2. Cytotoxic activity against the human cancer cells lines PC-3 and HT-29. Cytotoxicity against uninfected MT-4 cells and anti-HIV-1 activity using MT-4 cells infected with HIV-1$_{\text{IIIB}}$.

	PC-3	HT-29	MT-4	HIV-1$_{\text{IIIB}}$
Leaf extract (MeOH)	Percentage of growth inhibition ± SD (at 50 µg/ml)*		[a,b]CC$_{50}$ (µg/ml)	[a,c]EC$_{50}$ (µg/ml)
H. perforatum (1)	-14.4 ± 3.6	-11.9 ± 0.3	71.7	>71.7
H. kouytchense (2)	-53.1 ± 6.1	-29.3 ± 3.3	53.3	>53.3
H. polyphyllum (3)	50.9 ± 2.0	16.7 ± 3.3	40.0	>40.0
H. androsaenum (4)	-8.1 ± 3.4	-10.8 ± 3.8	66.5	>66.5
H. tetrapterum (5)	-20.6 ± 1.2	-16.9 ± 3.7	53.0	>53.0
H. inodorum (6)	9.9 ± 5.4	2.2 ± 2.4	42.7	>42.7
H. undulatum (7)	-42.9 ± 6.7	-24.2 ± 4.5	>100	>100
H. patulum (8)	3.0 ± 3.1	7.9 ± 0.7	55.0	>55.0
H. buckleyi (9)	30.9 ± 5.6	35.5 ± 3.8	41.0	>41.0
H. pulchrum (10)	-26.0 ± 6.6	-31.7 ± 3.8	49.5	>49.5
H. hircinum (11)	71.8 ± 1.8	56.7 ± 1.8	15.7	>15.7
H. calycinum (12)	-14.4 ± 5.6	-23.5 ± 3.7	43.6	>43.6
H. olympicum (13)	72.8 ± 0.2	81.3 ± 0.3	7.6	>7.6
H. frondosum (14)	-32.7 ± 6.3	-31.2 ± 1.8	50.8	>50.8
H. lanceolatum (15)	88.6 ± 0.6[d]	88.7 ± 1.8[d]	17.0	>17.0
H. roeperianum (16)	82.3 ± 0.6[e]	84.0 ± 4.5[e]	11.0	>11.0
H. roeperianum (stem bark extract)	73.1 ± 1.1[e] 60.4 ± 3.1[d]	73.3 ± 1.1[e] 52.5 ± 5.3[d]	6.0[e]	0.4[e]
H. peplidifolium (17)	48.0 ± 4.2	53.7 ± 3.6	41.0	>41.0
Digitonin	100 ± 0.2	99.9 ± 0.4	-	-
Efavirenz	-	-	40.0	0.002

[*] Negative values show increased proliferation/growth. This can be attributed to feeding effects (e.g. of sugars in extracts) or to growth factors like, e.g. phytoandrogens in PC-3 (Bobach *et al.*, 2014).
[a] Data represent mean values for three independent determinations. Variation among duplicate samples (SD) was less than 15%.
[b] Cytotoxicity concentration (CC): Compound concentration (µM) required to reduce the viability of mock-infected MT-4 cells by 50%, as determined by the MTT method. [c] Effective concentration (EC): Compound concentration (µM) required to achieve 50% protection of MT-4 cells from HIV-1 induced cytopathogenicity, as determined by the MTT method. [d] Crude methanol (80%) extract. [e] Crude chloroform extract.
Digitonin (125 µM) is the reference cytotoxic compound while efavirenz is the reference anti-HIV drug. DMSO (0.05% for activity against PC-3 and HT-29) was used as negative control.

2.2.3.2. Phytochemical investigation

Following the results of the three plant extract prioritization approaches presented herein, it appears that *H. olympicum*, *H. lanceolatum*, *H. roeperianum*, *H. peplidifolium*, and *H. polyphyllum* are the most relevant candidate *Hypericum* species prioritized for new compounds discovery. A detailed report on the isolation, structural elucidation, and biological activity of new compounds from these extracts is beyond the scope of the present work and will be disclosed in the future. However, it is noteworthy to mention that we isolated 27 compounds never described from the genus *Hypericum* (including 24 novel natural products which partly still await full characterization), belonging to different chemical classes, from *H. lanceolatum*, *H. roeperianum*, and *H. peplidifolium*. From these constituents of prioritized extracts, for instance, compounds **2.3-2.6** as a proof of concept are already resolved and depicted in Figure 2.5.

2.1 R = CH$_3$
2.2 R = CH$_2$CH$_3$

2.3

2.4

2.5

2.6
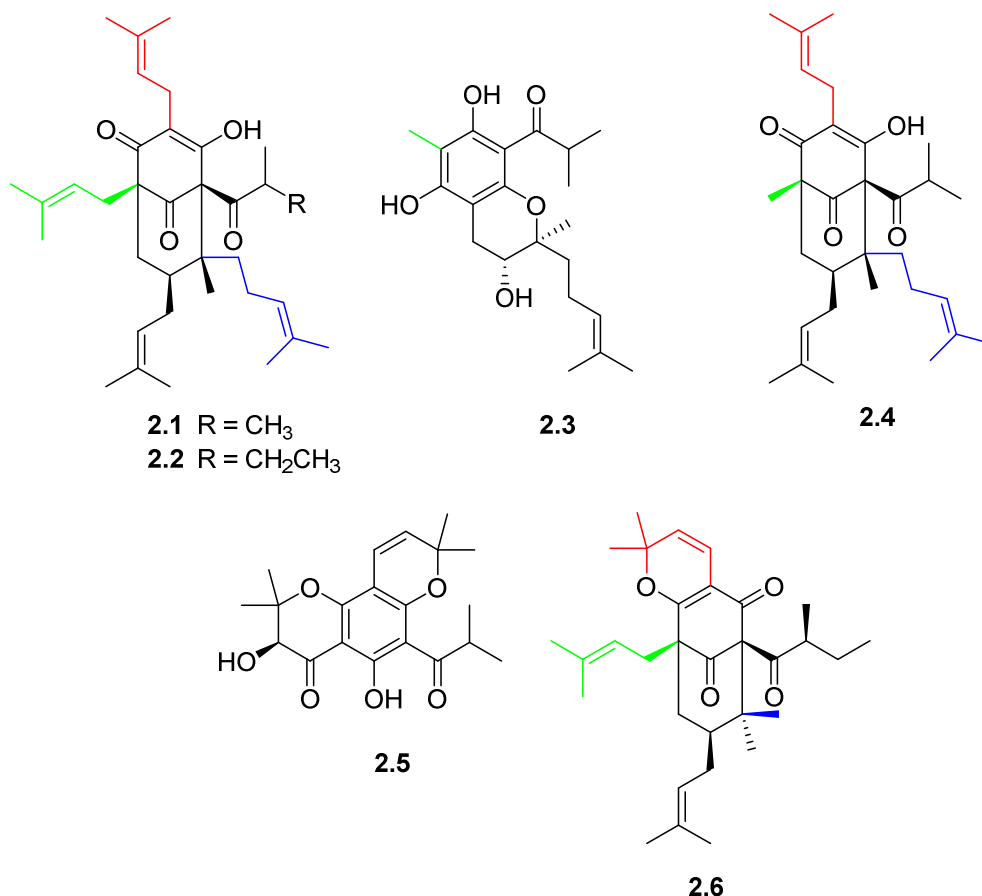
Fig. 2.5. Chemical structures of hyperforins (**2.1-2.2**) and selected compounds (**2.3-2.6**) from prioritized *Hypericum* species.

The novel compound **2.5** (selancin H) was isolated from *H. lanceolatum* and is the first natural product that consists of a 6-acyl-2,2-dimethylchroman-4-one derivative fused with a

dimethylpyran unit. Hyperselancin A (**2.6**) is an example of new polycyclic polyprenylated acylphloroglucinol isolated from *H. lanceolatum*. Detailed investigations of constituents from the leaf (part used in the present metabolomic study) and stem bark extracts of *H. roeperianum* were reported (see Chapters 4 and 5) (Fobofou *et al*., 2015b; Fobofou *et al*., 2014). Eleven unpreviously described prenylated acylphloroglucinol derivatives (selancins A-I and hyperselancins A and B) were isolated and elucidated from the leaf extract of *H. lanceolatum* (see Chapter 3) (Fobofou *et al*., 2016a). The chemical investigation of new constituents of *H. peplidifolium* was disclosed (see Chapter 6) (Fobofou *et al.*, 2016b). *H. polyphyllum* and *H. olympicum* still await completed phytochemical studies. However, our group recently reported the structure elucidation of hyperpolyphyllirin (**2.4**) from complex mixture (Porzel *et al*., 2014). The detection of unique acylphloroglucinols **2.3-2.6** (though compounds **2.3** and **2.4** were recently reported (Tanaka *et al*., 2010; Porzel *et al.*, 2014; Mitsopoulou *et al*., 2015)) from prioritized extracts is sufficient to demonstrate the power of metabolomic approaches for a semi-automated extract prioritization to boost new compound discovery in face of high chemical replication in plant extracts. The isolation procedure, ^{1}H and ^{13}C NMR data of pure compounds **2.3, 2.5,** and **2.6** (the proof of concept examples we selected among many) are described in detail in the upcoming chapters.

2.3. Experimental section

2.3.1. Plant material

The 17 *Hypericum* species used in this study were obtained from Germany, Cameroon, and the USA. All information on investigated samples and their origin is provided in Table 2.1. Seedlings of *Hypericums* 1 to 7 (see Table 2.1) were obtained from named companies and grown in the same field at our institute. Leaves were harvested in July/September 2009 and frozen (-80 °C) until investigation. Freshly collected *Hypericum* species 8 to 13 were kindly provided to us by the Frankfurt Botanical Garden (collected in June 2013) and kept at -80 °C until further investigation. Leaves of *H. frondosum* (14) collected in May 2014 and identified by Prof. Jeffrey Walck (Department of Biology, MSTU), were kindly provided from the Middle Tennessee State University (MTSU) Garden. *H. lanceolatum* (15), *H. roeperianum* (16), and *H. peplidifolium* (17A) were collected in Cameroon in August and October 2011 as specified in Table 2.1.

2.3.2. Sample preparation for LC-MS and NMR measurements

All the 17 *Hypericum* species (except *H. peplidifolium*) were extracted in the same manner. For each plant, three sample replicates were extracted in parallel under the same conditions. We used a one-pot extraction for MS and NMR analyses. For this, 200 mg of dried and powdered leaves

were extracted with 5 ml of methanol, containing umbelliferone (8 µl/ml, internal standard for LC-MS), for 15 minutes under ultrasound and centrifuged at 4000 G for 20 min.

For 1D and 2D-NMR, 3 ml of the supernatant were evaporated under a nitrogen stream to dryness and re-suspended in 800 µl methanol-D$_4$ containing HMDSO (0.936 mM) as an internal standard. The solution was centrifuged for 2 min at 13000 G. 700 µl of the supernatant was transferred to a NMR tube for measurements.

For LC-MS, 500 µl of leaves extract were placed on a SPE SA (Chromabond SA, Macherey-Nagel, Germany) cartridge (3 ml, 500 mg) pre-saturated with 3 ml methanol. The elution was performed with another 3 ml methanol. The eluate was evaporated under a nitrogen stream and re-suspended in 2 ml methanol containing umbelliferone (8 µl/ml). 1 ml was aliquoted using a syringe and placed into MS vials. Our choice of SPE SA cartridge derived from a comparison (results not shown) between SPE SA and SPE RP18 (Chromabond C18 ec, Macherey-Nagel, Germany) cartridges and some LC-MS runs to select the best SPE method for our complex matrices containing chlorophyll.

We could not obtain fresh material of *H. peplidifolium*, only the dried methanol extract of the aerial part (herb without flowers) could be provided to us by a Cameroonian colleague (Mr. Antoine Honoré Nkuete Lonfouo). To attempt as good of a comparison as possible, we weighted an equal mass of dried extract of *H. inodorum* (extracted as described above) in 500 µl (5.97 mg) and 3 ml (35.85 mg) methanol, respectively. These extracts, in three replicates, were re-suspended in methanol (500 µl and 3 ml) and prepared as described above for MS and NMR analyses and compared to the samples obtained by the standardized method described above.

2.3.3. LC-MS analyses

LC-MS analyses were performed on an AB-Sciex Triple TOF-5600 mass spectrometer (using the Analyst TF 1.6 software) coupled to a Waters Aquity UPLC equipped with a Macherey-Nagel Nucleoshell RP 18 column (150 x 2 mm, particle size 2.7 µm) applying the following binary gradient at a flow rate of 400 µl/min: 0-2 min, isocratic 95% A (0.3 mM ammonium formate in water), 5% B (acetonitrile); 2-19 min, linear, from 95 to 5% A; 19-22 min, isocratic 5% A; 22-22.01 min linear, from 5% B to 95% A; 22.01-24 min isocratic, 95% A. The injection volume was 5 µl (partial loop injection, loop volume 10 µl). The column temperature was 40 °C, and the injection needle was washed with 2 ml acetonitrile after each injection. MS data were acquired in SWATH-Mode (AB-Sciex MicroApp, version TF 1.6) with full scans from 65 to 1250 Daltons

with an accumulation time of 50 ms and SWATH-window with a width of 32 Daltons during 20 ms accumulation time. The cycle time was thus 0.833 seconds. The mass spectrometric analyses always were performed in high sensitivity mode. The ionization was performed by means of ESI (AB Sciex Deospray) under the following conditions: ion source gas I = 60, ion source gas II = 70, curtain gas = 35, temperature = 600 °C, ionspray floating voltage = -4500 in the negative mode, declustering potential = -35, ion release delay = 67, ion release width = 25. The collision energy for the full scan was -10. For the SWATH windows different collision energies (rolling collision energy, charge = 1, slope = 0.0575, intercept = 9, maximum CE = 80 V) were used. After every tenth sample, a calibration of the mass spectrometer with the aid of a Calibrant Delivery Systems (AB-Sciex) with the corresponding calibration solution (APCI Negative Calibration Solution for AB-Sciex triple-TOF System) was carried out. The evaluation of the peaks was performed using the AB Sciex programs Peak View version 1.2.0.3. The UV detector was a Waters ACQUITY 2996 PDA detector. The intensities of all wavelengths between 190-500 nm at a distance of 1.2 nm were measured. Thus, we obtained an absorption spectrum for each peak.

2.3.4. NMR analyses

All spectra were acquired on an Agilent (Varian) VNMRS 600 NMR spectrometer operating at a frequency of 599.83 MHz using a 5 mm inverse detection cryoprobe. The following parameters were used for recording ^{1}H NMR spectra: digital resolution 0.37 Hz/point (32 K complex data points), pulse width = 3 µs (45°), relaxation delay = 23.7 s, acquisition time = 2.7 s, number of transients = 40. Zero filling up to 128 K and an exponential window function with lb = 0.4 was used prior to Fourier transformation. 2D NMR spectra were acquired using standard CHEMPACK 5.1 pulse sequences (gHMBCAD) implemented in Varian VNMRJ 3.2C spectrometer software. HMBC spectra were measured over a bandwidth of 10 ppm in F2 (^{1}H) and 236 ppm in F1 (^{13}C) using two scans per 265 increments for F1 and 1024 complex data points in F2. HMBC analysis was optimized for a long range coupling of 8 Hz, a two-step $^1J_{CH}$ filter was used (130-165 Hz) with a 1.31 relaxation delay. The total acquisition time was 28 min (nt = 2 and ni = 256). Proton and carbon chemical shifts were referenced to internal hexamethyldisiloxane (HMDSO) at 0.062 ppm for proton and internal CD_3OD (49.0 ppm) for carbon.

2.3.5. NMR and LC-MS data processing and multivariate data analysis

For ^{1}H NMR, all spectra were automatically transformed to ESP files using ACD/NMR Manager lab version 10.0 software (Toronto, Canada). Spectral intensities were reduced to buckets of equal width (0.04 ppm) within the region of 12.0 to -0.4 ppm. The dark regions were set to 5.0-

4.7 (water) and 3.4-3.25 (methanol) using a macro. PCA was performed with R package (2.9.2) using custom written procedures after normalizing to HMDSO signal and excluding solvent regions.

For 2D NMR, all HMBC spectra were processed using a sinebell window function in F2, zero filling up to 1,024 K and a Gaussian window function in F1 prior to Fourier transformation to ESP files using the same ACD/NMR Manager lab version 10.0 software as above with a macro. For PCA analysis, spectral intensities were reduced to two-dimensional integrated regions, referred to as pixels, i.e. squares, of constant length and width in the spectral regions δ ^{13}C (- 6.0 to 231 ppm) in F1 and δ ^{1}H (- 0.4 to 8.5 ppm) in F2 and an intensity value per pixel (2D bucket). Pixel sizes were set at 0.925 ppm in the F1 dimension (^{13}C) and 0.04 ppm in the F2 dimension (^{1}H), with the noise factor set at 3. The dark regions were set as above, prior to multivariate analyses. PCA was performed with R (2.15.2) together with the Bioconductor package pcaMethods using custom-written procedure and normalization to sum of integral set at 10,000 (Farag *et al*., 2014).

For UPLC-MS, data acquired in negative ionization modes were exported to Excel by employing MarkerView (AB Sciex MS manufacturer software). This software approach employs peak picking, alignment, matching, and comparison. Principal component analysis (PCA) was performed with the program SIMCA-P Version 13.0 (Umetrics, Umeå, Sweden). All variables were mean centered and scaled to Pareto variance.

2.3.6. Biological assays

The experimental procedures for cytotoxic and anti-HIV assays were previously reported (Fobofou *et al.,* 2015b).

References:

Bilia, A.R., Bergonzi, M.C., Mazzi, G., Vincieri, F.F., **2001**. Analysis of plant complex matrices by use of nuclear magnetic resonance spectroscopy: St. John's Wort Extract. *J. Agric. Food Chem.* 49, 2115-2124.

Bobach, C., Schurwanz, J., Franke, K., Denkert, A., Sung, T.V., Kuster, R., Mutiso, P.C., Seliger, B., Wessjohann, L.A., **2014**. Multiple readout assay for hormonal (androgenic and antiandrogenic) and cytotoxic activity of plant and fungal extracts based on different prostate cancer cell line behavior. *J. Ethnopharmacol.* 155, 721-730.

Cragg, G.M., Newman, D.J., **2013**. Natural products: a continuing source of novel drug leads. *Biochem. Biophys. Acta* 1830, 3670-3695.

Crockett, S.L., Robson, N.K.B., **2011**. Taxonomy and chemotaxonomy of the genus *Hypericum*. *Medicinal Aromatic Plant Sci. Biotech.*5, 1-13.

Degenhardt, A., Wittlake, R., Steilwind, S., Liebig, M., Runge, C., Hilmer, J.M., Krammer, G., Gohr, A., Wessjohann, L., **2014**. Quantification of important flavour compounds in beef stocks and correlation to sensory results by "Reverse Metabolomics". Ed. Ferreira, V., Flavour Science, Elsevier, Amsterdam.

Dias, D.A., Urban, S., Roessner, U., **2012**. A historical overview of natural products in drug discovery. *Metabolites* 2, 303-336.

Drewes, S.E., van Vuuren, S.F., **2008**. Antimicrobial acylphloroglucinols and dibenzyloxy flavonoids from flowers of *Helichrysum gymnocomum*. *Phytochemistry* 69, 1745-1749.

Farag, M.A., Wessjohann, L.A., **2012**. Metabolome classification of commercial *Hypericum perforatum* (St. John's Wort) preparations via UPLC-qTOF-MS and chemometrics. *Planta Med.* 78, 488-496.

Farag, M.A., Mahrous, E.A., Lübken, T., Porzel, A., Wessjohann, L., **2014**. Classification of commercial cultivars of *Humulus lupulus* L. (hop) by chemometric pixel analysis of two dimensional nuclear magnetic resonance spectra. *Metabolomics* 10, 21-32.

Fobofou, S.A.T., Franke, K., Schmidt, J., Wessjohann, L., **2015a**. Chemical constituents of *Psorospermum densipunctatum* (Hypericaceae). *Biochem. Sys. Ecol.* 59, 174-176.

Fobofou, S.A.T., Franke, K., Sanna, G., Porzel, A., Bullita, E., La Colla, P., Wessjohann, L.A., **2015b**. Isolation and anticancer, anthelminthic, and antiviral (HIV) activity of acylphloroglucinols, and regioselective synthesis of empetrifranzinans from *H. roeperianum*. *Bioorg. Med. Chem.* 23, 6327-6334.

Fobofou, S.A.T. Franke, K., Arnold, N., Schmidt, J., Wabo, H.K., Tane, P., Wessjohann, L.A., **2014**. Rare biscoumarin derivatives and flavonoids from *Hypericum riparium*. *Phytochemistry* 105, 171-177.

Fobofou, S.A.T., Franke, K., Porzel, A., Brandt, W., Wessjohann, L.A., **2016a**. Tricyclic acylphloroglucinols from *Hypericum lanceolatum* and regioselective synthesis of selancins A and B. *J. Nat Prod.* 79, 743-753.

Fobofou, S.A.T., Harmon, C.R., Lonfouo, A.H., Franke, K., Wright, S.T., Wessjohann, L.A.., **2016b**. Prenylated phenyl polyketides and acylphloroglucinols from *Hypericum peplidifolium*. *Phytochemistry* 124, 108-113.

Harvey, A.L., **2008**. Natural products in drug discovery. *Drug Discov. Today* 13, 894-901.

Hou, Y., Braun, D.R., Michel, C.R., Klassen, J.L., Adnani, N., Wyche, T.P., Bugni, T.S., **2012**. Microbial strain prioritization using metabolomics tools for the discovery of natural products. *Anal. Chem.* 84, 4277-4288.

Huck, C., Abel, G., Popp, M., Bonn, G., **2006**. Comparative analysis of naphthodianthrone and phloroglucine derivatives in St. John's Wort extracts by near infrared spectroscopy, high-performance liquid chromatography and capillary electrophoresis. *Anal. Chim. Acta* 580, 223-230.

Kim, H.K., Choi, Y.H., Verpoorte, R., **2010**. NMR-based metabolomic analysis of plants. *Nat. Protoc.* 5, 536-549.

Lammerhofer, M., Weckwerth, W., **2013**. Metabolomics in practice: Successful strategies to generate and analyze metabolic data. Wiley VCH, Weinheim (Germany).

Macintyre, L., Zhang, T.,Viegelmann, C., Martinez, I.J.,Cheng, C., Dowdells, C., Abdelmohsen, U.R., Gernert, C., Hentschel, U., Edrada-Ebel, R., **2014**. Metabolomic tools for secondary metabolite discovery from marine microbial symbionts. *Mar. Drugs* 12, 3416-3448.

Maggi, F., Ferretti, G., Pocceshi, N., Menghini, L., Ricciutelli, M., **2004**. Morphological, histochemical and phytochemical investigation of the genus *Hypericum* of the Central Italy. *Fitoterapia* 75, 702-711.

Mahrous, E. A.; Farag, M.A., **2015**. Two dimensional NMR spectroscopic approaches for exploring plant metabolomes: A review. *J. Adv. Res.* 6, 3-15.

Mitsopoulou, K.P., Vidali, V.P., Maranti, A., Couladouros, E.A., **2015**. Isolation and structure elucidation of hyperibine J [revised structure of adhyperfirin (7-deprenyl-13-methylhyperforin)]: synthesis of hyperibone J. *Eur. J. Org. Chem.* 2015, 287-290.

Newman, D.J., Cragg, G.M., **2012**. Natural products as sources of new drugs over the 30 years from 1981 to 2010. *J. Nat. Prod.* 75, 311-335.

Newman, D.J., **2008**. Natural products as leads to potential drugs: an old process or the new hope for drug discovery? *J. Med. Chem.* 51, 2589-2599.

Porzel, A., Farag, M.A., Mülbradt, J., Wessjohann, L.A., **2014**. Metabolite profiling and fingerprinting of *Hypericum* species: A comparison of MS and NMR. *Metabolomics* 10, 574-588.

Raskin, I., Ribnicky, D.M., Komarnytsky, S., Ilic, N., Poulev, A., Borisjuk, N., Brinker, A., Moreno, D.A., Ripoll, C., Yakoby, N., O'Neal, J.M., Cornwell, T., Pastor, I., Fridlender, B., **2002**. Plants and human health in the twenty-first century. *Trends Biotechnol.* 20, 522-531.

Rasmussen, B., Cloarec, O., Tang, H.R., Staerk, D., Jaroszewski, J.W., **2006**. Multivariate analysis of integrated and full-resolution ^{1}H-NMR spectral data from complex pharmaceutical preparations: St. John's Wort. *Planta Med.* 72, 556-563.

Samat, N., Tan, P.J., Shaari, K., Abas, F., Lee, H.B., **2014**. Prioritization of natural extracts by LC-MS-PCA for the identification of new photosensitizers for photodynamic therapy. *Anal. Chem.* 86, 1324-1331.

Schmidt, B., Jaroszewski, J.W., Bro, R., Writt, M., Staerk, D., **2008**. Combining PARAFAC analysis of HPLC-PDA profiles and structural characterization using HPLC-PDA-SPE-NMR-MS experiments: commercial preparations of St. John's Wort. *Anal. Chem.* 80, 1978-1987.

Tanaka, N., Otani, M., Kashiwada, Y., Takaishi, Y., Shibazaki, A., Gonoi, T., Shiro, M., Kobayashi, J., **2010**. Petiolins J-M, prenylated acylphloroglucinols from *Hypericum pseudopetiolatum var. kiusianum*. *Bioorg. Med. Chem. Lett.* 20, 4451-4455.

Tautenhahn, R., Patti, G.J., Rinehart, D., Siuzdak, G., **2012**. XCMS Online: a web-based platform to process untargeted metabolomic data. *Anal. Chem.* 84, 5035-5039.

Tolonen, A., Hohtola, A., Jalonen, J., **2003**. Fast high-performance liquid chromatographic analysis of naphthodianthrones and phloroglucinols from *Hypericum perforatum* extracts. *Phytochem. Anal.* 14, 306-309.

Wessjohann, L.A., **2014**. Reverse metabolomics-Metabolomics in drug discovery: Connecting metabolomic profiles with phylogenetic, medicinal and flavoring properties. *Metabolomics & Systems Biol.* 4, 70.

Wessjohann, L.A., Ruijter, E., Garcia-Rivera, D., Brandt, W., **2005**. What can a chemist learn from nature's macrocycles? — A brief, conceptual view. *Mol. Diversity* 9, 171-186.

Wang, K., Wang, Y.Y., Gao, X., Chen, X.Q., Peng, L.Y., Li. Y., Xu, G., Zhao, Q.S., **2012**. Polycyclic polyprenylated acylphloroglucinols and cytotoxic constituents of *Hypericum androsaemum*. *Chem. Biodivers.* 9, 1213-1220.

Xu, G., Kan, W.L.T., Zhou, Y., Song, J.Z., Hang, Q.B., Qiao, C.F., Cho, C.H., Rudd, J. A., Lin, G., Xu, H.X., **2010**. Cytotoxic acylphloroglucinol derivatives from the twigs of *Garcinia cowa*. *J. Nat. Prod.* 73, 104-108.

Yuliana, N.D., Khatib, A., Choi, Y.H., Verpoorte, R., **2011**. Metabolomics for bioactivity assessment of natural products. *Phytother. Res.* 25, 157-169.

Chapter 3

Tricyclic acylphloroglucinols from *Hypericum lanceolatum* and regioselective synthesis of selancins A and B

Graphical abstract*
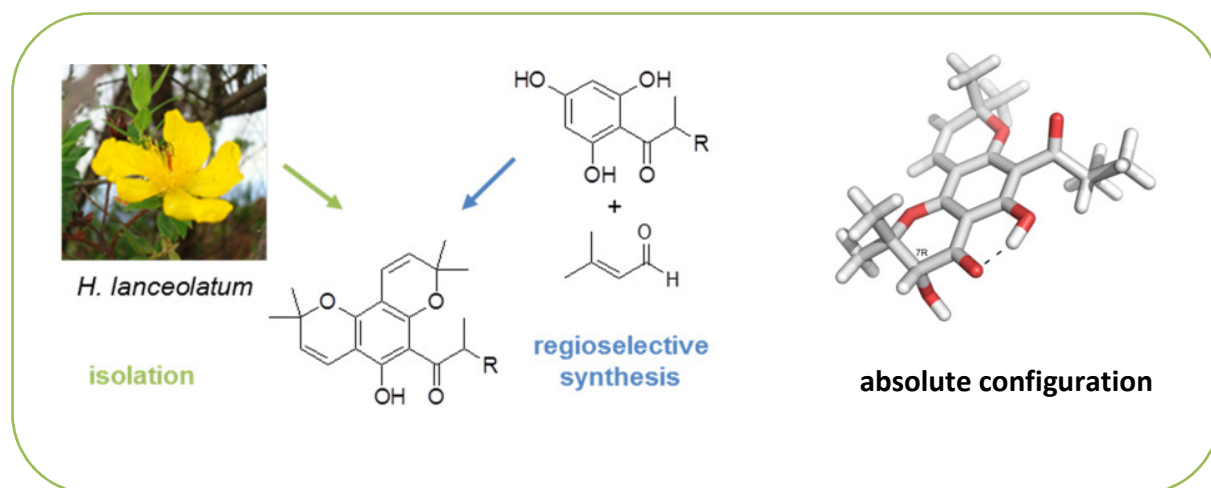
Highlights

- 11 new acylphloroglucinol derivatives were isolated from the leaves of *H. lanceolatum*

- Two unprecedented skeletons

- The known 3-*O*-geranylemodin is reported from the genus *Hypericum* for the first time

- The new compounds selancins A and B were synthesized regioselectively

- ^{1}H NMR profiles guided fractionation for new compounds discovery

Abstract

The chemical investigation of the chloroform extract of *Hypericum lanceolatum* Lam. guided by ^{1}H NMR, ESI-MS, and TLC profiles led to the isolation of 11 new tricyclic acylphloroglucinol derivatives, named selancins A-I (**3.1-3.9**) and hyperselancins A-B (**3.10-3.11**), along with the known compound 3-*O*-geranylemodin (**3.12**) which is described for a *Hypericum* species for the first time. Compounds **3.8** and **3.9** are the first examples of natural products with a 6-acyl-2,2-dimethylchroman-4-one core fused with a dimethylpyran unit. The new compounds **3.1-3.9** are rare acylphloroglucinol derivatives with two fused dimethylpyran units. Compounds **3.10-3.11** are derivatives of polycyclic polyprenylated acylphloroglucinols related to hyperforin, the active component of St. John's wort. Their structures were elucidated by UV, IR, extensive 1D and 2D NMR experiments, HR-ESI-MS, and comparison with the literature data. The absolute configurations of **3.5**, **3.8**, **3.10**, and **3.11** were determined by comparing experimental and calculated electronic circular dichroism (ECD) spectra. Compounds **3.1** and **3.2** were synthetized regioselectively in two steps. The cytotoxicity of the crude extract (88% growth inhibition at 50 μg/mL) and of compounds **3.1-3.6, 3.8**, **3.9**, and **3.12** (no significant growth inhibition up to a concentration of 10 mM) against colon (HT-29) and prostate (PC-3) cancer cell lines was determined. No anthelmintic or antiviral (HIV) activity was observed for the crude extract.

Keywords: Hypericaceae, Hyperselancins, prenylated and polycyclic compounds, natural products, chiroptical studies, ^{1}H NMR guided isolation.

3.1. Introduction

The great scientific interest and economic value of *Hypericum perforatum* (St. John's Wort), a medicinal herb mostly used for the treatment of mild to moderate depression, entailed the investigation of bioactive metabolites from other *Hypericum* species (Porzel *et al*., 2014; Fobofou *et al*., 2014). The most common secondary metabolites found within the genus *Hypericum* include phloroglucinols, xanthones, naphthodianthrones, flavonoids, and coumarins (Farag and Wessjohann, 2012; Athanasas *et al*., 2004; Crockett *et al*., 2008; Shui *et al*., 2012; Tanaka *et al*., 2009; Hecka *et al*., 2009; Kusari *et al*., 2008, Ang'edu *et al*., 1999). Acylphloroglucinols, of which hyperforin from *H. perforatum* is an outstanding example, are among the most relevant bioactive compounds isolated from *Hypericum* (Uwamorin and Nakada, 2013; Liu *et al*., 2013; Grey *et al*., 2007). Their structures and biological activities have attracted much attention in the medicinal and synthesis chemistry fields since the isolation of hyperforin in 1975 (Liu *et al*., 2013). They possess, among others, cytotoxic, antidepressant, antibacterial, and anti-inflammatory activities (Crockett *et al*., 2008; Shui *et al*., 2012; Liu *et al*., 2013; Verotta, 2003). The phloroglucinol core (1,3,5-trihydroxybenzene) of these compounds is often substituted by prenyl or geranyl moieties that are susceptible to cyclization and oxidation processes affording bi- or tricyclic derivatives as well as complex cage compounds (Athanasas *et al*., 2004; Beerhues, 2006; Liu *et al*., 2013). Recently, a revised structure for adhyperfirin with a *C*-methylated phloroglucinol core, named hyperpolyphyllirin from *H. polyphyllum*, was reported (Porzel *et al*., 2014).

Hypericum lanceolatum Lam. (Hypericaceae) has been prioritized for chemical investigation as part of a metabolomics driven isolation project aiming to study and compare the metabolomes, biosynthesis, and biological activities of prenylated aromatics and to find new or potential lead compounds from plants including various *Hypericum* species and accessions (Fobofou *et al*., 2014; Porzel *et al*., 2014; Farag and Wessjohann, 2012; Heinke *et al*., 2012; Heinke *et al*., 2013). *H. lanceolatum* is a medicinal plant occurring in the mountainous region of West Cameroon (Central Africa). Previous studies on this plant revealed the presence of xanthones, a polyprenylated phloroglucinol (isogarcinol), and terpenoids (Wabo *et al*., 2012). In Cameroonian traditional medicine, *Hypericum* plants are multipurpose remedies commonly used for the treatment of tumors, skin infections, epilepsies, infertility, venereal diseases, gastrointestinal disorders, intestinal worms, and viral diseases (Fobofou *et al*., 2014; Wabo *et al*., 2012; Zofou *et al*., 2011). Recently, the first isolation and structural elucidation of biscoumarins from Cameroonian *H. riparium* were reported (Fobofou *et al*., 2014). The aim of the present study was

to isolate and characterize the chemical constituents of *H. lanceolatum* and evaluate their biological activities.

3.2. Results and discussion

ESI-MS, TLC, and particularly ^{1}H NMR guided fractionation of the chloroform extract of the leaves of *H. lanceolatum* led to the isolation of 11 new acylphloroglucinol derivatives **3.1-3.11**, and the known compound, 3-*O*-geranylemodin (**3.12**). The characteristic deshielded proton signals around δ_H 9-14 in the ^{1}H NMR spectrum of acylphloroglucinols are caused by the presence of a free hydroxy group hydrogen bonded to the carbonyl group of the acyl moiety. This feature is readily visible in metabolite profiles of fractions and can be used for ^{1}H NMR-guided isolation to reduce replication (Schmidt *et al.*, 2012). The new compounds were trivially named selancins A-I (**3.1-3.9**) and hyperselancins A-B (**3.10-3.11**). The assigned compound names are based on the Cameroonian word "*Se*" which is used for *Hypericum* in the local language of Mbouda and also means "God" in the Bamendjida language. "Lancin" is derived from the source plant species *H. lanceolatum*, whose leaves are lanceolated.

The molecular formula of **3.1** was established as $C_{20}H_{24}O_4$ from the ^{13}C NMR and HR-ESI-FTMS that shows the deprotonated molecule ion at *m/z* 327.1601 [M-H]⁻, corresponding to nine indices of hydrogen deficiency. The NMR data (Tables 3.1 and 3.2) are similar to those of octandrenolone, a tricyclic acetophloroglucinol derivative, isolated from *Melicope erromangensis* (Rutaceae), bearing two non-symmetrical fused 2,2-dimethyl-2*H*-pyran rings (Winkelmann *et al.*, 2001; Muyard *et al.*, 1996). The main difference between the two compounds is that the acyl side chain in **3.1** is a 2-methylpropanoyl moiety while an acetyl group is present in octandrenolone (Muyard *et al.*, 1996). The characteristic signals of the 2-methylpropanoyl group are observed in the ^{1}H NMR spectrum as one methine septet at δ_H 3.84 (1H, *sept*, *J* = 6.6 Hz, H-2´) and two equivalent methyl groups at δ_H 1.19 (6H, *d*, *J* = 6.6 Hz, Me-3´/Me-4´). The structure assigned to compound **3.1** (Figure 3.1) was confirmed based on HMBC correlations from 9-OH to C-10, C-9, and C-8a; from H-8 to C-9, C-8a, C-4b, and C-6; from H-7 to C-8a, C-6, and C-13/C-14; from H-4 to C-10a, C-4b, C-4a, C-2, from H-3 to C- 4a, C-2, and C-11/C-12; and from H₃-3´/H₃-4´ to C-1´ and C-2´ as well as from H-2´ to C-1´ and C-3´/C-4´. The COSY spectrum reveals three spin systems (H-7/H-8, H-3/H-4, and H-2´/Me-3´/Me-4´) whereas five cross-peaks are displayed in the ROESY spectrum (H-7/H-8, H-3/H-4, H-2´/Me-3´/Me-4´, H-7/Me-13/Me-14, and H-3/Me-11/Me-12). The structure of compound **3.1**, selancin A (**3.1**), was therefore unambiguously defined as 1-(5-hydroxy-2,2,8,8-tetramethyl-2*H*,8*H*-pyrano[2,3-*f*]chromen-6-yl)-2-methylpropan-1-one.

A difference of 14 atomic mass units between **3.1** ($C_{20}H_{24}O_4$) and **3.2** ($C_{21}H_{26}O_4$) was derived from MS and NMR data. A comparison of the 1D and 2D NMR data of **3.2** with those of **3.1** show that the structural differences are restricted to the acyl side chain (Tables 3.1 and 3.2). HMBC correlations of Me-4´ with C-3´ (δ_C 26.8) and C-2´ (δ_C 46.0) and HMBC correlations of Me-5´ with C-1´ (δ_C 210.5) as well as with C-3´ and C-4´ clearly showed the replacement of the 2-methylpropanoyl substituent in **3.1** by a 2-methylbutanoyl side chain in **3.2**. Hence, the structure of compound **3.2** (Figure 3.1), selancin B (**3.2**), was elucidated as 1-(5-hydroxy-2,2,8,8-tetramethyl-2*H*,8*H*-pyrano[2,3-*f*]chromen-6-yl)-2-methylbutan-1-one.

The regioselective total synthesis of compounds **3.1** and **3.2** (racemic) was performed in two efficient steps (Scheme 3.1) starting with phloroglucinol. The synthetic routes afforded only one regiomer each (**3.1** and **3.2**) in 80 and 85% yield, respectively. The synthesis strategy involved Friedel-Craft acylation of phloroglucinol followed by an ethylenediamine diacetate-catalyzed (EDDA) double condensation of acylphloroglucinols to 3-methyl-2-butenal. The NMR and MS data of synthetic compounds **3.1** and **3.2** (racemic) are identical to those of natural selancin A (**3.1**) and selancin B (**3.2**) isolated from the leaves of *H. lanceolatum*. In order to assign the C-2´ absolute configuration of **3.2**, the sign of its optical rotation was compared with that of synthetic compound (*S*)-**3.2**, synthetized from (+)-(*S*)-2-methylbutanoic acid (Scheme 3.2). The specific rotations of (*S*)-**3.2** and **3.2** were found to be $[\alpha]^{25}_D$ +2 (*c* 0.24, CHCl$_3$) and $[\alpha]^{26}_D$ +13 (*c* 0.22, CHCl$_3$), respectively. This, supported by matching the experimental electronic circular dichroism (ECD) spectra of natural compound **3.2** and synthetic (*S*)-**3.2** (Figure S48, Supporting Information), confirms the (2´*S*)-configuration of the natural product **3.2**.

A variation of 18 atomic mass units (addition of H_2O) between **3.1** ($C_{20}H_{24}O_4$) and **3.3** ($C_{20}H_{26}O_5$) was derived from MS analysis. This difference was explained by the ^{1}H NMR spectrum (Table 3.1) which shows the replacement of the two doublets (H-3 and H-4) of a 2,2-dimethyl-2*H*-pyran moiety in **3.1** by the three signals (δ_H 3.81, *dd*, *J* = 5.8, 5.3, H-3; δ_H 2.85, *dd*, *J* = 17.1, 5.3, H-4a; and δ_H 2.60, *dd*, *J* = 17.1, 5.8, H-4b) of a 3-hydroxy-2,2-dimethyldihydropyran moiety in **3.3** (Lu *et al.,* 2008). The connection of the 3-hydroxy-2,2-dimethyldihydropyran moiety via C-4-C-4a was evident from HMBC correlations of H-4a/H-4b to C-10a, C-4b, C-4a, C-3, C-2 as well as from H-3 to C-4a, C-11, and C-12. ROESY interactions were observed between H-3/Me-11/Me-12 and H-4a/Me-11 as well as a weak association between H-4b/Me-12. The ROESY interaction between H-3/Me-11/Me-12 and the coupling constant of H-3 (δ_H 3.81, *dd*, *J* = 5.8 and 5.3 Hz) required 3-OH to be axial. However, it is not possible to determine the C-3 absolute configuration based on the axial orientation of 3-OH. On the basis of the above spectroscopic

evidence the structure of **3.3**, selancin C (**3.3**), was defined as 1-(5,9-dihydroxy-2,2,8,8-tetramethyl-9,10-dihydro-2*H*,8*H*-pyrano[2,3-*f*]chromen-6-yl)-2-methylpropan-1-one.

Figure 3.1. Chemical structures of compounds **3.1**-**3.12**.
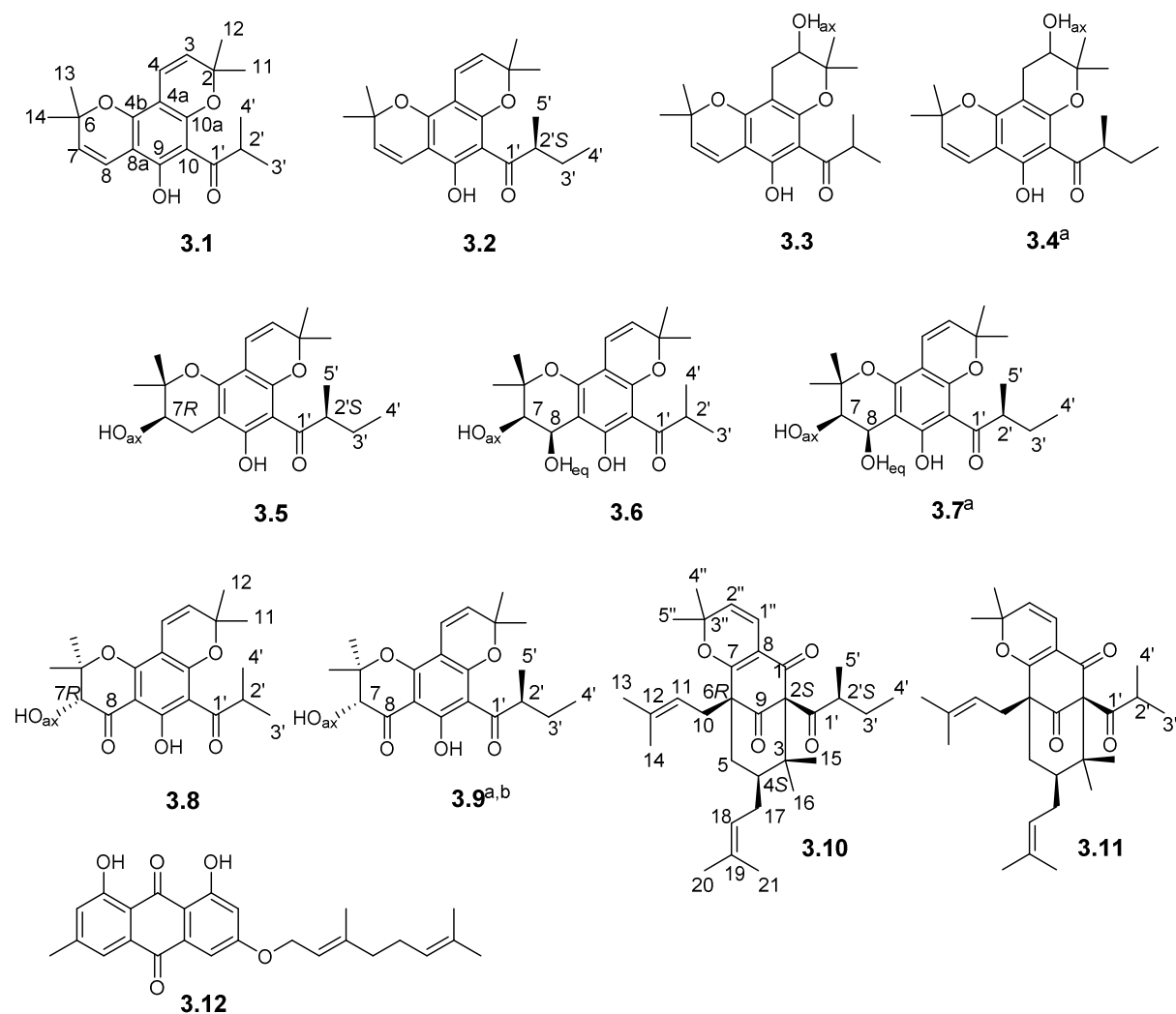
[a] (2´*S*) configuration tentatively assigned as in **3.2** due to the same biosynthetic origin (see Supporting Information).
[b] (7*R*) configuration tentatively assigned as in **3.8**.
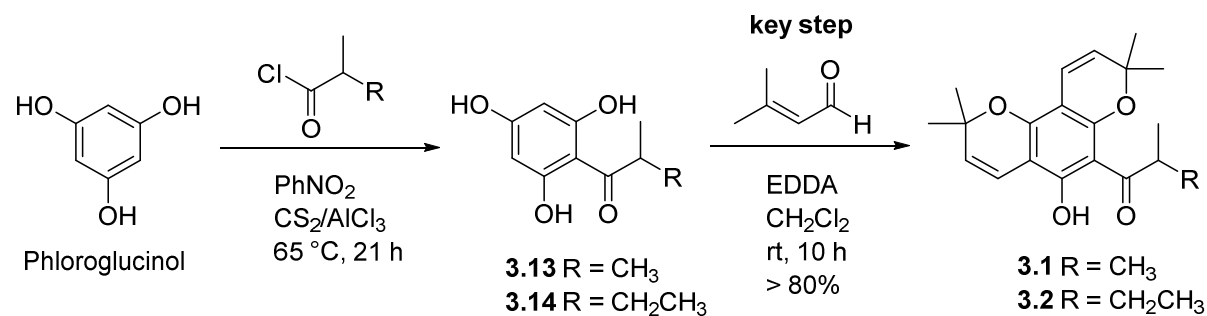
Scheme 3.1. Regioselective synthesis of acylphloroglucinol derivatives **3.1** and **3.2**.
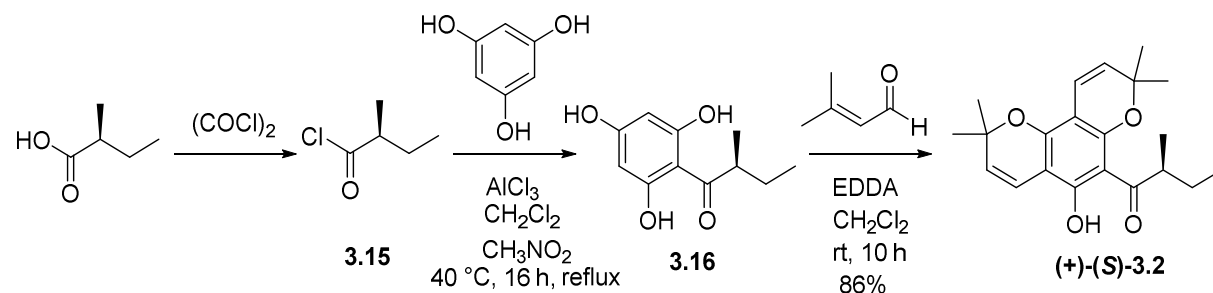
Scheme 3.2. Total synthesis of (+)-(*S*)-**3.2**.

The HR-ESI-FTMS data of compound **3.4** exhibits the deprotonated molecule at *m/z* 359.1864 [M-H]⁻, corresponding to the molecular formula $C_{21}H_{28}O_5$, which was also derived from ^{13}C NMR analysis. The 1D and 2D NMR data resemble those of selancin C (**3.3**), except in the acyl side chain. The difference of 14 mass units in compound **3.4** is attributed to a methylene group (δ_C 26.8, δ_H 1.85 *m*/1.41 *m*, 1H each) in the acyl side chain, which implies the replacement of the 2-methylpropanoyl unit of **3.3** by a 2-methylbutanoyl moiety in **3.4** (Tables 3.1 and 3.2) (Schmidt *et al*., 2012). Thus, the structure of compound **3.4**, selancin D (**3.4**), was identified as 1-(5,9-dihydroxy-2,2,8,8-tetramethyl-9,10-dihydro-2*H*,8*H*-pyrano[2,3-*f*]chromen-6-yl)-2-methylbutan-1-one. Compounds **3.3** and **3.4** are, therefore, 3-hydroxylated derivatives of **3.1** and **3.2**, respectively (Scheme S1, Supporting Information). Based on this consideration, the C-2′ absolute configuration of **3.4** was tentatively assigned to be *S* as in **3.2**.

Compound **3.5**, which has a molecular formula of $C_{21}H_{28}O_5$ as determined from HR-ESI-FTMS and ^{13}C NMR data, is a regiomer of **3.4**. They differ in the position of the 2,2-dimethyl-2*H*-pyran and 3-hydroxy-2,2-dimethyldihydropyran moieties as shown by 1D (Tables 3.1 and 3.2) and 2D NMR data. As for **3.3** and **3.4**, the ^1H NMR data (Table 3.1) of **3.5** show three characteristic signals (δ_H 3.80, *t*, *J* = 5.3, H-7; δ_H 2.87, *dd*, *J* = 17.1, 5.3, H-8a; and δ_H 2.65, *dd*, *J* =17.1, 5.3, H-8b) for a 3-hydroxy-2,2-dimethyldihydropyran moiety in addition to signals of a hydrogen-bonded hydroxy group (δ_H 14.30, *s*), a 2,2-dimethyl-2*H*-pyran and a 2-methylbutanoyl group. The position of the OH group at C-7 was supported by HMBC cross peaks from Me-13 (respectively, Me-14) to C-6, C-7, and C-14 (respectively, C-13). The key HMBC correlations from 9-OH to C-8a; from H-7 to C-8a; and from H-8a/H-8b to C-9, C-8a, C-4b, and C-7 established the connection of the 3-hydroxy-2,2-dimethyldihydropyran moiety via C-8-C-8a-C-4b on the phloroglucinol core. The linkage of the 2,2-dimethyl-2*H*-pyran moiety via C-4-C-4a-C-10a was indicated by the HMBC correlations from H-4 to C-10a, C-4b, C-2 as well as from H-3 to C-4a, and C-2. The 2-methylbutanoyl residue containing the carbonyl group hydrogen-bonded to the hydoxy group at C-9 was, therefore, deduced to be linked at C-10.

Table 3.1. ^{1}H NMR data [δ, *multiplicity, J* (Hz)] for compounds **3.1-3.9** (400 MHz, CDCl$_3$).

position	3.1	3.2	3.3	3.4	3.5	3.6	3.7	3.8	3.9
3	5.43, *d* (10.1)	5.44, *d* (9.7)	3.81, *dd* (5.8, 5.3)	3.80, *m*	5.41, *d* (10.1)	5.46, *d* (10.1)	5.46, *d* (10.1)	5.55, *d* (10.1)	5.55, *d* (10.1)
4	6.59, *d* (10.1)	6.60, *d* (9.7)	2.85, *dd* (17.1, 5.3); 2.60, *dd* (17.1, 5.8)	2.76, *dd* (17.1, 5.3); 2.60, *dd* (17.1, 5.3)	6.60, *d* (10.1)	6.43, *d* (10.1)	6.43, *d* (10.1)	6.55, *d* (10.1)	6.55, *d* (10.1)
7	5.46, *d* (10.1)	5.46, *d* (9.7)	5.43, *d* (10.1)	5.43, *d* (10.1)	3.80, *t* (5.3)	5.09, *d* (3.1)	5.09, *d* (3.1)	4.85, *s*	4.85, *s*
8	6.66, *d* (10.1)	6.66, *d* (9.7)	6.66 *d* (10.1)	6.67, *d* (10.1)	2.87, *dd* (17.1, 5.3); 2.65, *dd* (17.1, 5.3)	5.83, *d* (3.1)	5.83, *d* (3.1)		
11	1.49, *s*	1.49, *s*	1.39, *s*	1.39, *s*	1.48, *s*	1.53, *s*	1.53, *s*	1.59, *s*	1.59, *s*
12	1.49, *s*	1.50, *s*	1.40, *s*	1.40, *s*	1.48, *s*	1.51, *s*	1.51, *s*	1.57, *s*	1.58, *s*
13	1.44, *s*	1.44, *s*	1.43, *s*	1.43, *s*	1.38, *s*	1.44, *s*	1.44, *s*	1.39, *s*	1.39, *s*
14	1.44, *s*	1.44, *s*	1.43, *s*	1.43, *s*	1.33, *s*	1.12, *s*	1.12, *s*	1.30, *s*	1.30, *s*
2´	3.84, *sept* (6.6)	3.74, *sext* (7.0)	3.81, *sept* (6.8)	3.72, *sext* (7.0)	3.77, *sext* (7.0)	3.82, *sept* (6.6)	3.72, *sext* (6.6)	3.76, *sept* (7.0)	3.64, *sext* (6.6)
3´	1.19, *d* (6.6)	1.86, *m*; 1.40, *m*	1.17, *d* (6.8)	1.85, *m*; 1.41, *m*	1.86, *m*; 1.40, *m*	1.19, *d* (6.6)	1.86, *m*; 1.41, *m*	1.21, *d* (7.0)	1.86, *m*; 1.44, *m*
4´	1.19, *d* (6.6)	0.91, *t* (7.5)	1.17, *d* (6.8)	0.91, *t* (7.5)	0.91, *t* (7.5)	1.19, *d* (6.6)	0.92, *t* (7.5)	1.21, *d* (7.0)	0.93, *t* (7.0)
5´		1.16, *d* (7.0)		1.15, *d* (7.0)	1.16, *d* (7.0)		1.17, *d* (6.6)		1.19, *d* (6.6)
7-OH						8.30, *s*	8.30, *s*	8.98, *s*	8.97, *s*
8-OH						9.10, *s*	9.10, *s*		
9-OH	14.13, *s*	14.18, *s*	14.13, *s*	14.16, *s*	14.30, *s*	14.70, *s*	14.75, *s*	15.31, *s*	15.35, *s*

Table 3.2. ^{13}C NMR data (100 MHz, CDCl$_3$) for compounds **3.1-3.9**[a].

carbon	3.1	3.2	3.3	3.4	3.5	3.6	3.7	3.8	3.9
2	78.2, C	78.2, C	78.5, C	78.5, C	77.7, C	79.3, C	79.4, C	81.1, C	81.0, C
3	124.5, CH	124.6, CH	68.7, CH	68.7, CH	124.3, CH	125.0, CH	125.0, CH	125.1, CH	125.1, CH
4	116.5, CH	116.6, CH	26.8, CH$_2$	25.7, CH$_2$	116.8, CH	115.8, CH	115.8, CH	114.4, CH	114.5, CH
4a	102.1, C	102.2, C	98.1, C	98.1, C	102.2, C	98.2, C	98.3, C	98.2, C	98.3, C
4b	154.8, C	154.8, C	157.5, C	157.5, C	154.3, C	163.3, C	163.3, C	172.0, C	171.9, C
6	78.1, C	78.1, C	78.1, C	78.1, C	78.4, C	82.3, C	82.3, C	83.4, C	83.4, C
7	125.3, CH	125.3, CH	125.0, CH	125.0, CH	69.1, CH	91.9, CH	91.9, CH	88.8, CH	88.8, CH
8	116.3, CH	116.3, CH	116.3, CH	116.3, CH	25.6, CH$_2$	84.7, CH	84.8, CH	193.7, C	193.7, C
8a	102.5, C	102.5, C	102.6, C	102.6, C	99.6, C	102.2, C	103.8, C	104.1, C	104.2, C
9	161.1, C	161.1, C	160.6, C	160.5, C	164.3, C	163.4, C	163.3, C	165.6, C	165.6, C
10	104.6, C	105.2, C	104.6, C	105.2, C	105.9, C	105.3, C	106.4, C	105.3, C	105.8, C
10a	156.0, C	156.1, C	155.1, C	155.1, C	154.4, C	159.0, C	159.0, C	163.3, C	163.3, C
11	27.9, CH$_3$	27.8, CH$_3$	24.8, CH$_3$	24.8, CH$_3$	27.7, CH$_3$	28.2, CH$_3$	28.2, CH$_3$	28.5, CH$_3$	28.5, CH$_3$
12	27.9, CH$_3$	27.8, CH$_3$	21.7, CH$_3$	21.8, CH$_3$	27.8, CH$_3$	27.9, CH$_3$	27.8, CH$_3$	28.5, CH$_3$	28.4, CH$_3$
13	28.4, CH$_3$	28.4, CH$_3$	28.5, CH$_3$	28.5, CH$_3$	24.9, CH$_3$	21.3, CH$_3$	21.3, CH$_3$	21.9, CH$_3$	21.9, CH$_3$
14	28.4, CH$_3$	28.4, CH$_3$	28.6, CH$_3$	28.6, CH$_3$	22.1, CH$_3$	19.1, CH$_3$	19.1, CH$_3$	19.6, CH$_3$	19.6, CH$_3$
1´	210.7, C	210.5, C	210.4, C	210.3, C	210.5, C	210.9, C	210.8, C	211.0, C	210.9, C
2´	39.3, CH	46.0, CH	39.4, CH	46.1, CH	45.9, CH	39.2, CH	46.0, CH	39.6, CH	46.3, CH
3´	19.4, CH$_3$	26.8, CH$_2$	19.4, CH$_3$	26.8, CH$_2$	26.8, CH$_2$	19.3, CH$_3$	26.7, CH$_2$	19.2, CH$_3$	26.6, CH$_2$
4´	19.4, CH$_3$	11.9, CH$_3$	19.5, CH$_3$	11.9, CH$_3$	12.0, CH$_3$	19.4, CH$_3$	11.9, CH$_3$	19.2, CH$_3$	11.9, CH$_3$
5´	16.9, CH$_3$	16.9, CH$_3$	16.9, CH$_3$	16.9, CH$_3$	16.9, CH$_3$		16.8, CH$_3$		16.7, CH$_3$

[a]Assignment aided by 1D- and 2D-NMR data including HMBC, HSQC, and DEPT.

Further HMBC correlations were detected from 9-OH to C-9 and C-10, and from H-8a/H-8b to C-6. ROESY interactions were observed between H-7/Me-13/Me-14, which required 7-OH to be axial. On the basis of the above spectroscopic evidence the structure of **3.5**, selancin E (**3.5**), was defined as 1-(3,5-dihydroxy-2,2,8,8-tetramethyl-3,4-dihydro-2*H*,8*H*-pyrano[2,3-*f*]chromen-6-yl)-2-methylbutan-1-one. The absolute configuration of selancin E (**3.5**) was investigated by comparing its experimental and calculated ECD spectra. The calculations indicated that compound **3.5** has a 7*R* configuration with axial orientation of the 7-OH group (Figures 3.2 and S39, Supporting Information). However, it was not possible to unambiguously distinguish between (7*R*, 2´*S*) and (7*R*, 2´*R*) absolute configurations based on calculated data. Compared to the experimental data the (7*R*, 2´*S*) diastereoisomer exhibits a slightly better similarity factor (0.8963 at 24 nm shift) than the (7*R*, 2´*R*) epimer (0.8580 at 23 nm shift, Figure S39). Likewise, previously reported acylphloroglucinols as well as compound **3.2** possess the *S*-configuration at C-2´ (Shui *et al*., 2012; Xu *et al*., 2015). Therefore, the 2´*S* configuration (Figure 3.1) was tentatively assigned for **3.5**.

3.5
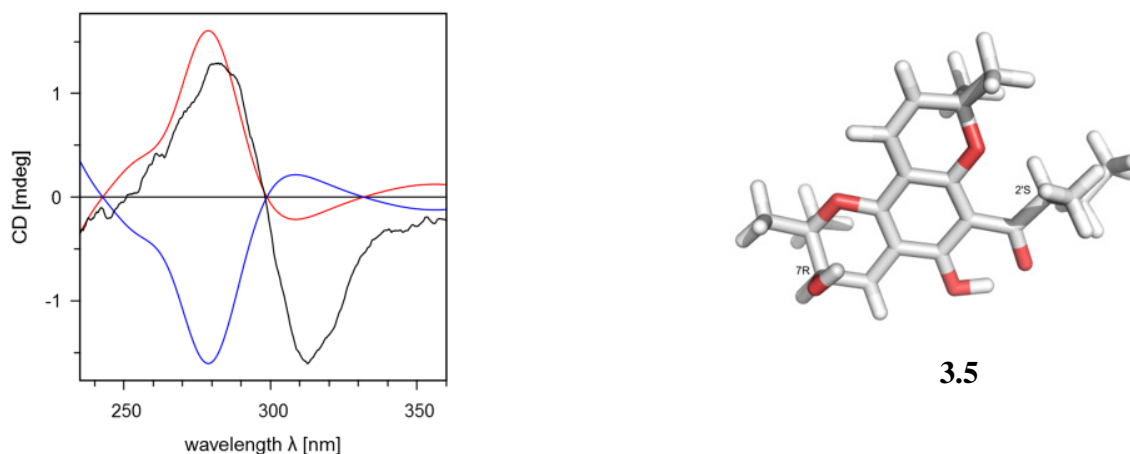
Figure 3.2. ECD spectra (7*R*, 2´*S*: red, 7*S*, 2´*R*: blue) of **3.5** in comparison to the experimental one (black). Similarity factor of 0.8963 at 24 nm shift.

The molecular formula of selancin F (**3.6**, $C_{20}H_{26}O_6$), as determined by HR-ESI-FTMS and ^{13}C NMR data, differs from that of selancin A (**3.1**, $C_{20}H_{24}O_4$) by the addition of two hydroxy groups. The NMR data of **3.1** and **3.6** are similar, except that signals of one of the two 2,2-dimethyl-2*H*-pyran moieties in **3.1** are substituted by those of a 3,4-dioxygenated dimethylchromane moiety (Tables 3.1 and 3.2; Figure 3.1) (Parsons *et al*., 1994; Jang *et al*., 2003). The ^1H NMR data (Table 3.1) of **3.6** shows signals of three hydroxy groups. The chemical shifts at δ_H 5.83 (*d*, *J* = 3.1 Hz; δ_C 84.7, C-8) and 5.09 (*d*, *J* = 3.1 Hz; δ_C 91.9, C-7) are assigned to the 3,4-dioxygenated dimethylchromane unit (Parsons *et al*., 1994; Jang *et al*., 2003). The 2,2-dimethyl-2*H*-pyran

58

moiety of **3.6** was connected via C-4-C-4a-C-10a as revealed by HMBC correlations from H-4 to C-10a, C-4b, C-4a, and C-2. The connection of the dioxygenated dimethylchromane moiety via C-8-C-8a-C-4b was consequently derived from 2D NMR data analysis. Further HMBC correlations were observed from 9-OH to C-10, C-9, and C-8a; from Me-14 to C-7, C-6, and C-13; as well as from Me-13 to C-7, C-6, and C-14. The relative configuration depicted in Figure 3.1 was established by 1D and 2D NMR. The ROESY correlations observed between H-8/Me-14 and H-7/Me-13/Me-14 suggest H-7 and Me-13 to be equatorial while H-8 and Me-14 are axially oriented. These observations, in addition to the ROESY correlation observed between H-7/H-8 and the small coupling constant ($^3J_{\text{H7-H8}}$ = 3.1 Hz), required H-7 and H-8 to be *cis* oriented. Compound **3.6**, selancin F (**3.6**), was therefore characterized as 1-(-3*R**,*4*S**,5-trihydroxy-2,2,8,8-tetramethyl-3,4-dihydro-2*H*,8*H*-pyrano[2,3-*f*]chromen-6-yl)-2-methylpropan-1-one.

Although selancin G (**3.7**, $C_{21}H_{28}O_6$) was not of good purity and rapidly decomposed, its ^1H and ^{13}C NMR signals could be readily assigned (Tables 3.1 and 3.2). The MS and NMR data resemble those of selancin F (**3.6**, $C_{20}H_{26}O_6$). A variation of 14 atomic mass units as determined from the HR-MS data is due to the replacement of a 2-methylpropanoyl unit by a 2-methylbutanoyl moiety (Tables 3.1 and 3.2). The chemical shifts and coupling constants of H-7 and H-8 are the same as in **3.6**, which implies the same relative configuration. The 2´*S* configuration was tentatively assigned for **3.7** as in **3.2** and previously reported acylphloroglucinols (Shui *et al*., 2012; Xu *et al*., 2015). Compound **3.7** was therefore assigned the structure 1-(-3*R**,*4*S**,5-trihydroxy-2,2,8,8-tetramethyl-3,4-dihydro-2*H*,8*H*-pyrano[2,3-*f*]chromen-6-yl)-2*S*-methylbutan-1-one.

The molecular formulas of compounds **3.8** and **3.9** were determined as $C_{20}H_{24}O_6$ and $C_{21}H_{26}O_6$ based on their negative ion HR-ESI-FTMS data, which reveal the [M-H]$^-$ ion peaks at *m/z* 359.1573 and 373.1729, respectively. These MS observations were supported by NMR data. Compounds **3.8** and **3.9** differ only in the acyl side chain as established by NMR and MS data. Compound **3.8** is similar to **3.6** except that C-8 (δ_C 193.7) is oxidized to a carbonyl group in **3.8** (Feng *et al*., 2010), as revealed by key HMBC correlations from H-7 (δ_H 4.85, *s*) to C-8, C-6, and C-13/C-14, as well as from Me-14 (respectively, Me-13) to C-7 (δ_C 88.8), C-6 (δ_C 83.4), and C-13 (respectively, C-14). The ROESY spectrum suggests H-7 to be equatorial oriented because it exhibits interactions with both Me-13 and Me-14 thus placing the 7-OH group axial. The absolute configuration of **3.8** was determined by comparing its experimental and calculated ECD spectra (Figures 3.3 and S40, Supporting Information). The calculations clearly indicated that compound **3.8** has a 7*R* configuration with axial orientation of the 7-OH group. The energetically preferred conformation is shown in Figure S40 (Supporting Information). Calculated spectra with equatorial

orientation of the 7-OH group do not fit with the experimental spectrum. On the basis of spectroscopic data, the structure of **3.8** (Figure 3.1), selancin I (**3.8**), was thus identified as 3*R*,5-dihydroxy-2,2,8,8-tetramethyl-6-(2-methylpropanoyl)-2,3-dihydro-4*H*,8*H*-pyrano[2,3-*f*]chromen-4-one. Similarly, compound **3.9**, selancin I (**3.9**), is 3*R*,5-dihydroxy-2,2,8,8-tetramethyl-6-(2*S*-methylbutanoyl)-2,3-dihydro-4*H*,8*H*-pyrano[2,3-*f*]chromen-4-one. (7*R*, 2´*S*) absolute configuration was tentatively assigned for **3.9** in comparison to its potential biosynthetic precursor (2´*S*)-**3.2** and its analog (7*R*)-**3.8** (Scheme S1, Supporting Information) (Shui *et al*., 2012; Xu *et al*., 2015).

The absolute configurations of **3.3**, **3.4**, and **3.9** were not determined since no reasonable conclusions could be drawn solely from ECD data. However, it can be presumed that they maintain the same configurations like their structural analogs **3.2**, **3.5**, or **3.8** due to the proposed biogenetic relationship (Scheme S1, Supporting Information). These compounds were not in sufficient quantities for further purification or chemical derivatization.

3.8a
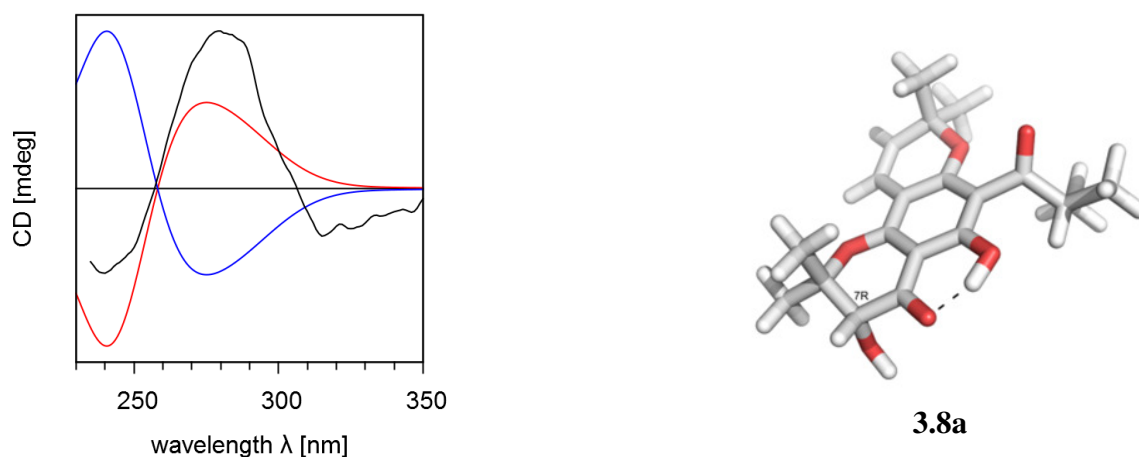
Figure 3.3: The Boltzmann weighted ECD spectra of **3.8** (7*R*: red, 7*S*: blue) in comparison to the experimental one (black). Similarity factor 0.9174 with a shift of -8 nm. Weighting factors see Fig. S40: **3.8a** (48.1 %), **3.8b** (38.2 %), and **3.8c** (13.7 %).

Hyperselancin A (**3.10**) has the molecular formula $C_{31}H_{44}O_4$ based on the HR-ESI-FTMS (*m/z* 481.3303, [M+H]$^+$) and ^{13}C NMR data. The assignment of carbon and proton signals of this compound was based on 1D and 2D NMR data, including DEPT, HSQC, HMBC, COSY, and ROESY. The ^1H NMR data (Table 3.3) of **3.10** indicate signals of four olefinic protons including two doublets of a 2,2-dimethyl-2*H*-pyran moiety at δ_H 6.49 (1H, *d*, *J* = 10.1 Hz, H-1´´) and 5.38 (1H, *d*, *J* = 10.1 Hz, H-2´´) as well as two triplets at δ_H 4.99 (1H, *t*, *J* = 6.6 Hz, H-11) and δ_H 4.92 (1H, *t*, *J* = 6.6 Hz, H-18) consistent with two prenyl units (Winkelmann *et al*., 2001; Wang *et al*.,

2012). It also indicates signals of six methyls at oxygenated and non-oxygenated sp^3 C-atoms and the four methyl groups of the two prenyl chains. The ^{13}C NMR data of **3.10** (Table 3.3) exhibit 31 carbon signals, including characteristic signals of a polyprenylated polycyclic acylphloglucinol (PPAP) containing a bicyclo[3.3.1]nonane-2,4,9-trione skeleton with two non-conjugated carbonyl groups (δ_C 208.6, C-1´; 206.8, C-9), one enolized keto group (δ_C 188.8, C-1; 114.1, C-8; 171.7, C-7), three quaternary carbons (δ_C 81.2, C-2; 55.1, C-6; 48.2, C-3), one methine (δ_C 44.7, C-4), one methylene (δ_C 38.4, C-5), and two methyl groups at C-3 (δ_C 26.5, C-16; 22.1, C-15) (Liu *et al.*, 2013; Winkelmann *et al.*, 2001; Wang *et al.*, 2012). Signals of the 2-methylbutanoyl moiety of PPAP-type compounds (δ_H 0.83, 3H, *t*, *J* = 7.5 Hz, Me-4´; 1.02, 3H, *d*, *J* = 6.1 Hz, Me-5´; 1.94 *m*/1.32 *m*, 1H each, diastereotopic C-3´ protons; 1.84, 1H, *m*, H-2´) are also displayed in the ^{1}H NMR spectrum of **3.10** (Table 3.3) (Liu *et al.*, 2013; Winkelmann *et al.*, 2001; Wang *et al.*, 2012). The COSY spectrum of **3.10** displays proton spin systems of H-1´´/H-2´´, H$_2$-10/H-11, H-18/H-17a/H-17b/H-4/H-5a, and H$_3$-5´/H-2´/H-3´a/H-3´b/H$_3$-4´. Inspection of the HMBC spectrum of **3.10** permitted the unambiguous placement of each substituent on the core structure. ROESY correlations were observed between H-17b/H-3´b, H-17b/H-5a, H-5a-H$_2$-10, and H-17a/Me-15. In addition to the COSY data, HMBC correlations from H-10 to C-6, C-7, C-9, C-11, and C-12, from H-5a (δ_H 2.11) to C-4, C-6, C-7, C-9, and C-17; from H-5b (δ_H 2.06) to C-7, C-9, and C-17; from H-1´´ to C-7, and C-3´´ as well as from H-2´´ to C-8 and C-3´´ confirmed the position of the prenyl and 2,2-dimethyl-2*H*-pyran groups. HMBC correlations from Me-15/Me-16 to C-2 (δ_C 81.2, C), C-3 (δ_C 48.2, C), C-4 (δ_C 47.7, CH), and C-16/C-15 require Me-15/Me-16 at C-3. Me-5´ of the C-2 acyl chain correlates to C-1´, C-2´, and C-3´. The chemical shift of the highly deshielded and non-oxygenated quaternary carbon C-2 (δ_C 81.2) indicates that it is surrounded by three carbonyl groups as extensively reported for PPAP-type compounds (Liu *et al.*, 2013; Winkelmann *et al.*, 2001; Wang *et al.*, 2012). The connectivity inferred by the HMBC spectrum is compatible only with structure **3.10**. According to these NMR data, the structure of compound **3.10** resembles therefore androforin A, scrobiculatone A, and papuaforin C, which were previously isolated from Guttiferae plants (Winkelmann *et al.*, 2001; Wang *et al.*, 2012; Porto *et al.*, 2000). Owing to the rigid structure of the bridged ring system, the substituents at C-2 and C-6 must be *cis* oriented as extensively reported for PPAPs (Liu *et al.,* 2013; Winkelmann *et al.*, 2001; Xu *et al.*, 2010). The C-4 relative configuration of **3.10** was assessed by NMR analysis. ROESY correlations observed between H-17b/H-5a, H-5a/H$_2$-10, and H-17a/Me-15 indicated that CH$_2$-17, Me-15, and CH$_2$-10 are *ß*-oriented. The absolute configuration of compound **3.10** was determined by comparing its experimental and calculated ECD spectra. The results (Figure 3.4) suggest the configuration at the four stereogenic centers to be (2*S*, 4*S*, 6*R*, 2´*S*). The most stable conformer agrees with ROESY

analysis and literature evidence where the chemical shift of C-4 (δ_C 45-49) in PPAPs with an α-oriented H-4 can be readily distinguished from that of C-4 (δ_C 41-44) in PPAPs with a β-oriented H-4 (Wang *et al*., 2012; Porto *et al*., 2000; Xu *et al*., 2010). On the basis of the above data, the structure of compound **3.10**, hyperselancin A, was established as 2,2,7,7-tetramethyl-6*S*-(2*S*-methylbutanoyl)-8*S*,10*R*-bis(3-methylbut-2-enyl)-2,6,7,8,9,10-hexahydro-5*H*-6,10-methanocycloocta[*b*]pyran-5,11-dione.

Table 3.3. ^{13}C and ^{1}H NMR data [δ, *multiplicity*, *J* (Hz)] for compounds **3.10** and **3.11** (CDCl$_3$).[a]

position	3.10 δ_C	3.10 δ_H	3.11 δ_C	3.11 δ_H
1	188.8, C		187.6, C	
2	81.2, C		81.1, C	
3	48.2, C		48.0, C	
4	47.7, CH	1.36, *m*	47.7, CH	1.36, *m*
5	38.4, CH$_2$	2.11, *m*	38.1, CH$_2$	2.11, *m*
		2.06, *m*		2.06, *m*
6	55.1, C		55.0, C	
7	171.7, C		171.8, C	
8	114.1, C		114.2, C	
9	206.8, C		206.7, C	
10	30.5, CH$_2$	2.45, *d* (6.6)	30.5, CH$_2$	2.45, *d* (6.6)
11	119.7, CH	4.99, *t* (6.6)	119.7, CH	5.02, *t* (6.6)
12	133.6, C		133.5, C	
13	26.0, CH$_3$	1.65, *s*	25.9, CH$_3$	1.67, *s*
14	18.1, CH$_3$	1.69, *s*	18.1, CH$_3$	1.53, *s*
15	22.1, CH$_3$	1.32, *s*	22.1, CH$_3$	1.32, *s*
16	26.5, CH$_3$	1.19, *s*	26.5, CH$_3$	1.20, *s*
17	29.5, CH$_2$	2.10, *m*	29.4, CH$_2$	2.10, *m*
		1.87, *m*		1.87, *m*
18	125.0, CH	4.92, *t* (7.0)	125.0, CH	4.92, *t* (7.5)
19	132.1, C		132.1, C	
20	25.8, CH$_3$	1.65, *s*	25.8, CH$_3$	1.65, *s*
21	18.1, CH$_3$	1.53, *s*	18.1, CH$_3$	1.68, *s*
1´	208.6, C		208.9, C	
2´	48.9, CH	1.84, *m*	41.9, CH	2.15, *m*
3´	26.7, CH$_2$	1.94, *m*	21.7, CH$_3$	1.03, *d* (6.6)
		1.32, *m*		
4´	11.7, CH$_3$	0.83, *t* (7.5)	20.6, CH$_3$	1.14, *d* (6.6)
5´	18.0, CH$_3$	1.02, *d* (6.1)		
1´´	115.5, CH	6.49, *d* (10.1)	115.4, CH	6.49, *d* (10.1)
2´´	124.0, CH	5.38, *d* (10.1)	124.0, CH	5.38, *d* (10.1)
3´´	82.5, C		82.5, C	
4´´	29.3, CH$_3$	1.51, *s*	29.3, CH$_3$	1.51, *s*
5´´	28.2, CH$_3$	1.37, *s*	28.1, CH$_3$	1.36, *s*

[a]Assignment aided by 1D- and 2D-NMR data including HMBC, HSQC, and DEPT.
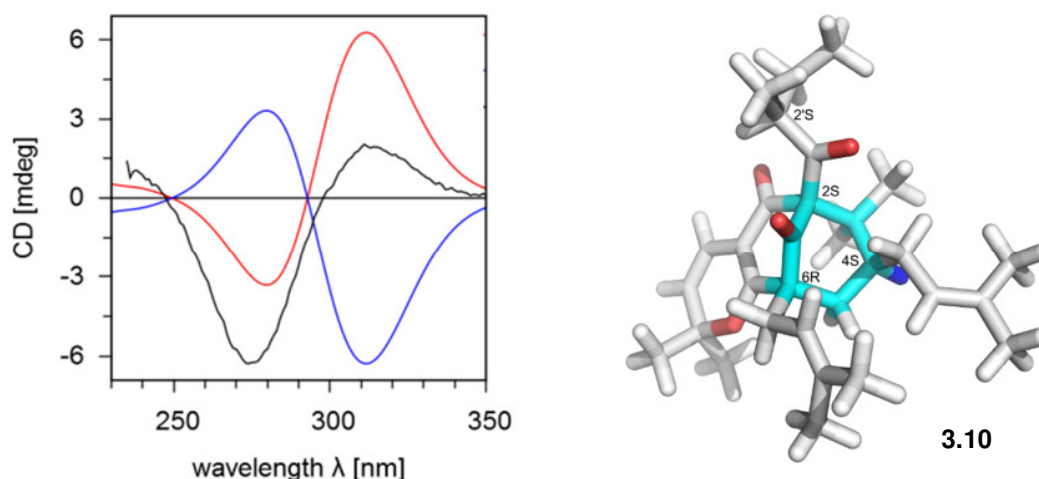
Figure 3.4. ECD spectra (red: calculated, black: experimental) and structure of **3.10** with 2*S*, 4*S*, 6*R*, 2´*S* configuration in boat conformation at 4*S* (cyan ring). Similarity factor = 0.9529, 9 nm shift. Blue spectrum: calculated spectrum with 2*R*, 4*R*, 6*S*, 2´*R* configuration.
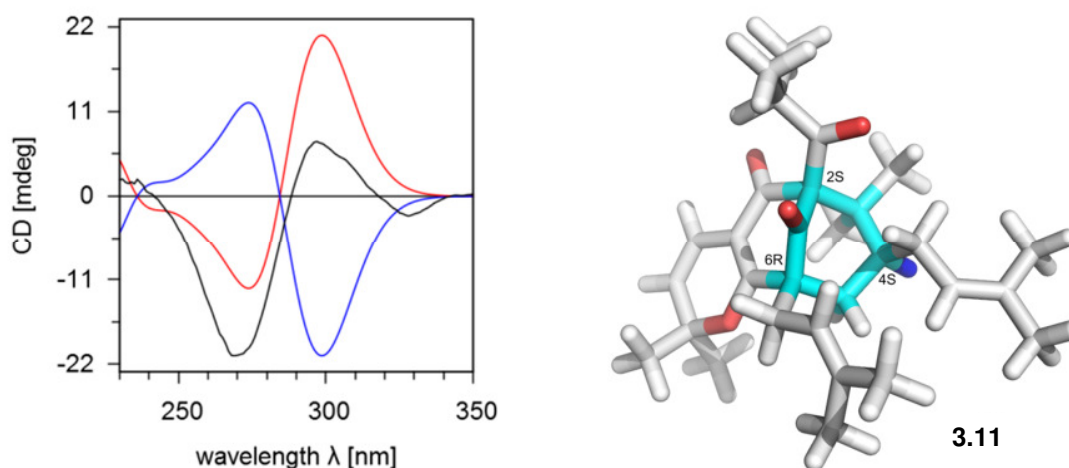
Figure 3.5: ECD spectra (red: calculated, black: experimental) and structure of compound **3.11** in 2*S*, 4*S*, 6*R* configuration with boat conformation (cyan ring). Similarity factor 0.9695, shift 2 nm. Blue spectrum: calculated spectrum with 2*R*, 4*R*, 6*S* configuration.

Hyperselancin B (**3.11**) has the molecular formula $C_{30}H_{42}O_4$ based on the HR-ESI-FTMS (*m/z* 467.3156, [M+H]$^+$) and ^{13}C NMR data. A difference of 14 atomic mass units is observed between **3.10** and **3.11**. The 1D and 2D NMR data of **3.11** indicates, that signals of the 2-methylbutanoyl group in **3.10** are replaced by signals of a 2-methylpropanoyl group (δ_H 1.14, 3H, *d*, *J* = 6.6 Hz, Me-4´; 1.03, 3H, *d*, *J* = 6.6 Hz, Me-3´; 2.15, 1H, *m*, H-2´) in **3.11**. This is confirmed by HMBC correlations from Me-4´/Me-3´ to C-1´ (δ_C 208.9). The ROESY data of **3.11** exhibits similar correlations as in **3.10**, which implies the same relative configuration. The absolute configuration of **3.11** was determined to be (2*S*, 4*S*, 6*R*) by comparing the experimental and calculated ECD

spectra (Figure 3.5). The results are consistent with NMR analysis. Analogues of hyperselancins A-B (PPAPs), including hyperforin (Porzel *et al.,* 2014), androforins (Wang *et al*., 2012), hypercohins (Liu *et al*., 2013), and papuaforins (Winkelmann *et al*., 2001), have been previously reported from *Hypericum* species.

The structure of 3-*O*-geranylemodin (**3.12**) was established by comparing its observed and reported spectroscopic data (Fobofou *et al*., 2015; Lenta *et al*., 2010). 3-*O*-geranylemodin is the first geranylated anthraquinone isolated from the genus *Hypericum*, although simple anthraquinones (e.g. emodin) and bisanthraquinones have been reported from this genus (Don *et al*., 2004; Wirz *et al*., 2000).

Compounds **3.1-3.9** belong to the rare group of acylphloroglucinol derivatives bearing two fused dimethylpyran units around a central benzene core. Only 18 compounds showing such structural features have been reported from nature, and they occur mainly in *Clusia ellipticifolia* (Clusiaceae or Guttiferae) and *Melicope erromangensis* (Rutaceae) (Muyard *et al*., 1996; Olivares *et al*., 1994). Some of the new derivatives reported here are partially oxidized. Compounds **3.8** and **3.9** are the first natural products that have a 6-acyl-2,2-dimethylchroman-4-one core fused with an additional dimethylpyran unit. Two key steps presumably govern the biosynthesis of compounds **3.1** and **3.2**: the diprenylation of the acylphloroglucinol core intermediate followed by cyclization. Compounds **3-9** might henceforth derive from **3.1** or **3.2** via oxidation processes (Jin *et al*., 2014; Schwinn *et al*., 2014; Bugos *et al*., 1998). The biosynthesis and diprenylation mechanisms of acylphloroglucinol intermediates have been disclosed (Zuurbier *et al*., 1998).

Considering that *Hypericum* species are used in the Cameroonian folk medicine for the treatment of various diseases, the crude MeOH extract obtained from the whole leaves powder of *H. lanceolatum* and compounds **3.1-3.6** and **3.8**, **3.9**, **3.12** were tested in a MT-4-cell-based assay against the human immunodeficiency virus type-1 (HIV-1), using efavirenz as reference inhibitor. The cytotoxicity against the MT4 cells was evaluated in parallel with the antiviral activity. As reported in Table 3.4, unfortunately, none of the tested compounds shows anti-HIV-1 activity, but they were also not cytotoxic against MT-4 cells. Compounds **3.1-3.6** and **3.8**, **3.9**, **3.12** were also screened for cytotoxicity against HT29 and PC3 cancer cell lines. Up to concentration of 10 μM no significant growth inhibition was determined. These compounds were also tested for antibacterial activity against representative human pathogenic Gram negative (*Escherichia coli)* and Gram positive (*Staphylococcus aureus*, and *Enterococcus faecalis*) bacteria. Ciprofloxacin

was used as reference compound. None of the tested compounds shows significant inhibitory activity (MIC > 1 mg/L).

Compounds **3.7** and especially **3.10** and **3.11** were not tested for any biological activity because they readily decomposed after isolation and spectroscopic measurements.

The anthelmintic activity of the crude methanolic extract against the model organism *Caenorhabditis elegans* was determined in a modified microtiter plate assay by enumeration of living and dead nematodes using a simple microscope view (Thomsen *et al*., 2012). At a test concentration of 500 µg/mL, the extract shows a nematode death percentage of only 2.52 ± 2.20 % (no activity).

Table 3.4. Cytotoxic and antiviral activity against MT-4 and HIV-1$_{IIIB}$, respectively, of the crude methanolic extract and of isolated compounds obtained from *Hypericum lanceolatum*.[a]

Hypericum lanceolatum	MT-4 CC_{50}[b]	HIV-1 $_{IIIB}$ EC_{50}[c]
Crude MeOH extract	17.0	>17.0
3.1	>100	>100
3.2	89.0	>89.0
3.3	38.5	>38.5
3.4	44.3	>44.3
3.5	45.8	>45.8
3.6	>100	>100
3.8	58.0	>58.0
3.9	53.0	>53.0
3.12	>100	>100
EFV	40.0	0.002

[a] Mean values of three independent determinations. Variation among duplicate samples was less than 15%.
[b] Compound concentration (µM) required to reduce the viability of mock-infected MT-4 cells by 50%, as determined by the MTT method.
[c] Compound concentration (µM) required to achieve 50% protection of MT-4 cells from the HIV-1 induced cytopathogeneticy, as determined by the MTT method.
EFV = reference anti-HIV-1 drug.

3.3. Experimental section

3.3.1. General experimental procedures

Optical rotations were measured using a JASCO P-2000 digital polarimeter. UV spectra were obtained on a JASCO V-560 UV/VIS spectrophotometer. ECD spectra in CHCl$_3$ were recorded using a JASCO J-815 spectrometer. IR (ATR) spectra were recorded using a Thermo Nicolet 5700 FT-IR spectrometer, in MeOH or CHCl$_3$. ^{1}H, ^{13}C NMR and 2D (gDQCOSY, ROESY (mixing time 200 ms), gHSQCAD, gHMBCAD) spectra were recorded on an Agilent DD2 400 NMR

spectrometer at 399.915 and 100.569 MHz, respectively. The ^{1}H NMR chemical shifts are referenced to internal TMS (δ_H 0.0); ^{13}C NMR chemical shifts are referenced to internal CDCl$_3$ (δ_C 77.0). The low resolution electrospray (ESI) mass spectra were performed on a SCIEX API-3200 instrument (Applied Biosystems, Concord, Ontario, Canada) combined with a HTC-XT autosampler (CTC Analytics, Zwingen, Switzerland). The samples were introduced via autosampler and loop injection. The HR-ESI mass spectra of compounds **3.1-3.12** as well as the corresponding MS^n measurements were obtained from an Orbitrap Elite mass spectrometer (Thermofisher Scientific, Bremen, Germany) equipped with an HESI electrospray ion source (spray voltage 4 kV; capillary temperature 275 °C, source heater temperature 40 °C; FTMS resolution 30.000). Nitrogen was used as sheath gas. The sample solutions were introduced continuously via a 500 μL-Hamilton syringe pump with a flow rate of 5 μL/min. The data were evaluated by the Xcalibur software 2.7 SP1.

HPLC was performed on a VARIAN PrepStar instrument equipped with a VARIAN ProStar PDA detector using a RP18 column (10 μm, 250 x 10 mm; flow rate 8.9 mL/min; detection 210 nm) and acetonitrile (HPLC grade, LiChrosolv, Merck KGaA, Germany) and double distilled water as solvents. Before HPLC separation samples were filtered using Solid Phase Extraction through a Chromabond C18ec SPE cartridge (Macherey-Nagel, 1 mL/100 mg). Column chromatography (CC) was run on silica gel (Merck, 63-200 and 40-63 μm) and Sephadex LH-20 (Fluka), while TLC was performed on precoated silica gel F$_{254}$ plates (Merck). Spots were visualized with a UV lamp at 254 and 366 nm or by spraying with vanillin-H$_2$SO$_4$-MeOH followed by heating at 100 °C.

3.3.2. Plant material

The leaves of *H. lanceolatum* Lam. were collected in August 2011 at Mount Bamboutos (Mbouda) in the West Region of Cameroon. The plant was identified by Mr. Nana Victor, botanist at the National Herbarium of Cameroon where a voucher specimen (No. 32356/HNC) is deposited.

3.3.3. Extraction and isolation

The air-dried and powdered leaves (750 g) of *H. lanceolatum* were sequentially and successively extracted with CHCl$_3$ (3 x 3 L) and MeOH (2 x 2 L) for one day under shaking to give the respective extracts, namely the CHCl$_3$ (68.82 g) and MeOH (15.63 g) extracts, after solvent evaporation under reduced pressure. For the evaluation of anthelmintic and cytotoxic activities, the whole powdered leaves (3 g) of *H. lanceolatum* were extracted in 80% MeOH (30

mL) under sonification for 30 minutes to afford a crude extract (140.2 mg) after filtration and solvent removal.

A portion of the CHCl$_3$ extract (42 g) was subjected to silica gel column flash chromatography, eluted with step gradients of *n*-hexane-EtOAc and EtOAc-MeOH to afford 23 fractions of 400 mL each, which were combined on the basis of their TLC profiles into seven main fractions (Fr. 1-Fr. 7). Fr. 1 (7.65 g) obtained from *n*-hexane-EtOAc (100:0 and 90:10) was further chromatographed on SiO$_2$ column, eluted with *n*-hexane-EtOAc to afford eight sub-factions (Fr.1$_1$-Fr. 1$_8$). Fr.1$_1$ (1.96 g, from *n*-hexane-EtOAc 90:10 and 80:20) also afforded eight sub-fractions (Fr.1$_{1a}$-Fr. 1$_{1h}$) after column chromatography (CC) on silica gel, eluted with step gradients of *n*-hexane-EtOAc (98:2, 95:5, 90:10, 0:100). Repeated chromatography of Fr.1$_{1a}$ (558 mg, obtained from *n*-hexane-EtOAc 98:2) on silica gel CC and preparative TLC, as well as final purification by reverse phase HPLC, eluted with H$_2$O-MeCN (30%→100% MeCN 0-20 min, 100% MeCN 20-25 min, 100%→30% MeCN 25-27 min, 30% MeCN 27-30 min) afforded compounds **3.1** (7.79 mg, t_R 6.43 min) and **3.2** (4.5 mg, t_R 7.25 min). Fr.1$_{1c}$ (151.4 mg), also obtained from *n*-hexane-EtOAc 98:2, was dissolved in THF and purified by semi-preparative HPLC, eluted with H$_2$O-MeCN (70→100% MeCN 0-20 min, 100% MeCN 20-25 min, 100→70% MeCN 25-27 min, 70→50% MeCN 27-30 min) to yield **3.6** (4.04 mg, t_R 9.08 min), **3.7** (2.9 mg, t_R 9.85 min), **3.8** (4.4 mg, t_R 9.34 min), **3.9** (1.8 mg, t_R 10.10 min), **3.10** (1.8 mg, t_R 17.42 min), **3.11** (1.78 mg, t_R 16.98 min), and **3.12** (2.2 mg, t_R 18.51 min). Fr. 2 (3.1 g) obtained from *n*-hexane-EtOAc (90:10 and 80:20) was further subjected on silica gel CC eluted with *n*-hexane containing increasing amounts of EtOAc to yield eight sub-fractions (Fr.2$_1$-Fr. 2$_8$). Fraction Fr. 2$_4$ (252.7 mg), obtained from *n*-hexane-EtOAc (80:20 and 70:30), was suspended in isopropyl alcohol, filtered by SPE and finally purified by semi-preparative HPLC, eluted with H$_2$O-MeCN (30%→100% MeCN 0-20 min, 100% MeCN 20-25 min, 100→30% MeCN 25-27 min, 30% MeCN 27-30 min) to afford compounds **3.3** (6.5 mg, t_R 3.88 min), **3.4** (3.5 mg, t_R 4.29 min), and **3.5** (2.6 mg, t_R 4.61 min).

Selancin A (**3.1**)*, 1-(5-hydroxy-2,2,8,8-tetramethyl-2H,8H-pyrano[2,3-f]chromen-6-yl)-2-methylpropan-1-one:* yellow oil; UV (CHCl$_3$) λ_{max} (log ε) 273 (4.49), 379 (3.38) nm; IR (ATR) υ_{max} (cm^{-1}) 3604, 2974, 2928, 2872, 1640, 1592, 1462, 1381, 1132, 997, 871, 709, 660; ^{1}H NMR data see Table 3.1; ^{13}C NMR data see Table 3.2; negative ion ESI-FTMS *m/z* 327.1601 [M-H]$^-$ (calcd for C$_{20}$H$_{23}$O$_4^-$, 327.1602).

Selancin B (**3.2**)*, 1-(5-hydroxy-2,2,8,8-tetramethyl-2H,8H-pyrano[2,3-f]chromen-6-yl)-2S-methylbutan-1-one:* yellow oil; [α]$^{26}_D$ +13 (*c* 0.2, CHCl$_3$); UV (CHCl$_3$) λ_{max} (log ε) 273 (4.47), 378

(3.37) nm; ECD (CDCl$_3$) Δε (nm) +1.8 (279) and -0.8 (317); IR (ATR) υ$_{max}$ (cm^{-1}) 3594, 2970, 2926, 2874, 1639, 1591, 1461, 1382, 1132, 880, 709, 660; ^{1}H NMR data see Table 3.1; ^{13}C NMR data see Table 3.2; negative ion ESI-FTMS *m/z* 341.1756 [M-H]$^-$ (calcd for C$_{21}$H$_{25}$O$_4^-$, 341.1758).

Selancin C (**3.3**)*, 1-(5,9-dihydroxy-2,2,8,8-tetramethyl-9,10-dihydro-2H,8H-pyrano[2,3-f]chromen-6-yl)-2-methylpropan-1-one:* yellow oil; [α]$^{25}_D$ +2 (*c* 0.3, CHCl$_3$); UV (CHCl$_3$) λ$_{max}$ (log ε) 279 (4.33), 354 (3.42) nm; ECD (CDCl$_3$) Δε (nm) +0.2 (293) and -0.04 (327); IR (ATR) υ$_{max}$ (cm^{-1}) 3444, 2975, 2929, 2872, 1634, 1594, 1424, 1381, 1125, 751, 717, 666; ^{1}H NMR data see Table 3.1; ^{13}C NMR data see Table 3.2; negative ion ESI-FTMS: [M-H]$^-$ at *m/z* 345.1712 (calcd for C$_{20}$H$_{25}$O$_5^-$, 345.1707).

Selancin D (**3.4**)*, 1-(5,9-dihydroxy-2,2,8,8-tetramethyl-9,10-dihydro-2H,8H-pyrano[2,3-f]chromen-6-yl)-2S-methylbutan-1-one:* yellow oil; [α]$^{25}_D$ +12 (*c* 0.3, CHCl$_3$); UV (CHCl$_3$) λ$_{max}$ (log ε) 279 (4.58), 357 (3.65) nm; ECD (CDCl$_3$) Δε (nm) +0.9 (292) and -0.6 (322); IR (ATR) υ$_{max}$ (cm^{-1}) 3444, 2972, 2929, 2874, 1613, 1594, 1423, 1379, 1123, 752, 718, 666; ^{1}H NMR data see Table 3.1; ^{13}C NMR data see Table 3.2; negative ion ESI-FTMS *m/z* 359.1867 [M-H]$^-$ (calcd for C$_{21}$H$_{27}$O$_5^-$, 359.1864).

Selancin E (**3.5**)*, 1-(3R,5-dihydroxy-2,2,8,8-tetramethyl-3,4-dihydro-2H,8H-pyrano[2,3-f]chromen-6-yl)-2S-methylbutan-1-one:* yellow oil; [α]$^{25}_D$ +7 (*c* 0.2, CHCl$_3$); UV (CHCl$_3$) λ$_{max}$ (log ε) 287 (5.04), 360 (4.12) nm; ECD (CDCl$_3$) Δε (nm) +0.6 (281) and -0.8 (313); IR (ATR) υ$_{max}$ (cm^{-1}) 3450, 2966, 2924, 2873, 1638, 1596, 1417, 1380, 1126, 754, 716, 666; ^{1}H NMR data see Table 3.1; ^{13}C NMR data see Table 3.2; negative ion ESI-FTMS *m/z* 359.1867 [M-H]$^-$ (calcd for C$_{21}$H$_{27}$O$_5^-$, 359.1864).

Selancin F (**3.6**)*, 1-(-3R*,4S*,5-trihydroxy-2,2,8,8-tetramethyl-3,4-dihydro-2H,8H-pyrano[2,3-f]chromen-6-yl)-2-methylpropan-1-one:* yellow oil; UV (CHCl$_3$), λ$_{max}$ (log ε) 269 (4.76), 279 (4.75) nm; IR (ATR) υ$_{max}$ (cm^{-1}) 3400, 2977, 2933, 2873, 1650, 1615, 1423, 1367, 1127, 1058, 749, 666; ^{1}H NMR data see Table 3.1; ^{13}C NMR data see Table 3.2; positive ion ESI-FTMS *m/z* 385.1625 [M+Na]$^+$ (calcd for C$_{20}$H$_{26}$O$_6$Na$^+$, 385.1622).

Selancin G (**3.7**)*, 1-(-3R*,4S*,5-trihydroxy-2,2,8,8-tetramethyl-3,4-dihydro-2H,8H-pyrano[2,3-f]chromen-6-yl)-2S-methylbutan-1-one:* yellow oil; ^{1}H NMR data see Table 3.1; ^{13}C NMR data see Table 3.2; positive ion ESI-FTMS *m/z* 399.1774 [M+Na]$^+$ (calcd for C$_{21}$H$_{28}$O$_6$Na$^+$, 399.1778). [α]$_D$, UV, and IR were not determined because of compound degradation.

Selancin H (**3.8**)*, 3R,5-dihydroxy-2,2,8,8-tetramethyl-6-(2-methylpropanoyl)-2,3-dihydro-4H,8H-pyrano[2,3-f]chromen-4-one:* yellow oil; $[\alpha]^{25}_D$ +1 (*c* 0.4, CHCl$_3$); UV (CHCl$_3$) λ_{max} (log ε) 265 (4.88), 357 (3.84) nm; ECD (CDCl$_3$) Δε (nm) +0.2 (279) and -0.03 (321); IR (ATR) υ_{max} (cm^{-1}) 3401, 2978, 2933, 2874, 1703, 1645, 1613, 1467, 1378, 1141, 1111, 747, 688, 666; ^{1}H NMR data see Table 3.1; ^{13}C NMR data see Table 3.2; negative ion ESI-FTMS *m/z* 359.1505 [M-H]$^-$ (calcd for C$_{20}$H$_{23}$O$_6^-$, 359.1500).

Selancin I (**3.9**)*, 3R,5-dihydroxy-2,2,8,8-tetramethyl-6-(2S-methylbutanoyl)-2,3-dihydro-4H,8H-pyrano[2,3-f]chromen-4-one:* yellow oil; $[\alpha]^{25}_D$ +10 (*c* 0.3, CHCl$_3$); UV (CHCl$_3$) λ_{max} (log ε) 266 (5.12), 357 (4.04) nm; ECD (CDCl$_3$) Δε (nm) +1.3 (271) and -0.7 (308); IR (ATR) υ_{max} (cm^{-1}) 3401, 2972, 2930, 2875, 1704, 1645, 1609, 1462, 1366, 1137, 1111, 749, 689, 667; ^{1}H NMR data see Table 3.1; ^{13}C NMR data see Table 3.2; negative ion ESI-FTMS *m/z* 373.1659 [M-H]$^-$ (calcd for C$_{21}$H$_{25}$O$_6^-$, 373.1657).

Hyperselancin A (**3.10**)*, 2,2,7,7-tetramethyl-6S-(2S-methylbutanoyl)-8S,10R-bis(3-methylbut-2-enyl)-2,6,7,8,9,10-hexahydro-5H-6,10-methanocycloocta[b]pyran-5,11-dione:* yellow oil; $[\alpha]^{25}_D$ -1 (*c* 0.3, CHCl$_3$); UV (CHCl$_3$) λ_{max} (log ε) 237 (4.65), 270 (4.63) nm; ECD (CDCl$_3$) Δε (nm) -3.6 (274) and +1.2 (311) cm^2 · mmol^{-1}; IR (ATR) υ_{max} (cm^{-1}) 2973, 2929, 1722, 1600, 1461, 1369, 1129, 751, 667; ^{1}H NMR and ^{13}C NMR data see Table 3.3; positive ion ESI-FTMS *m/z* 481.3303 [M+H]$^+$ (calcd for C$_{31}$H$_{45}$O$_4^+$, 481.3312).

Hyperselancin B (**3.11**)*, 2,2,7,7-tetramethyl-8S,10R-bis(3-methylbut-2-enyl)-6S-(2-methyl-propanoyl)-2,6,7,8,9,10-hexahydro-5H-6,10-methanocycloocta[b]pyran-5,11-dione:* yellow oil; $[\alpha]^{25}_D$ -9 (*c* 0.2, CHCl$_3$); UV (CHCl$_3$) λ_{max} (log ε) 235 (4.73), 271 (4.72) nm; ECD (CDCl$_3$) Δε (nm) +1.4 (269), 0.5 (298), and -0.2 (328); IR (ATR) υ_{max} (cm^{-1}) 2973, 2928, 1721, 1614, 1456, 1371, 1259, 1085, 752, 667; ^{1}H NMR and ^{13}C NMR data see Table 3.3; positive ion ESI-FTMS *m/z* 467.3147 [M+H]$^+$ (calcd for C$_{30}$H$_{43}$O$_4^+$, 467.3156).

3.4. Synthesis.

The synthetic procedure and spectroscopic data for compounds **3.13**, **3.14**, **3.15**, **3.16** and (+)-(*S*)-**3.2** are in the Supporting Information that can be found online at:

http://pubs.acs.org/doi/full/10.1021/acs.jnatprod.5b00673#showReferences

Synthesis of selancin A (3.1), 1-(5-hydroxy-2,2,8,8-tetramethyl-2*H*,8*H*-pyrano[2,3-*f*]chromen-6-yl)-2-methylpropan-1-one: Ethylene diamine diacetate (EDDA, 36 mg, 0.2 mmol) was added to a solution of 1-(2,4,6-trihydroxyphenyl)-2-methylpropanone (**3.13**, 196 mg, 1 mmol)

and 3-methyl-2-butenal (252 mg, 289 µL, 3.0 mmol) in CH_2Cl_2 (10 mL). The reaction mixture was stirred at room temperature for 10 h. After evaporation of the solvent under reduced pressure, the mixture was chromatographed through a silica gel column, eluted with *n*-hexane-EtOAc (95:5) to give selancin A (**3.1**) as yellow oil (80 %, 261 mg, 0.8 mmol, R_f = 0.5 in *n*-hexane:EtOAc (95:5)). ^{1}H NMR ($CDCl_3$) δ 14.14 (1H, *s*), 6.66 (1H, *d*, *J* = 10.1 Hz), 6.59 (1H, *d*, *J* = 10.1 Hz), 5.45 (1H, *d*, *J* = 10.1 Hz), 5.43 (1H, *d*, *J* = 10.1 Hz), 3.85 (1H, *sept*, *J* = 6.6 Hz), 1.49 (6H, *s*), 1.44 (6H, *s*), 1.19 (6H, *d*, *J* = 6.6 Hz); ^{13}C NMR ($CDCl_3$) δ 210.5, 161.1, 156.0, 154.8, 125.3, 124.5, 116.5, 116.3, 104.6, 102.5, 102.1, 78.2, 78.1, 39.3, 28.4, 27.9, 19.4; Positive ion ESI-FTMS: [M+H]$^+$ at *m/z* 329.1749 (calcd for $C_{20}H_{25}O_4^+$, 329.1747).

Synthesis of selancin B (3.2)*, 1-(5-hydroxy-2,2,8,8-tetramethyl-2*H*,8*H*-pyrano[2,3-*f*]chromen-6-yl)-2-methylbutan-1-one: EDDA (36 mg, 0.2 mmol) was added to a solution of 1-(2,4,6-trihydroxyphenyl)-2-methylbutanone (**3.14**, 210 mg, 1 mmol) and 3-methyl-2-butenal (252 mg, 289 µL, 3.0 mmol) in CH_2Cl_2 (10 mL). The reaction mixture was stirred at room temperature for 10 h. After removal of the solvent by evaporation under reduced pressure, the reaction mixture was chromatographed through a silica gel column, eluted with *n*-hexane-EtOAc (95:5) to give selancin B (**3.2**) as yellow oil (85 %, 290.1 mg, 0.85 mmol, R_f = 0.71 in *n*-hexane:EtOAc (95:5)). ^{1}H NMR ($CDCl_3$) δ 14.18 (1H, *s*), 6.66 (1H, *d*, *J* = 10.1 Hz,), 6.60 (1H, *d*, *J* = 10.1 Hz,), 5.45 (1H, *d*, *J* = 10.1 Hz), 5.44 (1H, *d*, *J* = 10.1 Hz), 3.74 (1H, *sext*, *J* = 6.6 Hz), 1.86 (1H, *m*), 1.50 (3H, *s*), 1.49 (3H, *s*), 1.44 (6H, *s*), 1.41 (1H, *m*), 1.17 (3H, *d*, *J* = 6.6 Hz), 0.91 (3H, *t*, *J* = 7.5 Hz); ^{13}C NMR ($CDCl_3$) δ 210.4, 161.1, 156.1, 154.7, 125.3, 124.6, 116.5, 116.3, 105.2, 102.5, 102.2, 78.2, 78.1, 46.0, 28.4, 28.3, 27.8, 26.8, 16.8, 11.9. Positive ion ESI-FTMS: [M+H]$^+$ at *m/z* 343.1907 (calcd for $C_{21}H_{27}O_4^+$, 343.1904).

3.5. Biological assays

Cell lines were purchased from American Type Culture Collection (ATCC). The absence of mycoplasma contamination was checked periodically by the Hoechst staining method. Cell lines supporting the multiplication HIV-1 virus were CD4+ human T-cells containing an integrated HTLV-1 genome (MT-4). IIIB laboratory strain of HIV-1 was obtained from the supernatant of the persistently infected H9/IIIB cells (NIH 1983).

3.5.1. Cytotoxicity assays against MT-4 cells

Exponentially growing MT-4 cells were seeded at an initial density of 1×10^5 cells/ml in 96-well plates in RPMI-1640 medium, supplemented with 10% fetal bovine serum (FBS), 100 units/mL penicillin G and 100 µg/mL streptomycin. Cell cultures were then incubated at 37 °C in

a humidified, 5% CO_2 atmosphere, in the absence or presence of serial dilutions of test compounds. Cell viability was determined after 96 hrs at 37 °C by the 3-(4,5-dimethylthiazol-2-yl)-2,5-diphenyl-tetrazolium bromide (MTT) method (Pauwels *et al.*, 1988).

3.5.2. Anti-HIV-1 assay

Sample's activity against HIV-1 was based on inhibition of virus-induced cytopathogenicity in MT-4 cell acutely infected with a multiplicity of infection (m.o.i.) of 0.01. Briefly, 50 µL of RPMI containing 1×10^4 MT-4 cells were added to each well of flat-bottom microtitre trays, containing 50 µL of RPMI with serial dilutions of test samples. Then, 20 µL of a HIV-1 suspension containing 100 $CCID_{50}$ were added. After 4-day incubation at 37 °C, cell viability was determined by the MTT method (Pauwels *et al.*, 1988).

3.5.3. Linear regression analysis

The extent of cell growth/viability and viral multiplication, at each drug concentration tested, was expressed as percentage of untreated controls. Concentrations resulting in 50% inhibition (CC_{50} or EC_{50}) were determined by linear regression analysis.

3.5.4. Antibacterial activity

The antibacterial activity of the selected compounds was evaluated on collection strains: *Escherichia coli* DSM 1103, *Staphylococcus aureus* DSM 2569, and *Enterococcus faecalis* DSM 2570. The antimicrobial activity was evaluated by determining the Minimum inhibitory concentration (MIC). MIC corresponds to the lowest concentration of an antibacterial compound that show complete growth inhibition. MIC was determined by the broth microdilution procedure according to the European Committee on Antimicrobial Susceptibility Testing (EUCAST 2003) (EUCAST, 2003). Ciprofloxacin was used as reference compound.

3.5.4.1. Antibacterial susceptibility testing procedure

Bacterial strains were grown on Tryptic soy agar (TSA) at 37 °C for 1 day. Cell suspensions of these recent cultures were prepared in sterile 0.85% saline solution by 4-5 colonies. The turbidity of the suspensions is adjusted to the McFarland 0.5 standard. Suspensions were diluted in cation-supplemented Mueller-Hinton broth to $3–7 \times 10^5$ CFU/ml. For each microorganism, 100 µl of the twofold serial dilutions of the antibacterial agents in cation-supplemented Mueller-Hinton broth and 100 µl of inoculum were added to each well of a microdilution plate. The concentration of each inoculum was confirmed by viable counts on Tryptic soy agar plates by plating the

appropriate dilution of the growth control well, immediately after inoculation, and incubating until visible growth. The inoculated plates were incubated at 37 °C in non-CO_2 incubator and in a humid atmosphere, and MICs were determined after 16-20 h. After agitation, plates were visually read with the aid of a reading mirror. MIC corresponds to the lowest compound concentration that show complete growth inhibition compared with the growth control.

3.5.5. Cytotoxicity assays against HT-29 and PC-3 cancer cells

This assay was performed for isolated compounds as we previously described (Fobofou *et al*., 2014).

3.5.6. Anthelmintic assays

This assay was performed as we previously described (Thomsen *et al*., 2012).

3.5.7. Computational methods. (See Supporting Information)

Appendix. Supporting Information

^{1}H and ^{13}C NMR spectra of isolated compounds **3.1**-**3.11** and synthetized compounds **3.1**, **3.2**, **3.13**, **3.14**, **3.16**, and (+)-(*S*)-**3.2**. Synthesis procedures of compounds **3.13**, **3.14**, **3.15**, **3.16**, and (+)-(*S*)-**3.2** and computational methods. This material is available free of charge via the Internet at: http://pubs.acs.org/doi/full/10.1021/acs.jnatprod.5b00673#showReferences

References

Ang'edu, C. A., Schmidt, J., Porzel, A., Gitu, P., Midiwo, J. O., Adam, G., **1999.** Coumarins from *Hypericum keniense* (Guttiferae). *Pharmazie* 54, 235-236.

Athanasas, K., Magiatis, P., Fokialakis, N., Skaltsounis, A.–L., Pratsinis, H., Kletsas, D., **2004**. Hyperjovinols A and B: Two new phloroglucinol derivatives from *Hypericum jovis* with antioxidant activity in cell cultures. *J. Nat. Prod.* 67, 973-977.

Beerhues, L., **2006**. Hyperforin. *Phytochemistry* 67, 2201-2207.

Bugos, R.C., Hieber, A.D., Yamamoto, H.Y., **1998**. Xanthophyll cycle enzymes are members of the lipocalin family, the first identified from plants. *J. Biol. Chem.* 273, 15321-15324.

Crockett, S.L., Wenzig, E.–M., Kunert, O., Bauer, R., **2008**. Anti-inflammatory phloroglucinol derivatives from *Hypericum empetrifolium. Phytochem. Lett.* 15, 37-43.

Don, M.J., Huang, Y.J., Huang, R.L., Lin, Y.L., **2004**. New phenolic principles from *Hypericum sampsonii. Chem. Pharm. Bull.* 52, 866-869.

European Committee on Antimicrobial Susceptibility Testing, **2003**. Determination of minimum inhibitory concentrations (MICs) of antibacterial agents by broth microdilution. EUCAST Discussion Document E. Def. 2003, 5.1. *Clin. Microbiol. Infect.* 9, 1–10.

Farag, M.A., Wessjohann, L.A., **2012**. Metabolome classification of commercial *Hypericum perforatum* (St. John's Wort) preparations via UPLC-qTOF-MS and chemometrics. *Planta Med.* 78, 488-496.

Feng, T., Wang, R.–R., Cai, X.–H., Zheng, Y.–T., Luo, X.–D., **2010**. Anti-human immunodeficiency virus-1 constituents of the bark of *Poncirus trifoliata*. *Chem. Pharm. Bull.* 58, 971-975.

Fobofou, S.A.T., Franke, K., Arnorld, N., Wabo, H.K., Tane, P., Wessjohann, L.A., **2014**. Rare biscoumarin derivatives and flavonoids from *Hypericum riparium*. *Phytochemistry* 105, 171-177.

Fobofou, S.A.T., Franke, K., Schmidt, J., Wessjohann, L., **2015**. Chemical constituents of *Psorospermum densipunctatum* (Hypericaceae). *Biochem. Syst. Ecol.* 59, 174-176.

Grey, C., Kyrylenko, S., Henning, L., Nguyen, L.H., Büttner, A., Pham, H.D., Giannis, A., **2007**. Phloroglucinol derivatives guttiferone G, aristoforin, and hyperforin: inhibitors of human sirtuins SIRT1 and SIRT2. *Angew. Chem. Int. Ed. Engl.* 46, 5219-5222.

Hecka, A., Maunit, B., Aubriet, F., Muller, J.F., **2009**. Study of active naphtodianthrone St John's wort compounds by electrospray ionization Fourier transform ion cyclotron resonance and multi-stage mass spectrometry in sustained off-resonance irradiation collision-induced dissociation and infrared multiphoton dissociation modes. *Rapid Commun. Mass Spectrom.* 23, 885-898.

Heinke, R., Arnold, N., Wessjohann, L., Schmidt, J., **2013**. Negative ion tandem mass spectrometry of prenylated fungal metabolites and their derivatives. *Anal. Bioanal. Chem.* 405, 177-189.

Heinke, R., Franke, K., Michels, K., Wessjohann, L., Ali, N.A.A., Schmidt, J., **2012**. Analysis of furanocoumarins from Yemenite *Dorstenia* species by liquid chromatography/electrospray tandem mass spectrometry. *J. Mass. Spectrom.* 47, 7-22.

Jang, D.S., Park, E.J., Kang, Y.–H., Hawthorne, M.E., Vigo, J.S., Graham, J.G., Cabieses, F., Fong, H.S., Mehta, R. G., Pezzuto, J.M., Kinghorn, A.D., **2003**. Potential cncer chemopreventive flavonoids from the stems of *Tephrosia toxicaria*. *J. Nat. Prod.* 66, 1166-1170.

Jin, M.L., Lee, D.Y., Um, Y., Lee, J.H., Park, C., Jetter, R., Kim, O.T., **2014**. Isolation and characterization of an oxidosqualene cyclase gene encoding a *β*-amyrin synthase involved in *Polygala tenuifolia* Willd. saponin biosynthesis. *Plant Cell Rep.* 33, 511-519.

Kusari, S., Lamshöft, M., Zühlke, S., Spiteller, M., **2008**. An endophytic fungus from *Hypericum perforatum* that produces hypericin. *J. Nat. Prod.* 71, 159-162.

Lenta, B.N., Devkota, K.P., Ngouela, S., Boyom, F.F., Naz, Q., Choudhary, M.I., Tsamo, E., Rosenthal, P.J., Sewald, N., **2008**. Anti-plasmodial and cholinesterase inhibiting activities of some constituents of *Psorospermum glaberrimum*. *Chem. Pharm. Bull*. 56, 222-226.

Liu, X., Yang, X.–W., Chen, C.–Q., Wu, C.–Y., Zhang, J.–J., Ma, J.–Z., Wang, H., Yang, L.–X., Xu, G., **2013**. Bioactive polyprenylated acylphloroglucinol derivatives from *Hypericum cohaerens*. *J. Nat. Prod*. 76, 1612-1618.

Liu, X., Yang, X.–W., Chen, C.–Q., Wu, C.–Y., Zhang, J.–J., Ma, J. .Z., Wang, H., Zhao, Q.–S., Yang, L.–X., **2013**. Hypercohones A–C, acylphloroglucinol derivatives with homo-adamantane cores from *Hypericum cohaerens*. *Nat. Prod. Bioprospect* 3, 233-237.

Lu, Y.-H., Wei, B.-L., Ko, H.-H., Lin, C.-N., **2008**. DNA strand-scission by phloroglucinols and lignans from heartwood of *Garcinia subelliptica* Merr. and Justicia plants. *Phytochemistry* 69, 225-233.

Muyard, F., Bissoue, A.N., Bevalot, F., Tillequin, F., Cabalion, P., Vaquette, J., **1996**. Acetophenones and other constituents from the roots of *Melicope erromangensis*. *Phytochemistry* 42, 1175-1179.

Olivares, E.M., Gonzales, J.G., Monache, F.D., **1994**. Benzophenones from *Clusia ellipticifolia*. *Phytochemistry* 36, 473-475.

Parsons, I.C., Gray, A.I., Hartley, T.G., Waterman, P.G., **1994**. Acetophenones and coumarins from stem bark and leaves of *Melicope stipitata*. *Phytochemistry* 37, 565-570.

Pauwels, R., Balzarini, J., Baba, M., Snoeck, D., Schols, D., Herdewijn, P., Desmyter, J., De Clercq, E., **1988**. Rapid and automated tetrazolium based colorimetric assay for the detection of anti-HIV compounds. *J. Virol. Methods* 20, 309–321.

Porto, A.L.M., Machado, S.M.F., Oliveira, C.M.A., Bittrich, V., Emaral, M.C.E., Marsaioli, A.J., **2000**. Polyisoprenylated benzophenones from *Clusia* floral resins. *Phytochemistry* 55, 755-768.

Porzel, A., Farag, M.A., Mülbradt, J., Wessjohann, L.A., **2014**. Metabolite profiling and fingerprinting of *Hypericum* species: A comparison of MS and NMR. *Metabolomics* 10, 574-588.

Schmidt, S., Jürgenliemk, G., Schmidt, T.J., Skaltsa, H., Heilmann, J., **2012**. Bi-, tri-, and polycyclic acylphloroglucinols from *Hypericum empetrifolium. J. Nat. Prod.* 75, 1697-1705.

Schwinn, K., Miosic, S., Davies, K., Thill, J., Gotame, T.P., Stich, K., Halbwirth, H., **2014**. The B-ring hydroxylation pattern of anthocyanins can be determined through activity of the flavonoid 3'-hydroxylase on leucoanthocyanidins. *Planta* 240, 1003-1010.

Shui, W.K.P., Rahman, M.M., Curry, J., Stapleton, P., Zloh, M., Malkinson, J.P., Gibbons, S.*,* **2012**. Antibacterial acylphloroglucinols from *Hypericum olympicum. J. Nat. Prod.* 75, 336-343.

Tanaka, N., Kashiwada, Y., Kim, S.–Y., Sekiya, M., Ikeshiro, Y., Takaishi, Y., **2009**. Xanthones from *Hypericum chinense* and their cytotoxicity evaluation. *Phytochemistry* 70, 1456-1461.

Thomsen, H., Reider, K., Franke, K., Wessjohann, L.A., Keiser, J., Dagne, E., Arnold, N., **2012**. Characterization of constituents and anthelmintic properties of *Hagenia abyssinica. Sci. Pharm.* 80, 433-446.

Uwamorin, M., Nakada, M., **2013**. Stereoselective total synthesis of (±)-hyperforin via intramolecular cyclopropanation. *Tetrahedron Lett.* 54, 2022-2025.

Verotta, L., **2003**. *Hypericum perforatum*, a source of neuroactive lead structures. *Curr. Top. Med. Chem.* 3, 187-201.

Wabo, H.K., Kowa, T.K., Lonfouo, A.H.N., Tchinda, A.T., Tane, P., Kikuchi, H., Frédérich, M., Oshima, Y., **2012**. Phenolic compounds and terpenoids from *Hypericum lanceolatum. Rec. Nat. Prod.* 6, 94-100.

Wang, K., Wang, Y.Y., Gao, X., Chen, X.Q., Peng, L.Y., Li. Y., Xu, G., Zhao, Q.S., **2012**. Polycyclic polyprenylated acylphloroglucinols and cytotoxic constituents of *Hypericum androsaemum. Chem. Biodivers.* 9, 1213-1220.

Winkelmann, K., Heilmann, J., Zerbe, O., Rali, T., Sticher, O., **2001**. New prenylated bi- and tricyclic phloroglucinol derivatives from *Hypericum papuanum. J. Nat. Prod.* 64, 701-706.

Wirz, A., Simmen, U., Heilmann, J., Calis, I., Meier, B., Sticher, O., **2000**. Bisanthraquinone glycosides of *Hypericum perforatum* with binding inhibition to CRH-1 receptors. *Phytochemistry* 55, 941-947.

Xu, G., Kan, W.L.T., Zhou, Y., Song, J.Z., Hang, Q.B., Qiao, C.F., Cho, C.H., Rudd, J.A., Lin, G., Xu, H.X., **2010**. Cytotoxic acylphloroglucinol derivatives from the twigs of *Garcinia cowa. J. Nat. Prod.* 73, 104-108.

Xu, W.-J., Zhu, M.-D., Wang, X.-B., Yang, M.-H., Luo, J., Kong, L.-Y., **2015**. Hypermongones A-J, rare methylated polycyclic prenylated acylphloroglucinols from the flowers of *Hypericum monogynum. J. Nat. Prod.* 78, 1093-1100.

Zofou, D., Kowa, T.K., Wabo, H.K., Ngemenya, M.N., Tane, P., Titanji, V.P.K., **2011**. *Hypericum lanceolatum* (Hypericaceae) as a potential source of new anti-malarial agents: a bioassay-guided fractionation of the stem bark. *Malar. J.* 10, 167. DOI: 10.1186/1475-2875-10-167.

Zuurbier, K.W.M., Fung, S.Y., Scheffer, J.J.C., Verpoorte, R., **1998**. In-vitro prenylation of aromatic intermediates in the biosynthesis of bitter acids in *humulus lupulus. Phytochemistry* 49, 2315-2322.

Chapter 4

Isolation and anticancer, antihelminthic, and antiviral (HIV) activity of acylphloroglucinols, and regioselective synthesis of empetrifranzinans from *Hypericum roeperianum*

Graphical abstract*
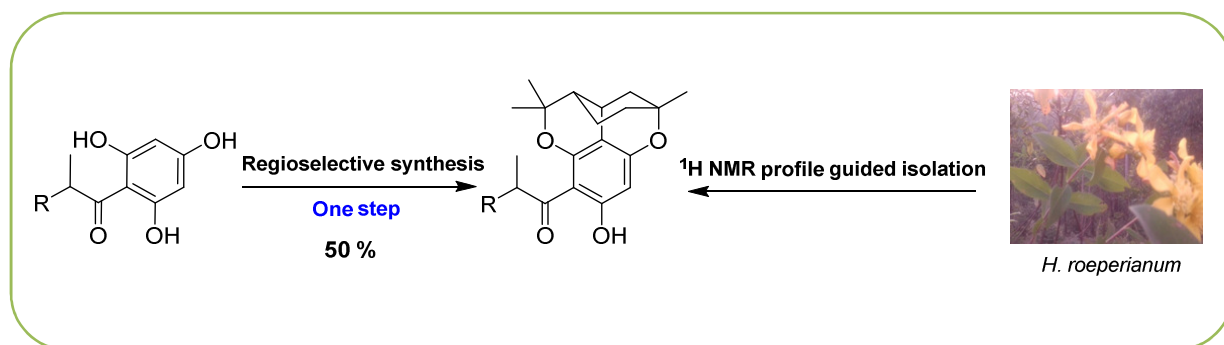
H. roeperianum

Highlights

- 10 acylphloroglucinols including 3 new natural products were isolated from *H. roeperianum* for the first time

- Empetrifranzinans A and C were synthesized regioselectively

- Significant anthelminthic activity was observed for the crude extract and compound **4.7**

- The structures of isolates were fully characterized by NMR and MS experiments

Abstract

From the ethno-medicinally used leaves of *Hypericum roeperianum* we isolated a new tricyclic acylphloroglucinol (**4.1**), a new tetracyclic acylphloroglucinol (**4.2**), and a new prenylated bicyclic acylphloroglucinol (**4.3**) together with four known prenylated (**4.4–4.7**) and three known tetracyclic acylphloroglucinol derivatives (**4.8–4.10**). Structure elucidation was based on UV, IR, $[\alpha]_D^{25}$, MS, 1D- and 2D-NMR experiments. Furthermore, empetrifranzinans A (**4.8**) and C (**4.9**) were synthesized regioselectively in only two steps. The isolated compounds were evaluated for their cytotoxicity against PC-3 and HT-29 cancer cell lines as well as antibacterial and anthelmintic activities. They were also tested in cell-based assays for cytotoxicity against MT-4 cells and for anti-HIV activity in infected MT-4 cells. Significant anthelmintic activity against *Caenorhabditis elegans* was exhibited by compound **4.7** (3-geranyl-1-(2′-methylbutanoyl)-phloroglucinol), which might provide a new lead.

Key words: Hypericaceae; *H. riparium*; Natural products; Madeleinol; ^{1}H NMR profile guided isolation; Acylphloroglucinol synthesis; Empetrifranzinans; Metabolic profiling.

76

4.1. Introduction

Plants of the genus *Hypericum* (Hypericaceae) are used worldwide as traditional medicine against a multitude of diseases. In China, *Hypericum sampsonii* Hance is used for the treatment of disorders such as backache, burns, diarrhea, snakebite, and swellings (Xia *et al*., 2007). *Hypericum laricifolium* Juss., with the common name 'Romerillo' has been used in traditional Ecuadorian medicine as a diuretic and for provoking menstruation (El-Seedi *et al*., 2003). In the folk medicine of Papua New Guinea, leaves of *Hypericum papuanum* Ridl. are applied to treat sores (Winkelmann *et al*., 2001). In Cameroonian traditional medicine, *Hypericum* plants are multipurpose remedies commonly used for the treatment of tumors, skin infections, epilepsy, infertility, venereal diseases, gastrointestinal disorders, intestinal worms, and viral diseases (Zofou *et al*., 2011; Wabo *et al*., 2012; Fobofou *et al*., 2014). In Turkey, *Hypericum empetrifolium* Willd. is used against kidney stones and gastric ulcers, in Greece as an anthelmintic and diuretic (Crockett *et al*., 2008). *Hypericum perforatum* L. (St. John's wort), the most popular species of the genus *Hypericum*, is well known in Europe and North America for the treatment of mild to moderate depression (Porzel *et al*., 2014; Farag and Wessjohann, 2012). It is believed that this multitude of biological effects occur through the action of various active compounds present in the plant (Verotta *et al*., 2003). Due to the great scientific interest and economic value associated with *H. perforatum*, many studies together with other species of the same genus have been carried out throughout the world (Porzel *et al*., 2014; Athanasas *et al*., 2004). The most common secondary metabolites found within the genus *Hypericum* include phloroglucinols, xanthones, naphthodianthrones, flavonoids, and coumarins (Farag and Wessjohann, 2012; Crockett *et al*., 2008; Porzel *et al*., 2014; Athanasas *et al*., 2004; Shui *et al*., 2012; Tanaka *et al*., 2009; Hecka *et al*., 2009, Ang'edu *et al*., 1999). Acylphloroglucinols, of which hyperforin from *H. perforatum* is an outstanding example, are among the most relevant bioactive compounds isolated from *Hypericum* (Uwamorin *et al*., 2013; Liu *et al*., 2013a). Their structures and biological activities have attracted wide attention in medicinal and synthetic chemistry fields since the isolation of hyperforin in 1975 (Liu *et al*., 2013a; Grey *et al*., 2007; Gartner *et al*., 2005). They possess, among others, cytotoxic, antidepressant, antibacterial, and anti-inflammatory activities (Crockett *et al*., 2008; Liu *et al*., 2013; Verotta *et al*., 2003; Shui *et al*., 2012). The phloroglucinol core of these compounds is often substituted by prenyl or geranyl moieties that are susceptible to cyclization and oxidation processes, affording bi- or tricyclic derivatives as well as complex cage compounds (Athanasas *et al*., 2004; Beerhues *et al*., 2006; Liu *et al*., 2013b).

Previously we have reported dimeric coumarins and flavonoids from the stem bark of *H. riparium* (Fobofou *et al*., 2014). As part of this continuing effort to study and compare the metabolomes of different *Hypericum* species and to find potential lead compounds (Fobofou *et al*., 2014; Porzel *et al*., 2014; Farag and Wessjohann, 2012), we have selected the leaves of *H. riparium* A.Chev. (synonym of *H. roeperianum* Schimp. ex A.Rich. according to The Plant List, http://www.theplantlist.org/, Hypericaceae) for chemical investigations, which led to the isolation of acylphloroglucinols **4.1**–**4.10**. The biological activities exhibited by the $CHCl_3$ extract of *H. roeperianum* as well as its chemical and chemotaxonomic significance fostered our effort in the isolation, structure elucidation, and more detailed study of specific biological activities of compounds **4.1**–**4.10** from *H. roeperianum* as well as the regioselective synthesis of compounds **4.8** and **4.9**.

4.2. Results and discussion

Column chromatography on silica gel and Sephadex LH-20 as well as semi-preparative HPLC led to the isolation of ten acylphloroglucinol derivatives (**4.1**–**4.10**) from the $CHCl_3$ extract of the leaves of *H. roeperianum* including one new tricyclic acylphloroglucinol (**4.1**), one new tetracyclic acylphloroglucinol (**4.2**), and one new prenylated bicyclic acylphloroglucinol (**4.3**) along with four known prenylated (**4.4**–**4.7**) and three known tetracyclic acylphloroglucinol derivatives (**4.8**-**4.10**). Their structures were established on the basis of spectroscopic evidence and comparison with the literature data. As acylphloroglucinol derivatives show characteristic deshielded proton signals around 9–14 ppm in the NMR spectrum, the isolation of compounds **4.1**–**4.10** was guided by ^{1}H NMR metabolite profiles of fractions. The geranylated phloroglucinol derivatives **4.6** and **4.7** were isolated as the major constituents from the leaves of *H. roeperianum*. These two compounds highly dominate the UPLC-PDA and ^{1}H NMR metabolite profiles (Figs. S1–S23; see Supporting Information) of the crude MeOH extract of the leaves of *H. riparium*. MeOH was identified as the best solvent of the solvents tested for extracting the whole metabolome of the plant.

Compound **4.1** was obtained as an optically active yellow oil, $[\alpha]_D^{25}$ −5.6 (*c* 0.35, MeOH). Its molecular formula was established as $C_{20}H_{28}O_5$ by means of HR-ESI-FTICR-MS (347.1859, [M−H]$^-$), indicating 7 double bond equivalents. The IR spectrum indicates the presence of hydroxyl (3277 cm^{-1}) and carbonyl (1602 cm^{-1}) groups. The ^{13}C NMR (Table 4.1) spectrum of compound **4.1** exhibits 20 signals, which were sorted by HSQC and DEPT into eight quaternary, four methine, three methylene, and five methyl carbons. The analysis of ^{1}H NMR and ^{13}C NMR (Table 4.1) suggests an acylphloroglucinol derivative (Athanasas *et al*., 2004; Tanaka *et al*., 2010).

The ^{1}H NMR spectrum of compound **4.1** reveals signals typical of a substituted (2-methylpropanoyl)phloroglucinol nucleus (Athanasas *et al.*, 2004; Tanaka *et al.*, 2010), exhibiting a highly deshielded hydrogen-bonded singlet at δ_H 13.83 (1H, *s*, 3-OH), a broad signal accounting for one hydroxyl group at δ_H 5.86 (1H, *bs*, 5-OH), one aromatic proton at δ_H 5.95 (1H, *s*, H-4), one methine septet at δ_H 3.77 (1H, *sept*, $J = 7.0$ Hz, H-2′), and two methyl groups at δ_H 1.15 (6H, *d*, $J = 7.0$ Hz, H-3′/H-4′). Additionally, many signals are observed between 3.46 and 0.91 ppm, including signals of one oxygenated methine at δ_H 3.46 (1H, *dd*, $J = 11.4, 4.0$ Hz, H-6″), one methine at δ_H 1.63 (1H, *m*, H-2″), two geminal protons at δ_H 2.68 (1H, *dd*, $J = 16.2, 5.3$ Hz, H-1″) and δ_H 2.36 (1H, *dd*, $J = 16.2, 13.2$ Hz, H-1″), and three singlet methyl groups (δ_H 1.13, C-8″; δ_H 0.91, C-9″; δ_H 1.28, C-10″). The carbon signals corresponding to the acylphloroglucinol moiety include one carbonyl group at (δ_C 210.4, C-1′), three deshielded oxygenated aromatic carbons (δ_C 165.2, C-3; δ_C 160.0, C-5; δ_C 156.0, C-1), two quaternary aromatic carbons (δ_C 105.4, C-2; δ_C 100.6, C-6), and one aromatic methine (δ_C 95.6, C-4). An inspection of the ^{1}H NMR and ^{13}C NMR spectra and degree of unsaturation of compound **4.1** suggests a tricyclic ring system because no additional double bond signal to the benzene ring is observed. Moreover, a characteristic signal of one oxygenated quaternary aliphatic carbon is observed in the ^{13}C NMR spectrum at δ_C 78.1 (C-3″). The ^{1}H and ^{13}C NMR signals of compound **4.1** resemble those reported for empetriferdinol [$C_{21}H_{30}O_5$, *m/z* 362, $[\alpha]_D^{25}$ +12 (*c* 0.1, MeOH)] (Schmidt *et al.*, 2012a), except for the signals of the acyl side-chain at C-2. The difference of 14 mass units in compound **4.1** is attributed to the fact that a 2-methylbutanoyl moiety is absent in **4.1** and is, instead, replaced by a 2-methylpropanoyl group. ROESY, COSY, HSQC, and HMBC experiments allowed for the determination of the tricyclic structure of **4.1**. Key observations in the HMBC spectrum were the correlation of Me-10″ (δ_H 1.28) to C-3″ (δ_C 78.1), C-2″ (δ_C 45.8), and C-4″ (δ_C 35.7) and the correlation of H-2″ (δ_H 1.63) to C-6 (δ_C 100.6), C-10″ (δ_C 19.7), C-7″ (δ_C 38.4), C-6″ (δ_C 78.0), C-1″ (δ_C 17.3), C-8″ (δ_C 27.2), C-9″ (δ_C 14.2). Pertinent correlations are observed from H-1″ (δ_H 2.36 and δ_H 2.68) to C-7″, C-5, C-6, C-2″, C-3″, and C-1; from H-6″ to C-8″ and C-9″; from H-4″ (δ_H 1.82 and δ_H 2.08) to C-6″, C-5″, C-10″ and C-2″; from H-9″ to C-6″, C-2″, C-7″, and C-8″; from H-4 to C-2, C-3, C-5, C-6 as well as from H-3′ to C-1′, C-2′, and C-4′. The COSY spectrum (Fig. 4.2) reveals correlations between H-6″ and H-5″, H-5″ and H-4″, H-1″ and H-2″, H-2′ and H-4′ as well as H-2′ and H-3′. ROESY interactions between H-6″ and H-2″, between H-6″ and Me-8″ as well as between Me-10″ and Me-9″ indicate the relative configuration of compound **4.1**. Compound **4.1**, which is reported herein for the first time, was therefore characterized to be 1-[(2R^*,4aR^*,9aR^*)-2,6,8-trihydroxy-1,1,4a-trimethyl-2,3,4,4a,9,9a-hexahydro-1*H*-xanthen-5-

yl]-2-methylpropan-1-one, trivially named madeleinol A (**4.1**). Madeleinol is a dedication to the principal investigator's mother named Madeleine.
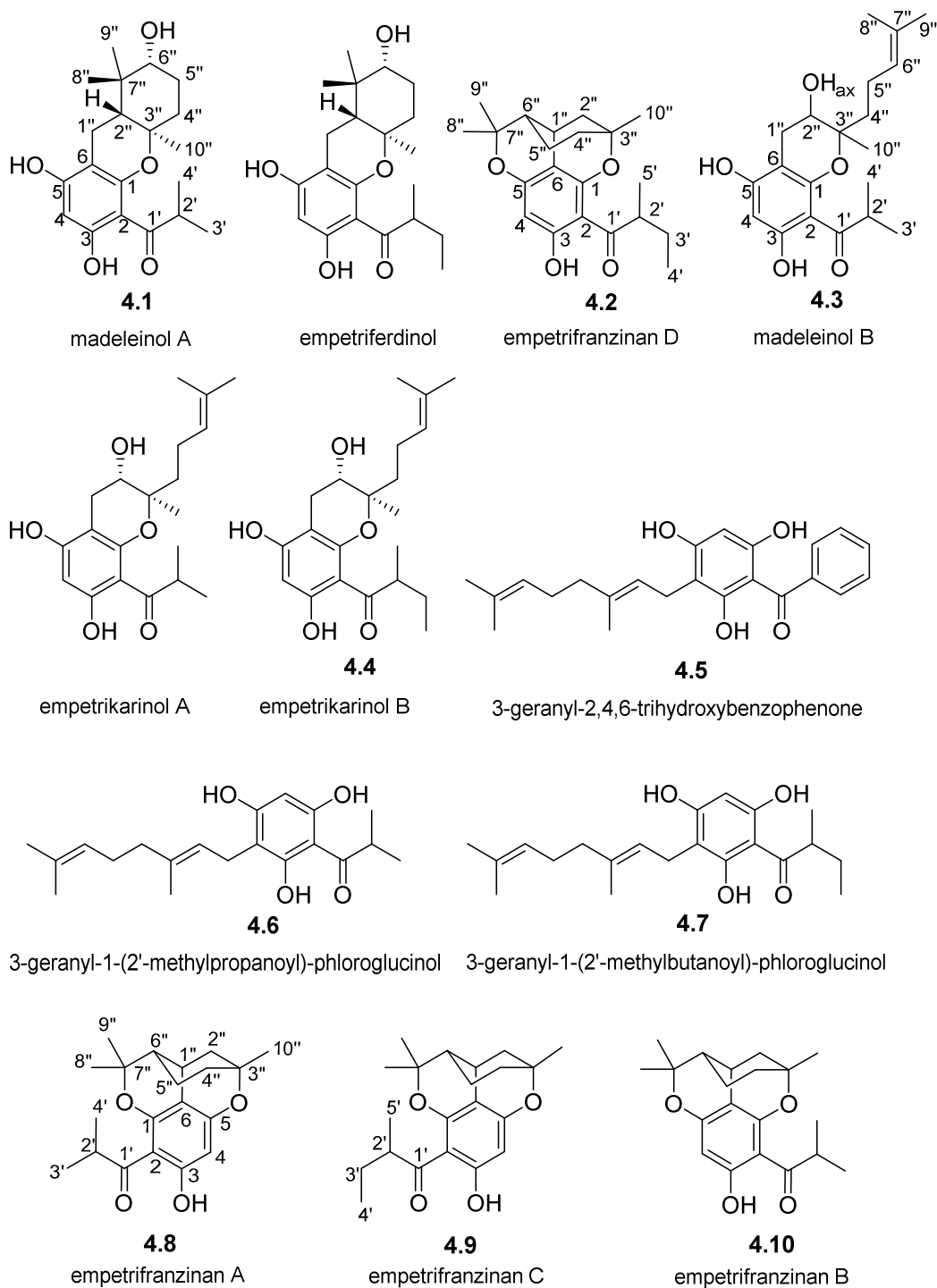
Fig. 4.1. Structures and trivial names of compounds **4.1-4.10**, empetriferdinol and empetrikarinol A.
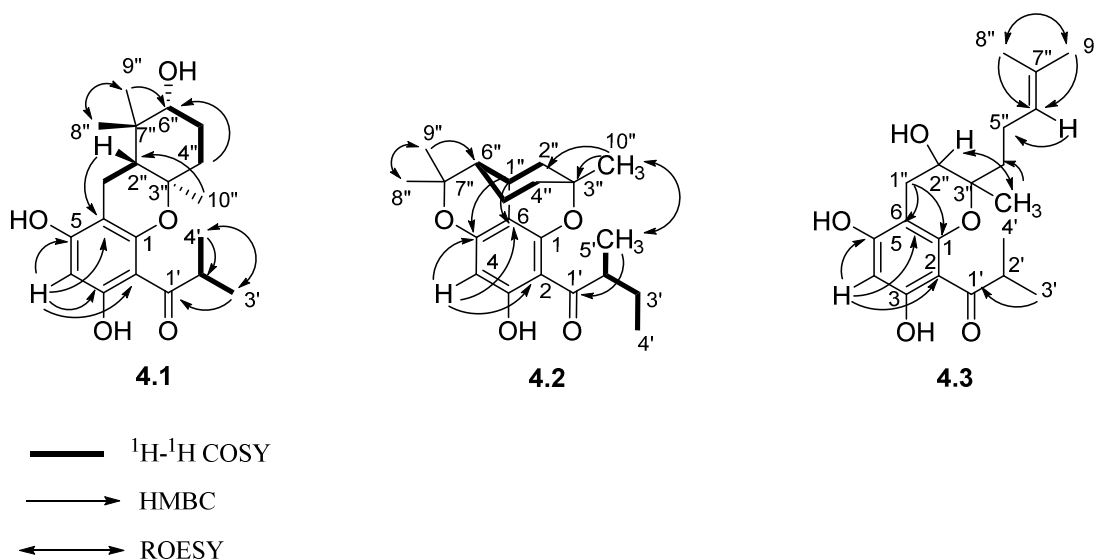
Fig. 4.2. Some selected 2D NMR correlations for compounds **4.1-4.3**.

Compound **4.2** was isolated as a slightly yellowish amorphous and optically active substance, $[\alpha]_D^{25}$ +28.7 (*c* 0.27, CHCl$_3$). The HR-ESI-FTICR-MS indicates a quasi-molecular ion peak at *m/z* 343.1916 ([M−H]$^-$) consistent with the molecular formula C$_{21}$H$_{28}$O$_4$, corresponding to 8 degrees of unsaturation. The ^{1}H (Table 4.1) and ^{13}C NMR (Table 4.1) data of compound **4.2** are indicative of an acylphloroglucinol derivative (Athanasas *et al.*, 2004; Tanaka *et al.*, 2010; Schmidt *et al.*, 2012a; Gibbons *et al.*, 2005). The ^{1}H NMR exhibits one signal of an aromatic methine singlet (δ_H 6.03, H-4) and duplicate signals of one highly deshielded hydrogen-bonded singlet (δ_H 13.87, 3-OH) (Shui *et al.*, 2012; Schmidt *et al.*, 2012a), one methine sextet (δ_H 3.66, *J* = 7.5 Hz, H-2′), one methyl doublet (δ_H 1.16, *J* = 7.5 Hz, H-5′), one methyl triplet (δ_H 0.96, *J* = 7.5 Hz, H-4′), and two diastereotopic methine multiplets (δ_H 1.84, H-3′a; δ_H 1.39, H-3′b). These observations are in agreement with the presence of a substituted (2-methylbutanoyl)-phloroglucinol derivative (Shui *et al.*, 2012; Schmidt *et al.*, 2012a), The ^{13}C NMR spectrum (Table 4.1) of compound **4.2** displays signals of 21 carbon atoms, which were sorted by DEPT and HSQC experiments into eight quaternary, four methine, four methylene, and five methyl carbons. The carbon signals corresponding to the acylphloroglucinol moiety include one carbonyl group (δ_C 209.7, C-1′) three deshielded (oxygenated) aromatic carbons (δ_C 158.2, C-1; δ_C 165.8, C-3; δ_C 162.8, C-5), two quaternary aromatic carbons (δ_C 106.0, C-2; δ_C 106.6, C-6), and one aromatic methine (δ_C 98.7, C-4) (Shui *et al.*, 2012; Schmidt *et al.*, 2012a), The ^{1}H and ^{13}C NMR data of compound **4.2** are similar to those of petiolin K and empetrifranzinan A–C (Fig. 4.1) recently reported in the literature (Tanaka *et al.*, 2010; Schmidt *et al.*, 2012a). In these interesting naturally occurring tetracyclic compounds, a menthane moiety is linked to the acylphloroglucinol core via one –C–C– and two –

C–O–C– bridges, forming a citran moiety (Tanaka *et al*., 2010; Schmidt *et al*., 2012a). Signals of a menthane skeleton are observed in the ^{1}H NMR spectrum (Table 4.1) of **4.2** as one methine broad singlet (δ_H 2.83, H-1″) and six methine multiplets (δ_H 2.20, H-2″a; δ_H 1.88, H-2″b; δ_H 1.84, H-4″a; δ_H 1.49, H-4″b; δ_H 1.33, H-5″a; δ_H 0.88, H-5″b) (Schmidt *et al*., 2012a). In addition, the ^{1}H NMR spectrum reveals three methyl groups as singlets (δ_H 1.09, H-8″; δ_H 1.53, H-9″; δ_H 1.44, H-10″). The HMBC spectrum (Fig. 4.2) of **4.2** reveals important correlations from H-1″ to C-1, C-5, C-6, C-2″, C-3″, C-5″, C-6″, and C-7″ in good agreement with the presence of one –C–C– bridge in the structure of **4.2** and enables the linkage of the 4 rings. The signals of two oxygenated aliphatic carbon atoms (δ_C 76.5, C-3″ and δ_C 84.9, C-7″) in the ^{13}C NMR spectrum and some important HMBC correlations, including from Me-8″ to C-6″, C-7″, and C-9″ as well as from Me-10″ to C-2″, C-3″, and C-4″, corroborate the presence of two –C–O–C– bridges in the molecule. The COSY spectrum shows correlations between H-2′ and the diastereotopic H-3′a/b protons; H-2′ and Me-5′, H-3′a/b and Me-4′, H-1″ and H-2″a/b, H-1″ and H-6″, H-4″a/b and H-5″a/b, as well as between H-5″a/b and H-6″. The 1D and 2D-NMR data of **4.2** as well as the key ROESY correlation observed between Me-10″ and Me-4′/Me-5′ indicate that it is a new derivative of empetrifranzinan B (**4.10**, C$_{20}$H$_{26}$O$_4$, *m/z* 330) (Schmidt *et al*., 2012a). The difference of 14 mass units in compound **4.2** agrees with the absence of a 2-methylpropanoyl group, replaced by a 2-methylbutanoyl group in the structure of **4.2**. Given all the spectroscopic data above, compound **4.2** was then characterized as 1-(1,9-epoxy-3-hydroxy-6,6,9-trimethyl-6a,7,8,9,10,10a-hexahydro-6*H*-benzo[*c*]chromene-2-yl)-2-methylbutan-1-one, which is a new acylphloroglucinol derivative and named empetrifranzinan D (**4.2**), based on similar compounds empetrifranzinans A–C (**4.8**–**4.10**).

The structures of the polycyclic compounds **4.8**, **4.9**, and **4.10** (Fig. 4.1) were similarly elucidated by comparing their spectroscopic (including 2D NMR) and physicochemical data with those disclosed in the literature, and they were respectively identified to be empetrifranzinan A (**4.8**), empetrifranzinan C (**4.9**), and empetrifranzinan B (**4.10**), recently reported as antiproliferative constituents of *H. empetrifolium* (Schmidt *et al*., 2012a). Acylphloroglucinols containing a citran moiety in their structures, with a menthane substructure C- and O-connected to the aromatic ring, have previously been reported from Guttiferae *sensu stricto*, isolated from the genera *Hypericum* and *Clusia* (Tanaka *et al*., 2010; Schmidt *et al*., 2012a).

In order to provide additional evidence for the proposed regiomeric structures (**4.2**, **4.8**, **4.9**, and **4.10**) alongside 2D NMR spectroscopic data and to obtain more material for our biological activity testing, we performed the total and regioselective synthesis of compounds **4.8** and **4.9** in

two efficient steps (Scheme 4.1). The key synthetic route used provided only one regiomer each (**4.8** and **4.9**) with 50% yield.

Table 4.1. ^{13}C NMR (δ) and ^{1}H NMR data [δ, *multiplicity*, *J* (Hz)] for compounds **4.1-4.3** (CDCl$_3$).

Position	4.1[a] ^{13}C	^{1}H	4.2[a] ^{13}C	^{1}H	4.3[b] ^{13}C	^{1}H
1	156.0		158.2		155.7	
2	105.4		106.0		105.4	
3	165.2		165.8		165.7	
4	95.6	5.95 *s*	98.4	6.03 *s*	96.3	5.97 *s*
5	160.0		162.8		159.8	
6	100.6		106.6		97.9	
1'	210.4		209.7		210.4	
2'	39.3	3.77 *sept* (7.0)	45.4	3.66 *sext* (7.5)	39.4	3.85 *sept* (6.6)
3'	19.3	1.15 *d* (7.0)	26.8	1.39 *m*	19.2	1.18 *d* (6.6)
				1.84 *m*		
4'	19.5	1.15 *d* (7.0)	12.0	0.96 *t* (7.5)	19.7	1.18 *d* (6.6)
5'			17.0	1.16 *d* (7.5)		
1''	17.3	2.36 *dd* (16.2, 13.2)	27.5	2.83 *bs*	25.2	2.60 *dd* (16.5, 6.6)
		2.68 *dd* (16.2, 5.3)				2.89 *dd* (16.5, 5.5)
2''	45.8	1.63 *m*	34.8	1.88 *m*	66.4	3.95 *dd* (6.6,5.5)
				2.20 *m*		
3''	78.1		76.5		80.7	
4''	37.5	1.82 *dd* (12.7, 4.0)	37.5	1.49 *m*	37.5	1.71 *m*
		2.08 *dt* (12.7, 3.5)		2.84 *m*		1.77 *m*
5''	28.1	1.65 *m*	22.0	0.88 *m*	22.0	2.15 *m*
		1.90 *m*		1.33 *m*		
6''	78.0	3.46 *dd* (11.4, 4.0)	46.0	2.04 *ddd* (7.5, 5.3, 2.2)	123.4	5.09 *t* (7.0)
7''	38.4		84.9		132.6	
8''	27.2	1.13 *s*	24.2	1.03 *s*	25.7	1.69 *s*
9''	14.2	0.91 *s*	29.6	1.53 *s*	17.6	1.60 *s*
10''	19.7	1.28 *s*	28.8	1.44 *s*	19.0	1.38 *s*
3-OH		13.83 *s*		13.87 *s*		13.81 *s*
5-OH		5.86 *bs*				5.43 *s*

[a] ^{13}C NMR (100 MHz), ^{1}H NMR (400 MHz)
[b] ^{13}C NMR (150 MHz), ^{1}H NMR (600 MHz)
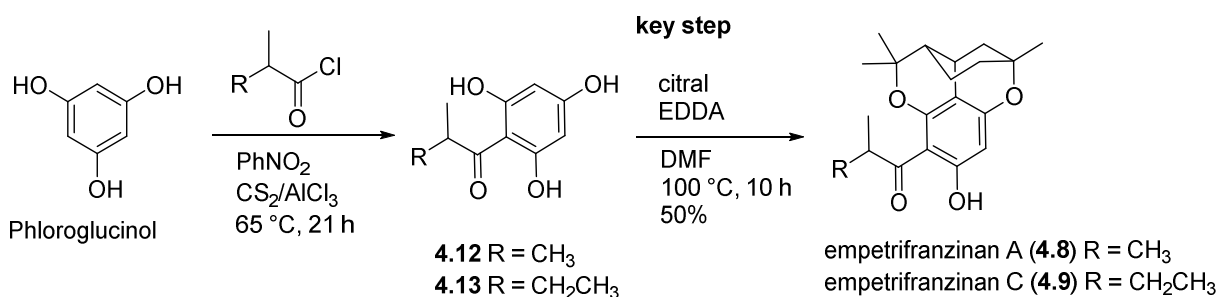
Scheme 4.1. Regioselective synthesis of acylphloroglucinol derivatives **4.8** and **4.9**.

The synthetic strategy involved Friedel–Craft acylation of phloroglucinol followed by an ethylenediamine diacetate-catalyzed (EDDA) cyclization by a domino aldol-type/electrocyclization/H-shift/hetero-Diels–Alder reaction of acylphloroglucinols and citral or *trans,trans*-farnesal (Wang and Lee, 2011). This reaction was previously applied for the

regioselective synthesis of acylphloroglucinols bearing citrans, like the petiolin D regioisomer (Wang and Lee, 2011). The spectroscopic data (Tables S1 and S2, see Supporting Information) of synthetic compounds **4.8** and **4.9** are identical to those of empetrifranzinan A (**4.8**) and empetrifranzinan C (**4.9**) isolated from *H. roeperianum* (this work) and also previously reported from *H. empetrifolium* (Schmidt *et al*., 2012a).

Compound **4.3** was isolated as an optically active yellow oil, $[\alpha]_D^{25}$ +6.8 (*c* 0.10, MeOH). Its molecular formula was determined to be $C_{20}H_{28}O_5$ from its HR-ESI-FTMS, which shows the base peak at *m/z* 347.1857 ([M−H]$^-$), consistent with 7 degrees of unsaturation. The IR spectrum shows the presence of hydroxyl (3306 cm^{-1}) and carbonyl (1614 cm^{-1}) groups. As in case of **4.1**, the ^{1}H (Table 4.1) and ^{13}C NMR (Table 4.1) data of compound **4.3** are in agreement with the presence of a (2-methylpropanoyl)-phloroglucinol moiety in the molecule (Tanaka *et al*., 2010; Schmidt *et al*., 2012b). Additional signals of a prenyl chain (Schmidt *et al*., 2012a; Gibbons *et al*., 2005), including one methine triplet (δ_H 5.09, C-6″), one methylene multiplet (δ_H 2.15, C-5″), and two methyl singlets (δ_H 1.69, C-9″; δ_H 1.60, C-8″) are revealed in the ^{1}H NMR spectrum. This is supported by HMBC correlations (Fig. 4.2) from Me-8″ to C-6″, C-7″, and C-9″ as well as from Me-9″ to C-6″, C-7″, and C-8″. The molecular formula and 1D and 2D NMR data of compound **4.3** are similar to those reported for empetrikarinol A (Schmidt *et al*., 2012a), except the ROESY spectrum which shows in **4.3** a key interaction between H-2″ (δ_H 3.95, *dd*, *J* = 6.6, 5.5 Hz) and Me-10″ (δ_H 1.38) in accordance with an equatorial position of H-2″. Furthermore, empetrikarinol A shows an optical rotation of $[\alpha]_D^{21}$ −24 (*c* 0.1, MeOH) (Schmidt *et al*., 2012a), whereas for **4.3** a value of $[\alpha]_D^{25}$ +6.8 (*c* 0.1, MeOH) was determined. Therefore, compound **4.3** is presumably a stereoisomer of empetrikarinol A, which is reported herein for the first time and named madeleinol B (**4.3**).

The structures of remaining known phloroglucinol derivatives were assigned by comparing their spectroscopic and physical data with those previously reported in the literature. These compounds were identified as empetrikarinol B (**4.4**) isolated from *H. empetrifolium* (Schmidt *et al*., 2012a), 3-geranyl-2,4,6-trihydroxybenzophenone (**4.5**) isolated from *Tovomita krukovii* (Guttiferae) (Zhang *et al*., 2002), 3-geranyl-1-(2′-methylpropanoyl)-phloroglucinol (**4.6**) (Crockett *et al*., 2008), and 3-geranyl-1-(2′-methylbutanoyl)-phloroglucinol (**4.7**) (Crockett *et al*., 2008). Compounds **4.6** and **4.7** were reported as constituents of *H. empetrifolium* and *H. punctatum* (Crockett *et al*., 2008; Sarkisian *et al*., 2012).

Compounds **4.1**–**4.10** were tested in a cell-based assay against the human immunodeficiency virus type-1 (HIV-1), using efavirenz as the reference inhibitor. Cytotoxicity against uninfected

MT-4 cells was evaluated in parallel with the antiviral activity. As reported in Table 4.2, none of the isolated compounds shows significant anti-HIV activity at concentrations below those cytotoxic for exponentially growing MT-4 cells.

Compounds **4.1**–**4.10** were also tested for antibacterial activity against representative human pathogenic Gram negative (*Escherichia coli* DSM 1103) and Gram positive (*Staphylococcus aureus* DSM 2569, and *Enterococcus faecalis* DSM 2570) bacteria. Ciprofloxacin was used as reference compound. None of the tested compounds shows significant inhibitory activity (MIC >1 mg/L). Olympicin A, which differs from compound **4.7** only by the position of the geranyl group shifted onto the 2-OH group (in olympicin A) of the phloroglucinol core, showed potent antibacterial activity (Shui *et al*., 2012). The lack of activity of compounds **4.6** and **4.7** in comparison to olympicin A could be due to different protocols and strains used or to the aforementioned structural differences.

Table 4.2. Cytotoxicity and antiviral activity of compounds (µM) and MeOH extract (µg/mL) obtained from *H. roeperianum* leaves (**4.1-4.10**) against HIV-1$_{\text{IIIB}}$.[a]

Hypericum roeperianum	MT-4 CC$_{50}$ (µM)[b]	HIV-1$_{\text{IIIB}}$ EC$_{50}$ (µM)[c]
Leaf extract	11.0 µg/mL	> 11.0 µg/mL
4.1	41.0	> 41.0
4.2	> 100	> 100
4.3	84.0	> 84.0
4.4	45.0	> 45.0
4.5	69.0	> 69.0
4.6	> 100	> 100
4.7	26.7	> 26.7
4.8	18.7	> 18.7
4.9	45.0	> 45.0
4.10	> 100	> 100
Efavirenz	40.0	0.002

[a] Data represent mean values for three independent determinations. Variation among duplicate samples (SD) was less than 15%.

[b] Cytotoxic concentration (CC): Compound concentration (µM) required to reduce the viability of mock-infected MT-4 cells by 50%, as determined by the MTT method. Efavirenz is the reference drug. For extracts: µg/mL.

[c] Effective concentration (EC): Compound concentration (µM) required to achieve 50% protection of MT-4 cells from the HIV-1 induced cytopathogeneticy, as determined by the MTT method. For extracts:µg/mL.

The CHCl$_3$ extract as well as compounds **4.1**–**4.10** were screened for cytotoxicity against HT-29 and PC-3 cancer cell lines. The CHCl$_3$ extract (from the leaves) exhibits cytotoxic activities indicated by a growth inhibition of the cell lines of 84% and 82%, respectively, at a concentration of 50 µg/mL. No inhibition was observed at 0.5 µg/mL. As shown in Figure 4.3, the isolated compounds **4.7**–**4.10** show weak cytotoxic effects (growth inhibition of 20–40%) against PC-3 at

a tested concentration of 10 μM while compounds **4.1–4.6** are inactive (less than 20% of growth inhibition). They were all inactive (inhibition of less than 20%) at 10 nM. Compounds **4.4**, **4.7**, **4.9–4.10** show weak cytotoxic activities (growth inhibition of 20–51%) against the cancer cell line HT-29 (Fig. 4.4).
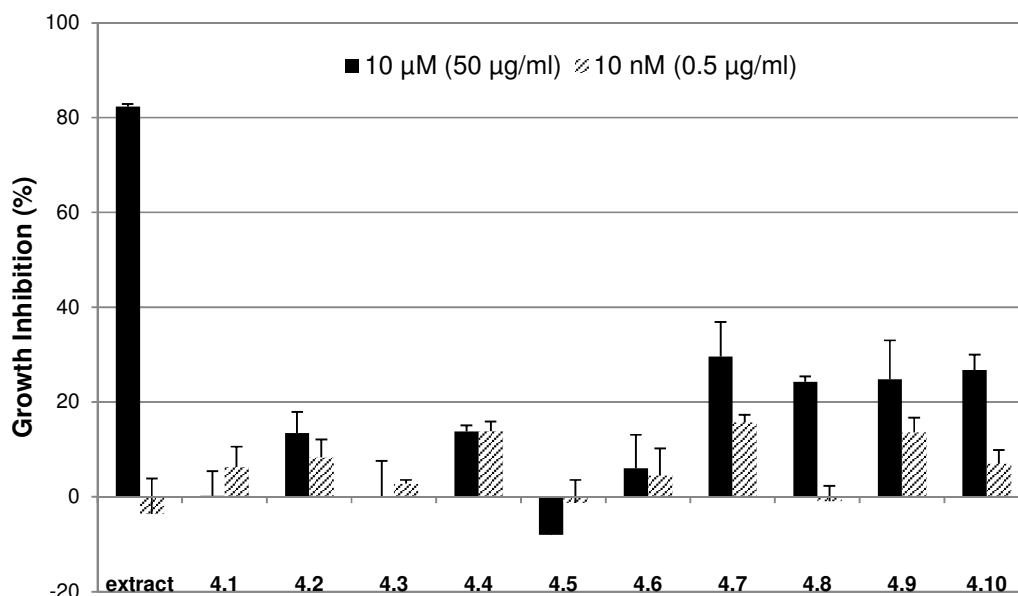
Figure 4.3. Cytotoxic activities of the CHCl₃ extract (leaves) and compounds **4.1-4.10** against the human prostate cancer cell line PC-3. The results are expressed as percentage of inhibition ± SD. Compounds were tested at two different concentrations of 10 μM and 10 nM while extracts were tested at 50 μg/mL and 0.5 μg/mL. Digitonin at 125 μM was used as positive control (100% growth inhibition). 0.05% DMSO was used as negative control.
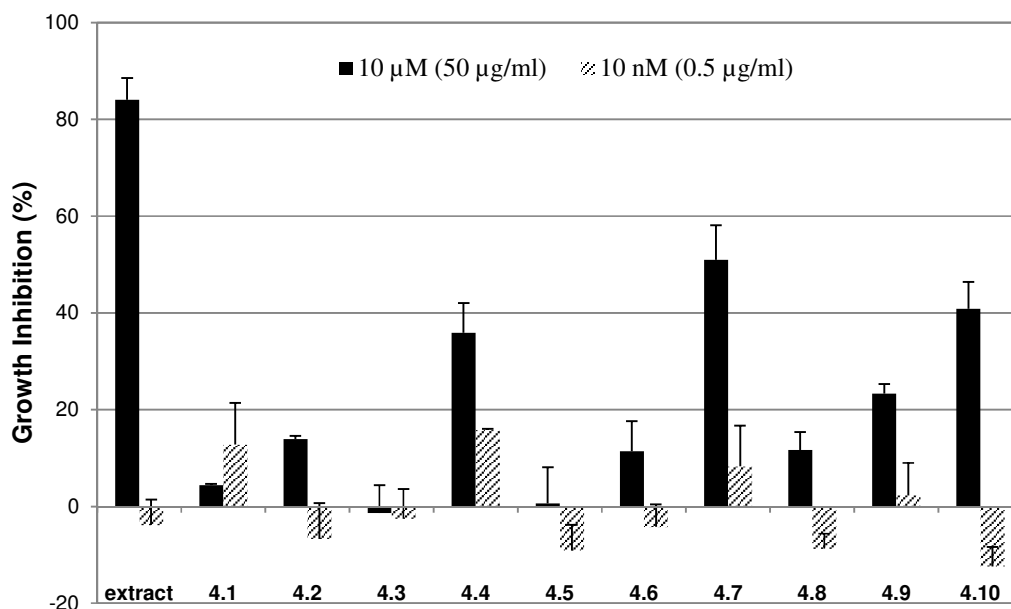
Figure 4.4. Cytotoxic activities of the CHCl₃ extract (leaves) and compounds **4.1-4.10** against the human colon cancer cell line HT-29. The results are expressed as percentage of inhibition ± SD. Compounds were tested at two different concentrations of 10 μM and 10 nM while extracts were tested at 50 μg/mL and 0.5 μg/mL. Digitonin at 125 μM was used as positive control (100% growth inhibition). 0.05% DMSO was used as negative control.

Compounds **4.1**–**4.10** were found not active at 10 nM. Compound **4.7**, one of the two major constituents (**4.6** and **4.7**) of the leaves, shows the highest cytotoxic effects among the tested acylphloroglucinols (Figures 4.3 and 4.4). An initial explanation or presumption of the difference of activity observed between the prenylated compounds **4.6**–**4.7** and **4.3**–**4.4** may be the length of the acyl chain as (2-methylbutanoyl)-phloroglucinols are more potent than (2-methylpropanoyl)-phloroglucinols in the present study. However, a contrary effect is observed between the two pairs of citran acylphloroglucinols **4.8**–**4.9** and **4.2**, **4.10**. Another activity-relevant feature is the prenyl side chain; the loss of a prenyl side chain can decrease the activity. For instance, the tricyclic acyphloroglucinol **4.1**, which is derived biosynthetically from prenylated phloroglucinols, does not cause any growth inhibition of the cell lines. Cytotoxic and antiproliferative phloroglucinols, including hyperforin, have been already reported from the genus *Hypericum* (Liu *et al.*, 2013; Schmidt *et al.*, 2012a; Schmidt *et al.*, 2012b).
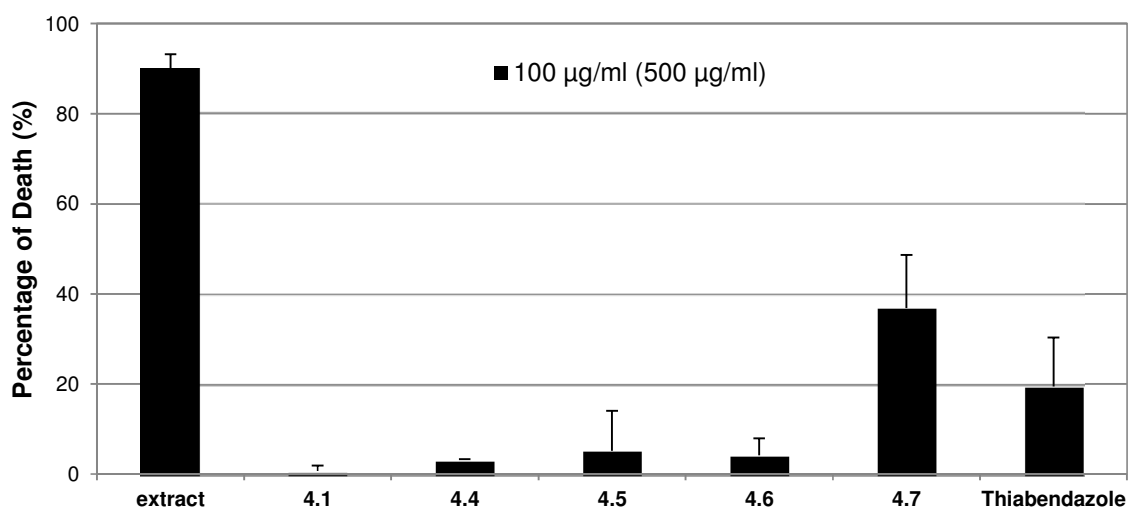
Figure 4.5. Anthelmintic activities of the CHCl$_3$ extract (dried leaves, 500 µg/mL) and compounds **4.1, 4.4-4.7** (100 µg/mL) against *Caenorhabditis elegans*. The results are expressed as percentage of death worms ± SD. 2% DMSO (3 ± 3 %) was used as negative control while ivermectin 10 µg/mL (99 ± 1 %) was used as positive control. Thiabendazole is a reference anthelmintic drug.

Some natural phloroglucinol derivatives, including aspidin and desaspidin from *Dryopteris filix-mas* (Dryopteridaceae) as well as kosins from *Hagenia abyssinica* (Rosaceae), have also been reported to show anthelmintic properties (Thomsen *et al.*, 2012; Bowden *et al.*, 1965; Magalhaes *et al.*, 2010). One of the objectives of the United Nations Millennium Development Goals is to halt or reverse the incidence of infections caused by neglected tropical diseases like helminths as billions of people suffer from helminthic diseases worldwide resulting in many thousands of deaths annually (Millennium Development Goals, 2014; Smout *et al.*, 2010). Although some effective anthelmintic drugs are available, recent treatment failures have occurred apparently due to the

development of genetic resistance in nematodes (Thomsen *et al*., 2013). Thus, there is a need for new and inexpensive drugs able to act longer before the resistance sets in. As described by Thomsen *et al*. (2012), the non-parasitic nematode *Caenorhabditis elegans* can be used as a model organism for inexpensive and rapid initial screening for the detection of compounds active against parasitic helminths. Preliminary anthelmintic activities of the $CHCl_3$ extract from the leaves of *H. roeperianum* and compounds **4.1**, **4.4–4.7** against the model organism *Caenorhabditis elegans* (Bristol N2 wild type strain) were determined in a modified microtiter plate assay by enumeration of living and dead nematodes using a microscope (Thomsen *et al*., 2013). At a test concentration of 100 µg/mL, compound **4.7** shows a nematode death percentage of 37 ± 12% (Fig. 4.5) while the reference drug thiabendazole exhibits a percentage of death of 19 ± 11%. Compounds **4.1**, **4.4–4.6** are inactive. They show a percentage of death ranging from 0.7% to 5.1%. All the tested compounds are inactive at 12.5 µg/mL (results not shown). The known compound **4.7**, one of the two major constituents of the extract, may be responsible for the observed anthelmintic activity of the $CHCl_3$ extract. It hints to a potential anthelmintic lead structure, which may be structurally modified on its acyl side chain in order to investigate its structure activity relationship. An initial observation of the structures of **4.6** and **4.7** and their anthelmintic activities allows us to speculate that longer acyl side chains may give more active compounds. However, such alterations also enhance the lipophilicity and thus the bioavailability. Thus, it is yet unclear if the improved activities are based on better target binding or on better bioavailability.

4.3. Conclusion

In summary, we isolated and identified new constituents of *H. roeperianum* for the first time, namely compounds **4.1–4.10**, which include some very minor compounds and three new natural products. Two acylphloroglucinols (**4.8** and **4.9**) bearing citran moieties were successfully synthetized in only two steps. Their anthelmintic (**4.1**, **4.4–4.7**), cytotoxic (**4.1–4.10**) and anti HIV (**4.1–4.10**) activities were evaluated. Compounds **4.4**, **4.7**, **4.9–4.10** exhibit weak cytotoxic effects against cancer cell lines. The crude $CHCl_3$ extract and compound **4.7** show anthelmintic activity against *Caenorhabditis elegans*. This may explain the use of *Hypericum* species in Cameroonian traditional medicine against intestinal worm infections. Even though this is a preliminary screening, the force of our study lies on the ability of Hypericaceae natural products to provide yet unexplored structures with the potential for anthelmintic, cytotoxic or anti-HIV activity. Also, acylphloroglucinols have significance as chemotaxonomic markers in *Hypericum* species (Crockett, 2012; Crockett and Robson, 2011). Based on this and similar studies on *Hypericum*, it will be interesting to evaluate the activity profiles of more species and compare them by

established metabolomics approaches for chemotaxonomic significance as well as for differences or specificities in bio-markers and bioactivities.

4.4. Experimental

4.4.1. General experimental procedures

Acetonitrile (HPLC grade, LiChrosolv) was obtained from Merck KGaA, Germany; double distilled water was used for HPLC analysis. HPLC was performed on a VARIAN PrepStar instrument equipped with a VARIAN ProStar PDA detector. Column chromatography was run on silica gel (Merck, 63–200 and 40–63 μm) and Sephadex LH-20 (Fluka), while TLC was performed on precoated silica gel F_{254} plates (Merck). Spots were visualized with a UV lamp at 254 and 366 nm, or by spraying with vanillin–H_2SO_4–MeOH followed by heating at 100 °C. UV spectra were obtained on a JASCO V-560 UV/VIS spectrophotometer. IR (ATR) spectra were recorded using a Thermo Nicolet 5700 FT-IR spectrometer, in MeOH or $CHCl_3$. Optical rotation was measured using a JASCO P-2000 digital polarimeter. ^1H and ^{13}C NMR spectra were recorded on an Agilent DD2 400 NMR spectrometer at 400 and 100 MHz and on an Agilent VNMRS 600 NMR spectrometer at 600 and 150 MHz, respectively. 2D NMR spectra were recorded on an Agilent VNMRS 600 NMR spectrometer using standard pulse sequences implemented in Agilent VNRMJ software. The ^1H chemical shifts are referenced to internal TMS (δ_H 0.0); ^{13}C chemical shifts are referenced to internal $CDCl_3$ (δ_C 77.0) and CD_3OD (δ_C 49.0), respectively.

The low resolution electrospray (ESI) mass spectra were performed on a SCIEX API-3200 instrument (Applied Biosystems, Concord, Ontario, Canada) combined with a HTC-XT autosampler (CTC Analytics, Zwingen, Switzerland). The samples were introduced via autosampler and loop injection.

The negative ion high resolution ESI mass spectrum of compound **4.3** was obtained from an Orbitrap Elite mass spectrometer (Thermofisher Scientific, Bremen, Germany) equipped with an HESI electrospray ion source (spray voltage 4 kV; capillary temperature 275 °C, source heater temperature 40 °C; FTMS resolution 60.000). Nitrogen was used as sheath gas. The sample solutions were introduced continuously via a 500 μl Hamilton syringe pump with a flow rate of 5 μl/min. The data were evaluated by the Xcalibur software 2.7 SP1.

The negative ion high resolution ESI mass spectra of compounds **4.1**–**4.2** and **4.4**–**4.10** were obtained from a Bruker Apex III Fourier transform ion cyclotron resonance (FT-ICR) mass spectrometer (Bruker Daltonics, Billerica, USA) equipped with an Infinity™ cell, a 7.0 Tesla

superconducting magnet (Bruker, Karlsruhe, Germany), an RF-only hexapole ion guide and an external electrospray ion source (Agilent, off axis spray). Nitrogen was used as drying gas at 150 °C. The sample solutions were introduced continuously via a syringe pump with a flow rate of 120 μl/h. The data was acquired with 512 k data points, zero filled to 2048 k by averaging 16 scans and evaluated using the Bruker XMASS software (Version 7.0.8).

4.4.2. Plant material

The leaves of *Hypericum roeperianum* Schimp. ex A.Rich. were collected in August 2011 at Mount Bamboutos (Mbouda) in the West Region of Cameroon. The plant was identified as *H. riparium* A.Chev. by Mr. Nana Victor, a botanist at the National Herbarium of Cameroon where a voucher specimen (No. 33796/HNC) is deposited. *H. riparium* A.Chev. is presently treated as synonym of *H. roeperianum* Schimp. ex A.Rich. *H. roeperianum* is commonly found on Mount Bamboutos and other highlands in the south of Cameroon.

4.4.3. Extraction and isolation

The air-dried and powdered leaves (400 g) of *H. roeperianum* were sequentially extracted with $CHCl_3$ (3 × 5 L) and MeOH (3 × 2 L) for one day under shaking to give the respective extracts, namely the $CHCl_3$ (23.74 g) and MeOH (6.10 g) extracts, after evaporation under reduced pressure. The MeOH extract from the leaves of *H. roeperianum* used for UPLC-PDA analysis, anti-bacterial and anti-HIV assays, was obtained using an extraction procedure previously described for *Hypericum* species (Porzel *et al.*, 2014).

The $CHCl_3$ extract (23.48 g) from the leaves was subjected to silica gel column chromatography, eluted with step gradients of *n*-hexane–EtOAc and EtOAc–MeOH. Fractions were collected using a fraction collector (Retriever II). They were combined on the basis of their TLC profiles into 6 main fractions (Fr. 1A–Fr. 6A): Fr. 1A (170.8 mg), Fr. 2A (12.36 g), Fr. 3A (8.66 g), Fr. 4A (1.76 g), Fr. 5A (1.9 g), Fr. 6A (81.6 mg). Fr. 2A (12.36 g) obtained from *n*-hexane–EtOAc (90:10) was chromatographed on Sephadex LH-20 column (69 × 3 cm), eluted with CH_2Cl_2–MeOH (1:1), to give eight sub-fractions (Fr. $2A_1$–Fr. $2A_8$).

Fr. $2A_3$ (1.71 g) was subjected to column chromatography over silica gel eluted with *n*-hexane containing increasing amounts of EtOAc (from 100:0 to 50:50 with 5% increment) and 100% MeOH to yield 13 fractions (Fr. $2A_{3a}$–Fr. $2A_{3m}$). A portion of Fr. $2A_{3k}$ (79 mg), obtained from *n*-hexane–EtOAc (80:20), was purified through a RP18 column (5 μm, 120 × 2 mm, flow rate 17 mL/min, detection 210 nm) by semi-preparative HPLC on a Varian PrepStar eluted with

H_2O-MeCN (10→100% MeCN 0–20 min, 100→10% MeCN 20–25 min, 10% MeCN 27–30 min) to afford compounds **4.6** (30 mg, t_R 15.17 min) and **4.7** (34.2 mg, t_R 15.65 min). An initial approach to separate Fr. 2A$_{3c}$, a mixture of citran acylphloroglucinols plus other impurities as revealed by the ^{1}H NMR profile, by CC or HPLC as described above failed. Fr. 2A$_{3c}$ (193 mg) was then firstly separated by silica preparative thin layer chromatography (PTLC) and eluted with a mixture of toluene–EtOAc–HOAc (98:2:0.5), to afford two fractions after extraction and evaporation: Fr. 2A$_{3c1}$ (R_f = 0.32) and Fr. 2A$_{3c2}$ (R_f = 0.5). Fr. 2A$_{3c1}$ (115.6 mg) was suspended in MeCN and filtered. The resulting filtrate (53 mg) was further suspended in MeCN and filtered through a Chromabond C18 ec (Macherey-Nagel, 1 mL/100 mg), and finally purified through a RP18 column (5 μm, 120 × 2 mm, flow rate 17 mL/min, detection 210 nm) by semi-preparative HPLC on a Varian PrepStar eluted with H_2O–MeCN (30→100% MeCN 0–20 min, 100→30% MeCN 20–25 min, 30% MeCN 27–30 min) to yield **4.2** (2.3 mg, t_R 16.03 min), **4.8** (4.6 mg, t_R 14.51 min), **4.9** (6.3 mg, t_R 15.76 min), and **4.10** (4.5 mg, t_R 15.11 min).

Fr. 4A (1.76 g), obtained from *n*-hexane–EtOAc (90:10 and 50:50) and EtOAc–MeOH (100:0), was further chromatographed on Sephadex LH-20 column (69 × 3 cm), eluted with CH_2Cl_2–MeOH (1:1), to give five fractions (Fr. 4A$_1$–Fr. 4A$_5$). Fr. 4A$_3$ (407 mg) was dissolved in MeCN and filtered through a Chromabond C18 ec (1 mL/100 mg). A portion of the resulting filtrate was purified using RP18 HPLC (5 μm, 120 × 2 mm, flow rate 17 mL/min, detection 210 nm) on a Varian PrepStar instrument and eluted with H_2O–MeCN (30→100% MeCN 0-20 min, 100→30% MeCN 20–25 min, 30% MeCN 27–30 min) to give **4.1** (1.9 mg, t_R 8.04 min), **4.4** (2 mg, t_R 12.29 min), **4.5** (2.7 mg, t_R 13.30 min), and also **4.6** (3 mg, t_R 13.77 min) and **4.7** (3 mg, t_R 14.63 min). The remaining portion (67.5 mg) of the filtrate was purified using RP18 HPLC (10 μm, 250 × 10 mm, flow rate 8.9 mL/min, detection 210 nm) on the same instrument as above and also eluted with H_2O–MeCN (30→100% MeCN 0–20 min, 100→30% MeCN 20–25 min, 30% MeCN 27–30 min) to afford **4.3** (2.9 mg, t_R 13.82 min).

Madeleinol A (**4.1**), *1-((2R*,4aR*,9aR*)-2,6,8-trihydroxy-1,1,4a-trimethyl-2,3,4,4a,9,9a-hexahydro-1H-xanthen-5-yl)-2-methylpropan-1-one:* yellow oil; $[α]_D^{25}$ −5.6 (*c* 0.35, MeOH); UV (MeOH), $λ_{max}$ (log $ε$): 292 (2.06) nm; IR (ATR) $ν_{max}$ (cm^{-1}): 3277, 2965, 2935, 2870, 1603, 1504, 1419, 1380, 1233, 1127, 1022, 824, 752, 696, 666; ^{1}H NMR data see Table 4.1; ^{13}C NMR data see Table 4.1; negative ion ESI-FTICR-MS: [M−H]$^-$ at *m/z* 347.1859 (calcd for $C_{20}H_{27}O_5^-$, 347.1864).

Empetrifranzinan D (**4.2**), *1-(1,9-epoxy-3-hydroxy-6,6,9-trimethyl-6aS*,7R*,8,9R*,10,10a-hexahydro-6H-benzo[c]chromene-2-yl)-2-methylbutan-1-one:* white yellowish amorphous

compound; $[\alpha]_D^{25}$ +28.7 (*c* 0.27, CHCl$_3$); UV (MeOH), λ_{max} (log ε): 294 (2.30) nm; IR (ATR) ν_{max} (cm^{-1}): 2967, 2924, 2873, 1614, 1577, 1454, 1368, 1230, 1124, 924, 851, 831, 793, 757; ^{1}H NMR data see Table 4.1; ^{13}C NMR data see Table 4.1; negative ion ESI-FTICR-MS: [M−H]$^-$ at *m/z* 343.1916 (calcd for C$_{21}$H$_{27}$O$_4^-$, 343.1915).

Madeleinol B (**4.3**), *1-[3,5,7-trihydroxy-2-methyl-2-(4-methylpent-3-enyl)chroman-8-yl]-2-methylpropan-1-one:* yellow oil; $[\alpha]_D^{25}$ +6.8 (*c* 0.10, MeOH); UV (MeOH), λ_{max} (log ε): 291 (1.77) nm; IR (ATR) ν_{max} (cm^{-1}): 3306, 2966, 2928, 2873, 1614, 1511, 1422, 1380, 1234, 1141, 1094, 1048, 997, 827, 756, 698; ^{1}H NMR data see Table 4.1; ^{13}C NMR data see Table 4.1; negative ion ESI-FTMS: [M−H]$^-$ at *m/z* 347.1857 (calcd for C$_{20}$H$_{27}$O$_5^-$, 347.1864).

4.4.4. Synthesis

4.4.4.1. Synthesis of 1-(2,4,6-trihydroxyphenyl)-2-methylpropanone (4.12)

Anhydrous phloroglucinol (**4.11**, 10.0 g, 79.30 mmol) was suspended in nitrobenzene (80 mL). 40 mL of carbon disulfide (40 mL, CS$_2$) was added at room temperature under stirring. AlCl$_3$ (48.35 g, 362.61 mmol) was added in two portions. The reaction mixture was stirred at room temperature for 30 min to give a pale brownish solution. Isobutyl chloride (10 mL) was added and the reaction mixture was heated at 65 °C for 21 h to give a dark mixture, which was poured onto an ice-water bath. Concentrated HCl was added until pH 1–2 was reached, and the aqueous phase (400 mL) was filtered and extracted with chloroform (200 mL × 3). The chloroform of the extract was evaporated using a rotavap and the resulting residue was lyophilized to give a crude product (6.36 g), which was chromatographed through a silica gel column, eluted with *n*-hexane/EtOAc (25:75 and 40:60) to give compound **4.12** as yellow oil (4.89 g, 24.9 mmol, 31%, R_f = 0.39 in *n*-hexane/EtOAc (75:25)). ^{1}H NMR (CD$_3$OD) δ_H: 5.86 (s, 2H), 4.96 (*brs*, 2× OH), 4.01 (*sept*, *J* = 6.6 Hz, 1H), 1.16 (*d*, *J* = 6.6 Hz, 6H). ^{13}C NMR δ_C: 211.7, 165.7, 104.6, 95.8, 39.8, 19.6. Positive ion ESI-FTMS: [M+H]$^+$ at *m/z* 197.0805 (calcd for C$_{10}$H$_{13}$O$_4^+$, 197.0808).

4.4.4.2. Synthesis of 1-(2,4,6-trihydroxyphenyl)-2-methylbutanone (4.13)

Anhydrous phloroglucinol (5.23 g, 41.47 mmol) was suspended in nitrobenzene (40 mL). 40 mL of carbon disulfide (40 mL, CS$_2$) was added at room temperature under stirring. AlCl$_3$ (22.67 g, 170.02 mmol) was added in two portions. The reaction mixture was stirred at room temperature for 30 min to give a pale brownish solution. 2-Methylbutyryl chloride (5 g, 41.47 mmol) was added and the reaction mixture heated at 65 °C for 21 h to give a dark mixture, which was poured onto an ice-water bath (400 mL). Concentrated HCl was added to reach pH 1-2.

The aqueous phase was filtered and successively extracted with chloroform (250 mL × 3) and ethyl acetate (250 mL × 3). These unified extracts were freed from solvent using a rotavap and the residue was chromatographed through a silica gel column (*n*-hexane/EtOAc 70:30) to give compound **4.13** as yellow oil (2.32 g, 11.04 mmol, 27%, R_f = 0.42 in *n*-hexane/EtOAc (70:30)). ^{1}H NMR (CD$_3$OD) δ_H: 12.22 (*brs*, 1H), 5.91 (*s*, 2H), 5.17 (*brs*, 2× OH), 3.91 (*sext*, *J* = 6.6 Hz, 1H), 1.84 (*m*, 1H), 1.40 (*m*, 1H), 1.16 (*d*, *J* = 6.6 Hz, 3H), 0.93 (*t*, *J* = 7.45 Hz, 3H). ^{13}C NMR δ_C: 211.6, 165.40, 165.36, 115.2, 95.9, 46.5, 27.9, 16.9, 12.2. Positive ion ESI-FTMS: [M−H]$^-$ at *m/z* 209.0818 (calcd for C$_{11}$H$_{13}$O$_4^-$, 209.0819).

4.4.4.3. Synthesis of empetrifranzinan A (4.8)

To 196 mg (1 mmol) of **4.12** and citral (183 mg, 1.2 mmol) in DMF (10 mL) was added ethylene diamine diacetate (EDDA, 0.036 g, 0.2 mmol) at room temperature. The reaction mixture was heated at 100 °C for 10 h. After completion of the reaction as indicated by ESI-MS and TLC, the reaction mixture was cooled to room temperature. Water (30 mL) was added and the mixture was extracted with ethyl acetate (30 mL × 3). The combined organic extracts were freed from volatiles in a rotavap in vacuo, and the crude product (yellowish brownish oil, 397 mg) was purified by column chromatography on silica gel, eluted with *n*-hexane/EtOAc (95:5) to afford **4.8** as yellow compound (163.4 mg, 0.5 mmol, 50%, R_f = 0.31 in *n*-hexane/EtOAc (95:5)). ^{1}H and ^{13}C NMR see Table S1; positive ion HRESI-FTMS: [M+H]$^+$ at *m/z* 331.1905 (calcd for C$_{20}$H$_{27}$O$_4^+$, 331.1904).

4.4.4.4. Synthesis of empetrifranzinan C (4.9)

To 210.23 mg (1 mmol) of compound **4.13** and citral (183 mg, 1.2 mmol) in DMF (10 mL) was added ethylene diamine diacetate (EDDA, 0.036 g, 0.2 mmol) at room temperature. The reaction mixture was heated at 100 °C for 10 h. After completion of the reaction as indicated by ESI-MS and TLC, the reaction mixture was cooled to room temperature. Water (30 mL) was added and the mixture was extracted with ethyl acetate (50 mL × 3). The combined organic extracts were freed from solvent in a rotavap in vacuo, and the crude product (yellow oil, 431.8 mg) was purified by column chromatography on silica gel, eluted with *n*-hexane/EtOAc (95:5) to afford compound **4.9** as yellow oil (173.9 mg, 0.5 mmol, 50%, R_f = 0.33 in *n*-hexane/EtOAc (95:5)). ^{1}H and ^{13}C NMR see Table S2; positive ion HRESI-FTMS: [M+H]$^+$ at *m/z* 345.2067 (calcd for C$_{21}$H$_{29}$O$_4^+$, 345.2060).

4.4.5. Biological assays

4.4.5.1. Cells and viruses

Cell lines were purchased from American Type Culture Collection (ATCC). The absence of mycoplasma contamination was checked periodically by the Hoechst staining method.

Cell lines supporting the multiplication HIV-1 virus were CD4+ human T-cells containing an integrated HTLV-1 genome (MT-4). IIIB laboratory strain of HIV-1, were obtained from the supernatant of the persistently infected H9/IIIB cells (NIH 1983).

4.4.5.2. Cytotoxicity assays

The human prostate cancer cell line PC-3 and the colon cancer cell line HT-29 were maintained in RPMI 1640 medium supplemented with 10% fetal bovine serum, 1% l-alanyl-l-glutamine (200 mM) and 1.6% HEPES (1 M). ca. 5×10^2 PC-3 cells and ca. 1.5×10^3 HT-29 cells were seeded overnight into 96-well plates and exposed to a serial dilution of each compound (10 μM and 10 nM) and extract (50 and 0.50 μg/mL) for three days. Cytotoxicity was determined utilizing modified XTT method (0.25 mg/mL XTT, 6.5 μM PMS) as described by Scudiero *et al*. 1988.

Exponentially growing MT-4 cells were seeded at an initial density of 1×10^5 cells/mL in 96-well plates in RPMI-1640 medium, supplemented with 10% fetal bovine serum (FBS), 100 Units/mL penicillin G and 100 μg/mL streptomycin. Cell cultures were then incubated at 37 °C in a humidified, 5% CO_2 atmosphere, in the absence or presence of serial dilutions of test compounds. Cell viability was determined after 96 h at 37 °C by the 3-(4,5-dimethylthiazol-2-yl)-2,5-diphenyl-tetrazolium bromide (MTT) method (Pauwels *et al*., 1988).

4.4.5.3. Antibacterial assays

These assays were performed as described by the European Committee on Antimicrobial Susceptibility (EUCAST) testing (EUCAST, 2003).

4.4.5.4. Anthelmintic assays

This assay was performed as described by Thomsen *et al*. 2012.

4.4.5.5. Anti-HIV-1 assay

Activity against HIV-1 was based on the inhibition of virus-induced cytopathogenicity in MT-4 cell acutely infected with a multiplicity of infection (m.o.i.) of 0.01. Briefly, 50 μL of RPMI

containing 1×10^4 MT-4 cells was added to each well of flat-bottom microtitre trays, containing 50 μL of RPMI without or with serial dilutions of test compounds. Then, 20 μL of a HIV-1 suspension containing 100 $CCID_{50}$ were added. After a 4-day incubation at 37 °C, cell viability was determined by the MTT method (Pauwels *et al.*, 1988).

4.4.5.6. Linear regression analysis

The extent of cell growth/viability and viral multiplication at each drug concentration tested was expressed as a percentage of the untreated controls. Concentrations resulting in 50% inhibition (CC_{50} or EC_{50}) were determined by linear regression analysis.

Appendix. Supporting Information (this is available online)

Supplemental data associated with this chapter can be found in the online and published version at http://www.sciencedirect.com/science/article/pii/S0968089615300110.

References

Ang'edu, C.A., Schmidt, J., Porzel, A., Gitu, P., Midiwo, J.O., Adam, G., **1999.** Coumarins from *Hypericum keniense* (Guttiferae). *Pharmazie* 54, 235-236.

Athanasas, K., Magiatis, P., Fokialakis, N., Skaltsounis, A.–L., Pratsinis, H., Kletsas, D., **2004**. Hyperjovinols A and B: Two new phloroglucinol derivatives from Hypericum jovis with antioxidant activity in cell cultures. *J. Nat. Prod.* 67, 973-977.

Beerhues, L., **2006**. Hyperforin. *Phytochemistry* 67, 2201-2207.

Bowden, K., Broadbent, J.L., Ross, W.J., **1965**. Some simple anthelmintics. *Br. J. Pharmacol.* 24, 714-724.

Crockett. S.L., **2012**. Secondary chemistry of *Hypericum*—Taxonomic implications. *Phytotaxa* 71, 104-111.

Crockett, S.L., Robson, N.K., **2011**. Taxonomy and Chemotaxonomy of the Genus *Hypericum. Med. Aromat. Plant Sci. Biotechnol.* 5, 1-13.

Crockett, S.L., Wenzig, E.–M., Kunert, O., Bauer, R., **2008**. Anti-inflammatory phloroglucinol derivatives from *Hypericum empetrifolium. Phytochem. Lett.* 15, 37-43.

El-Seedi, H.R., Ringbom, T., Torsell, K., Borhlin, L., **2003**. Constituents of *Hypericum laricifolium* and their cyclooxygenase (COX) enzyme activities. *Chem. Pharm. Bull.* 51, 1439-1440.

European Committee on Antimicrobial Susceptibility Testing (EUCAST), **2003**. Determination of minimum inhibitory concentrations (MICs) of antibacterial agents by broth microdilution. EUCAST Discussion Document E. Def. 2003, 5.1. *Clin. Microbiol. Infect.* 9, 1–10.

Farag, M.A., Wessjohann, L.A., **2012**. Metabolome classification of commercial *Hypericum perforatum* (St. John's Wort) preparations via UPLC-qTOF-MS and chemometrics. *Planta Med.* 78, 488-496.

Fobofou, S.A.T., Franke, K., Arnorld, N., Wabo, H.K., Tane, P., Wessjohann, L.A., **2014**. Rare biscoumarin derivatives and flavonoids from *Hypericum riparium. Phytochemistry* 105, 171-177.

Gartner, M., Müller, T., Simon, J.C., Giannis, A., Sleeman, J.P., **2005**. Aristoforin, a novel stable derivative of hyperforin, is a potent anticancer agent. *ChemBioChem* 6, 171-177.

Gibbons, S., Moser, E., Hausmann, S., Stavri, M., Smith, E., Clennett, C., **2005**. An anti-staphylococcal acylphloroglucinol from *Hypericum foliosum*. *Phytochemistry* 66, 1472-1475.

Grey, C., Kyrylenko, S., Henning, L., Nguyen, L.H., Büttner, A., Pham, H.D., Giannis, A., **2007**. Phloroglucinol derivatives guttiferone G, aristoforin, and hyperforin: inhibitors of human sirtuins SIRT1 and SIRT2. *Angew. Chem. Int. Ed. Engl.* 46, 5219-5222.

Hecka, A., Maunit, B., Aubriet, F., Muller, J.F., **2009**. Study of active naphtodianthrone St John's wort compounds by electrospray ionization Fourier transform ion cyclotron resonance and multi-stage mass spectrometry in sustained off-resonance irradiation collision-induced dissociation and infrared multiphoton dissociation modes. *Rapid Commun. Mass Spectrom.* 23, 885-898.

Liu, X., Yang, X.–W., Chen, C.–Q., Wu, C.–Y., Zhang, J.–J., Ma, J.–Z., Wang, H., Yang, L.–X., Xu, G., **2013a**. Bioactive polyprenylated acylphloroglucinol derivatives from *Hypericum cohaerens*. *J. Nat. Prod.* 76, 1612-1618.

Liu, X., Yang, X.–W., Chen, C.–Q., Wu, C.–Y., Zhang, J.–J., Ma, J.Z., Wang, H., Zhao, Q.–S., Yang, L.–X., **2013b**. Hypercohones A–C, acylphloroglucinol derivatives with homo-adamantane cores from *Hypericum cohaerens*. *Nat. Prod. Bioprospect* 3, 233-237.

Magalhaes, L.G., Kapadia, G.I., Da Silva, T.L.R., Caixeta, S.C., Perreira, N.A., Rodrigues, V., Da Silva, F.A.A., **2010**. In vitro schistosomicidal effects of some phloroglucinol derivatives from *Dryopteris* species against *Schistosoma mansoni* adult worms. *Parasitol. Res*. 106, 395-401.

Millennium Development Goals (MDGs), **2014**. Retrieved March 25, 2014, from http://www.who.int/mediacentre/factsheets/fs290/en/.

Pauwels, R., Balzarini, J., Baba, M., Snoeck, D., Schols, D., Herdewijn, P., Desmyter, J., De Clercq, E., **1988**. Rapid and automated tetrazolium based colorimetric assay for the detection of anti-HIV compounds. *J. Virol. Methods* 20, 309–321.

Porzel, A., Farag, M.A., Mülbradt, J., Wessjohann, L.A., **2014**. Metabolite profiling and fingerprinting of *Hypericum* species: A comparison of MS and NMR. *Metabolomics* 10, 574-588.

Sarkisian, S.A., Janssen, M.J., Matta, H., Henry, G.E., LaPlante, K.L., Rowleyi, D.C., **2012**. Inhibition of bacterial growth and biofilm production by constituents from *Hypericum spp*. *Phytother. Res*. 26, 1012-1016.

Schmidt, S., Jürgenliemk, G., Schmidt, T.J., Skaltsa, H., Heilmann, J., **2012a**. Bi-, tri-, and polycyclic acylphloroglucinols from *Hypericum empetrifolium*. *J. Nat. Prod.* 75, 1697-1705.

Schmidt, S., Jürgenliemk, G., Skaltsa, H., Heilmann, J., **2012b**. Phloroglucinol derivatives from *Hypericum empetrifolium* with antiproliferative activity on endothelial cells. *Phytochemistry* 77, 218-225.

Scudiero, D.A., Schoemaker, R.H., Monks, A., Tierney, S., Nofziger, T.H., Currens, M.J., Seniff, D., Boyd, M.R., **1988**. Evaluation of a soluble tetrazolium/formazan assay for cell growth and drug sensitivity in culture using human and other tumor cell lines. *Cancer Res*. 48, 4827-4833.

Shui, W.K.P., Rahman, M.M., Curry, J., Stapleton, P., Zloh, M., Malkinson, J.P., Gibbons, S*.,* **2012**. Antibacterial acylphloroglucinols from *Hypericum olympicum*. *J. Nat. Prod*. 75, 336-343.

Smout, M. J, Kotze, A.C., McCarthy, J.S., Loukas, A., **2010**. A novel high throughput assay for anthelmintic drug screening and resistance diagnosis by real-time monitoring of parasite motility. *PLoS Negl. Trop. Dis.* 4, 1-10.

Tanaka, N., Kashiwada, Y., Kim, S.–Y., Sekiya, M., Ikeshiro, Y., Takaishi, Y., **2009**. Xanthones from *Hypericum chinense* and their cytotoxicity evaluation. *Phytochemistry* 70, 1456-1461.

Tanaka, N., Otani, M., Kashiwada, Y., Takaishi, Y., Shibazaki, A., Gonoi, T., Shiro, M., Kobayashi, J., **2010**. Petiolins J-M, prenylated acylphloroglucinols from *Hypericum pseudopetiolatum* var. *kiusianum*. *Bioor. Med. Chem. Lett.* 20, 4451-4455.

Thomsen, H., Reider, K., Franke, K., Wessjohann, L.A., Keiser, J., Dagne, E., Arnold, N., **2012**. Characterization of constituents and anthelmintic properties of *Hagenia abyssinica*. *Sci. Pharm*. 80, 433-446.

Thomsen, H., Reider, K., Franke, K., Fobofou, S., Wessjohann, L.A., Keiser, J., Arnold, N. Abstract of Posters, 1st European Conference on Natural Products: Research and Applications, DECHEMA; Frankfurt, **2013**; Abstract 150.

Uwamorin, M., Nakada, M., **2013**. Stereoselective total synthesis of (±)-hyperforin via intramolecular cyclopropanation. *Tetrahedron Lett.* 54, 2022-2025.

Verotta, L., **2003**. *Hypericum perforatum*, a source of neuroactive lead structures. *Curr. Top. Med. Chem.* 3, 187-201.

Wabo, H.K., Kowa, T.K., Lonfouo, A.H.N., Tchinda, A.T., Tane, P., Kikuchi, H., Frédérich, M., Oshima, Y., **2012**. Phenolic compounds and terpenoids from *Hypericum lanceolatum*. *Rec. Nat. Prod.* 6, 94-100.

Wang, Xue., Lee, Y.R., **2011**. Efficient synthesis of polycycles bearing prenylated, geranylated, and farnesylated citrans: application to 3′-prenylrubranine and petiolin D regioisomer. *Tetrahedron* 67, 9179-84.

Winkelmann, K., Heilmann, J., Zerbe, O., Rali, T., Sticher, O., **2001**. New prenylated bi- and tricyclic phloroglucinol derivatives from *Hypericum papuanum*. *J. Nat. Prod.* 64, 701-706.

Xiao, Z.H.Y., Mu, Q., Shiu, W.K.P., Zeng, Y.H., Gibbons, S., **2007**. Polyisoprenylated benzoylphloroglucinol derivatives from *Hypericum sampsonii*. *J. Nat. Prod.* 70, 1779-1782.

Zhang, Z., Elsohly, H.N., Jacob, M.R., Pasco, D.S., Walker, L.A., Clark, A.M., **2002**. Natural products inhibiting *Candida albicans* secreted aspartic proteases from *Tovomita krukovii*. *Planta Med.* 68, 49-54.

Zofou, D., Kowa, T.K., Wabo, H.K., Ngemenya, M.N., Tane, P., Titanji, V.P.K., **2011**. *Hypericum lanceolatum* (Hypericaceae) as a potential source of new anti-malarial agents: a bioassay-guided fractionation of the stem bark. *Malar. J.* 10, 167. DOI: 10.1186/1475-2875-10-167.

Chapter 5

Rare biscoumarin derivatives and flavonoids from *Hypericum roeperianum*: bichromonol, the first example of anti-HIV biscoumarin from the genus *Hypericum*

Graphical abstract*

New anti-HIV compound   **Absolute configuration**
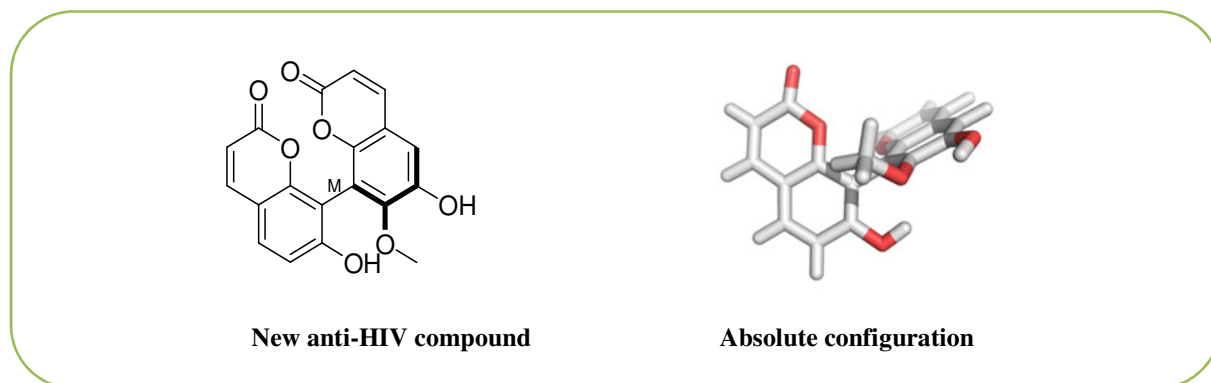
Highlights

- The crude extract of *H. roeperianum* exhibits significant anti-HIV-1 activity

- Ten compounds were isolated from *H. roeperianum* stem bark for the first time

- Novel biscoumarins were isolated and characterized by 1D and 2D NMR spectroscopy

- Bichromonol, a novel biscoumarin, exhibits significant anti-HIV activity

- First examples of biscoumarins from the genus *Hypericum*

Abstract

Chemical investigation of the methanol extract of the stem bark of *H. roeperianum* led to the isolation of five new natural products, 7,7´-dihydroxy-6,6´-biscoumarin (**5.1**), 7,7´-dihydroxy-8,8´-biscoumarin (**5.2**), 7-methoxy-6,7´-dicoumarinyl ether (**5.3**), 2´-hydroxy-5´-(7´´-methoxycoumarin-6´´-yl)-4´-methoxyphenylpropanoic acid (**5.4**), 6,7´-dihydroxy-7-methoxy-8,8´-biscoumarin (**5.5**) named bichromonol (**5.5**), together with one known 7,7´-dimethoxy-6,6´-biscoumarin (**5.6**), two flavones, 2´-methoxyflavone (**5.7**) and 3´-methoxy-flavone (**5.8**), and two steroids, stigmast-4-en-3-one (**5.9**) and ergosta-4,6,8,22-tetraen-3-one (**5.10**). In addition, tetradecanoic acid (**5.11**), *n*-pentadecanoic acid (**5.12**), hexadecanoic acid (**5.13**), *cis*-10-heptadecenoic acid (**5.14**), octadecanoic acid (**5.15**) campesterol (**5.16**), stigmasterol (**5.17**), *ß*-sitosterol (**5.18**), stigmastanol (**5.19**), *ß*-eudesnol (**5.20**), 1-hexadecanol (**5.21**), and 1-octadecanol (**5.22**) were identified by GC-MS analysis. The new compound **5.4** consists of an unusual phenylpropanoic acid derivative fused with a coumarin unit, while compounds **5.2**, **5.3,** and **5.5** are rare members of C8-C8´ or C7-O-C6 linked biscoumarins. Their structures were elucidated by UV, IR, extensive 1D- and 2D-NMR experiments and electrospray (ESI) high resolution mass spectrometry (MS) including detailed MS/MS studies. The absolute configuration at the biaryl axis of bichromonol (**5.5**) was determined by comparing the experimental electronic circular dichroism (ECD) spectrum with those calculated for the respective atropisomers. This is the first report on the isolation of biscoumarins from the genus *Hypericum*, although simple coumarin derivatives were reported from this genus in the literature. The isolated compounds were evaluated for their cytotoxicity against PC-3 and HT-29 cancer cell lines and antibacterial activities. They were also tested in cell-based assays for cytotoxicity against MT-4 cells and for anti-HIV activity in infected MT-4 cells. Interestingly, compound **5.1** and bichromonol (**5.5**) exhibit significant activity at EC_{50} = 6.6-12.0 µM against HIV-1 wild type and its resistant strains. Especially against the resistant variants A17 and EFV[R], bichromonol is more effective than the commercial drug nevirapine and might thus provide new anti-HIV leads. The biscoumarins show no significant cytotoxic or antibacterial activities.

Keywords: *Hypericum roeperianum*; absolute configuration; biscoumarins; flavones; biological activities.

5.1. Introduction

Hypericum is a genus within the plant family Guttiferae (Mabberley, 1997). The genus comprises more than 450 species which occur widely in temperate regions of the world (Crockett and Robson, 2011). The widespread interest in the genus *Hypericum* started with the discovery of the medicinal properties of St. John's wort (*Hypericum perforatum*), which is extremely popular in Europe and North America for the treatment of mild-to-moderately severe depressions (Sarris, 2007). *H. perforatum* has been intensively investigated throughout the world both chemically and pharmacologically (Farag and Wessjohann, 2012). The genus *Hypericum* has been the source of diverse classes of bioactive phenolic and polyketide compounds (Kingauf *et al*., 2005). However, only a small proportion of the over 450 *Hypericum* species, other than the popular medicinal supplement St. John's wort (*H. perforatum*), have even been chemically characterized (Crispin *et al*., 2013; Porzel *et al*., 2013). Previous studies on *Hypericum* species revealed several bioactive compounds including dianthrones, flavonoids, anthraquinones, xanthones, coumarins, benzophenones, phloroglucinols, and less frequently chalcones, benzopyrans, steroids, and terpenoids (Ang'edu *et al*., 1999; Chung *et al*., 1999; Schmidt *et al*., 2012; Shiu and Gibbons, 2009; Tanaka *et al*., 2009; Wabo *et al*., 2012; Wirz *et al*., 2000; Wu *et al*., 1998). The biological activities of these compounds such as antimicrobial, cytotoxicity, anti-depressive, anti-oxidant, and anti-inflammatory have been also reported.

Hypericum roeperianum Schimp. ex A.Rich. (synonym: *Hypericum riparium* A.Chev.) is used in Cameroonian folk medicine for the treatment of epilepsy, microbial diseases, and mental disorder. It is also used by AIDS patients. Previous studies on the root of this plant species revealed the occurrence of xanthones, a phloroglucinol, daucosterol, and betulinic acid (Tala *et al*., 2013).

In our ongoing investigation of *Hypericum* species, we isolated and identified or characterized six biscoumarins (**5.1-5.6**), two flavonoids (**5.7-5.8**), and two steroids (**5.9-5.10**) from the stem bark of *H. roeperianum*. The biological activities of the crude extracts and the isolated compounds were evaluated. This is, to the best of our knowledge, the first report of biscoumarins from the genus *Hypericum*.

5.2. Results and discussion

Compound **5.1** was obtained as white crystals, m.p. 312-314 °C. The molecular formula was determined to be $C_{18}H_{10}O_6$ from its ESI-FTMS, which shows the base peak at *m/z* 321.0411 ([M-H]$^-$). The mass spectral behavior of the [M-H]$^-$ ion is characterized by losses of CO_2 and H_2O

followed by a CO expulsion (Figure S1, see Supporting Information). The IR spectrum shows absorption bands of hydroxyl (3278 cm^{-1}) and α,β-unsaturated lactone (1728 cm^{-1}) groups. The ^{1}H NMR spectrum (Table 5.1) exhibits two doublets at δ_H 6.11 (1H, *d*, *J* = 9.2 Hz, H-3) and 7.91 (1H, *d*, *J* = 9.2 Hz, H-4) corresponding to protons H-3 and H-4 of a coumarin moiety, and two aromatic protons at δ_H 6.67 (1H, *s*, H-8) and 7.61 (1H, *s*, H-5) characteristic of a 1,2,4,5-tetrasubstituted benzene ring. The molecular formula $C_{18}H_{10}O_6$, the IR spectrum and the number of proton signals in the ^{1}H NMR spectrum suggest compound **5.1** to be an oxygenated biscoumarin derivative. The important ROESY correlations observed between H-4 and H-5 as well as between H-3 and H-4 enabled us to unambiguously establish the substitution pattern of compound **5.1** (Fig. 5.2). The assignment of all carbon atoms signals was done using HSQC and HMBC experiments. The HMBC (Fig. 5.2) correlation observed between the proton at δ_H 7.61 (H-5) and the oxygenated aromatic carbon at δ_C 167.3 (C-7) suggests a linkage at C-6 position. Further pertinent HMBC correlations were observed from H-4 to C-8a and C-2, from H-3 to C-2 and C-4a, from H-5 to C-8a, C-4, and C-6 as well as from H-8 to C-6, C-8a, C-7, and C-4a. On the basis of the above spectral data, compound **5.1** was then characterized as 7,7´-dihydroxy-6,6´-biscoumarin. To the best of our knowledge, this compound is described here for the first time. Compounds **5.1** and **5.2** are structural isomers of 7,7´-dihydroxy-6,8´-biscoumarin (bicoumol), which is a C6-C8´ linked biscoumarin, previously isolated from *Trifolium repens* (Basa, 1988).

Compound **5.2** was obtained as white crystals, m.p. 300-302 °C, [α]$^{25}_D$ -5.5 (*c* 0.62 mM, CHCl$_3$). Its molecular formula of $C_{18}H_{10}O_6$, deduced from MS and NMR spectra is the same as that of **5.1**. The ESI-FTMS exhibits a peak at *m/z* 321.0414 ([M-H]$^-$) corresponding to the molecular formula $C_{18}H_8O_5$. The fragmentation behavior of the [M-H]$^-$ ion of compound **5.2** is very similar to that of the biscoumarin **5.1** (Figure S1, see Supporting Information). However, in contrast to **5.1** a successive loss of two CO_2 units is observed in its MS^2 spectrum. Furthermore, the abundance ratio of the ions *m/z* 275/277 is quite different (see Experimental). The IR spectrum shows the presence of hydroxyl (3378 cm^{-1}) and carbonyl (1731 cm^{-1}) groups. The ^{1}H NMR spectrum (Table 5.1) of compound **5.2** shows two doublets at δ_H 6.56 (1H, *d*, *J* = 9.7 Hz, H-3) and 8.24 (1H, *d*, *J* = 9.7 Hz, H-4) ascribed to protons H-3 and H-4 of a coumarin moiety. It also shows two additional signals at δ_H 7.96 (1H, *d*, *J* = 8.8 Hz, H-5) and 7.82 (1H, *d*, *J* = 8.8 Hz, H-6) characteristic of a 1,2,3,4-tetrasubstituted benzene ring. The ^{13}C NMR spectrum (Table 5.2) reveals nine carbon signals, which are only half of the number of carbon atoms in the molecular formula of $C_{18}H_{10}O_6$, suggestive for a symmetrical dimeric structure for compound **5.2**. These carbon signals were sorted by a DEPT experiment as four methines and five quaternary carbon

atoms, including one carbonyl group at δ_C 159.4 (C-2) and two oxygenated aromatic carbon atoms at δ_C 157.7 (C-7) and 148.8 (C-8a).
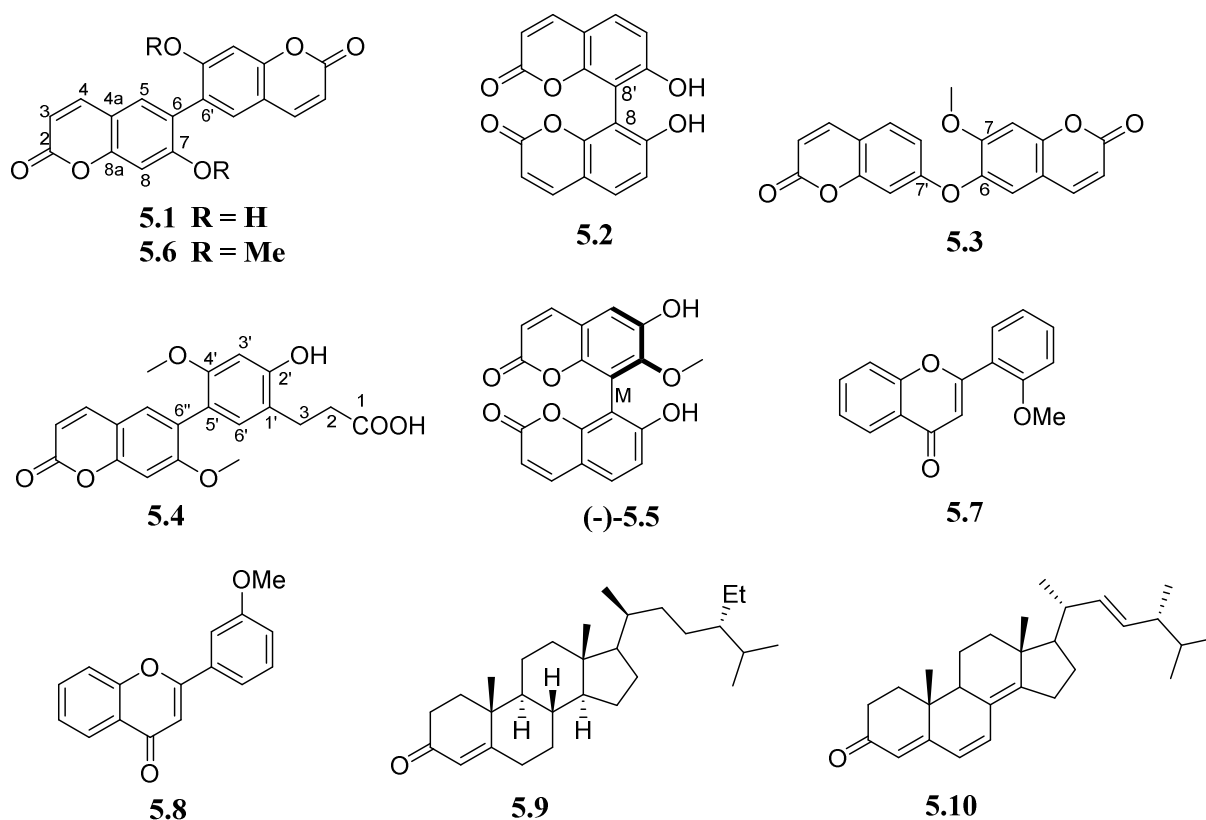
Fig. 5.1. Constitutions of compounds **5.1-5.10**.

The ROESY correlation between H-4 and H-5 suggests compound **5.2** to be a C-8 and C-8′ linked biscoumarin. This was further confirmed by its HMBC spectrum (Fig. 5.2), which shows correlations from H-5 to C-4, C-6, C-7, and C-8a. Additional important HMBC correlations were observed from H-6 to C-4a, C-5, C-7, and C-8, from H-3 to C-2 and C-4a, and from H-4 to C-2, C-5, C-4a, and C-8a. Compound **5.2** was thus unambiguously characterized as 7,7′-dihydroxy-8,8′-biscoumarin and is reported herein for the first time as a natural product. It was, however, already obtained from hydrolysis of edgeworoside C, its rhamnosidic derivative, isolated from *Edgeworthia chrysantha* (Thymelaeaceae) (Baba *et al.*, 1990). Compound **5.2** belongs to the rare class of natural C8-C8′ linked biscoumarins as only very few have been reported so far. The optical activity of this compound indicates a hindered rotation at the biaryl axis.

Compound **5.3** was obtained as white crystals, m.p. 115-117 °C. Its molecular formula was established as $C_{19}H_{12}O_6$ by means of ESI-FTMS (337.0712, [M+H]$^+$). The mass spectral fragmentation of the [M+H]$^+$ ion is dominated by a radical loss of methyl. Further decompositions

are mainly characterized by successive losses of CO (Figure S2) as previously described for ESI ion trap MS data of furanocoumarins (Kang *et al.* 2008, Yang *et al.* 2010, Heinke *et al.* 2012).

5.1 R = OH   **5.2**   **5.3**

5.4   **5.5**
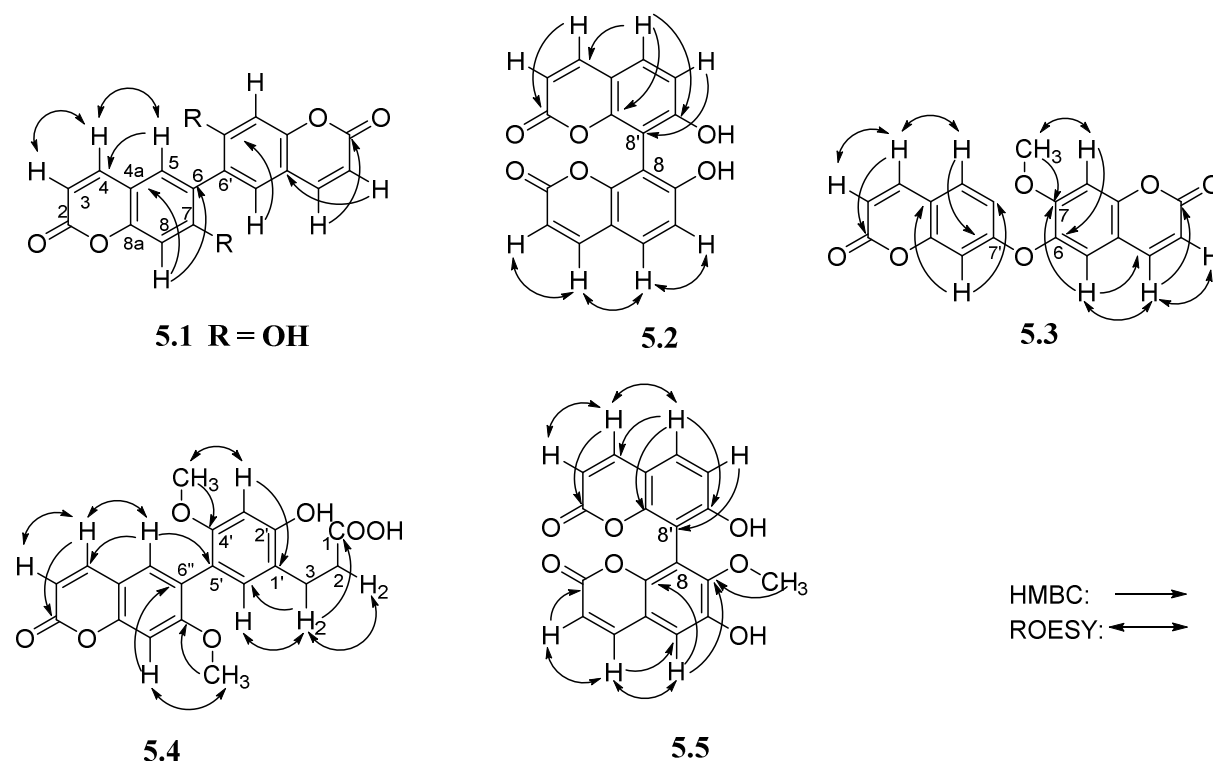
HMBC: ⟶
ROESY: ⟷

Fig. 5.2. Selected HMBC and ROESY correlations of compounds **5.1.-5.5**.

The IR spectrum reveals the presence of carbonyls (1727 cm^{-1}) and aromatic moieties (1613, 1558 and 1501 cm^{-1}). The ^{1}H NMR spectrum (Table 5.1) shows the presence of twelve proton signals including one methoxyl group at δ_H 3.87 (7-OMe). The observation of four distinct doublets at δ_H 6.30 (1H, *d*, *J* = 9.5 Hz, H-3´), 6.35 (1H, *d*, *J* = 9.2 Hz, H-3), 7.60 (1H, *d*, *J* = 9.2 Hz, H-4), and 7.66 (1H, *d*, *J* = 9.5 Hz, H-4´) corresponding to two coumarin units, suggests that **5.3** is an unsymmetrical coumarin dimer. The ^{1}H NMR spectrum also displays two signals at δ_H 6.98 (1H, *s*, H-8) and 7.22 (1H, *s*, H-5) characteristic of aromatic protons of a 1,2,4,5-tetrasubstituted benzene ring as well as signals of aromatic protons of a 1,3,4-trisubstituted benzene ring at δ_H 6.76 (1H, *d*, *J* = 2.6 Hz, H-8´), 6.88 (1H, *dd*, *J* = 8.8, 2.6 Hz, H-6´), and 7.57 (1H, *d*, *J* = 8.8 Hz, H-5´). The ^{13}C NMR spectrum (Table 5.2) reveals nineteen carbon signals including two carbonyl groups at δ_C 160.6 (C-2) and 160.7 (C-2´), one methoxyl signal at δ_C 56.5 as well as five oxygenated aromatic carbon signals at δ_C 161.2 (C-7´), 155.6 (C-8a´), 154.9 (C-7),

153.1 (C-8a), and 139.8 (C-6). ROESY, COSY, HSQC, and HMBC correlations allowed the determination and the linkage position of the two coumarin units (Fig. 5.2).

Table 5.1. ^{1}H NMR data [δ, *multiplicity*, *J* (Hz)] for compounds **5.1-5.5** at 600 MHz.

Position	5.1[a]	5.2[b]	5.3[c]	5.4[a]	5.5[a]	5.6[c]
2				2.54 *t* (7.5)		
3	6.11 *d* (9.2)	6.56 *d* (9.7)	6.35 *d* (9.2)	2.82 *t* (7.5)	6.31 *d* (9.7)	6.30 *d* (9.6)
4	7.91 *d* (9.2)	8.24 *d* (9.7)	7.60 *d* (9.2)		7.65 *d* (9.7)	7.65 *d* (9.6)
5	7.61 *s*	7.96 *d* (8.8)	7.22 *s*		7.14 *s*	7.31 *s*
6		7.82 *d* (8.8)				
8	6.67 *s*		6.98 *s*			6.91 *s*
3′	6.11 *d* (9.2)	6.56 *d* (9.7)	6.30 *d* (9.5)	6.50 *s*	6.17 *d* (9.7)	6.30 *d* (9.6)
4′	7.91 *d* (9.2)	8.24 *d* (9.7)	7.66 *d* (9.5)		7.93 *d* (9.7)	7.65 *d* (9.6)
5′	7.61 *s*	7.96 *d* (8.8)	7.57 *d* (8.8)		7.57 *d* (8.3)	7.31 *s*
6′		7.82 *d* (8.8)	6.88 *dd* (8.8, 2.6)	6.89 *s*	6.95 *d* (8.3)	
8′	6.67 *s*		6.76 *d* (2.6)			6.91 *s*
3″				6.25 *d* (9.2)		
4″				7.90 *d* (9.2)		
5″				7.37 *s*		
8″				6.98 *s*		
7-OMe			3.87 *s*		3.69 *s*	3.84 *s*
7′-OMe						3.84 *s*
4′-OMe				3.67 *s*		
7″-OMe				3.83 *s*		

[a] In CD_3OD
[b] In DMSO-d_6
[c] In $CDCl_3$

The COSY spectrum reveals correlations between protons H-4 and H-3, H-4′ and H-3′, H-5′ and H-6′, and between H-6′ and H-8′. Protons H-4 and H-5; H-8 and 7-OMe; H-4′ and H-5′ show correlations in the ROESY spectrum indicating the attachment of the methoxyl group to C-7 and the linkage of the two coumarin units through C-7′ and C-6. This was further corroborated by the HMBC spectrum which shows pertinent correlations from 7-OMe to C-7, from H-5 to C-7, C-8a, C-6, and C-4, from H-8 to C-6, C-7, C-8a, and C-4a, from H-4 to C-2, C-5, and C-8a as well as from H-5′ (δ_H 7.57) to C-7′ (δ_C 161.2), C-4′, and C-8a′. Additional HMBC correlations are observed from H-6′ to C-8′, C-4a′, and C-7′, from H-4′ to C-8a′, C-5′, and C-2′, and also from H-3′ to C-2′ and C-4a′. The high chemical shifts of C-7′ (δ_C 161.2) and C-6 (δ_C 139.8) together with the HR-ESI-MS data suggest that the two coumarin moieties are linked through an oxygen bridge at C-6 and C-7′. Thus the structure of compound **5.3** was unambiguously determined as 7-methoxy-6,7′-dicoumarinyl ether.

Compound **5.4** was obtained as white yellowish crystals, m.p. 162-164 °C, [α]$^{25}_D$ +5.1 (*c* 6.5 mM, MeOH). Its molecular formula was determined to be $C_{20}H_{18}O_7$ from the ESI-FTMS (369.0988 [M-H]$^-$). The MS^2 spectrum of the [M-H]$^-$ ion shows a loss of CO_2 as base peak ion. The further fragmentation is characterized by loss of the substituents as methyl and methoxy radicals, respectively, as well as MeOH (see Experimental and Figure S3).

Table 5.2. ^{13}C NMR data (δ) for compounds **5.1-5.5**.

Position	**5.1**[a, d, e]	**5.2**[b, e]	**5.3**[c, e]	**5.4**[a, d, f]	**5.5**[a, d, e]	**5.6**[c, f]
1				179.9		
2	164.5	159.4	160.6	36.5	163.3	161.0
3	110.4	114.5	114.4	26.7	115.1	113.5
4	146.7	144.9	142.6		145.9	143.3
4a	111.9	115.0	112.1		116.6	112.1
5	131.1	129.0	120.3		114.6	130.0
6	128.6	108.8	139.8		148.8	123.4
7	167.3	157.7	154.9		151.9	160.4
8	106.1	110.1	101.3		116.2	99.3
8a	157.1	148.8	153.1		147.6	155.7
1´				120.8		
2´	164.5	159.4	160.7	157.9	163.7	161.0
3´	110.4	114.5	114.3	100.5	112.0	113.5
4´	146.7	144.9	143.0	157.2	146.5	143.3
4a´	111.9	115.0	114.0		113.1	112.1
5´	131.1	129.0	129.0	118.5	130.5	130.0
6´	128.6	108.8	113.1	133.5	114.4	123.4
7´	167.3	157.7	161.2		161.6	160.4
8´	106.1	110.1	103.8		108.9	99.3
8a´	157.1	148.8	155.6		155.0	155.7
2´´				163.5		
3´´				113.1		
4´´				146.1		
4a´´				113.3		
5´´				131.6		
6´´				127.7		
7´´				162.6		
8´´				99.7		
8a´´				156.3		
7-OMe			56.5		61.1	56.2
7´-OMe						56.2
4´-OMe				56.1		
7´´-OMe				56.6		

[a] In CD_3OD
[b] In DMSO-d_6
[c] In $CDCl_3$
[d] Assignment supported with HSQC and HMBC correlation signals(600 MHz)
[e] Measured at 150 MHz
[f] Measured at 100 MHz

The IR spectrum reveals absorption bands due to hydroxyl (3402 cm^{-1}), carboxylic and carbonyl (2925 and 1713 cm^{-1}) groups as well as aromatic rings (1613, 1560 and 1510 cm^{-1}). The ^{1}H NMR spectrum (Table 5.1) shows two doublets at δ_H 6.25 (1H, *d*, *J* = 9.2 Hz, H-3´´) and 7.90 (1H, *d*, *J* = 9.2 Hz, H-4´´) attributable to H-3´´ and H-4´´ of a coumarin nucleus, and two singlets at δ_H 6.98 (1H, *s*, H-8´´) and 7.37 (1H, *s*, H-5´´) assignable to H-5´´ and H-8´´. This indicates a 6´´-substituted-7´´-oxygenated coumarin unit (Franke *et al*., 2002). Signals of two additional aromatic protons at δ_H 6.50 (1H, *s*, H-3´) and 6.89 (1H, *s*, H-6´), two methoxyl groups at δ_H 3.67 (3H, *s*, 4´-OMe) and 3.83 (3H, *s*, 7´´-OMe) as well as signals of four aliphatic protons at δ_H 2.54 (2H, *t*, *J* = 7.5 Hz, H-2) and δ_H 2.82 (2H, *t*, *J* = 7.5 Hz, H-3) were observed in the ^{1}H NMR

spectrum. The signals of protons H-1, H-2, H-3´, and H-6´ are characteristic of 5´-substituted-2´,4´-dioxygenated phenylpropanoic acid derivatives (Ioset *et al.*, 2000; Marumoto and Miyazawa, 2011; Rahmani *et al.,* 1994). The signals in the ^{1}H and ^{13}C NMR spectra (Table 5.2) as well as the connectivity between the coumarin unit and the phenylpropanoic acid derivative were assigned unambiguously using ROESY, COSY, HSQC, and HMBC experiments. The COSY spectrum reveals correlations between protons H-3 and H-4, and between H-1´´ and H-2´´. Important ROESY correlations (Fig. 5.2) are observed between H-3´´ and H-4´´, H-4´´ and H-5´´, H-8´´ and 7´´-OMe confirming the presence of a 6´´-substituted-7´´-methoxycoumarin unit. The ROESY spectrum also reveals correlations between H-2 and H-3, H-3 and H-6´, and between H-3´ and 4´-OMe, indicating that the two different units are linked between C-6´´ and C-5´. This was further confirmed by the HMBC spectrum (Fig. 5.2) which shows pertinent correlations from H-5´´ to C-5´, C-7´´, C-4´´, and C-8a´´, from H-8´´ to C-6´´, C-7´´, C-8a´´, and C-4a´´, from H-3´ to C-5´ and C-1´, from H-6´ to C-4´ and C-3, from 7´´-OMe to C-7´´, from 4´-OMe to C-4´, from H-3 to C-6´, C-2´, C-1, and C-2 as well as from H-2 to C-1´, C-1, and C-3. The correlation appearing between H-3 (δ_H 2.82) and C-1 (δ_C 179.9) in the HMBC spectrum is in good agreement with the presence of a propanoic acid moiety in the molecule. On the basis of the above spectroscopic data, the structure of compound **5.4** was unambiguously characterized as 2´-hydroxy-5´-(7-methoxycoumarin-6´´-yl)-4´-methoxyphenylpropanoic acid, which is a new coumarin-hydrocinnamic acid conjugate. Compound **5.4** also hints at a potential biosynthetic path to 6,6´-biscoumarins like **5.6** (or vice versa).

Compound **5.5** was isolated as an optically active yellow and amorphous substance, $[\alpha]^{25}_D$ -81.7 (*c* 6.0 mM, MeOH). The HR-ESI-FTMS indicates a quasi-molecular ion peak at *m/z* 351.0525 ([M-H]$^-$) consistent with the molecular formula $C_{19}H_{11}O_7^-$. The MS^2 spectrum of the [M-H]$^-$ ion shows a loss of MeOH as base peak ion. Further fragmentations are mainly characterized by successive losses of CO_2 and CO as previously described for MS/MS data of coumarins (Kang *et al.,* 2008, Yang *et al.,* 2010, Heinke *et al.,* 2012). The IR spectrum shows absorption bands of hydroxyl (3353 cm^{-1}) and carbonyl (1698 cm^{-1}) groups. The ^{1}H NMR spectrum (Table 5.1) shows the presence of eight proton signals including one methoxyl group (δ_H 3.69, 7-OMe). The observation of four distinct doublets at δ_H 6.31 (1H, *d*, *J* = 9.7 Hz, H-3), δ_H 7.90 (1H, *d*, *J* = 9.7 Hz, H-4), δ_H 6.17 (1H, *d*, *J* = 9.7 Hz, H-3´), δ_H 7.93 (1H, *d*, *J* = 9.7 Hz, H-4´) corresponding to two coumarin units signals suggests that **5.5** is an unsymmetrical coumarin dimer (Franke *et al.*, 2002). The ^{1}H NMR spectrum (Table 5.1) also shows two signals at δ 6.95 (1H, *d*, *J* = 8.3 Hz, H-6´) and δ 7.57 (1H, *d*, *J* = 8.3 Hz, H-5´), characteristic of aromatic protons of a 1,2,3,4-tetrasubstituted benzene ring as well as one signal at δ_H 7.14 (1H, *s*, H-5) attributable to

the proton of a 1,2,3,4,5-pentasubstituted benzene nucleus. The ^{1}H (Table 5.1) and ^{13}C NMR (Table 5.2) signals as well as the connectivity between the two coumarin units through a C-8/C-8′ biaryl axis were assigned unambiguously using DEPT, ROESY, COSY, HSQC, and HMBC spectroscopy. The ^{13}C NMR spectrum (Table 5.2) reveals nineteen carbon signals including two carbonyl groups (δ_C 163.8, C-2; δ_C 163.7, C-2′), one methoxyl group (δ_C 61.1, 7-OMe) as well as five oxygenated aromatic carbon signals (δ_C 148.8, C-6; δ_C 151.9, C-7; δ_C 147.6, C-8a; δ_C 161.6, C-7′; δ_C 155.0, C-8a′). The COSY spectrum reveals correlations between H-3 and H-4, H-3′ and H-4′ as well as between H-5′ and H-6′. Key interactions are observed in the ROESY spectrum (Fig. 5.2) between H-4 and H-3/H-5, H-4′ and H-3′/H-5′ as well as between H-5′ and H-6′. In addition, no ROESY correlation of the OMe group can be detected. These findings indicate the attachment of the methoxyl group to C-7 and the connection of the two coumarin units via C-8 and C-8′. This was further supported by the HMBC spectrum (Fig. 5.2) which reveals correlations from 7-OMe to C-7, from H-5 to C-4, C-8a, C-7, and C-6, from H-5′ to C-4′, C-8a′, and C-7′ as well as from H-6′ to C-4a′ and C-8′. On the basis of the above spectroscopic data, the structure of compound **5.5** was characterized as 6,7′-dihydroxy-7-methoxy-8,8′-biscoumarin and trivially named bichromonol (**5.5**).

The absolute configuration of bichromonol (**5.5**) was determined by comparing its experimental electronic circular dichroism (ECD) spectrum (in MeOH) with those calculated by quantum mechanical methods for both configurations S_a (or M) and R_a (or P) for 30 singlet and triplet states. The force field optimizations yielded two low energy conformations for each atropisomer (Sa, Ra) which were subsequently optimized with density functional theory (DFT) calculations. The two stable conformations of the Sa configuration are shown in Figure 5.3. The most stable conformation **5.5a** is characterized by the dihedral angles 8a-8-8′-8a′ = -67.9° and 8-7-O-C = -71.4°, whereas for the 3.39 kcal/mol less stable conformation dihedral angles of -102.5° and 37.3° resulted. For both conformations in Sa as well as Ra configurations the ECD spectra were calculated for 30 singlet and triplet states. The calculated spectra in comparison to the experimental one are displayed in Figures 5.4A-C. The comparison of the calculated with the experimental ECD spectrum clearly shows that the compound is preferentially populated in the Sa-configuration (Figures 5.4A-C). The rather good agreement between the calculated and experimental spectrum for the triplet states (Figure 5.4B) obviously indicates the triplet states contribute much more to the spectrum than the singlet states. Based on the foregoing evidence, the absolute configuration of compound **5.5** was with very high likelihood assigned to be Sa (or M).

5.5a   **5.5b**

Figure 5.3. The two low energy conformations of compound **5.5** with the Sa (or M) atropisomer configuration constructed using MOE 2013.0801. **5.5a:** The most stable conformation (dihedral angles 8a-8-8´-8a´ = -67.9°, 8-7-O-C = -71.4°). **5.5b:** the 3.39 kcal/mol less stable conformation (dihedral angles 8a-8-8´-8a´ = -102.5°, 8-7-O-C = 37.3°).
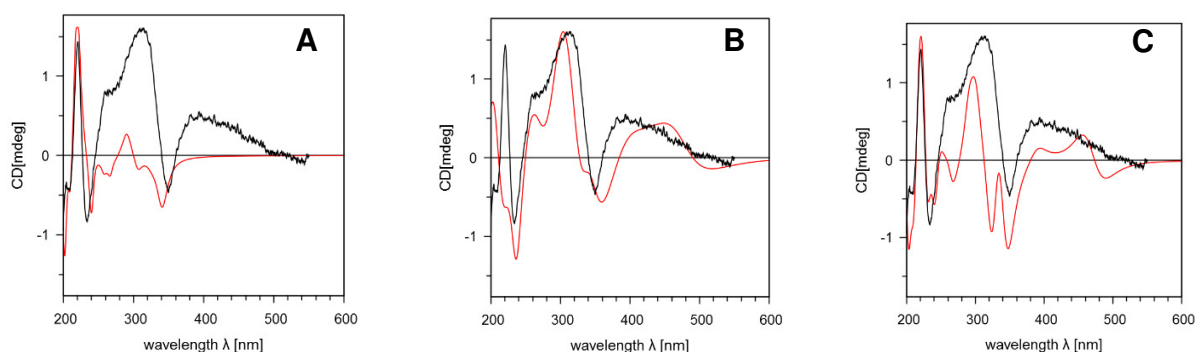
Figure 5.4. Comparison of the Boltzmann weighted calculated ECD spectrum (red line) with the experimental spectrum (black line) for both low energy conformations of the Sa configuration. **A.** Calculations for singlet states only. The calculated similarity factor is 0.4402 at 4 nm shift whereas the one for the Ra enantiomer would be only 0.2156. **B.** Calculations for triplet states only. The calculated similarity factor is 0.8062 at 12 nm shift whereas the one for the Ra enantiomer would be only 0.1266. **C.** Calculations for both singlet and triplet states. The calculated similarity factor is 0.6768 at 5 nm shift whereas the one for the Ra enantiomer would be only 0.1870.

Compound **5.6** was obtained as white crystals, m.p. 318-320 °C. The ESI-FTMS indicates an $[M+H]^+$ ion at *m/z* 351.0868 consistent with the molecular formula $C_{20}H_{14}O_6$, suggesting that **5.6** could be a dimethoxylated derivative of **5.1**. The stable ion at *m/z* 305 (base peak) formed from the $[M+H]^+$ ion in an initial step by loss of a methoxy and a methyl radical is further decomposed by successive CO losses (Figure S4). The IR spectrum shows the presence of carbonyls (1742 cm^{-1}) and aromatic rings (1620, 1560 and 1508 cm^{-1}). Only five signals at δ_H 6.30 (2H, *d*, *J* = 9.6 Hz, H-3/H-3´), 6.90 (2H, *s*, H-8/H-8´), 7.31 (2H, *s*, H-5/H-5´), 7.65 (2H, *d*, *J* = 9.6 Hz, H-4/H-4´), and 3.84 (6H, *s*, 7-and 7´-OMe) appear in the ^{1}H NMR spectrum (Table 5.1). This suggests the presence of a 6,7-disubstituted coumarin moiety. The ^{13}C NMR spectrum (Table 5.2) reveals nine carbon signals, which are only half of the number of carbon atoms in the molecular formula of $C_{20}H_{14}O_6$, suggesting a symmetrical dimeric structure for compound **5.6**. The ROESY correlations (Fig. 5.2) between H-4 and H-3/H-5; 7-OMe and H-8 as well as the HMBC correlations (Fig. 5.2) from H-5 to C-7, C-4, and C-8a are in good agreement with a C6-C6´ linked biscoumarin. The

HMBC spectrum reveals further correlations from H-5 to C-6, from H-8 to C-6, C-7, C-8a, and C-4a, from H-4 to C-2, C-5, C-8a, and C-4a as well as from H-3 to C-2 and C-4a. Thus, compound **5.6** was identified to be 7,7´-dimethoxy-6,6´-biscoumarin previously reported by Hou *et al.* (2010) as a constituent of *Urtica dentata* Hand, but not in other *Urtica* species recently surveyed (Farag *et al.*, 2013). We report its full set of spectroscopic data which were not published previously. This study is the first report on the isolation of biscoumarins from the genus *Hypericum*. Simple monomeric coumarin and isocoumarin derivatives have been reported from *Hypericum keniense* and *Hypericum annulatum*, respectively (Ang'edu *et al.*, 1999; Nedialkov *et al.*, 2007).

The structures of further isolated compounds were established by comparing their spectroscopic data with those previously reported in the literature. These compounds were identified as 2´-methoxyflavone (**5.7**), 3´-methoxyflavone (**5.8**), stigmast-4-en-3-one (**5.9**), and ergosta-4,6,8,22-tetraen-3-one (**5.10**) (Budzianowski *et al.*, 2005; Chorot *et al.*, 1997; Li and Wu, 1997). Compounds **5.7** and **5.8** are isolated from plants of the genus *Hypericum* for the first time. Flavonoid derivatives including rutin, quercetin, wightianin, apigenin, isoquercetin, and hyperoside have been reported as constituents of the genus *Hypericum* (Farag and Wessjohann, 2012). In addition, tetradecanoic acid (**5.11**), *n*-pentadecanoic acid (**5.12**), hexadecanoic acid (**5.13**), cis-10-heptadecenoic acid (**5.14**), octadecanoic acid (**5.15**) campesterol (**5.16**), stigmasterol (**5.17**), *ß*-sitosterol (**5.18**), stigmastanol (**5.19**), *ß*-eudesnol (**5.20**), 1-hexadecanol (**5.21**), and 1-octadecanol (**5.22**) were identified from non-polar fractions after trimethylsilylation by GC-MS.

The *n*-hexane and CHCl$_3$ extracts as well as compounds **5.2-5.10** were screened for cytotoxicity against HT29 and PC3 cancer cell lines. The *n*-hexane and CHCl$_3$ extracts exhibit cytotoxic activities indicated by a growth inhibition of the cell lines of more than 89 and 66 %, respectively, at a concentration of 50 µgml^{-1}. Up to concentration of 10 µM no significant growth inhibition (growth inhibition < 10% against HT-29 and < 25% against PC3) was determined for compounds **5.2-5.4** and **5.6-5.10**. Compound **5.5** exhibits a growth inhibition of the cell lines HT-29 and PC-3 of 21.4% and 41.7%, respectively. These results may suggest possible synergistic effects between the constituents. The crude (80% MeOH) extract was tested for anthelmintic activity against *caenorhabditis elegans*. No significant activity was observed (percentage of nematodes death of 23 %). Compounds **5.1-5.8** were tested for antibacterial activity against representative human pathogenic Gram negative (*Escherichia coli)*, and Gram positive (*Staphylococcus aureus*, and *Enterococcus faecalis*) bacteria. Ciprofloxacin was used as reference compound. None of tested compounds shows significant inhibitory activity (MIC > 1 mg/L).

In the course of our collection of Cameroonian *Hypericum* species for metabolomic profiles and biological activities comparison with their European and American counterparts, we heard from Cameroonian local population that the *H. roeperianum* is traditionally used against mental disorders (epilepsy and madness) and by AIDS patients. This raised our curiosity and we decided to evaluate its anti-HIV properties in order to determine whether it can really help HIV-infected people, and ultimately find new anti-HIV lead compounds. The $CHCl_3$ extract from *H. roeperianum* and isolated compounds **5.1**-**5.8** were tested in cell-based assay against the human immunodeficiency virus type-1 (HIV-1), using efavirenz as reference inhibitor. The cytotoxicity against the MT-4 cells was evaluated in parallel with the antiviral activity. The $CHCl_3$ extract exhibits significant anti-HIV-1_{IIIB} activity (EC_{50} = 0.4 µg/ml) associated with moderate cytotoxicity (CC_{50} = 6 µg/ml) against MT-4 cells. As reported in Table 5.3, compound **5.1** and bichromonol (**5.5**) show relevant activity (EC_{50} = 11.8 and 8.7 µM, respectively) associated with a moderate cytotoxicity (CC_{50} = 54 µM) for bichromonol and no cytotoxicity for **5.1** (CC_{50} = 100 µM). Since a critical issue in the long-term clinical management of HIV disease is the development of drug resistance, we decided to evaluate bichromonol (**5.5**) against a panel of viruses possessing mutations that confer selective resistance either to nucleoside/nucleotide reverse transcriptase inhibitors (NRTIs) or non-nucleoside reverse transcriptase inhibitors (NNRTIs) and that often appear during highly active anti-retroviral therapy therapy (HAART), reducing its effectiveness. Bichromonol (**5.5**) shows significant activity with EC_{50} ranging from 6.6 to 12.0 µM on all the tested HIV-1 mutant strains as depicted in Table 5.4.

Table 5.3. Cytotoxicity and antiviral activity of compounds (**5.1-5.8**) (µM) and $CHCl_3$ extract (µg/mL) obtained from *H. roeperianum* stem bark against HIV-1_{IIIB}.[a]

Hypericum roeperianum	MT-4 CC_{50} (µM)[b]	HIV-1_{IIIB} EC_{50} (µM)[c]
Stem bark extract	6.0 µg/mL	0.4 µg/mL
5.1	> 100	11.8
5.2	> 100	> 100
5.3	> 100	> 100
5.4	> 100	> 100
5.5	54.0	8.7
5.6	> 100	42.0
5.7	> 100	> 100
5.8	> 100	> 100
Efavirenz	40.0	0.002

[a] Data represent mean values for three independent determinations. Variation among duplicate samples (SD) was less than 15%. [b] Cytotoxic concentration (CC): Compound concentration (µM) required to reduce the viability of mock-infected MT-4 cells by 50%, as determined by the MTT method. Efavirenz is the reference drug. For extracts: µg/mL. [c] Effective concentration (EC): Compound concentration (µM) required to achieve 50% protection of MT-4 cells from the HIV-1 induced cytopathogeneticy, as determined by the MTT method. For extracts:µg/mL.

It is noteworthy to mention that its activity on some of the resistant strains is higher than that of the reference anti-HIV drug nevirapine (Table 5.4). The activity exhibited by the new compound **5.5** demonstrated its potential as anti-HIV drug and the role of natural products to provide unique chemical entities in drug discovery programs. Studies based on various coumarins from plant sources and their synthetic analogs indicate that some of them behave like potent non-nucleoside RT-inhibitors, other than inhibitors of HIV-integrase or HIV-protease (Kostova, 2006). However, the major approved anti-HIV drugs fall into five categories: the nucleoside/nucleotide reverse transcriptase inhibitors (NRTIs), the non-nucleoside reverse transcriptase inhibitors (NNRTIs), the protease inhibitors (PIs), entry inhibitors, and integrase inhibitors (Vicini *et al.*, 2009). Studies to identify the mode of action for dimeric coumarins as new anti-HIV-leads are ongoing.

Table 5.4. Cytotoxicity and antiviral activity of bichromonol (**5.5**) against HIV-1 and its NNRTI-(N119, A17, EFV^R) and NRTI-(AZT^R, MDR) resistant variants.

Bioassay (µM)		bichromonol (**5.5**)	nevirapine^c	azidothymidine^c	efavirenz^e
Cytotoxicity (CC$_{50}$)^a	MT-4	54.0	>100	>100	40
Anti-HIV activity against HIV-1$_{IIIB}$ and its resistant variants (EC$_{50}$)^b	HIV-1$_{IIIB}$	**8.7**	0.08	0.02	0.002
	N119 (Y1811C)	**6.7**	6.3	0.02	0.03
	A17 (K103N, Y181C)	**8.3**	80	0.01	0.08
	EFV^R (K103R, V179D, P225H)	**6.6**	100	0.02	12.0
	AZT^R (67N, 70R, 215F, 219Q)	**6.6**	0.07	0.3	0.003
	MDR (74V, 41L, 106A, 215Y)	**12.0**	5.0	0.08	0.01

^{a} Cytotoxicity concentration (CC): Compound concentration (µM) required to reduce the viability of mock-infected MT-4 cells by 50%, as determined by the MTT method. ^{b} Effective concentration (EC): Compound concentration (µM) required to achieve 50% protection of MT-4 cells from HIV-1 induced cytopathogenicity, as determined by the MTT method. ^{c} Efavirenz, azidothymidine, and nevirapine are the reference anti-HIV drugs.

In conclusion, the significant anti-HIV-1 activity of *H. roeperianum* stem bark extract supports its use in the Cameroonian traditional medicine by AIDS patients. However, further studies are still required to evaluate its toxicity, pharmacodynamics, and therapeutic benefits. The isolated compound **5.1** and bichromonol (**5.5**) might provide new anti-HIV leads.

5.3. Experimental

5.3.1. General experimental procedures

Column chromatography was run on silica gel (Merck, 63-200 and 40-63 µm) and Sephadex LH-20 (Fluka), while TLC was performed on precoated silica gel F_{254} plates (Merck). Spots were visualized with an UV lamp at 254 and 366 nm or by spraying with vanillin-H_2SO_4-MeOH followed by heating at 100 °C. Melting points were determined using a LEICA DM LS2 melting point instrument and were uncorrected.

UV spectra were obtained on a JASCO V-560 UV/VIS spectrophotometer. IR spectra were recorded using a Thermo Nicolet 5700 FT-IR spectrometer, in MeOH or $CHCl_3$. Optical rotations were measured using a JASCO P-2000 digital polarimeter.

^{1}H and ^{13}C NMR spectra were recorded on an Agilent DD2 400 NMR spectrometer at 400 and 100 or 150 MHz, respectively. High frequency (600 MHz) ^{1}H and 2D NMR spectra were recorded on an Agilent VNMRS 600 NMR spectrometer. The chemical shifts of ^{1}H spectra are given in ppm (δ), relative to TMS as internal standard and coupling constants (J) are in Hz. Chemical shifts of ^{13}C NMR spectra are referenced to $CDCl_3$ (δ_C 77.0) or CD_3OD (δ_C 49.0).

The low resolution electrospray (ESI) mass spectra were performed on a SCIEX API-3200 instrument (Applied Biosystems, Concord, Ontario, Canada) combined with a HTC-XT autosampler (CTC Analytics, Zwingen, Switzerland). The samples were introduced via autosampler and loop injection.

The positive and negative ion high resolution ESI mass spectra, respectively, of compounds **5.1** to **5.6** as well as the corresponding MS^n measurements of them were obtained from an Orbitrap Elite mass spectrometer (Thermofisher Scientific, Bremen, Germany) equipped with an HESI electrospray ion source (spray voltage 4 kV; capillary temperature 275 °C, source heater temperature 40 °C; FTMS resolution 60.000). Nitrogen was used as sheath gas. The sample solutions were introduced continuously via a 500 µl Hamilton syringe pump with a flow rate of 5µl min^{-1}. The data were evaluated by the Xcalibur software 2.7 SP1.

The positive ion high resolution ESI mass spectra of compounds **5.7** to **5.10** were obtained from a Bruker Apex III Fourier transform ion cyclotron resonance (FT-ICR) mass spectrometer (Bruker Daltonics, Billerica, USA) equipped with an Infinity™ cell, a 7.0 Tesla superconducting magnet (Bruker, Karlsruhe, Germany), an RF-only hexapole ion guide and an external electrospray ion

source (Agilent, off axis spray). Nitrogen was used as drying gas at 150 °C. The sample solutions were introduced continuously via a syringe pump with a flow rate of 120µl h^{-1}. The data were acquired with 512k data points, zero filled to 2048k by averaging 16 scans and evaluated using the Bruker XMASS software (Version 7.0.8).

The GC/EIMS measurements were performed on a QP-2010 Ultra (Shimadzu Corporation, Kyoto, Japan) by using the following conditions: electron energy 70 eV, detected mass range *m/z* 40-700; source temperature 200°C; column: ZB-5MS (Phenomenex, 30 m x 0.25 mm, 0.25 µm film thickness), injector temperature 220 °C, interface temperature 290 °C, carrier gas helium, column flow 0.9 mlmin^{-1}, flow control mode: linear velocity, split injection, split ratio 5.0, column temperature program: 170 °C for 1 min, then raised to 290 °C at a rate of 10 °C min^{-1}and then hold on 290 °C for 27 min. The trimethylsilylation was carried out by dissolving of a few µg of the sample in 5 µl dichloromethane and treatment with *ca.* 20 µl *N*-methyl-*N*-trimethylsilyltrifluoroacetamide (MSTFA) at 60 °C for 60 min. The obtained EI mass spectra were evaluated by the NIST 11 Mass Spectral Library.

5.3.2. Plant material

The stem bark of *Hypericum riparium* A. Chev. (*H. roeperianum* as accepted name) was collected in August 2011 at Mount Bamboutos (Mbouda) in the West Region of Cameroon. The plant was identified by Mr. Nana Victor, botanist at the National Herbarium of Cameroon where a voucher specimen (No. 33796/HNC) is deposited.

5.3.3. Extraction and isolation

The air-dried and powdered stem bark (1 kg) was exhaustively extracted with 80% MeOH (3 × 7.5 l) at room temperature for one day, including 30 min in ultrasound bath to speed up extraction, and filtered. After evaporation of the methanol in *vacuo*, the resulting aqueous phase was successively partitioned (3 x 3 l) with *n*-hexane (1.14 g), CHCl$_3$ (3.23 g), and EtOAc (1.61 g). These were evaporated to dryness to give the respective extracts.

The CHCl$_3$ extract (2.7 g) was subjected to silica gel column chromatography, eluted with step gradients of *n*-hexane-EtOAc and EtOAC-MeOH. Fractions were collected using a fraction collector (Retriever II). They were combined on the basis of their TLC profiles into 11 main fractions (Fr. 1-Fr. 11): Fr. 2 (171.4 mg), Fr. 3 (249.9 mg), Fr. 4 (60 mg), Fr. 5 (320 mg), Fr. 6 (320 mg), Fr. 7 (240 mg), Fr. 8 (161 mg), Fr. 9 (161 mg), Fr. 10 (210 mg), Fr. 11 (30 mg). Compound **5.2** (2 mg, R_f = 0.58 in *n*-hexane-EtOAc (1:1)) crystallized from Fr. 5. The filtrate

obtained from Fr. 5 (145.9 mg) was chromatographed on a silica gel column (0.04-0.063 mm, 99 g), eluted with CH_2Cl_2-MeOH (100:0, 98:2, 96:4, 90:10, 0:100) to yield, after combination, 7 sub-fractions (Fr. 5a-Fr. 5g): Fr. 5a (2 mg), Fr.5b (10.2 mg), Fr.5c (8.7 mg), Fr. 5d (28.3 mg), Fr.5e (63 mg), Fr. 5f (15.5 mg), Fr. 5g (25.5 mg). Fr. 5b eluted with 100% CH_2Cl_2 was dried to afford compound **5.6** (10.2 mg, R_f = 0.70 in CH_2Cl_2-MeOH (98:2)). Fr. 5e (63 mg), obtained from CH_2Cl_2-MeOH (98:2 and 96:4), was purified through Sephadex LH-20 column eluted with MeOH to afford bichromonol (**5.5**) (1.4 mg, R_f = 0.34 in CH_2Cl_2-MeOH (90:10)). Fr. 5g (25.5 mg) obtained from CH_2Cl_2-MeOH (10:90 and 0:100) was submitted to gel permeation chromatography through Sephadex LH-20, eluted with MeOH to yield compound **5.1** (trace, R_f = 0.42 in $CHCl_3$-MeOH (85:15)). Fr. 3 (249.9 mg) was subjected to column chromatography over silica gel (0.04-0.063 mm, 35 g) eluted with *n*-hexane containing increasing amounts of EtOAc (100:0, 95:5, 90:10, 80:20, 70:30, 60:40, 50:50, 40:60, and 0:100) and 100% MeOH to yield 10 fractions. Compound **5.3** (2 mg, R_f = 0.60 in *n*-hexane-EtOAc (1:1)) crystallized from fractions eluted with *n*-hexane-EtOAc (70:30 and 60:40). Fr. 7 (240 mg) was further chromatographed through a silica gel column using a stepwise gradient of CH_2Cl_2-MeOH (100:0, 98:2, 96:4, 94:6, 90:10, 80:20, 50:50, 0:100) as eluent to give 13 sub-fractions (Fr. 7a-Fr. 7m). Fr. 7k (CH_2Cl_2-MeOH (80:20 and 90:10)) was eluted with MeOH over Sephadex LH-20 to yield compound **5.4** (2.4 mg, R_f = 0.40 in CH_2Cl_2-MeOH (90:10)). Fr. 2 was trimethylsilylated and analyzed by GC-MS. The TMS derivatives of octadecanoic acid (**5.15**), campesterol (**5.16**), stigmasterol (**5.17**), sitosterol (**5.18**) and stigmastanol (**5.19**) were identified by comparing their EI-MS with those available in the NIST 11 Mass Spectral Library.

The *n*-hexane extract (1.18 g) was chromatographed over Sephadex LH-20 eluted with a mixture of *n*-hexane-CH_2Cl_2-MeOH (7:4:0.5) and then MeOH to give 7 major fractions (Fr. A-Fr. G) which were combined based on their TLC profiles. Fr. A (182 mg) was further chromatographed on silica gel, eluted with a gradient of *n*-hexane-EtOAc to afford compounds **5.9** (15 mg, R_f = 0.30 in *n*-hexane-EtOAc (90:10)) and **5.10** (2.7 mg, R_f = 0.27 in *n*-hexane-EtOAc (90:10)). Repeated chromatography of Fr. C (186.1 mg) on silica gel with a gradient of *n*-hexane-EtOAc yielded compounds **5.7** (2 mg, R_f = 0.22 in *n*-hexane-EtOAc (75:25)) and **5.8** (2.7 mg, R_f = 0.30 in *n*-hexane:EtOAc 75:25). Fr. D was trimethylsilylated and analyzed by GC-MS. The TMS ester or ether of tetradecanoic acid (**5.11**), pentadecanoic acid (**5.12**), hexadecanoic acid (**5.13**), cis-10-heptadecenoic acid (**5.14**), ß-eudesnol (**5.20**), 1-hexadecanol (**5.21**), and 1-octadecanol (**5.22**) were identified by comparing their EI-MS data with those available in the NIST 11 database.

7,7´-Dihydroxy-6,6´-biscoumarin (**5.1**):white crystal, m.p. 312-314°C; UV (MeOH), λ_{max} (log ε): 201 (3.98), 257 (3.51), 284 (3.42), 354 (3.41); IR (ATR) υ_{max} (cm^{-1}): 3278, 2922, 1728, 1603, 1495, 1388, 1225, 815, 735 cm^{-1}; ^{1}H NMR data see Table 5.1; ^{13}C NMR data see Table 5.2; negative ion ESI-FTMS [*m/z* (rel. int., %)]: [M-H]$^-$ at *m/z* 321.0411 (calcd. for $C_{18}H_9O_6^-$ 321.0405). MS^2 [*m/z* 321 (7)]: *m/z* 303.0303 [M-H-H$_2$O]$^-$(100, calcd. for $C_{18}H_7O_5^-$ 303.0299), 277.0510 [M-H-CO$_2$]$^-$ (25, calcd. for $C_{17}H_9O_4^-$ 277.0506), 275.0354 [M-H-H$_2$O-CO]$^-$ (34, calcd. for $C_{17}H_7O_4^-$ 275.0350).

7,7´-Dihydroxy-8,8´-biscoumarin (**5.2**): white crystal, m.p. 300-302 °C, $[\alpha]^{25}_D$ -5.5 (*c* 0.62 mM, CHCl$_3$); UV (MeOH),λ_{max} (log ε): 271 (1.56), 281 (1.67), 327 (1.02), 343 (0.92); IR (ATR) υ_{max} (cm^{-1}): 3378, 2922, 2851, 1731, 1615, 1600, 1457, 1258, 840, 763; ^{1}H NMR data see Table 5.1; ^{13}C NMR data see Table 5.2; negative ion ESI-FTMS [*m/z* (rel. int., %)]: [M-H]$^-$ at *m/z* 321.0414 (calcd. for $C_{18}H_9O_6^-$, 321.0405). MS^2 [*m/z* 321 (8)]: *m/z* 303.0306 [M-H-H$_2$O]$^-$ (100, calcd. for $C_{18}H_7O_5^-$ 303.0299), 277.0513 [M-H-CO$_2$]$^-$ (72, calcd. for $C_{17}H_9O_4^-$ 277.0506), 275.0354 [M-H-H$_2$O-CO]$^-$ (35, calcd. for $C_{17}H_7O_4^-$ 275.0350), 233.0613 [M-H-2CO$_2$]$^-$ (13, calcd. for $C_{16}H_9O_2^-$ 233.0608).

7-Methoxy-6,7´-dicoumarinyl ether (**5.3**): white crystal, m.p. 115-117 °C; UV (MeOH), λ_{max} (log ε): 295 (1.78), 326 (1.98); IR (ATR) υ_{max} (cm^{-1}): 1727, 1613, 1558, 1502, 1288, 1229, 987, 853, 750; ^{1}H NMR data see Table 5.1; ^{13}C NMR data see Table 5.2; positive ion ESI-FTMS [*m/z* (rel. int., %)]: [M+H]$^+$ at *m/z* 337.0712 (calcd. for $C_{19}H_{13}O_6^+$, 337.0707). MS^2 [*m/z* 337 (54)]: *m/z*322.0481 [M+H-Me]$^+$ (100, calcd. for $C_{18}H_{10}O_6^+$322.0472). MS^3 [*m/z* 322 (0)]: 321.0403 [M+H-CH$_4$]$^+$ (40, calcd. for $C_{18}H_9O_6^+$ 321.0394), 305.0454 [M+H-Me-OH]$^+$ (72, calcd. for $C_{18}H_9O_5^+$ 305.0444), 294.0532 [M+H-Me-CO]$^+$ (100, calcd. for $C_{17}H_{10}O_5^+$ 294.0523), 293.0454 [M+H-CH$_4$-CO]$^+$ (60, calcd. for $C_{17}H_9O_5^+$ 293.0444), 277.0504 [M+H-Me-OH-CO]$^+$ (43, calcd. for $C_{17}H_9O_4^+$ 277.0495), 265.0504 [M+H-CH$_4$-2CO]$^+$ (84, calcd. for $C_{16}H_9O_4^+$ 265.0495).

2´-Hydroxy-5´-(7-methoxycoumarin-6´´-yl)-4´-methoxyphenylpropanoic acid (**5.4**): white yellowish crystal, m.p. 162-164 °C, $[\alpha]^{25}_D$ +5.1 (*c* 6.5 mM, MeOH); UV (MeOH), λ_{max} (log ε): 200 (2.13), 286 (1.31), 324 (1.21); IR (ATR) υ_{max} (cm^{-1}): 3402, 2924, 2851, 1713, 1613, 1560, 1510, 1231, 1201, 975, 826, 770; ^{1}H NMR data see Table 5.1; ^{13}C NMR data see Table 5.2; negative ion ESI-FTMS [*m/z* (rel. int., %)]: [M-H]$^-$ at *m/z* 369.0988 (calcd. for $C_{20}H_{17}O_7^-$, 369.0980). MS^2 [*m/z* 369 (3)]: *m/z* 351.0879 [M-H-H$_2$O]$^-$ (61, calcd. for $C_{20}H_{15}O_6^-$ 351.0874), 337.0722 [M-H-MeOH]$^-$ (29, calcd. for $C_{19}H_{13}O_6^-$ 337.0718), 325.1087 [M-H-CO$_2$]$^-$ (100, calcd. for $C_{19}H_{17}O_5^-$ 325.1081), 310.0852 [M-H-CO$_2$-Me]$^-$ (13, calcd. for $C_{18}H_{14}O_5^-$ 310.0847), 305.0461 [M-H-2MeOH]$^-$ (23,

calcd. for $C_{18}H_9O_5^-$ 305.0455). MS^3 [*m/z* 351 (2)]: 336.0644 [M-H-H_2O-Me]$^-$ (100, calcd. for $C_{19}H_{12}O_6^-$ 336.0639), 335.0563 [M-H-H_2O-CH_4]$^-$ (37, calcd. for $C_{19}H_{11}O_6^-$ 335.0561), 323.0930 [M-H-H_2O-CO]$^-$ (30, calcd. for $C_{19}H_{15}O_5^-$ 323.0925), 305.0462 [M-H-H_2O-Me-OMe]$^-$ (28, calcd. for $C_{18}H_9O_5^-$ 305.0455). MS^4 [*m/z* 310(0)]: 279.0668 [M-H-CO_2-Me-OMe]$^-$ (100, calcd. for $C_{17}H_{11}O_4^-$ 279.0663). MS^5 [*m/z* 279 (0)]: 264.0432 [M-H-CO_2-2Me-OMe]$^-$ (100, calcd. for $C_{16}H_8O_4^-$ 264.0428).

Bichromonol (**5.5**), *6,7´-dihydroxy-7-methoxy-8,8´-biscoumarin*: yellow amorphous powder; $[\alpha]^{25}_D$ -81.7 (*c* 6 mM, MeOH); UV (MeOH), λ_{max} (log ε): 287 (1.49), 321 (1.51) nm; IR (ATR) υ_{max} (cm^{-1}): 3353, 2940, 2937, 1698, 1599, 1503, 1452, 1426, 1398, 1316, 1240, 1144, 1121, 1018, 834, 759; ^1H NMR data see Table 5.1; ^{13}C NMR data see Table 5.2; negative ion ESI-FTMS [*m/z* (rel. int., %)]: [M-H]$^-$ at *m/z* 351.0525 (calcd. for $C_{19}H_{11}O_7^-$, 351.0510). MS^2 [*m/z* 351 (48)]: *m/z* 319.0253 [M-MeOH]$^-$ (100, calcd for $C_{18}H_7O_6^-$, 319.0248). MS^3 [*m/z* 319 (100)]: *m/z* 291.0305 [M-MeOH-CO]$^-$ (100, calcd for $C_{17}H_7O_5^-$, 291.0299), 275.0357 [M-MeOH-CO_2]$^-$ (16, calcd for $C_{17}H_7O_4^-$, 275.0305). MS^4 [*m/z* 291 (100)]: *m/z* 263.0357 [M-MeOH-CO-CO]$^-$ (100, calcd for $C_{16}H_7O_4^-$, 263.0305), 247.0400 [M-MeOH-CO-CO_2]$^-$ (14, calcd for $C_{16}H_7O_3^-$, 247.0401). MS^5 [*m/z* 263 (100)]: *m/z* 235.0409 [M-MeOH-CO-CO-CO]$^-$ (100, calcd for $C_{15}H_7O_3^-$, 235.0401).

7,7´-Dimethoxy-6,6´-biscoumarin (**5.6**): white crystal, m.p. 318-320 °C; IR (ATR) υ_{max} (cm^{-1}): 2919, 1742, 1602, 1560, 1488, 1264, 1206, 985, 887, 817, 746; ^1H NMR data see Table 5.1; ^{13}C NMR data see Table 5.2; positive ion ESI-FTMS [*m/z* (rel. int., %)]: [M+H]$^+$ at *m/z* 351.0868 (calcd. for $C_{20}H_{15}O_6^+$ 351.0863). MS^2 [*m/z* 351 (23)]: *m/z* 305.0453 [M+H-Me-OMe]$^+$ (100, calcd. for $C_{18}H_9O_5^+$ 305.0444). MS^3 [*m/z* 305 (29)]: *m/z* 277.0503 [M+H-Me-OMe-CO]$^+$ (79, calcd. for $C_{17}H_9O_4^+$ 277.0495), 261.0554 [M+H-Me-OMe-CO_2]$^+$ (83, calcd. for $C_{17}H_9O_3^+$ 261.0546), 249.0554 [M+H-Me-OMe-2CO]$^+$ (100, calcd. for $C_{16}H_9O_3^+$ 249.0546). MS^4 [*m/z* 249 (29)]: *m/z* 221.0605 [M+H-Me-OMe-3CO]$^+$ (100, calcd. for $C_{15}H_9O_2^+$ 221.0597).

2´-Methoxyflavone (**5.7**): yellow gum; IR (ATR) υ_{max} (cm^{-1}): 2923, 1618, 1465, 1369, 1251, 748, 665; ^1H NMR (CDCl$_3$, 400 MHz): 8.24 (1H, *dd*, 7.9/1.8 Hz, H-5), 7.91 (1H, *dd*, 7.9/1.8, H-6´), 7.68 (1H, *ddd*, 8.3/7.0/1.8 Hz, H-7), 7.53 (1H, *dd*, 8.3/0.9 Hz, H-8), 7.49 (1H, *ddd*, 8.8/7.5/1.8, H-4´), 7.41 (1H, *td*, 7.9/7.0/0.9 Hz, H-6),) 7.15 (1H, *s*, H-3), 7.11 (1H, *td*, 7.5/0.9 Hz, H-5´), 7.06 (1H, *d*, 8.8 Hz, H-3´), 3.95 (3H, *s*, 2´-OMe); ^{13}C NMR (CDCl$_3$, 100 MHz): 178.9 (C-4), 160.9 (C-2), 158.0 (C-2´), 156.5 (C-9), 133.5 (C-7), 132.4 (C-4´), 129.3 (C-6´), 125.6 (C-5), 124.9 (C-6), 123.8 (C-10), 120.8 (C-5´), 120.7 (C-1´), 118.0 (C-8), 112.7 (C-3), 111.8 (C-3´), 55.7 (2´-OMe); positive ion ESI-FTICR-MS: [M+H]$^+$ at *m/z* 253.0858 (calcd. for $C_{16}H_{13}O_3^+$, 253.0859).

3´-Methoxyflavone (**5.8**): yellow gum; IR (ATR) υ_{max}(cm^{-1}): 2922, 1708, 1626, 1605, 1570, 1214, 749, 667; ^{1}H NMR (CDCl$_3$, 400 MHz): 8.24 (1H, *dd*, 7.9/1.3, H-5), 7.71 (1H, *m*, H-7), 7.58 (1H, *d*, 8.3 Hz, H-8), 7.53 (1H, *m*, H-6´), 7.46-7.42 (3H, *m*, H-6/H-2'/H-5´), 7.09 (1H, *dd*, 8.3/2.2, H-4´), 6.84 (1H, *s*, H-3), 3.91 (3H, *s*, 3´-OMe); ^{13}C NMR (CDCl$_3$, 100 MHz): 178.5 (C-4), 163.3 (C-2), 160.0 (C-3´), 156.3 (C-9), 133.8 (C-6), 133.2 (C-1´), 130.1 (C-5´), 125.7 (C-5), 125.3 (C-6), 124.0 (C-10), 118.8 (C-6´), 118.1 (C-8), 117.2 (C-4´), 111.8 (C-2´), 107.8 (C-3), 55.5 (3´-OMe); positive ion ESI-FTICR-MS: [M+Na]$^+$ at *m/z* 275.0678 (calcd. for C$_{16}$H$_{12}$O$_3$Na$^+$, 275.0679).

Stigmast-4-en-3-one (**5.9**): white powder; IR (ATR) υ_{max} (cm^{-1}): 2933, 1671, 1615, 1463, 1228, 1186, 865, 751; ^{1}H NMR (CDCl$_3$, 400 MHz): 5.72 (1H, *brs*,H-4), 1.18 (3H, *s*, H-19), 0.92 (3H, *d*, 6.6 Hz, H-21), 0.85 (3H, *t*, 7.5 Hz, H-29), 0.84 (3H, *d*, 7.5 Hz, H-26), 0.82 (3H, *d*, 7.0 Hz, H-27), 0.71 (3H, *s*, H-18); ^{13}C NMR (CDCl$_3$, 100 MHz): 199.6 (C-3), 171.7 (C-5), 123.7 (C-4), 56.0 (C-17), 55.9 (C-14), 53.8 (C-9), 45.8 (C-24), 42.3 (C-13), 39.6 (C12), 38.6 (C-10), 36.1 (C-20), 35.7 (C-1), 35.6 (C-8), 34.0 (C-22), 33.9 (C-2), 33.0 (C-6), 32.1 (C-7), 29.1 (C-25), 28.2 (C-16), 26.0 (C-23), 24.2 (C-15), 23.1 (C-28), 21.0 (C-11), 19.8 (C-26), 19.0 (C-27), 18.7 (C-21), 17.4 (C-19), 12.0 (C-18), 11.9 (C-29);positive ion ESI-FTICR-MS: [M+Na]$^+$ at *m/z* 435.3597 (calcd. for C$_{29}$H$_{48}$ONa$^+$, 435.3597).

Ergosta-4,6,8,22-tetraen-3-one (**5.10**): yellow oil; IR (ATR) υ_{max} (cm^{-1}): 2922, 1738, 1663, 1585, 1460, 1193, 970, 755; ^{1}H NMR (CDCl$_3$, 400 MHz): 6.61 (1H, *d*, 9.2 Hz, H-6), 6.03 (1H, *d*, 9.2, H-7), 5.74 (1H, *s*), 5.23 (2H, *m*), 1.06 (3H, *d*, 6.6 Hz, H-24), 1.00 (3H, *s*, H-19), 0.96 (3H, *s*, H-18), 0.93 (3H, *d*, 7.0 Hz, H-27), 0.85 (3H, *d*, 6.6 Hz, H-26), 0.82 (3H, *d*, 7.0 Hz, H-21); ^{13}C NMR (CDCl$_3$, 100 MHz): 199.5 (C-3), 164.4 (C-5), 156.1 (C-8), 135.0 (C-22), 134.0 (C-7), 132.5 (C-23), 124.5 (C-6), 124.4 (C-9), 123.0 (C-4), 55.7 (C-17), 44.3 (C-14), 44.0 (C-13), 42.9 (C-24), 39.3 (C-20), 36.8 (C-10), 35.6 (C-12), 34.1 (C-1), 34.1 (C-2), 33.1 (C-25), 29.7 (C-11), 27.7 (C-16), 25.4 (C-15), 21.2 (C-26), 20.0 (C-27), 19.7 (C-21), 19.0 (C-19), 17.6 (C-24´), 16.4 (C-18); positive ion ESI-FTICR-MS: [M+Na]$^+$ at *m/z* 415.2971 (calcd. for C$_{28}$H$_{40}$ONa$^+$, 415.2971).

Tetradecanoic acid, trimethylsilyl ester (**5.11**): RT = 6.20 min, EIMS *m/z* (rel. int. %): 300 [M]$^+$ (10) for C$_{17}$H$_{36}$O$_2$Si$^+$, 285 (80), 257 (6), 145 (15), 132 (41), 117 (100), 73 (62).

n-Pentadecanoic acid, trimethylsilyl ester (**5.12**): RT = 6.82 min, EIMS *m/z* (rel. int. %): 314 [M]$^+$ (9)for C$_{18}$H$_{38}$O$_2$Si$^+$, 299 (99), 145 (32), 132 (32), 117 (100), 73 (65), 55 (18).

Hexadecanoic acid, trimethylsilyl ester (**5.13**): RT = 7.94 min, EIMS *m/z* (rel. int. %): 328 [M]$^+$ (10) for C$_{19}$H$_{40}$O$_2$Si$^+$, 313 (95), 285 (7), 145 (26), 132 (52), 117 (100), 73 (78).

cis-10-Heptadecenoic acid, trimethylsilyl ester (**5.14**): RT = 8.68 min, EIMS *m/z* (rel. int. %): 340 [M]$^+$ (-) for $C_{20}H_{40}O_2Si^+$, 250 (11), 169 (23), 145 (21), 129 (25), 117 (45), 73 (100), 69 (20), 55 (22).

Octadecanoic acid, trimethylsilyl ester (**5.15**): RT = 9.66 min, EIMS *m/z* (rel. int. %): 342 [M]$^+$ (-) for $C_{21}H_{44}O_2Si^+$, 356 (15), 341 (98), 201 (11), 145 (28), 132 (55), 117 (100), 73 (62).

Campesterol, trimethylsilyl ether (**5.16**): RT = 20.14 min, EIMS *m/z* (rel. int. %): 472[M]$^+$ (48) for $C_{31}H_{56}OSi^+$, 382 (100), 367 (37), 343 (69), 255 (20), 207 (40), 129 (84), 121 (34).

Stigmasterol, trimethylsilyl ether (**5.17**): RT = 20.62 min, EIMS *m/z* (rel. int. %): 484 [M]$^+$ (51) for $C_{32}H_{56}OSi^+$, 394 (58), 379 (19), 255 (45), 129 (49), 83 (100), 69 (33), 55 (36).

ß-Sitosterol, trimethylsilyl ether (**5.18**): RT = 21.69 min, EIMS *m/z* (rel. int. %): 486 [M]$^+$ (56) for $C_{32}H_{58}OSi^+$, 471 (12), 396 (100), 381 (35), 357 (74), 255 (21), 129 (86), 121 (29), 95 (33), 73 (30).

Stigmastanol, trimethylsilyl ether (**5.19**): RT = 22.17 min, EIMS *m/z* (rel. int. %): 488 [M]$^+$ (61) for $C_{32}H_{60}OSi^+$, 473 (74), 431 (19), 398 (41), 383 (40), 306 (29), 230 (16), 215 (100), 121 (23), 107 (27), 95 (30), 75 (59).

ß-Eudesnol (**5.20**): RT = 4.96 min, EIMS *m/z* (rel. int. %): 222 [M]$^+$ (4) for $C_{15}H_{26}O^+$, 207 (8), 189 (18), 164 (25), 149 (67), 135 (9), 122 (32), 108 (36), 93 (25), 79 (24), 59 (100).

1-Hexadecanol, trimethylsilyl ether (**5.21**): RT = 6.85 min, EIMS *m/z* (rel. int. %): 314 [M]$^+$ (0) for $C_{19}H_{42}OSi^+$, 299 (100), 103 (17), 97 (26), 75 (34), 69 (16), 43 (9).

1-Octadecanol, trimethylsilyl ether (**5.22**): RT = 8.91 min, EIMS *m/z* (rel. int. %): 342 [M]$^+$(0) for $C_{21}H_{46}OSi^+$, 327 (100), 125 (5), 103 (12), 97 (17), 75 (28), 57 (13), 55 (8).

5.3.4. Cytotoxicity assays

The human prostate cancer cell line PC-3 and the colon cancer cell line HT-29 were maintained in RPMI 1640 medium supplemented with 10 % fetal bovine serum, 1 % L-alanyl-L-glutamine (200 mM) and 1,6 % hepes (1 M). 5×10^2 PC-3 cells and 1.5×10^3 HT-29 cells were seeded overnight into 96-well plates and exposed to a serial dilution of each compound (10 µM and 10 nM) and extract (50 and 0.50 µgml^{-1}) for three days. The *n*-hexane and CHCl$_3$ extracts show respectively 88 (or -46) and 66 % (or -42 %) inhibition of the proliferation on HT-29 cell lines and PC-3 cell growth inhibition of 90 (37) and 68 (15) % at concentration of 50 µgml^{-1} (0.50 µgml^{-1}).

Cytotoxicity was determined utilizing modified XTT method (0.25 mgml^{-1} XTT, 6.5 µM PMS) (Scudiero *et al.*, 1988).

5.3.5. Cytotoxicity against MT-4 cells and anti-HIV activity

See Section 4.5 (Chapter 4) for general cytotoxic and anti-HIV activitiy.

5.3.6. Computational methods

The three dimensional structure of compound **5.5** was constructed using MOE 2013.0801. A conformational search by rotating the bond 8-8´ and the C7-OMe group with energy optimization was carried out with the Merck molecular force field (MMFF) (Halgren, 1996). Subsequently, all quantum mechanical calculations were performed with TURBOMOLE 6.5 using the graphical interface TmoleX. The force field minimum-energy structures were optimized with DFT-B3LYP (TZVPP) (Stephens *et al.*, 1994). The CD spectra were calculated with the same method and basis set using Time-dependent density functional theory (TD-DFT) in TURBOMOLE. Visualization and comparison of the calculated spectra with the experimental one was performed with SpecDis Version 1.61 (Bruhn *et al.*, 2013).

Appendix. Supporting Information (this is available online)

A supplemental data associated with this chapter can be found in the online and published part at http://www.sciencedirect.com/science/article/pii/S003194221400199X.

References

Ang'edu, C.A., Schmidt, J., Porzel, A., Gitu, P., Midiwo, J.O., Adam, G., **1999**. Coumarins from *Hypericum keniense* (Guttiferae). *Pharmazie* 54, 235-236.

Baba, K., Taniguti, M., Yoneda, Y., Kozawa, M., **1990**. Coumarin glycosides from *Edgeworthia chrysantha*. *Phytochemistry* 29, 247-249.

Basa, S.C., **1988**. Natural biscoumarins. *Phytochemistry* 27, 1933-1941.

Budzianowski, J., Morozowska, M., Wesolowska, M., **2005**. Lipophilic flavones of *Primula veris* L. from field cultivation and *in vitro* cultures. *Phytochemistry* 66, 1033-1039.

Bruhn, T., Schaumlöffel, A., Hemberger, Y., Bringmann, G., **2013**. SpecDis: quantifying the comparison of calculated and experimental electronic circular dichroism spectra. *Chirality* 25, 243-249.

Crockett, S.L., Robson, N.K.B., **2011**. Taxonomy and chemotaxonomy of the genus *Hypericum. Medicinal Aromatic Plant Sci. Biotech.* 5, 1-13.

Crispin, M.C., Hur, M., Park, T., Kim, H.Y., Wurtele, E. S., **2013**. Identification and biosynthesis of acylphloroglucinols in *Hypericum gentianoides. Physiol. Plant.*148, 354-370.

Chorot, V., Ropletal, L., Jahodar, L., Patel, A.V., Dacke, C.G., Blunden, G., **1997**. Ergosta-4,6,8,22-tetraen-3-one from the edible fungus, *Pleurotus ostreatus* (oysterfungus). *Phytochemistry* 48, 1669-1671.

Farag, M.A., Wessjohann, L.A., **2012**. Metabolome classification of commercial *Hypericum perforatum* (St. John's Wort) preparations via UPLC-qTOF-MS and chemometrics. *Planta Med*. 78, 488-496.

Farag, M.A., Weigend, M., Luebert, F., Brokamp, G., Wessjohann, L.A., **2013**. Phytochemical, phylogenetic, and anti-inflammatory evaluation of 43 *Urtica* accessions (stinging nettle) based on UPLC–Q-TOF-MS metabolomic profiles. *Phytochemistry* 96, 170–183.

Franke, K., Porzel, A., Schmidt, J., **2002**. Flavone-coumarin hybrids from *Gnidia socotrana*. *Phytochemistry* 61, 873-878.

Halgren, T.A., **1996**. Merck molecular force field. I. Basis, form, scope, parameterization, and performance of MMFF94. *J. Comp. Chem.* 17, 490-519,

Heinke, R., Franke, K. Michels, K., Ali, N.A.A., Wessjohann, L., Schmidt, J., **2012**. Analysis of Furanocoumarins from Yemenite *Dorstenia* Species by Liquid Chromatography/Electrospray Tandem Mass Spectrometry. *J. Mass Spectrom.* 47, 7-22.

Hou, W.-R., Su, Z.-Q., Pi, H.-F., Yao, G.-M., Zhang, P., Luo, X., Xie, S.-N., Xiang, M., **2010**. Immunosuppressive constituents from *Urtica dentata* Hand. *J. Asian Nat. Prod. Res.* 12, 707-713.

Ioset, J.-R., Marston, A., Gupta, M.P., Hostettmann, K., **2000**. Antifungal and larvicidal compounds from the root bark of *Cordia alliodora*. *J. Nat. Prod.* 63, 424-426.

Kang, J., Zhou, L., Sun, J., Han, J., Guo, D.-A., **2008**. Chromatographic fingerprint analysis and characterization of furocoumarins in the roots of *Angelica dahurica* by HPLC/DAD/ESI-MS^n technique. *J. Pharm. Biomed. Anal.* 47, 778-785.

Klingauf, P., Beuerle, T., Mellenthin, A., El-Moghazy, S.A.M., Boubakir, Z., Beerhues, L., **2005**. Biosynthesis of the hyperforin skeleton in *Hypericum calycinum* cell cultures. *Phytochemistry* 66, 139-145.

Kostova, L., **2006**. Coumarins as inhibitors of HIV reverse transcriptase. *Curr. HIV. Res.* 4, 347-363.

Li, W.-S., Wu, S.-Li., **1997**. Xanthones and triterpenoids from *Hypericum geminiflorum*. *Chin. Pharmaceut. J. (Taipei)* 49, 145-156.

Mabberley, D.J., **1997**. The Plant-Book. A portable dictionary of the vascular plants, 2nd ed. Cambridge University Press, Cambridge (UK).

Marumoto, M., Miyazawa, M., **2001**. Microbial reduction of coumarin, psoralen, and xanthyletin by *Glomerella cingulata*. *Tetrahedron* 67, 495-500.

Nedialkov, P.T., Dimitrova, D.-Z., Girreser, U., Kitanov, G.M., **2007**. A new isocoumarin from *Hypericum annulatum*. *Nat. Prod. Res.* 21, 1056-1060.

Porzel, A., Farag, M.A., Mülbradt, J., Wessjohann, L.A., **2014**. Metabolite profiling and fingerprinting of *Hypericum* species: A comparison of MS and NMR metabolomics. *Metabolomics* 10, 574-588.

Rahmani, M., Taufiq-Yap, Y.H., Ismail, H.B.M., Sukari, A., Waterman, P.G., **1994**. New coumarin and dihydrocinnamic acid derivatives from two Malaysian populations of *Micromelum minutum*. *Phytochemistry* 32, 561-564.

Sarris, J., **2007**. Herbal medicines in the treatment of psychiatric disorders: a systematic review. *Phytother. Res.* 21, 703-716.

Schmidt, S., Jürgenliemk, G., Skaltsa, H., Heilmann, J., **2012**. Phloroglucinol derivatives from *Hypericum empetrifolium* with antiproliferative activity on endothelial cells. *Phytochemistry* 77, 218-225.

Scudiero, D.A., Schoemaker, R.H., Monks, A., Tierney, S., Nofziger, T.H., Currens, M.J., Seniff, D., Boyd, M.R., **1988**. Evaluation of a soluble tetrazolium/formazan assay for cell growth and drug sensitivity in culture using human and other tumor cell lines. *Cancer Res*. 48, 4827-4833.

Shiu, W.K.P., Gibbons, S., **2009**. Dibenzofuran and pyranone metabolites from *Hypericum revolutum* ssp. *revolutum* and *Hypericum choisianum*. *Phytochemistry* 70, 403-406.

Stephens, P.J., Devlin, F.J., Chabalowski, C.F., Frisch, M.J.J., **1994**. Ab Initio calculation of vibrational absorption and circular dichroism spectra using density functional force fields. *Phys. Chem*. 98, 11623-11627.

Tala, M.F., Tchakam, P.D., Wabo, H.K., Talontsi, F.M., Tane, P., Kuiate, J.R., Tapondjou, L.A., Laatsch, H., **2013**. Chemical constituents, antimicrobial and cytotoxic activities of *Hypericum riparium* (Guttiferae). *Rec. Nat. Prod*. 7, 65-68.

Tanaka, N., Kashiwada, Y., Kim, S.-Y., Sekiya, M., Ikeshiro, Y., Takaishi, Y., **2009**. Xanthones from *Hypericum chinense* and their cytotoxicity activity evaluation. *Phytochemistry* 70, 1456-1461.

Vicini, P., Matteo I., La Colla, P., Loddo, R., **2009**. Anti-HIV evaluation of benzo[*d*]isothiazole hydrazones. *Eur. J. Med.Chem*. 44, 1801-1809.

Wabo, H.K., Kowa, T.K., Lonfouo, A.H.N., Tchinda, A.T., Tane, P., Kikuchi, H., Frederich, M., Oshima, Y., **2012**. Phenolic compounds and terpenoids from *Hypericum lanceolatum*. *Rec. Nat. Prod.* 6, 94-100.

Wirz, A., Simmen, U., Heilmann, J., Calis, I., Meier, B., Sticher, O., **2000**. Bisanthraquinone glycosides of *Hypericum perforatum* with binding inhibition to CRH-1 receptors. *Phytochemistry* 55, 941-947.

Wu, Q.-L., Wang, S.-P., Du, L.-J., Xiao, P.-G., **1998**. Xanthones from *Hypericum japonicum* and *H. henryi*. *Phytochemistry* 49, 1395-1402.

Yang, W., Ye, M., Liu, M., Kong, D., Shi, R., Shi, X., Zhang, K., Wang, Q., Lantong, Z., **2010**. A practical strategy for the characterization of coumarins in *Radix Glehniae* by liquid chromatography coupled with triple quadrupole-linear ion trap mass spectrometry. *J. Chromatogr. A* 1217, 4587-4600.

Chapter 6

Prenylated phenyl polyketides and acylphloroglucinols from *Hypericum peplidifolium*

Graphical abstract*

Ten acetophenone derivatives including new pyranones and furans, along with known acylphloroglucinol type-compounds were isolated from the chemically unexplored *Hypericum peplidifolium*.

antifungal pyranone   **unusual prenylated furan**   **prenylated phenyl polyketide**
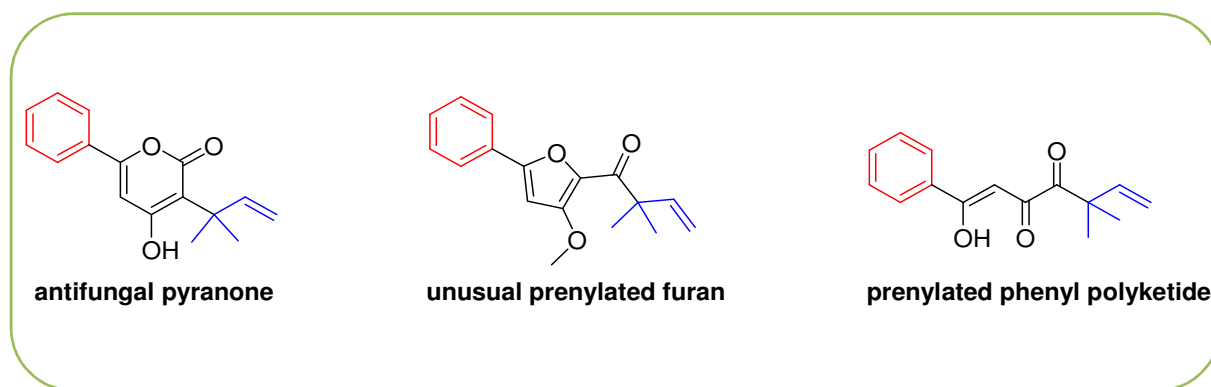
Highlights

- First report on constituents and biological activity of *Hypericum peplidifolium*
- Detection of an unusual prenylated furan ring from the genus *Hypericum*
- Isolation, characterization, and bioactivity evaluation of phenyl polyketides and acylphloroglucinols
- Complete structural elucidation by HR-MS, 1D- and 2D-NMR
- Occurrence of rare methylated acylphloroglucinols

Abstract

In search for new or chemo-taxonomically relevant bioactive compounds from chemically unexplored *Hypericum* species, four previously undescribed natural products, named peplidiforones A-D were isolated and characterized from *Hypericum peplidifolium* A. Rich., together with six known compounds. The structures of all compounds were elucidated by extensive 1D- and 2D-NMR experiments, high resolution mass spectrometric analyses (HR-MS), and by comparison with data reported in the literature. Seven of these compounds are phenyl polyketides while three are acylphloroglucinol type compounds. Peplidiforone C, which possesses an unusual carbon skeleton consisting of a furan ring substituted by a 2,2-dimethylbut-3-enoyl moiety, is the first example of a prenylated furan derivative isolated from the genus *Hypericum*. The cytotoxicity, antifungal, and anti-herpes simplex virus type 1 (HSV-1) activities of extracts and compounds are described.

Keywords: *Hypericum peplidifolium*; Hypericaceae; polyketide derivatives; furans; pyranones; prenylated natural products.

6.1. Introduction

The genus *Hypericum* belongs to the family Hypericaceae and comprises more than 450 species widely occurring in temperate regions of the world and tropical highlands (Mabberley, 1997; Crockett and Robson, 2011). The discovery of the anti-depressive properties of St. John's wort (*Hypericum perforatum*) fostered the widespread interest in the genus *Hypericum* (Sarris, 2007). However, only a small proportion of the *Hypericum* species, other than the popular medicinal supplement St. John's wort, have even been chemically characterized (Fobofou *et al*., 2014; Crispin *et al*., 2013; Porzel *et al*., 2014). The most common secondary metabolites found within the genus *Hypericum* include dianthrones, flavonoids, anthraquinones, xanthones, coumarins, benzophenones, phloroglucinols, and less frequently chalcones, benzopyrans, steroids and terpenoids (Fobofou *et al*., 2014; Ang'edu *et al*., 1999; Schmidt *et al*., 2012a; Shiu and Gibbons, 2009; Tanaka *et al*., 2009; Wabo *et al*., 2012; Wirz *et al*., 2000; Wu *et al*., 1998). In the aforementioned references, biological activities of these compounds such as antimicrobial, cytotoxic, anti-depressive, anti-oxidant, and anti-inflammatory effects were also reported.

Hypericum species are used in the Cameroonian folk medicine for the treatment of tumors, epilepsy, microbial diseases, and mental disorders (Tala *et al*., 2013, Wabo *et al.,* 2012). *Hypericum peplidifolium* A.Rich. (sect. *Humifusoideum*) is a perennial herb occurring in a mountainous region of West Cameroon (Central Africa) and which is endemic to sub-Saharan Africa in general. To the best of our knowledge, there is no previous report on its chemistry, or biological activity of its extract or constituents. As part of our ongoing efforts to explore secondary metabolites from the genus *Hypericum* and the Hypericaceae family in general (Fobofou *et al.,* 2015a, b; Fobofou *et al*., 2014; Porzel *et al*., 2014; Farag and Wessjohann, 2012; Ang'edu *et al*., 1999), we have investigated chemical constituents from the whole plant of *H. peplidifolium* for the first time. In the course of our study, we isolated and characterized seven mono-substituted phenyl derivatives (**6.1-6.7**) including four new compounds named peplidiforones A-D (**6.1-6.4**), together with three known acylphloroglucinols (**6.8-6.10**). Furthermore, the cytotoxic, antifungal, and antiviral activities of compounds **6.1-6.10** were investigated.

6.2. Results and discussion

The EtOAc extract, obtained by liquid-liquid partition from the crude extract of *H. peplidifolium*, was fractionated by column chromatography on silica gel and purified through reverse phase (RP18) HPLC to afford compounds **6.1-6.10.**

Peplidiforone A (**6.1**) has a molecular formula of $C_{16}H_{16}O_3$ calculated from its negative ion HR-ESI-MS displaying an $[M-H]^-$ ion at *m/z* 255.1035 (calcd. 255.1027 for $C_{16}H_{15}O_3^-$). The ^1H NMR spectrum (Table 6.1) reveals signals of a reverse *C*-prenyl chain (Heinke *et al.,* 2011) at δ_H 6.45 (1H, *dd*, *J* = 17.9, 10.5 Hz, H-2´´), 5.55 (1H, *d*, *J* = 17.9 Hz, H-3´´a), 5.45 (1H, *d*, *J* = 10.5 Hz, H-3´´b), and δ_H 1.56 (2 × 3H, *s*, 3H-4´´ and 3H-5´´) as well as a signal of one hydroxyl group at δ_H 7.83 (1H, *s*, 4-OH) and characteristic signals of the aromatic ring and singlet proton of a 6-phenyl-3,4-(disubstituted)-pyran-2-one at δ_H 7.78 (2H, *m*, H-2´ and H-6´), 7.43 (3H, *m*, H-3´, H-4´, and H-5´), and δ_H 6.32 (1H, *s*, H-5) (Kikuchi *et al.,* 1985a; Kikuchi *et al.,* 1985b). The ^{13}C NMR (Table 6.1) spectrum exhibits sixteen carbon signals, which were sorted by DEPT and HSQC experiments into six quaternary, seven methine, one methylene, and two methyl carbons. The oxygenated carbon signals at δ_C 165.1 (C-4), 162.6 (C-2), and 158.4 (C-6) agree with the presence of a 4-hydroxy-3,6-(disubstituted)-pyran-2-one in the molecule as previously reported for similar compounds (Hohmann *et al.,* 2009; Sun *et al.,* 2014). The chemical shifts and multiplicities of ^1H NMR data of **6.1** are very similar to those of hyperenone B, a 4*H*-pyran-4-one derivative with the molecular formula $C_{16}H_{16}O_3$ isolated from *Hypericum mysorense* (^{13}C NMR data were not reported for hyperenone B) (Kikuchi *et al.,* 1985b). Peplidiforone A (**6.1**) and hyperenone B represent tautomers with the same substitution pattern differing only with respect to the position of the hydroxyl and carbonyl groups at the pyran nucleus. In fact, all proton and carbon signals of **6.1** were assigned based on DEPT, HSQC, and HMBC spectra. The HMBC correlations (Fig. 6.2) from 4-OH (δ_H 7.83) to C-3 (δ_C 107.1), C-4 (δ_C 165.1), and C-5 (δ_C 98.5) established the position of the hydroxyl group at C-4 in **6.1**, and henceforth an *α*-pyranone moiety in peplidiforone A (**6.1**) rather than a *γ*-pyranone like in hyperenone B. The HMBC correlations from H-2´/H-6´ to C-6, C-3´/C-5´, and C-4´ confirm the position of the phenyl group at C-6. Further HMBC correlations are observed from H-5 (δ_H 6.32) to C-1´ (δ_C 131.0), C-3 (δ_C 107.1), and C-6 (δ_C 162.6), from H-3´/H-4´/H-5´ to C-1´/C-2´/C-6´; from H-2´´ to C-1´´, C-4´´/C-5´´, from the diastereotopic H-3´´a/H-3´´b protons to C-1´´ and C-2´´ as well as from Me-4´´/Me-5´´ to C-1´´/C-2´´/C-3´´. Based on the above spectroscopic evidences, the structure of **6.1** was established as depicted in Fig. 6.1.

Peplidiforone B (**6.2**) has the molecular formula $C_{16}H_{16}O_3$ as deduced from the positive ion HR-ESI-MS, which reveals a $[M+H]^+$ ion at *m/z* 257.1173 (calcd. 257.1172 for $C_{16}H_{17}O_3^+$). Compounds **6.1** and **6.2** have the same molecular formula, but they differ in the substitution of the pyrone moiety as determined by ^1H and ^{13}C NMR data (Table 6.1). The hydroxyl group and the terminal double bond of isoprenyl signals are not observed in the NMR spectra of **6.2**. In compound

6.2, a dihydrofuran ring adjacent to the α-pyrone is formed by a nucleophilic attack of the ɣ-OH of the α-pyrone on the terminal double bond of the isoprenyl group as confirmed by observing a tertiary methyl group doublet ($δ_H$ 1.42) and an oxymethylene quartet ($δ_H$ 4.58) in the ^{1}H NMR spectrum. Structural isomers like **6.1** and **6.2** can occur naturally as exemplified by the two isomers malbranpyrroles E and F discovered by intact-cell mass spectrometry and LC-SPE-NMR from *Malbranchea sulfurea* (Yang *et al., 2009*).
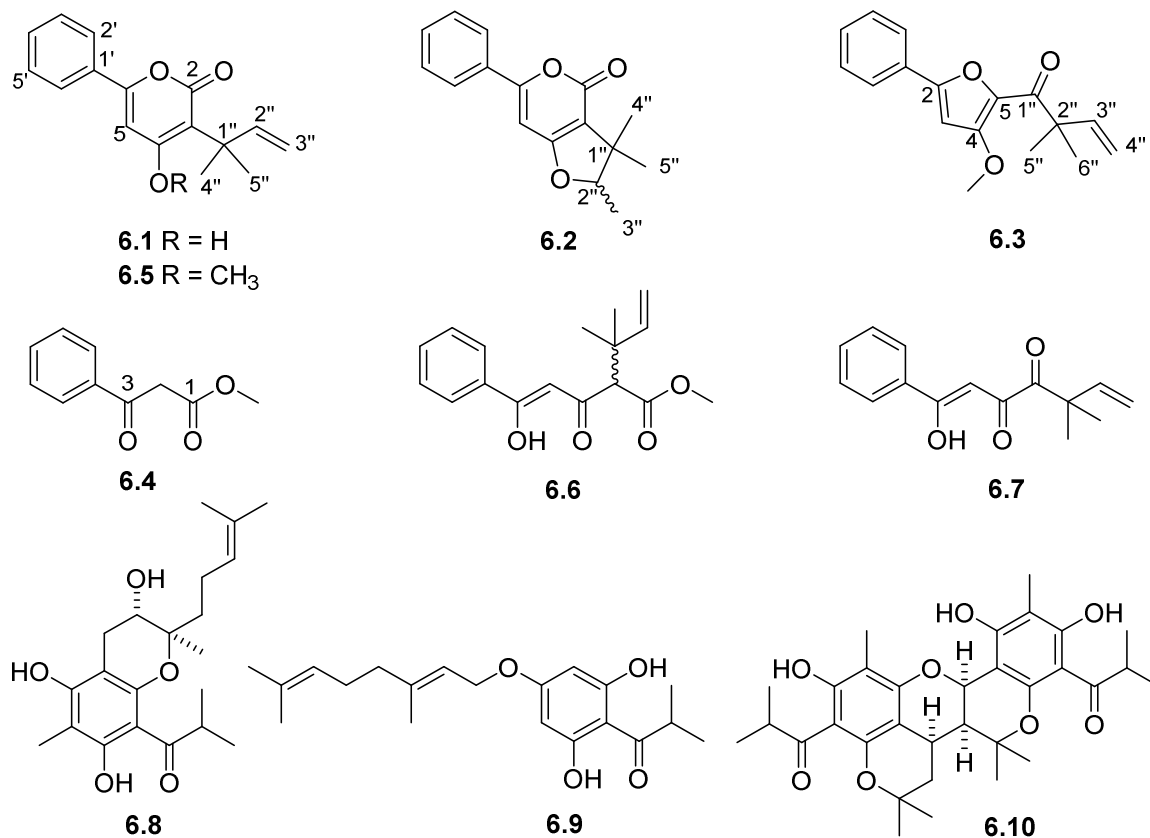
Fig. 6.1. Structures of compounds **6.1**-**6.10** from *H. peplidifolium.*
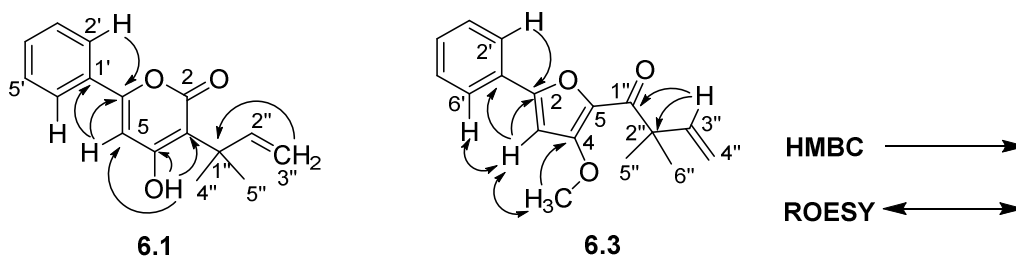
Fig. 6.2. Selected important 2D NMR correlations of compounds **6.1** and **6.3**.

Table 6.1: ^{13}C NMR data [100 MHz] and ^{1}H NMR data [400 MHz, δ, *multiplicity*, *J* (Hz)] for compounds **6.1-6.4** in CDCl₃.

No.	6.1 ^{13}C	6.1 ^{1}H	6.2 ^{13}C	6.2 ^{1}H	6.3 ^{13}C	6.3 ^{1}H	6.4 ^{13}C	6.4 ^{1}H
1							167.8 C	
2	162.6 C		160.8 C		157.0 C		45.8 CH₂	4.02 *s*
3	107.1 C		109.3 C		106.7 CH	6.32 *s*	192.2 C	
4	165.1 C		169.5 C		163.9 C			
5	98.5 CH	6.32 *s*	93.3 CH	6.49 *s*	158.5 C			
6	158.4 C		162.9 C					
1´	131.0 C		131.6 C		132.4 C		128.5 C	
2´	125.4 CH	7.78 *m*	125.8 CH	7.81 *m*	125.9 CH	7.60 *m*	128.5 CH	7.94 *m*
3´	128.8 CH	7.43 *m*	130.9 CH	7.45 *m*	131.3 CH	7.44 *m*	128.8 CH	7.51 *m*
4´	128.8 CH	7.43 *m*	128.8 CH	7.45 *m*	128.9 CH	7.44 *m*	133.8 CH	7.61 *m*
5´	128.8 CH	7.43 *m*	130.9 CH	7.45 *m*	131.3 CH	7.44 *m*	128.8 CH	7.51 *m*
6´	125.4 CH	7.78 *m*	125.8 CH	7.81 *m*	125.9 CH	7.60 *m*	128.5 CH	7.94 *m*
1´´	39.6 C		42.9 C		195.6 C			
2´´	148.8 CH	6.45 *dd* (17.9, 10.5)	92.2 C	4.58 *q* (6.6)	49.4 C			
3´´	114.9 CH₂	5.55 *d* (17.9) 5.45 *d* (10.5)	14.5 CH₃	1.42 *d* (6.6)	140.1 CH	6.17 *dd* (17.5, 10.5)		
4´´	25.4 CH₃	1.56 *s*	20.2 CH₃	1.24 *s*	114.9 CH₂	5.26 *d* (17.5) 5.25 *d* (10.5)		
5´´	25.4 CH₃	1.56 *s*	25.5 CH₃	1.43 *s*	23.5 CH₃	1.48 *s*		
6´´					23.5 CH₃	1.48 *s*		
OMe					51.7 CH₃	3.75 *s*	52.5 CH₃	3.74 *s*
4-OH		7.83 *s*						

Signals assignment was based on 1D- and 2D-NMR including DEPT, HSQC, and HMBC.

The structure assignment of **6.2** is fully supported by 2D NMR data. The HMBC correlations observed from H-2´/H-6´ (δ_H 7.81) to C-6 (δ_C 162.9), from H-5 (δ_H 6.49) to C-1´ (δ_C 131.6), C-6 (δ_C 162.9), C-3 (δ_C 109.3), and C-4 (δ_C 169.5), from H-2´´(δ_H 4.58) to C-1´´ (δ_C 42.9), C-4´´ (δ_C 20.2), and C-5´´ (δ_C 25.5), from Me-4´´ (resp. M-5´´) to C-3, C-1´´, C-2´´ and Me-5´´ (resp. Me-4´´) as well as from Me-3´´ to C-1´´, and C-2´´ (δ_C 92.2) require that the phenyl group is connected at C-6 and the dihydrofuran ring fused at C-3-C-4 on the α-pyrone nucleus. ROESY correlations between H-2´/H-6´ and H-5 further confirm the C-6-position of the phenyl group. Less importantly, COSY correlations are observed between H-2´´ and Me-3´´ and between H-2´/H-6´ and H-3´/H-4´/H-5´. Thus, the structure of peplidiforone B (**6.2**) is confirmed by different spectroscopic data as depicted in Fig. 6.1. The very low specific optical rotation ([α]^{25}_D +0.8 (*c*

0.11 M, MeOH)) of compound **6.2**, being almost zero, indicates the co-existence of both *R*- and *S*-configurations (at C-2˝) in a comparable or equal proportion in the solution, which does not allow the determination of the absolute configuration. Furthermore, no Cotton effect (i.e. zero CD) was detected in the experimental electronic circular dichroism (ECD) spectrum of **6.2** which supports the presence of a complete racemic (1:1) mixture (see Fig. S22, Supporting Information). The occurrence of natural racemates can be explained by a non-enzymatic ring closure such as also proposed for the formation of tramadol as the racemic (±)-(1*R*,2*R*)-compound (Lecerf-Schmidt *et al*., 2015).

Peplidiforone C (**6.3**) has the molecular formula $C_{17}H_{18}O_3$ as calculated from the positive ion HR-ESI-MS exhibiting an $[M+H]^+$ ion at *m/z* 271.1332 (calcd. 271.1329 for $C_{16}H_{19}O_3^+$). Its structure was determined by the interpretation of its ^1H (Table 6.1), ^{13}C (Table 6.1), DEPT, HSQC, HMBC, COSY, and NOESY spectra. The observation of ^1H NMR signals at δ_H 6.17 (1H, *dd*, *J* = 17.5, 10.5 Hz, H-3˝), 5.26 (1H, *d*, *J* = 17.5 Hz, H-4˝a), 5.25 (1H, *d*, *J* = 10.5 Hz, H-4˝b), and δ_H 1.48 (2 × 3H, *s*, 3H-5˝ and 3H-6˝) and HMBC correlations from Me-5˝ (resp Me-6˝) to C-1˝ (δ_C 195.6), C-3˝ (δ_C 140.1), C-4˝ (δ_C 116.2), and (resp. Me-5˝) suggest the presence of a 2,2-dimethylbut-3-enoyl moiety in the molecule. This is further supported by HMBC correlations (Fig. 6.2) from H-3˝ to C-1˝, C-2˝ (δ_C 49.4), Me-5˝/Me-6˝ and from the diastereotopic H-4˝a/H-4˝b protons to C-2˝ and C-3˝. The signal at δ_H 3.75 (3H, *s*, 4-OMe; δ_C 51.7) in the proton spectrum corresponds to one methoxyl group. Characteristic proton signals of the phenyl group are exhibited at δ_H 7.60 (2H, *m*, H-2´/H-6´) and 7.44 (3H, *m*, H-3´/H-4´/H-5´) in the ^1H NMR spectrum of **6.3**. After elucidation of the phenyl, methoxyl, and 2,2-dimethylbut-3-enoyl groups of the molecule; its remaining four carbons (δ_C 163.9, C; 158.5, C; 157.0, C; 106.7, CH), one singlet proton (δ_H 6.32, *s*, 1H, H-3), and one oxygen atom, which all together account for three degrees of unsaturation, require the presence of a tri-substituted furan ring. The substitution pattern on the furan ring was unambiguously determined by the detailed inspection of HMBC and NOESY spectra (Fig. 6.2). NOESY interactions H-3/4-OMe and H-3/H-2´/H-6´ established the connection of the phenyl, methoxyl, and 2,2-dimethylbut-3-enoyl groups at C-2, C-4, and C-5, respectively. This is supported by HMBC correlations from H-3 to C-1´ and C-2; from H-2´/H-6´ to C-2 (δ_C 157.0); and from 4-OMe to C-4 (δ_C 163.9). Further HMBC correlations are revealed from H-3´/H-4´/H-5´ to C-1´, C-2´/C-6´; from H-2´/H-6´ to C-6´/C-2´. No HMBC connectivity to C-5 was monitored. Additional NOESY interactions were observed between H-2´/H-6´ and H-3´/H-5´ as well as between H-3˝ and H-4˝. The two systems H-2´/H-6´/H-3´/H-4´/H-5´ and H-3˝/H-4˝ are observed in the COSY spectrum. The above spectroscopic data enabled us to elucidate the

structure of peplidiforone C as shown in Fig. 6.1. Peplidiforone C (**6.3**) is the first prenylated furan derivative isolated from the genus *Hypericum*. A furan ring substituted by a methoxyl or 2,2-dimethylbut-3-enoyl moiety (prenyl derivative) is unusual in the nature. Furanic compounds are very rare in *Hypericum*. According to a database search (Reaxys, on 20. 08. 2015) only 4 benzofuran derivatives are known (Ang'edu *et al*., 1999, Shiu and Gibbons, 2009).

Peplidiforone D (**6.4**) was identified to be methyl 3-oxo-3-phenylpropanoate by comparison of its NMR (Table 6.1) and MS data with those reported in the literature for the synthetic methyl 3-oxo-3-phenylpropanoate (Li *et al.,* 2009). However, our study is the first recorded isolation of compound **6.4** as a natural product.

The known natural products **6.5**-**6.10** were identified by comparing their spectroscopic data including 2D NMR with those previously reported for compounds isolated from the genus *Hypericum*. Compounds **6.6** and **6.7** were characterized as mysorenone-A and mysorenone-C, being previously described as constituents of *Hypericum mysorense* (Kikuchi *et al.,* 1985a; Kikuchi *et al.,* 1985b). These two compounds can be assigned as derivatives or extended polyketides of **6.4** which underwent prenylation. Compound **6.5** was identified to be 4-methoxy-3-(2-methylbut-3-en-2-yl)-6-phenyl-2*H*-pyran-2-one (**6.5**) and represents the *O*-methylated derivative of peplidiforone A (**6.1**) that was previously isolated from *H. mysorense* (Vishwakarma *et al.,* 1983). The acylphloroglucinols **6.8**-**6.10** were determined to be petiolin J (**6.8,** methylated acylphloroglucinol), previously found in *H. pseudopetiolatum var. kiusianum* (Tanaka *et al.,* 2010), 1-(4-(E-3,7-dimethylocta-2,6-dienyloxy)-2.6-dihydroxylphenyl)-2-methylpropan-1-one (**6.9**) detected in *H. jovis* (Athanasas *et al.,* 2004), and hyperevoline (**6.10,** methylated acylphloroglucinol derivative) also isolated from *H. revolutum* (Decosterd *et al.,* 1987). The NMR and [α]$^{25}_{D}$ data of compound **6.8** match those previously reported by Tanaka *et al.* (2010) for petiolin J in accordance with the relative configuration shown in Fig 6.1. The configuration of hyperevoline (**6.10**) was not previously described. However, the ^{1}H NMR data (J ~5 Hz) indicate *cis* relative configurations of the protons of the three stereogenic centers. Methylated acylphloroglucinols are rare in nature. Recently, we reported hyperpolyphillirin, a methylated polycyclic polyprenylated acylphloroglucinol, from *H. polyphyllum* (Porzel *et al*., 2014). Acylphloroglucinols methylated at the *meta* position relative to the acyl group as in compound **6.8** and **6.10** seem to be biosynthetic precursors for complex polycyclic polyprenylated derivatives (Xu *et al*., 2015). Petiolin-J (**6.8**) is the methylated acylphloroglucinol derivative of empetrikarinols A and B. The two latter were reported for the first time from *H. empetrifolium* (Schmidt *et al*., 2012b) and later empretrikarinol B, along with some previously undescribed

prenylated acylphloroglucinol derivatives, were isolated from *H. roeperianum* (Fobofou *et al.*, 2015b).

As shown before, the prenylated and non-prenylated compounds **6.5-6.10** are found within the genus *Hypericum*. Therefore, in general, the occurrence of the described compounds in *Hypericum peplidifolium* is also of chemotaxonomic relevance with respect to *Hypericum* species and plants of the Hypericaceae family. The family Hypericaceae was formerly based on morphological features together with Clusiaceae combined to Guttiferae. There is an ongoing discussion whether Hypericaceae should be considered as separate family or as subfamily within Guttiferae (Fobofou *et al.*, 2015a; Crocket & Robson, 2011; Hegnauer, 1989). Also within the Hypericaceae the chemotaxonomic distinctions are challenging (Crocket & Robson, 2011). Interestingly, the phenyl polyketides **6.1**-**6.7** or similar compounds were so far only isolated from *H. peplidifolium* (section Humifusoideum), *H. mysorense* (section Campylosporus, Kikuchi *et al.*, 1985a,b) and *H. riparium* (section Campylosporus, Tala *et al.*, 2015). According to the phylogenetic network established by Robson, both sections of the Hypericaceae are closely related (Robson, 2003; Crocket & Robson, 2011). Therefore, this compound class might be considered as valuable chemotaxonomic marker. In contrast to the phenyl polyketides, prenylated acylphloroglucinol derivatives are widely distributed within Hypericaceae and Clusiaceae. However, the potential chemo-taxonomic significance of the rare methylated acylphloroglucinols should be further investigated.

Since *Hypericum* species are used in the Cameroonian folk medicine against tumors and microbial diseases, the cytotoxic, antifungal, and antiviral activities of crude extracts and isolated compounds were evaluated. The MeOH and EtOAc extracts of *H. peplidifolium* as well as compounds **6.1**, **6.3** and **6.5-6.8** were tested for cytotoxicity against HT29 and PC3 cancer cell lines. The MeOH and EtOAc extracts exhibit cytotoxic activities indicated by a growth inhibition of the cell lines of 54% and 35% for HT29 and 48% and 36% for PC3, respectively, at a concentration of 50 µg/ml. Both extracts do not show any activity at 0.5 µg/ml against the tested cells. Up to a concentration of 10 µM, no significant growth inhibition (less than 22%) was determined for compounds **6.1, 6.3, 6.5-6.8**. The antifungal and anti-herpes simplex virus type 1 (HSV-1) activities of extracts and isolated compounds (**6.1-6.10**) are summarized in Table 6.2. The MeOH and EtOAc extracts exhibit significant antifungal activity against *Botrytis cinerea* (84 ± 13 and 62 ± 3%, resp.) and moderate activity against *Septoria tritici* (41 ± 8 and 32 ± 2%, resp.) at a concentration of 400 µg/ml. Compounds **6.1** and **6.5** display the highest antifungal activity (among the tested pure compounds) with growth inhibitions ranging from 34 to 47% at 83.3 µM. The extracts and pure compounds do not exhibit any antifungal activity against *B. cinerea* and *S.*

tritici up to a concentration of 0.1 mg/ml for extracts and 28 µM for pure compounds. None of the tested samples exhibit significant anti HSV-1 activity, failing to meet our minimum requirement of 50% inhibition of virus at a tested concentration of 100 µg/ml. At this concentration, none of the samples show cytotoxicity (less than 20% inhibition) to the cells (vero cells, see description in the Supporting Information). Surprisingly, for unknown reasons, when some compounds were combined with the virus, cell mortality was increased. This means, compounds **6.1** and **6.6** and acylphloroglucinols **6.8-6.10** might increase the virulence of HSV-1. In conclusion, moderate antifungal and cytotoxic (HT-29 and PC-3) activities were observed for *H. peplidifolium* extracts. However, none of the isolated compounds exhibits significant biological activities in these initial tests, which would encourage a detailed biological investigation (e.g. dose dependent studies).

Table 6.2. Antifungal and antiviral activities of extracts and compounds **6.1**-**6.10** from *Hypericum peplidifolium* against *Botrytis cinerea*, *Septoria tritici*, and HSV-1.

H. peplidifolium	Growth inhibition (% ± SD)		
	B. cinerea[b]	*S. tritici*[b]	HSV-1[c]
Crude extract	84 ± 13	41 ± 8	11 ± 7
EtOAc extract	62 ± 3	32 ± 2	23 ± 3
6.1	40 ± 4	38 ± 3	(35 ± 6)
6.2	nd [a]	nd	1 ± 7
6.3	14 ± 2	21 ± 4	11 ± 4
6.4	nd	nd	9 ± 7
6.5	34 ± 4	47 ± 3	nd
6.6	43 ± 1	10 ± 7	(18 ± 6)
6.7	-22 ± 2	2 ± 2	1 ± 3
6.8	4 ± 10	29 ± 4	(18 ± 1)
6.9	nd	nd	(37 ± 6)
6.10	nd	nd	(35 ± 6)

[a] not determined.

[b] Extracts were tested at 400 µg/ml and pure compounds at 83.3 µM. DMSO was used as negative control while pyraclostrobin served as positive control.

[c] Sample concentration was 100 µg/ml. All the samples demonstrated less than 20% cell death (Vero cells ATCC, CCL-81) at 100 µg/ml. Values in parenthesis indicate a higher percentage of cell death occurred with the extract with virus than in cells exposed to virus alone without extract. The IC_{50} of acyclovir (known control) was determined to be 4.75 ± 0.87 µg/ml. The use of DMSO do not have any effect on assays.

6.3. Experimental

6.3.1. General experimental procedures

Acetonitrile (HPLC grade, LiChrosolv) was obtained from Merck KGaA, Germany; double distilled water was used for HPLC analysis. HPLC was performed on a VARIAN PrepStar instrument equipped with a VARIAN ProStar PDA detector. Column chromatography was run on silica gel (Merck, 63-200 and 40-63 µm), while TLC was performed on precoated silica gel F_{254} plates (Merck). Spots were visualized with a UV lamp at 254 and 366 nm or by spraying with vanillin-H_2SO_4-MeOH followed by heating at 100 °C. UV spectra were obtained on a JASCO V-560 UV/VIS spectrophotometer. IR (ATR) spectra were recorded using a Thermo Nicolet 5700 FT-IR spectrometer, in MeOH or $CHCl_3$. Optical rotation was measured using a JASCO P-2000 digital polarimeter. ^1H and ^{13}C NMR spectra were recorded on an Agilent DD2 400 NMR spectrometer at 399.915 and 100.569 MHz, respectively. gDQCOSY, ROESY/NOESY (mixR = 200 ms), gHSQCAD, and gHMBCAD spectra were recorded on an Agilent DD2 400 NMR spectrometer. The ^1H chemical shifts are referenced to internal TMS (δ_H 0.0); ^{13}C chemical shifts are referenced to internal $CDCl_3$ (δ_C 77.0) or CD_3OD (δ_C 49.0).

The low resolution electrospray (ESI) mass spectra were performed on a SCIEX API-3200 instrument (Applied Biosystems, Concord, Ontario, Canada) combined with a HTC-XT autosampler (CTC Analytics, Zwingen, Switzerland). The samples were introduced via autosampler and loop injection.

The high resolution ESI mass spectra of compounds **6.1-6.10** as well as the corresponding higher collision dissociation (HCD) measurements (normalized collision energy 50%) were obtained from an Orbitrap Elite mass spectrometer (Thermofisher Scientific, Bremen, Germany) equipped with an HESI electrospray ion source (spray voltage 4 kV; capillary temperature 275 °C, source heater temperature 40 °C; FTMS resolution 30.000). Nitrogen was used as sheath gas. The sample solutions were introduced continuously via a 500 µl Hamilton syringe pump with a flow rate of 5 µl/min. The data was evaluated by the Xcalibur software 2.7 SP1.

6.3.2. Plant material

Hypericum peplidifolium A. Rich. was collected in October 2011 at Mount Bamboutos (Mbouda) in the West Region of Cameroon. The plant was identified by Mr. Fulbert Tadjouteu, botanist at the National Herbarium of Cameroon where a voucher specimen (No. 26774/SFR-Cam) is deposited.

6.3.3. Extraction and isolation

The dried aerial parts of the plant (87 g) was macerated in MeOH (3 × 1.5 L) at room temperature during 72 hours to give the respective extract (38 g) after evaporation of the solvent under reduced pressure. A portion of the resulting extract (3.9 g) was then partitioned between ethyl acetate and water (1:1). The ethyl acetate layer contained 3.6 g of dried material which was chromatographed on a silica gel column, eluted with step gradients of *n*-hexane-EtOAc (100:0, 90:10, 80:20, 70:30, 50:50, and 100:0) and EtOAc-MeOH (90:10, 80:20, 50:50, and 0:100). Twenty-six fractions of 200 mL each were collected and combined on the basis of their TLC and ^{1}H NMR profiles into five main fractions (Fr. 1-Fr. 5). Fr. 1 (259.8 mg) obtained from *n*-hexane-EtOAc (100:0 and 90:10) was further chromatographed on a silica gel column, eluted with *n*-hexane containing an increasing amount of EtOAc, to give 4 sub-fractions (Fr. 1.1-Fr.1.4). Fr. 1.2 (86.5 mg) and Fr. 1.3 (82.4 mg) obtained from *n*-hexane-EtOAc (85:15) were purified by RP18 HPLC (5 µm, 120 x 2 mm, flow rate 8.9 ml/min, detection 210 nm) , eluted with H_2O-MeCN (30→100% MeCN 0-20 min, 100% MeCN 20-25 min, 100→30% MeCN 25-27 min, 30% MeCN 27-30 min), to afford compound **6.6** (21 mg, t_R 11.62 min) and compounds **6.2** (7.6 mg, t_R 9.37 min), **6.4** (2.8 mg, t_R 5.24 min), **6.9** (2.8 mg, t_R 12.88 min), and **6.10** (3.6 mg, t_R 16.89 min), respectively. Fr. 2 (112.5 mg), obtained from *n*-hexane-EtOAc (80:20), contained four main compounds which were separated by RP18 HPLC, eluted with H_2O-MeCN as described above, to yield compounds **6.1** (5.0 mg, t_R 7.07 min), **6.3** (5.3 mg, t_R 10.20 min), **6.5** (7.5 mg, t_R 9.96 min), and **6.7** (2.1 mg, t_R 2.55 min). Fr. 4 (167.6 mg), obtained from *n*-hexane-EtOAc (70:30), was submitted onto RP18 HPLC, eluted with H_2O-MeCN (15→100% MeCN 0-20 min, 100% MeCN 20-25 min, 100→15% MeCN 25-27 min, 15% MeCN 27-30 min), to afford **6.8** (3.2 mg, t_R 13.61 min).

Peplidiforone A (**6.1**): amorphous compound, ^{1}H NMR data see Table 6.1; ^{13}C NMR data see Table 6.1; negative ion HR-ESI-FTMS [*m/z* (rel. int., %)]: [M-H]$^-$ at *m/z* 255.1035 (calcd. for $C_{16}H_{15}O_3^-$, 255.1027). negative ion ESI-HCD-MS [*m/z* 255.1026 (65)]: *m/z* 211.1128 [M-H-CO_2]$^-$ (100, calcd. for $C_{15}H_{15}O^-$ 211.1128).

Peplidiforone B (**6.2**): colorless oil, $[\alpha]^{25}_D$ +0.8 (*c* 0.11 M, MeOH); UV (MeOH), λ_{max} (log ε): 239 (1.22), 269 (0.72), 330 (1.03); IR (ATR) υ_{max} (cm^{-1}): 2968, 1710, 1623, 1579, 1563, 1496, 1453, 1417, 1383, 1202, 1025, 945, 928, 838, 764, 689; ^{1}H NMR data see Table 6.1; ^{13}C NMR data see Table 6.1; positive ion HR-ESI-FTMS [*m/z* (rel. int., %)]: [M+H]$^+$ at *m/z* 257.1173 (calcd. for $C_{16}H_{17}O_3^+$ 257.1172). positive ion ESI-HCD-MS [*m/z* 257 (38)]: *m/z* 215.0704 [M+H-C_3H_6]$^+$

(50, calcd. for $C_{13}H_{11}O_3^+$ 215.0703), 201.0547 $[M+H-C_4H_8]^+$ (100, calcd. for $C_{12}H_9O_3^+$ 201.0546), 147.0440 $[M+H-C_7H_{10}O]^+$ (34, calcd. for $C_9H_7O_2^+$ 147.0441), 105.0333 $[M+H-C_9H_{12}O_2]^+$ (60, calcd. for $C_7H_5O^+$ 105.0335).

Peplidiforone C (**6.3**): colorless oil; UV (MeOH), λ_{max} (log ε): 271 (1.70); 338 (0.63); IR (ATR) υ_{max} (cm^{-1}): 2977, 2950, 1761, 1721, 1643, 1449, 1434, 1331, 1157, 1048, 1001, 982, 764, 686; ^{1}H NMR data see Table 6.1; ^{13}C NMR data see Table 6.1; positive ion HR-ESI-FTMS [*m/z* (rel. int., %)]: $[M+H]^+$ at *m/z* 271.1332 (calcd. for $C_{17}H_{19}O_3^+$ 271.1329). positive ion ESI-HCD-MS [*m/z* 271 (13)]: *m/z* 229.0860 $[M+H-C_3H_6]^+$ (49, calcd. for $C_{14}H_{13}O_3^+$ 229.0859), 215.0704 $[M+H-C_4H_8]^+$ (100, calcd. for $C_{13}H_{11}O_3^+$ 215.0703), 105.0333 $[M+H-C_{10}H_{14}O_2]^+$ (37, calcd. for $C_7H_5O^+$ 105.0335).

Peplidiforone D (**6.4**): colorless oil; ^{1}H NMR data see Table 6.1; ^{13}C NMR data see Table 6.1; HR-ESI-MS: $[M-H]^-$ at *m/z* 177.0565 (calcd. for $C_{10}H_9O_3^-$, 177.0557).

6.3.4. Cytotoxicity assays

The human prostate cancer cell line PC-3 and the colon cancer cell line HT-29 were maintained in RPMI 1640 medium supplemented with 10% fetal bovine serum, 1% L-alanyl-L-glutamine (200 mM) and 1.6% hepes (1 M). 5×10^2 PC-3 cells and 1.5×10^3 HT-29 cells were seeded overnight into 96-well plates and exposed to a serial dilution of each compound (10 µM and 10 nM) and extract (50 and 0.50 µg/ml) for three days. Cytotoxicity was determined utilizing a modified XTT method (0.25 mg/ml XTT, 6.5 µM PMS) (Scudiero *et al.*, 1988).

6.3.5. Antifungal bioassay

Crude extracts and pure compounds were tested in 96-well microtiter plate assays against the phytopathogenic ascomycetes *Botrytis cinerea* Pers. and *Septoria tritici* Desm. according to the fungicide resistance action committee (FRAC) with the following modifications (FRAC, 2015a, 2015b, 2015c). Briefly, crude extracts were examined at 1250 and 416.7 µg/ml, while pure compounds were tested at 250, 83.3 and 27.8 µM. The solvent DMSO was used as negative control (max. concentration 2.5%), while the commercial fungicide pyraclostrobin (Sigma Aldrich, Germany) served as positive control (100% inhibition at 83.3 µM). Five to seven days after inoculation, pathogen growth was evaluated by measurement of the optical density (OD) at λ 405 nm with a TecanGENios Pro microplate reader (5 measurements per well using multiple reads in a 3×3 square). Each experiment was carried out in triplicates.

6.3.6. Antiviral assay

Antiviral activity of pure compounds and crude extract against herpes simplex virus, type 1 (HSV-1, ATCC, VR-1383) was tested in a plaque assay using Vero monolayer in a 96-well plate (Vero cells, ATCC, CCL-81). Cell viability was determined by the addition of PrestoBlue (Invitrogen) and spectrophotometric reading for fluorescence using Softmax Pro (Molecular Devices, Ca). The methods (unpublished) used for this assay are described in detail in the supplemental material.

Appendix. Supporting Information (this is available online)

Supplemental material (antiviral assays, ^{1}H and ^{13}C NMR spectra of compounds **6.1-6.10**, ECD spectrum and chiral HPLC chromatogram of compound **6.2**) associated with this chapter is available online at http://www.sciencedirect.com/science/article/pii/S0031942216300206.

References

Ang'edu, C.A., Schmidt, J., Porzel, A., Gitu, P., Midiwo, J.O., Adam, G., **1999**. Coumarins from *Hypericum keniense* (Guttiferae). *Pharmazie* 54, 235-236.

Athanasas, K., Magiatis, P., Fokialakis, N., Skaltsounis, A.L., Pratsinis, H., Kletsas, D., **2004**. Hyperjovinols A and B: Two new phloroglucinol derivatives from *Hypericum jovis* with antioxidant activity in cell cultures. *J. Nat. Prod.* 67, 973-977.

Crockett, S.L., Robson, N.K.B., **2011**. Taxonomy and Chemotaxonomy of the genus *Hypericum*. *Medicinal Aromatic Plant Sci. Biotech.* 5, 1-13.

Crispin, M.C., Hur, M., Park, T., Kim, H.Y., Wurtele, E.S., **2013**. Identification and biosynthesis of acylphloroglucinols in *Hypericum gentianoides*. *Physiol. Plant*. 148, 354-370.

Decosterd, L.A., Stoeckli-Evans, H., Msonthi, J.D., Hostettmann, K., **1987**. New antifungal chromenyl ketones and their pentacyclic dimers from *Hypericum revolutum* VAHL. *Helv. Chim. Act.* 70, 1694-1702.

Farag, M.A., Wessjohann, L.A., **2012**. Metabolome classification of commercial *Hypericum perforatum* (St. John's Wort) preparations via UPLC-qTOF-MS and chemometrics. *Planta Med*. 78, 488-496.

Fobofou, S.A.T., Franke, K., Arnold, N., Schmidt, J., Wabo, H.K., Tane, P., Wessjohann, L.A., **2014**. Rare biscoumarin derivatives and flavonoids from *Hypericum riparium*. *Phytochemistry* 105, 171-177.

Fobofou, S.A.T., Franke, K., Schmidt, J., Wessjohann, L., **2015a**. Chemical constituents of *Psorospermum densipunctatum* (Hypericaceae). *Biochem. Syst. Ecol*. 59, 174-176.

Fobofou, S.A.T., Franke, K. Sanna, G., Porzel, A., Bullita, E., La Colla, P., Wessjohann, L.A., **2015b.** Isolation and anticancer, anthelmintic, and antiviral (HIV) activity of acylphloroglucinols, and regioselective synthesis of empetrifranzinans from *Hypericum roeperianum*. *Bioorg. Med. Chem*., 23, 6327-6334.

FRAC, **2015a**. www.frac.info; approved monitoring method by FRAC: BOTRCI microtiter monitoring method BASF 2009 V2.

FRAC, **2015b**. www.frac.info; approved monitoring method by FRAC: SEPTTR microtiter monitoring method BASF 2009 V1.

FRAC, **2015c**. www.frac.info; approved monitoring method by FRAC: PHYTIN microtiter method sporangia BASF 2006 V1.

Hegnauer, R., **1989**. Chemotaxonomie der Pflanzen, Vol. 8. Birkhäuser Verlag, Basel.

Heinke, R., Franke, K., Porzel, A., Wessjohann, L.A., Ali, N.A., Schmidt, J., **2011**. Furanocoumarins from *Dorstenia foetida*. *Phytochemistry* 72, 929-934.

Hohmann, C., Schneider, K., Bruntner, C., Brown, R., Jones, A.L., Goodfellow, M., Krämer, M., Imhoff, J.F., Nicholson, G., Friedler, H-.P., Süssmuth, R.D., **2009**. *J. Antibiot*. 62, 75-79.

Kikuchi, T., Kadoka, S., Matsuda, S., Tanaka, K., Namba, T., **1985a**. Studies on the constituents of medicinal related plants in Sri Lanka. II. Isolation and structures of new γ-pyrone and related compounds from *Hypericum mysorense* HEYNE. *Chem. Pharm. Bull*. 33, 557-564.

Kikuchi, T., Kadota, S., Matsuda, S., Tanaka, K., **1985b**. Studies on the constituents of medicinal and related plants in Sri Lanka. IV. Isolation and structure determination of hyperenone-B, mysorenone-B, and Mysorenone-C from *Hypericum mysorense* HEYNE and synthesis of hyperenone-A and -B. *Chem. Pham. Bull*. 33, 1969-1974.

Lecerf-Schmidt, F., Haudecoeur, R., Peres, B., Queiroz, M.M.F., Marcourt, L., Challal, S., Queiroz, E.F., Taiwe, G.S., Lomberget, T., Le Borgne, M., Wolfender, J.-L., De Waard, M., Robins, R.J., Boumendjel, A, **2015**. Biomimetic synthesis of tramadol. *Chem. Commun*. 51, 14451-14453.

Li, H., He, Z., Guo, X., Li, W., Zhao, X., Li, Z., **2009**. Iron-catalysed selective oxidation of *N*-methyl amines: Highly efficient synthesis of methylene-bridged bis-1,3-dicarbonyl compounds. *Org. Lett*. 11, 4176-41-79.

Mabberley, D.J., **1997**. The Plant-Book. A portable dictionary of the vascular plants, 2nd ed. Cambridge University Press, Cambridge (UK).

Porzel, A., Farag, M.A., Mülbradt, J., Wessjohann, L.A., **2014**. Metabolite profiling and fingerprinting of *Hypericum* species: A comparison of MS and NMR metabolomics. *Metabolomics* 10, 574-588.

Robson, N.K.B., **2003**. *Hypericum* botany. Ed. Ernst, E., *Hypericum*: The genus *Hypericum*, Taylor and Francis, New York (USA).

Sarris, J., **2007**. Herbal medicines in the treatment of psychiatric disorders: a systematic review. *Phytother. Res*. 21, 703-716.

Schmidt, S., Jürgenliemk, G., Skaltsa, H., Heilmann, J., **2012a**. Phloroglucinol derivatives from *Hypericum empetrifolium* with antiproliferative activity on endothelial cells. *Phytochemistry* 77, 218-225.

Schmidt, S., Jürgenliemk, G., Schmidt, T. J., Skaltsa, H., Heilmann, J., **2012b**. Bi-, tri-, and polycyclic acylphloroglucinols from *Hypericum empetrifolium*. *J. Nat. Prod*. 75, 1697-1705.

Scudiero, D.A., Schoemaker, R.H., Monks, A., Tierney, S., Nofziger, T.H., Currens, M.J., Seniff, D., Boyd, M.R., **1988**. Evaluation of a soluble tetrazolium/formazan assay for cell growth and drug sensitivity in culture using human and other tumor cell lines. *Cancer Res*. 48, 4827-4833.

Shiu, W. K. P., Gibbons, S., **2009**. Dibenzofuran and pyranone metabolites from *Hypericum revolutum* ssp. *revolutum* and *Hypericum choisianum*. *Phytochemistry* 70, 403-406.

Sun, X., Kong, X., Gao, H., Zhu, T., Wu, G., Gu, Q., Li, D., **2014**. Two new meroterpenoids produced by the endophytic fungus *Penicillium* sp. SXH-65. *Arch. Pharm. Res*. 37, 978-982.

Tala, M.F. Talontsi, F. M., Zeng, G.-Z., Wabo, H.K., Tan, N.-H., Spiteller, M., Tane, P., **2015**. Antimicrobial and cytotoxic constituents from native Cameroonian medicinal plant *Hypericum riparium*. *Fitoterapia*, 102, 149-55.

Tala, M.F., Tchakam, P.D., Wabo, H.K., Talontsi, F.M., Tane, P., Kuiate, J.R., Tapondjou, L.A., Laatsch, H., **2013**. Chemical constituents, antimicrobial and cytotoxic activities of *Hypericum riparium* (Guttiferae). *Rec. Nat. Prod*. 7, 65-68.

Tanaka, N., Kashiwada, Y., Kim, S.-Y., Sekiya, M., Ikeshiro, Y., Takaishi, Y., **2009**. Xanthones from *Hypericum chinense* and their cytotoxicity activity evaluation. *Phytochemistry* 70, 1456-1461.

Tanaka, N., Otani, M., Kashiwada, Y., Takaishi, Y., Shibazaki, A., Gonoi, T., Shiro, M., Kobayashi, J., **2010**. Petiolins J-M, prenylated acylphloroglucinols from *Hypericum pseudopetiolatum* var. *kiusianum*. *Bioorg. Med. Chem. Lett.* 20, 4451-4455.

Vishwakarma, R.A., Kapil, R.S., Popli, S.P., **1983**. Studies in medicinal plants: Part X-Chemical constituents of *Hypericum mysorense*. *Ind. J. Chem.* 222, 612-613.

Wabo, H. K., Kowa, T.K., Lonfouo, A.H.N., Tchinda, A.T., Tane, P., Kikuchi, H., Frederich, M., Oshima, Y., **2012**. Phenolic compounds and terpenoids from *Hypericum lanceolatum*. *Rec. Nat. Prod.* 6, 94-100.

Wirz, A., Simmen, U., Heilmann, J., Calis, I., Meier, B., Sticher, O., **2000**. Bisanthraquinone glycosides of *Hypericum perforatum* with binding inhibition to CRH-1 receptors. *Phytochemistry* 55, 941-947.

Wu, Q.-L., Wang, S.-P., Du, L.-J., Xiao, P.-G., **1998**. Xanthones from *Hypericum japonicum* and *H. henryi*. *Phytochemistry* 49, 1395-1402.

Xu, W.-J., Zhu, M.-D., Wang, X.-B.; Yang; M.-H., Luo, J., Kong, L.Y., **2015**. Hypermongones A-J, rare methylated polycyclic polyprenylated acylphloroglucinols from the flowers of *Hypericum monogynum*. *J. Nat. Prod.* 78, 1093-1100.

Yang, Y.-L., Liao, W.-Y., Liu, W.-Y., Liaw, C.-C., Shen, C.-N., Huang, Z.-Y., Wu, S.-H., **2009**. Discovery of new natural products by intact-cell mass spectrometry and LC-SPE-NMR: Malbranpyrroles, novel polyketides from thermophilic fungus *Malbranchea sulfurea*. *Chem. Eur. J.* 15, 11573-11580.

Chapter 7

New source report: chemical constituents of *Psorospermum densipunctatum* (Hypericaceae)

Graphical abstract*

P. densipunctatum   vismiaquinone   proanthocyanidin B-1
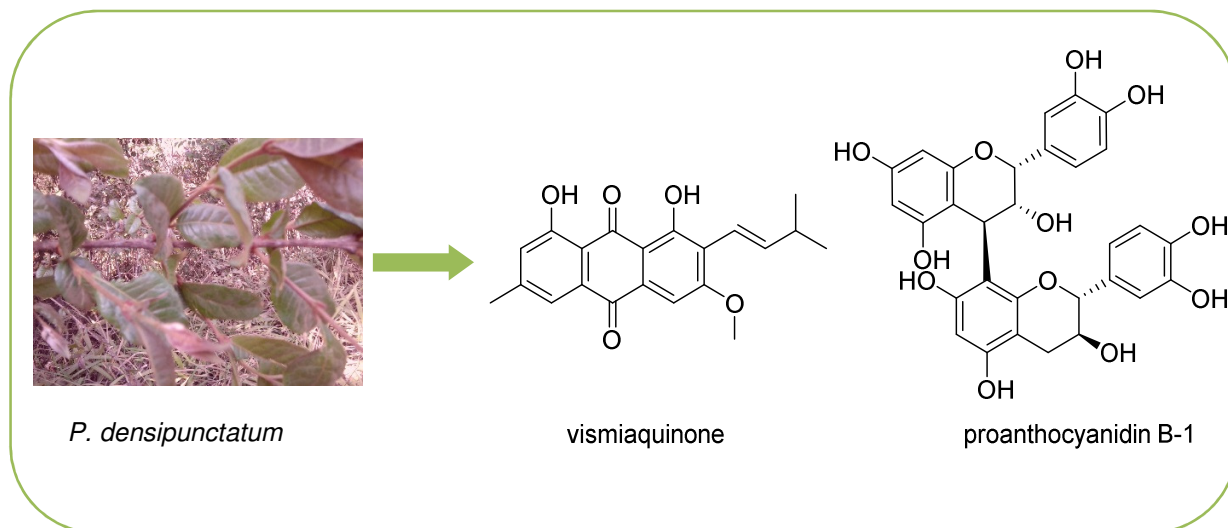
Highlights

- Characterization of three prenylated anthraquinones and five proanthocyanidins from the chemically unexplored *P. densipunctatum*

- First report on proanthocyanidins from the genus *Psorospermum*

- Discussion on the chemotaxonomic significance of the isolated compounds

Abstract

The present work describes the chemistry of the phytochemically unexplored *Psorospermum densipunctatum*, which (like *Hypericum* species) belongs to the family Hypericaceae. Eight natural products, including three prenylated anthraquinones (**7.1-7.3**) and five proanthocyanidins (**7.5-7.8**) were isolated from *P. psorospermum* for the first time. The occurrence of prenyltated compounds in this plant is of high chemotaxonomic significance since they can be markers of the family Hypericaceae. Also, this is the first report of proanthocyanidins (**7.5-7.8**) from the genus *Psorospermum*.

Keywords: Prenylated anthraquinones; Proanthocyanidins; *Psorospermum densipunctatum*; Hypericaceae.

7.1. Subject and source

Psorospermum densipunctatum Engl. is a shrub or small tree occurring in grassland and forest edges in mountain regions of Cameroon. The twigs of *P. densipunctatum* Engl. were collected in January 2013 on the border of the lake Awing in Bamenda, Northwest Region of Cameroon. The plant was identified by Mr. Nana Victor, botanist at the National Herbarium of Cameroon where a voucher specimen (No. 37315/HNC) is deposited.

The genus *Psorospermum* belongs to the tribe Vismieae of Hypericaceae. In Africa, *Psorospermum* species are used to treat wounds, spiders or scorpions bite, skin diseases (like scabies, dermatitis, and eczemas), and leprosy (Lenta *et al.,* 2009; Poumale *et al.,* 2008; Tsaffack *et al.,* 2009, 2013). In our continuing effort to investigate plants of the Hypericaceae family (Fobofou *et al.,* 2014; Porzel *et al.,* 2014), we report the isolation and structural elucidation of compounds from *P. densipunctatum* for the first time.

7.2. Previous work

To the best of our knowledge, there is no chemical investigation reported on *P. densipunctatum* Engl.

7.3. Present study

The air-dried and powdered twigs (2 kg) were macerated with MeOH (1 × 6 L and 2 × 4 L) under shaking for one day. The obtained extracts were evaporated under reduced pressure to give a dark gum (36 g). The crude MeOH extract (34 g) from the twigs was subjected to silica gel column chromatography, eluted with step gradients of *n*-hexane-EtOAc and EtOAc-MeOH. Fractions were combined on the basis of their TLC profiles into 7 main fractions (Fr. 1-Fr. 7). Fr. 1 (653.3 mg) obtained from *n*-hexane-EtOAc (100:0 and 90:10) was further chromatographed on a silica gel column, eluted isocratically with *n*-hexane-EtOAc (98:2) to give three sub-fractions (Fr.1_1-Fr. 1_3). 3-Geranyloxyemodin (**7.1**, 28 mg, R_f = 0.42 in *n*-hexane:EtOAc 95:5) was crystallized from Fr.1_1. Fr. 1_2 was purified on Sephadex LH 20 eluted with CH_2Cl_2:MeOH (1:1) and submitted on a Chromabond SiOH cartridge and eluted with *n*-hexane:EtOAc (97:3) to yield vismiaquinone A (**7.2**, 5 mg, R_f = 0.38 in *n*-hexane:EtOAc 95:5). Fr. 2 (574.2 mg) was chromatographed on silica gel, eluted with *n*-hexane containing an increasing amount of EtOAc, to give 7 sub-fractions (Fr. 2_1-Fr. 2_7). Fr. 2_5 obtained from *n*-hexane:EtOAc (90:10 and 80:20) was purified by Sephadex LH 20 and silica gel columns to afford 2-geranylemodin (**7.3**, 0.5 mg, R_f = 0.67 in *n*-hexane:EtOAc 80:20). Fr. 5 (6.7 g) was further chromatographed on silica gel column, eluted with $CHCl_3$ containing an increasing amount of MeOH, to give 9 sub-fractions: Fr.

5_1-Fr. 5_9. A portion of Fr. 5_7 (151.4 mg) obtained from CHCl₃:MeOH (70:30 and 50:50) was purified using RP18 HPLC (5 µm, 120 × 2 mm, flow rate 8.9 ml/min, detection 210 nm) on a
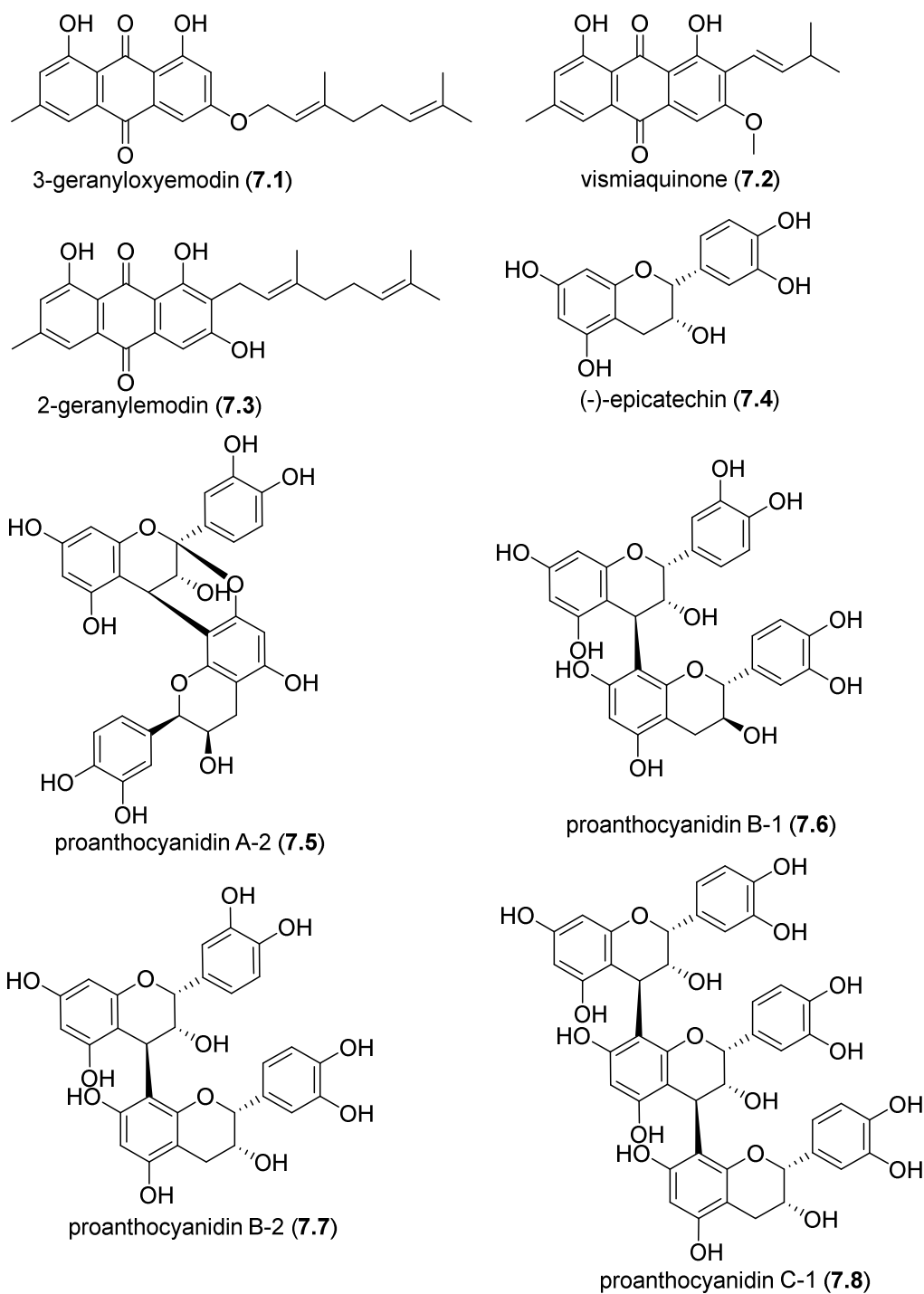
Figure 7.1. Chemical structures of compounds **7.1-7.8** isolated from *P. densipunctatum*.

Varian PrepStar instrument and eluting with H₂O-MeCN (2→100% MeCN 0-20 min, 100→2% MeCN 20-25 min, 2% MeCN 27-30 min) to give proanthocyanidin A-2 (**7.5**, 3.5 mg, t_R 7.08 min),

proanthocyanidin B-1 (**7.6**, 1 mg, t_R 6.74 min), proanthocyanidin B-2 (**7**, 18.6 mg, t_R 5.38 min), and proanthocyanin C-1 (**7.8**, 15.3 mg, t_R 5.91 min). A portion of Fr. 5_3 was purified by semi-preparative HPLC as described above to afford (-)-epicatechin (**7.4**, 33.7 mg, t_R 6.20 min). The structures of the isolated and known compounds were determined by their spectroscopic data ($[\alpha]^{25}_D$, NMR, and ESI-HRMS) and compared with those previously reported in the literature for **7.1-7.3** (Lenta *et al.*, 2009; Poumale *et al.*, 2008) and **7.4-7.8** (Foo *et al.*, 2000; Foo and Karchesy, 1989; Lou *et al.*, 1999; Mohri *et al.*, 2009; Saito *et al.*, 2004) (Figure 7.1).

7.4. Chemotaxonomic significance

The family Hypericaceae was formerly based on morphological features together with Clusiaceae combined to Guttiferae. There is an ongoing discussion whether Hypericaceae should be treated as separate family or as subfamily within Guttiferae (Hegnauer, 1989; Crocket & Robson, 2011; Kubitzki 2007).

In this study, eight naturally occurring compounds including the three anthraquinones 3-geranyloxyemodin (**7.1**), vismiaquinone A (**7.2**), 2-geranylemodin (**7.3**), and the five proanthocyanidins (-)-epicatechin (**7.4**), proanthocyanidin A-2 (**7.5**), proanthocyanidin B-1 (**7.6**), proanthocyanidin B-2 (**7.7**), and proanthocyanin C-1 (**7.8**) were isolated for the first time from *P. densipunctatum* (Hypericaceae). Interestingly, compounds **7.4-7.8** are reported herein from the genus *Psorospermum* for the first time, however, catechins and proanthocyanidins generally occur within the subfamily Hypericoidae (Hegnauer, 1989). Proanthocyanidins are widely distributed in nature, among others, as constituents of cranberry (*Vaccinum* genus, Ericaceae), douglas fir (*Pseudotsuga menziesii*, Pinaceae), and peanut skins (*Arachis hypogaea*, Fabaceae) (Foo *et al.*, 2000; Foo and Karchesy, 1989; Lou *et al.*, 1999). The prenylated and geranylated anthraquinones **7.1-7.3** were previously isolated from various *Psorospermum* species including the Cameroonian *P. androseamifolium* Baker, *P. glaberrimum* Hochr., *P. aurantiacum* Engl., *P. adamauense* Engl. and *P. febrifugum* Spach. (Lenta *et al.,* 2009; Poumale *et al.,* 2008; Tiani *et al.,* 2013; Tsaffack *et al.,* 2009, 2013). The isolation of the anthraquinones **7.1-7.3** from *P. densipunctatum* is a relevant contribution with respect to the chemotaxomy of *Psorospermum* species and plants of the Hypericaceae family in general. Especially, the occurrence of prenylated or geranylated anthraquinones within Guttiferae seems to be restricted to the subfamily Hypericoidae and supports thus the consideration as own family Hypericaceae. Therefore, these compounds can be considered as valuable chemotaxonomic markers (Hegnauer, 1989; Genovese *et al.*, 2012).

7.5. Experimental

See Sections 3.3 and 5.3 for general experimental procedures. These can be also found as supplemental material at http://dx.doi.org/10.1016/j.bse.2015.01.018.

3-Geranyloxyemodin (**7.1**): yellow compound; ^{1}H NMR (600 MHz, CDCl$_3$): 12.29 (1H, s), 12.13 (1H, *s*), 7.62 (1H, *d*, 1.3), 7.37 (1H, *d*, 2.6), 7.07 (1H, *d*, 1.3), 6.68 (1H, *d*, 2.6), 5.47 (1H, *bt*, 6.6), 5.09 (1H, *bt*, 7.0), 4.68 (1H, *d*, 6.6), 2.45 (3H, *s*), 2.13 (4H, *m*), 1.78 (3H, *s*), 1.67 (3H, *s*), 1.61 (3H, *s*); ^{13}C NMR (100 MHz, CDCl$_3$): 190.7, 182.1, 166.0, 165.1, 162.5, 148.4, 142.9, 135.2, 133.2, 132.0, 124.5, 123.6, 121.2, 118.0, 113.7, 110.1, 108.8, 107.5, 65.8, 39.5, 26.2, 25.7, 22.1, 17.7, 16.8; negative ion HR-ESI-FTMS: [M-H]$^-$ at *m/z* 405.1719 (calcd. for C$_{25}$H$_{25}$O$_5^-$, 405.1707).

Vismiaquinone A (**7.2**): reddish compound; ^{1}H NMR (600 MHz, CDCl$_3$):12.97 (1H, *s*), 12.11 (1H, *s*), 7.63 (1H, *d*, 1.10), 7.42 (1H, *s*), 7.08 (1H, *bs*), 6.93, (1H, *dd*, 16.5, 6.8), 6.67 (1H, *dd*, 16.5, 1.1), 4.05 (3H, *s*), 2.53 (1H, *m*), 2.45 (3H, *s*), 1.14 (1H, *d*, 6.6); ^{13}C NMR (100 MHz, CDCl$_3$): 191.5, 182.0, 163.0, 162.5, 148.5, 146.8, 124.4, 121.1, 115.8, 103.4, 56.3, 33.4, 22.5, 22..2, 110.9, 120.7, 162.9, 149.1, 114.2, 132.9; negative ion HR-ESI-FTMS: [M-H]$^-$ at *m/z* 351.1249 (calcd. for C$_{21}$H$_{19}$O$_5^-$, 351.1238).

2-Geranylemodin (**7.3**): yellow compound; ^{1}H NMR (600 MHz, DMSO-*d$_6$*): 12.52 (1H, s), 12.04 (1H, *s*), 7.52 (1H, *d*, 1.3), 7.26 (1H, *s*), 7.19 (1H, *d*, 1.3), 5.18 (1H, *t*, 7.3), 5.02 (1H, *t*, 8.1), 2.42 (3H, *s*), 2.0 (4H, *m*), 1.92 (2H, *m*), 1.75 (3H, *s*), 1.57 (3H, *s*), 1.51 (3H, *s*); ^{13}C NMR (150 MHz, DMSO-*d$_6$*): 190.1, 181.4, 162.0, 161.7, 161.4, 148.3, 135.3, 133.9, 130.7, 124.1, 124.0, 121.1, 120.7, 120.5, 118.0, 113.5, 108.2, 26.1, 25.5, 21.5, 17.5, 16.0; negative ion HR-ESI-FTMS: [M-H]$^-$ at *m/z* 405.1712 (calcd. for C$_{25}$H$_{25}$O$_5^-$, 405.1707).

Epicatechin (**7.4**): brown and optically active compound; [α]$^{25}_D$ -50 (*c* 0.4, CH$_3$OH); ^{1}H NMR (400 MHz, CD$_3$OD): 6.97 (1H, *d*, 1.8), 6.78 (1H, *dd*, 8.3, 1.8), 6.75 (1H, *d*, 8.3), 5.94 (1H, *d*, 2.2), 5.92 (1H, *d*, 2.2), 4.81 (1H, *bs*), 4.17 (1H, *m*), 2.86 (1H, *dd*, 16.7, 3.1), 2.73 (1H, *dd*, 16.7, 4.4); ^{13}C NMR (100 MHz, CD$_3$OD): 158.0, 157.7, 157.4, 145.9, 145.8, 132.3, 119.4, 115.9, 115.3, 100.1, 96.4, 95.9, 79.9, 67.5, 29.2; negative ion HR-ESI-FTMS: [M-H]$^-$ at *m/z* 289.0727 (calcd. for C$_{15}$H$_{13}$O$_6^-$, 289.0718).

Proanthocyanidin A-2 (**7.5**): brown and optically active compound; [α]$^{25}_D$ + 35 (*c* 0.3, CH$_3$OH); ^{1}H NMR (400 MHz, CD$_3$OD): 7.15 (1H, *d*, 2.2), 7.14 (1H, *d*, 2.2), 7.02 (1H, *dd*, 8.3, 2.2), 6.98 (1H, *dd*, 8.3, 2.2), 6.81 (2H, *d*, 8.3), 6.09 (1H, *s*), 6.07 (1H, *d*, 2.2), 6.01 (1H, *d*, 2.2), 4.91 (1H, *bs*), 4.41 (1H, *d*, 3.5), 4.24 (1H, *m*), 4.06 (1H, *d*, 3.5), 2.95 (1H, *dd*, 17.1, 4.8), 2.76 (1H, *dd*, 17.1,

2.6). ^{13}C NMR (100 MHz, CD_3OD): 158.1, 157.0, 156.6, 154.3, 152.3, 152.2, 146.8, 146.3, 146.0, 145.7, 132.5, 131.2, 120.4, 119.8, 116.1, 116.0, 115.7, 115.6, 107.2, 104.3, 102.4, 100.2, 98.3, 96.6, 96.5, 81.8, 68.1, 67.0, 29.9, 29.3; negative ion HR-ESI-FTMS: [M-H]$^-$ at *m/z* 575.1210 (calcd. for $C_{30}H_{23}O_{12}^-$, 575.1195).

Proanthocyanidin B-1 (**7.6**): brown and optically active compound; $[\alpha]^{25}_D$ + 51 (*c* 0.3, CH_3OH); ^1H NMR (400 MHz, CD_3OD): 6.98 (1H, *d*, 1.8), 6.89 (1H, *d*, 1.8), 6.82-6.66 (4H, *m*), 6.07-6.04 (2H, *m*), 5.99 (1H, *d*, 2.2), 4.92 (1H, *bs*), 4.81 (1H, *bs*), 4.57 (1H, *bs*), 4.18-4.14 (1H, *m*), 4.03-4.00 (1H, *m*), 2.87-2.80 (1H, *m*), 2.72-2.65 (1H, *m*). ^{13}C NMR (100 MHz, CD_3OD): 158.0, 156.3, 155.6, 146.0, 145.8, 145.7, 132.4, 119.4, 115.9, 115.9, 115.3, 115.2, 100.6, 97.4, 96.8, 96.1, 83.4, 79.7, 77.3, 67.5, 37.7, 29.6; negative ion HR-ESI-FTMS [M-H]$^-$: *m/z* 577.1355 (calcd. for $C_{30}H_{25}O_{12}^-$, 577.1351).

Proanthocyanidin B-2 (**7.7**): brown and optically active compound; $[\alpha]^{25}_D$ + 31 (*c* 0.5, CH_3OH); ^1H-NMR (400 MHz, CD_3OD): 7.10 (1H, *bs*), 6.64-6.95 (4H, *m*), 5.81-6.10 (3H, *m*), 5.05 (1H, *bs*), 4.90-4.99 (1H, *bs*), 4.52-4.69 (1H, *m*), 4.2-4.35 (1H, *m*), 3.91 (1H, *bs*), 2.86-2.98 (1H, *m*), 2.71-2.85 (1H, *m*). ^{13}C NMR (100 MHz, CD_3OD): 158.3, 157.8, 156.5, 154.6, 145.9, 145.6, 132.6, 132.1, 119.3, 115.9, 115.3, 101.5, 100.5, 97.4, 96.5, 96.1, 79.7, 77.1, 73.5, 67.0, 37.1, 29.7; negative ion HR-ESI-FTMS [M-H]$^-$: *m/z* 577.1361 (calcd. for $C_{30}H_{25}O_{12}^-$, 577.1351).

Proanthocyanidin C-1 (**7.8**): brown and optically active compound; $[\alpha]^{25}_D$ + 64 (*c* 0.3, CH_3OH); ^1H NMR (400MHz, CD_3OD): 7.16-7.09 (1H, *bs*), 7.06-7.00 (1H, *bs*), 6.98-6.88 (2H, *m*), 6.85-6.64 (5H, *m*), 6.11-6.02 (1H, *bs*), 6.02-5.97 (1H, *bs*), 5.97-5.87 (2H, *m*), 5.28-5.17 (1H, *bs*), 5.12-5.03 (1H, *bs*), 5.02-4.96 (1H, *bs*), 4.75-4.64 (1H, *bs*), 4.57 (1H, *bs*), 4.32 (1H, *bs*), 4.06-3.96 (2H, m), 3.00-2.90 (1H, *m*), 2.86-2.76 (1H, *m*); ^{13}C NMR (100 MHz, CD_3OD): 158.3, 157.9, 157.3, 156.8, 156.6, 154.6, 146.0, 145.8, 145.7, 143.1, 132.7, 132.5, 132.1, 119.1, 116.0, 115.3, 107.6, 100.6, 96.7, 96.3, 73.5, 79.7, 77.1, 72.9, 66.8, 37.4, 29.8; negative ion HR-ESI-FTMS [M-H]$^-$: *m/z* 865.1991 (calcd. for $C_{45}H_{37}O_{18}^-$, 865.1985).

References

Crockett, S.L., Robson, N.K.B., **2011**. Taxonomy and chemotaxonomy of the genus *Hypericum. Medicinal Aromatic Plant Sci. Biotech.* 5, 1-13.

Foo, L.Y., Lu, Y., Howell, A.B., Vorsa, N., **2000**. The structure of cranberry proanthocyanidins which inhibit adherence of uropathogenic P-fimbriated *Escherichia coli* in vitro. *Phytochemistry* 54, 173-181.

Foo, L.Y., Karchesy, J.J., **1989**. Procyanidin dimers and trimers from Douglas fir inner bark. *Phytochemistry* 28, 1743-1447.

Genovese, S., Epifano, F., Curini, M., Kremer, D., Carlucci, G., Locatelli, M., **2012**. Screening for oxyprenylated anthraquinones in Mediterranean *Rhamnus* species. *Biochem. Syst. Ecol.* 43, 125-127.

Hegnauer, R., **1989**. Chemotaxonomie der Pflanzen, Vol. 8. Birkhäuser Verlag, Basel (Switzerland).

Kubitzki, K., **2007**. The Families and genera of flowering plants. Flowering Plants. Eudicots, Vol. 9. Springer Verlag, Berlin Heidelberg (Germany).

Lenta, B. N., Devkota, K.P., Ngouela, S., Boyom, F.F., Naz, Q., Choudhary, M.I., Tsamo, E., Rosenthal, P.J., Sewald, N., **2009**. Anti-plasmodial and cholinesterase inhibiting activities of some constituents of *Psorospermum glaberrimum*. *Chem. Pharm. Bull.* 56, 222-226.

Lou, H., Yamazaki, Y., Sasaki, T., Uchida, M., Tanaka, H., Oka, S., **1999**. A-type proanthocyanidins from peanut skins. *Phytochemistry* 51, 297-308.

Mohri, Y., Sagehashi, M., Yamada, T., Hattori, Y., Morimura, K., Hamauzu, Y., Kamo, T., Hirota, M., Makabe, H., **2009**. An efficient synthesis of procyanidins using equimolar condensation of catechin and/or epicatechin catalyzed by ytterbium triflate. *Heterocycles* 79, 549-563.

Porzel, A., Farag, M.A., Mülbradt, J., Wessjohann, L., **2014**. Metabolite profiling and fingerprinting of *Hypericum* species: a comparison of MS and NMR metabolomics. *Metabolomics* 10, 574-588.

Poumale, H.M.P., Randrianasolo, R., Rakotoarimanga, J.V., Raharisololalao, A., Krebs, H.C., Tchouankeu, J.C., Ngadjui, B.T., **2008**. Flavonoid glycosides and other constituents of *Psorospermum androsaemifolium* Baker (Clusiaceae). *Chem. Pharm. Bull*. 56, 1428-1430.

Saito, A., Doi, Y., Tanaka, A., Matsuura, N., Ubukata, M., Nakajima, N., **2004**. Systematic synthesis of four epicatechin series procyanidin trimers and their inhibitory activity on the Maillard reaction and antioxidant activity. *Bioorg. Med. Chem.* 12, 4783-4790.

Fobofou, S.A.T., Franke, K., Arnold, N., Schmidt, J., Wabo, H.K., Tane, P., Wessjohann, L., **2014**. Rare biscoumarin derivatives and flavonoids from *Hypericum riparium*. *Phytochemistry* 105, 171-177.

Tiani, G.M., Ahmed, I., Krohn, K., Green, I.R., Nkengfack, A.E., **2013**. Kenganthranol F, a new anthranol from Psorospermum aurantiacum. *Nat. Prod. Commun*. 8, 103-104.

Tsaffack, M., Nguemeving, J.R., Kuete, V., Ndejouong, T.B.S., Mkounga, P., Penlap, B.V., Hultin, P.G., Tsamo, E., Nkengfack, A.E., **2009**. Two new antimicrobial dimeric compounds: febrifuquinone, a vismione-anthraquinone coupled pigment and adamabianthrone, from two *Psorospermum* Species. *Chem. Pharm. Bull*. 57, 1113-1118.

Tsaffack M., Ouahouo, W.B.M., Nguemeving, J.R., Mkounga, P., Kuete, V., Olov, S., Meyer, M., Nkengfack, A.E., **2013**. Antimicrobial prenylated xanthones and anthraquinones from barks and fruits of *Psorospermum adamauense* Engl. *Nat. Prod. J*. 3, 60-65.

8. General discussion and perspectives of ongoing and future research

Plants of the genus *Hypericum* are popular for phytotherapy and thus used worldwide as traditional remedies or phytodrugs. For instance, St. John's wort (*Johanniskraut*) is available as phytodrug in German pharmacies and was elected as medicinal plant of the year 2015 in the country. Despite this worldwide popularity, it is estimated that the chemistry of more than 60% of the about 450 *Hypericum* species remains unknown (Crockett and Robson, 2011). The main objective of our research work was to compare the metabolomic profiles of different *Hypericum* species using NMR and LC-MS together with multivariate data analysis (e.g. PCA), evaluate their biological activities, and select for futher investigation those, that might potentially lead to new bioactive compounds or at least compounds different from those highly redundant in *H. perforatum*. In this regard, 17 *Hypericum* species (that is ca. 3.8% of the overall *Hypericum* species) collected in Europe, USA, and Cameroon were chemically (extraction and analysis by LC-MS and NMR) investigated and tested for biological activity (Chapter 2).

To investigate the most promising candidates from as many *Hypericum* species as possible was an ambitious goal which required some strategies. In the search for high-throuput and holistic approaches, we hypothetized that methods which can rapidly cluster *Hypericum* species with respect to their similarity in metabolite profiles (or biological activities) can assist in prioritizing some species for bioactive compounds discovery. Species which are in the same group contain similar metabolites but may mostly differ in the concentration of the compounds they contain, while outliers contain different compound classes. Untargeted NMR and/or LC-MS metabolomics and multivariate data analysis can be easily applied to such experimental models or hypotheses because the samples can be rapidly prepared and analyzed by NMR or LC-MS. The ^{1}H NMR, for instance, contains the fingerprints or signatures of compounds present in the plant extract. Knowledge of characteristic NMR signals of natural products allow to map interesting compound classes or sometimes even special single compounds in extracts prior any time comsuming isolation. The principal component analysis (PCA) can help to reduce the large data obtained from the extracts, 51 in this work (17 *Hypericum* extracts × 3 replicates) and visualize clusters and outliers. Furthermore, the PCA loading plot allows to determine NMR or MS signals of compounds making differences among groups. Such compounds can be easily isolated guided by their MS or NMR signals. Nevertheless, that ions from some compounds, even major ones, can be suppressed during LC-MS analysis, or low abundant compounds can be easily ionized and thus be overproportionally visible is a limitation principally of MS or UV detection methods. On the other

hand, the low sensitivity of NMR makes very low abundant metabolites undetectable by this analytical technique.

As shown before (Chapter 2), *H. olympicum*, *H. lanceolatum*, *H. roeperianum*, *H. peplidifolium*, and *H. polyphyllum* are the most discriminated species from NMR-PCA or LC-MS-PCA analyses and do not cluster in the group of *H. perforatum*. Consequently, these plants are expected to contain new natural products and should count among the *Hypericum* species prioritized for phytochemical studies. Also, they are statistically not expected to be rich in metabolites that are present in *H. perforatum*. Chemical investigation of *H. lanceolatum*, *H. roeperianum*, and *H. peplidifolium* afforded 27 natural products never before described from the genus *Hypericum* (Chapters 3-6). Most of the compounds isolated in this work have not been reported from *H. perforatum* nor even from the other 12 *Hypericum* species (see Table 2.1, Chapter 2) investigated in this study and which, for the majority of them, cluster in the group of *H. perforatum* as shown on the PCA plots (Chapter 2). Furthermore, unusual natural products (e.g. peplidiforone C, selancins H and I) were isolated from the prioritized *Hypericum* species. In addition, we evaluated some biological activities such as cytotoxic or anti-HIV properties of all the 17 *Hypericum* species. Interestingly, species belonging to the same group have almost the same cytotoxic activitiy profiles. This further supports the hypothesis that they have similar chemistry. However, in most of the cases (e.g. *H. roeperianum*) the cytotoxic, anti-HIV or anthelmintic activity decreased with fractionation and the isolated compounds were not as active as hoped for. This may imply additive or synergetic effects among the constituents of the investigated species, but other reasons can not be excluded. Still, we characterized the significant anti-HIV and anthelmintic constituents of *H. roeperianum*, namely dimeric coumarins (**5.1**, **5.5**, and **5.6**) against HIV and acylphloroglucinols (**4.7**) against *C. elegans*. Compound **4.7** is more potent against *C. elegans* than the reference anthelmintic drug thiabendazole while compound **5.5** is more active against some drug resistant HIV strains (A17 and EFV^R) than the reference anti-HIV compound nevirapine (Chapters 4 and 5). Thus, compounds **5.5** and **4.7** (Fig. 8.1) represent valuable hits for the development of anti-HIV and anthelmintic drugs, respectively, for the treatment of human pathologies. Against the virus HIV$_{IIIB}$, compound **5.1** exhibits the highest selectivity index (SI = CC$_{50}$/EC$_{50}$, based on cytotoxicity), followed by compounds **5.5** (EC$_{50}$ = 8.7 µM and CC$_{50}$ = 54.0 µM) and **5.6**, respectively. In fact, compounds **5.1** and **5.6** are not cytotoxic against MT-4 cells (CC$_{50}$ > 100 µM) and exhibit anti-HIV activity (EC$_{50}$ = 11.8 and 42.0 µM for **5.1** and **5.6**, resp.) in MT-4 cells infected with HIV virus. Thus, **5.1** may also provide new anti-HIV leads. However, it was not tested on drug resistant HIV variants because it could be isolated in trace amounts only.

5.1 R = H
5.6 R = CH$_3$
(-)-5.5
4.7
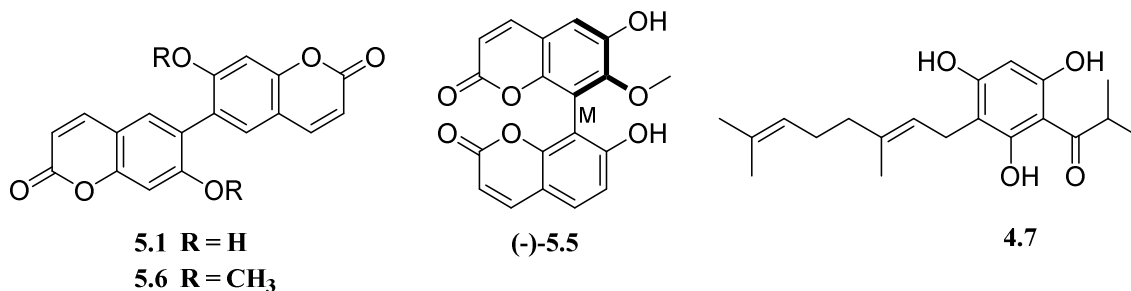
Fig. 8.1. Most prominent anti-HIV (**5.1, 5.5,** and **5.6**) and anthelmintic (**4.7**) compounds discovered within this thesis.

Although additive or synergetic effects might be assumed for constituents of *H. roeperianum*, it is noteworthy to know that the isolated biscoumarins are less cytotoxic against MT-4 cells than the crude extract, while the latter shows significant anti-HIV activity (EC$_{50}$ = 0.4 µg/ml) associated with cytotoxicity (CC$_{50}$ = 6.0 µg/ml), which hints at a yet undiscovered principle. Compound **5.6**, the methylated derivative of **5.1**, shows less anti-HIV activity than **5.1**. This means, the methylation decreased the anti-HIV activity of **5.1**. Nonetheless, no effect of the methylation was observed on the cytotoxicity against MT-4 cells. Investigation of the anti-HIV mode of action of dimeric coumarins is ongoing. However, previous studies showed that some coumarins are inhibitors of HIV reverse transcriptase, others are protease inhibitors or integrase inhibitors (Yu *et al*., 2003). This means they inhibit various stages of HIV replication. Recents studies also showed that some anti-HIV drugs (entry/fusion inhibitors) act by inteferring the entry of HIV virons to human cells (Kuritzkes, 2009).

In Chapter 4 was shown that longer acyl side chains (i.e. higher lipophilicity) on compound **4.7** might increase the anthelmintic activity. A good perspective of this work would be to synthetize derivatives of **4.7** for the sake of more active compounds. Also, given the anti-HIV activity exhibited by biscoumarins, another outlook would be the synthesis of compounds **5.1, 5.5,** and **5.6** and a series of derivatives in order to establish the structure-activity relationship. From our initial investigation, the synthesis of such compounds would be possible. However, we could not achieve compound **5.2** via boronic coumarin followed by coumarin-coumarin coupling reaction under the conditions shown in Scheme 8.1. Nevertheless, it would be highly plausible to obtain compounds like **5.2** via aryl-aryl coupling (compounds **8.3** and **8.4**) followed by condensation reactions (e.g. Pechmann condensation) as depicted in scheme 8.2. The syntheses of precusors (**8.3** and **8.4**) of biscoumarins were achieved, but the conditions tried for the Pechmann condensation were not yet successful and need to be improved.
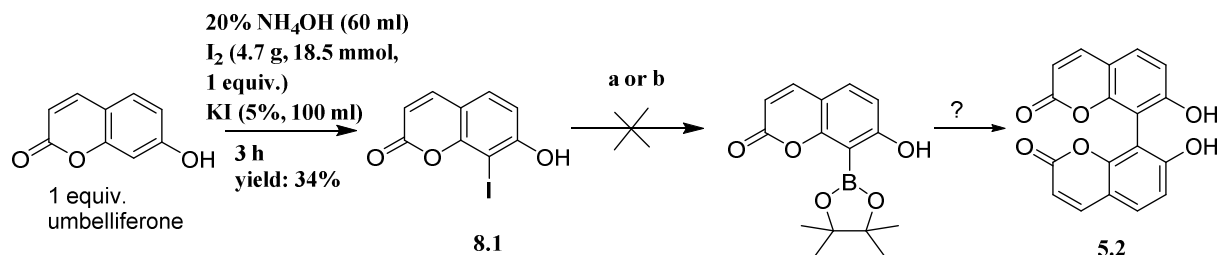
Conditions: a) Pd(PPh₃)₄ 0.02 mmol 0.1 equiv, KOAc (1.23 mmol) 1.23 mmol 6 equiv, (Bpin)₂ 77 mg, 0.3 mmol, 90 °C, solvent (DMF, 10 ml), under nitrogen. **b)** Pd(OAc)₂ (2.7 mg, 0.012 mmol, 0.02 equiv.), CuI (22.8 mg, 0.12 mmol, 0.2 equiv.), PPh₃ (3.1 mg, 0.012 mmol, 0.02 equiv.), Cs₂CO₃ (293.2 mg, 0.9 mmol, 1.5 equiv.), (BPin)₂ (228 mg, 0.9 mmol, 1.5 equiv.), solvent (CH₃CN, 3 ml), room temperature, under dry nitrogen.

Scheme 8.1. Initial investigation of a synthetic route toward biscoumarin (**5.2**) via Pd-catalyzed coumarin-coumarin coupling starting with umbelliferone.
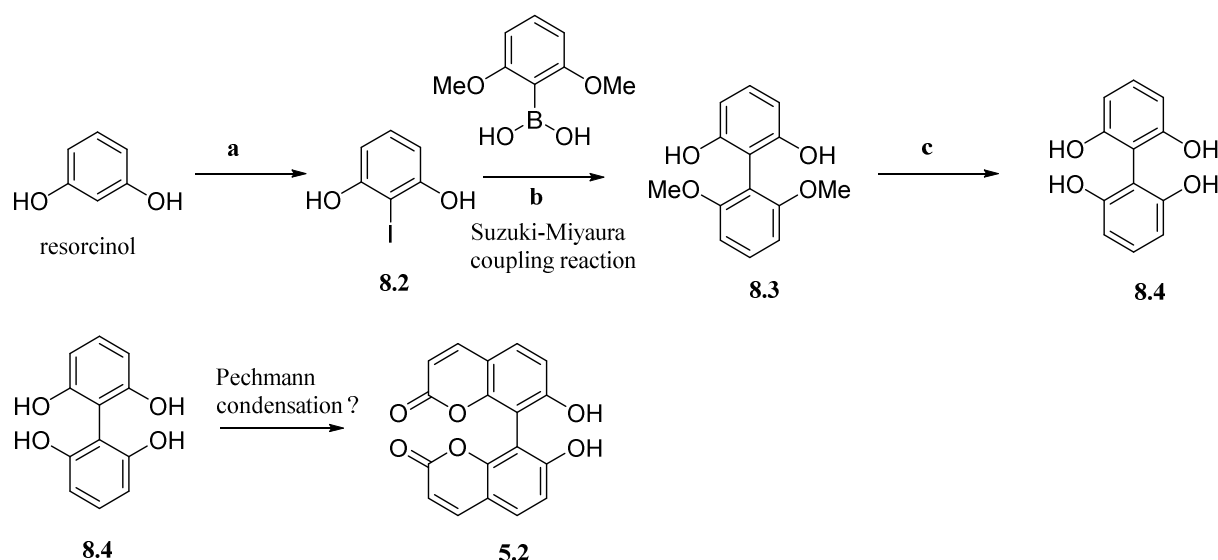
Conditions: a) resorcinol (1.10 g, 10 mmol), iodine (2.72 g, 10.7 mmol), NaHCO₃ (0.94 g, 11.2 mmol), solvent (water, 10 ml), r.t., 20 min, 59%. **b)** Compound **8.2** (585.3 mg, 2.48 mmol), 3, 5.dimethoxyphenylboronic acid (607.81 mg, 3.34 mmol), Pd(PPh₃)₄ (285.8 mg, 0.25 mmol), 2M Na₂CO₃ (20 ml), solvent (toluene, 100 ml), 80 °C overnight and under argon atmosphere, 44%. **c)** Compound **8.3** (64.5 mg, 0.27 mmol, in 10 ml of dry DCM), BBr₃ (0.84 ml, 1 M solution in DCM), under dry nitrogen, -70 °C to r.t. overnight, 51%.

Scheme 8.2. Initial investigation of the synthetic route toward biscoumarin (**5.2**) via biaryl coupling starting with resorcinol.

Besides the synthesis of new bioactive compounds and their analogs, it would also be worthwhile to investigate more *Hypericum* species for compound discovery starting, for example, with *H. olympicum* and *H. polyphyllum*. As previously stated (Chapter 2), the phytochemical investigation of *H. polyphyllum* therefore is ongoing in our lab. It is also planned to evaluate several *Hypericum* species extracts and compounds for their effects on the central nervous system and its diseases (e.g. depression, epilepsy, Alzheimer's, or Parkinson's disease) because *Hypericum* is traditionally mostly used for the treatment of such ailments. For instance, Barnes

(2014) reported that *H. frondosum* has been used for the treatment of conditions ranging from muscle pain and skin burns to depression, attention deficit hyperactivity disorder (ADHD), and Parkinson's disease. The phytochemical investigation of *H. frondosum* is ongoing. This species was not discriminated after LC-MS-PCA or ^{1}H NMR-PCA analysis, which means it probably contains almost the same compounds as *H. perforatum*. However, it was very slightly separated by HMBC-PCA analysis (see PCA score plots in Chapter 2). We are currently working on the fractionation and chemical analysis of *H. frondosum* (results not shown). Initial ^{1}H NMR and HR-MS profilings of the obtained fractions indicate that the major fractions contain flavonoid glycosides and chlorogenic acid derivatives. This was confirmed by comparing the ^{1}H NMR of fractions with that of authentic and pure chlorogenic acid. In general, these results agree with the observation from the ^{1}H-NMR-PCA and LC-MS-PCA analyses and further support our method for plant extract prioritization. Nevertheless, characteristic proton NMR signals of prenyl chains (around 5-6 ppm) can be observed in the ^{1}H NMR spectra of very minor and less polar fractions. Due to our interest in prenylated compounds, we futher separated these fractions (results not shown), but, unfortunately, among the minor compounds obtained so far only compounds **8.5** and **8.6** were in good quantitiy and sufficiently pure for structure elucidation by 1D- and 2D-NMR. Compound **8.5**, a tetraprenyltoluqinol previously reported from the brown alga *Cystoseira jabukae* (Amico *et al.*, 1985), was identified in the genus *Hypericum* for the first time. The structure was elucidated as 2´-geranylgeranyl-6´-methylquinone and depicted in Figure 8.2. The structure determination of the prenylated compound **8.6** is in progress.

8.5
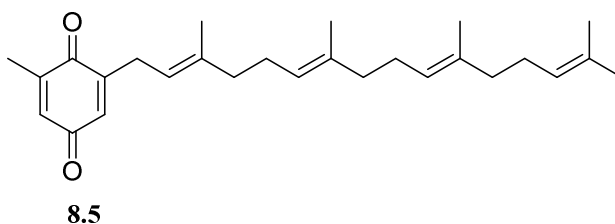
Figure 8.2. Compound **8.5** isolated from minor fractions obtained from *H. frondosum.*

Beyond the investigation of bioactive compounds from *Hypericum* species, one of the important projects is the chemical study and biological activity evaluation of unexplored plants from other genera of the Hypericaea family, e.g. look into their chemotaxonomic relevance, for new bioactive compounds discovery, and, in general, to understand the role of prenylation and prenylated compounds in nature. For instance, as previously discussed (Chapter 7), the isolation of prenylated anthraquinones from *Psorospermun densipunctatum* (Hypericaceae) supports the

chemotaxonomic significance of prenylated compounds in plants of the Hypericaceae family. In addition, most of the compounds we isolated from *Hypericum* species are prenylated.

Finally, this work demonstrated the role of natural products in drug discovery programs and, in particular, members of the genus *Hypericum* as potential source of new bioactive compounds with cytotoxic, anti-HIV, and anthelmintic activity.

References

Barnes, T., **2014**. Plant of the week: Shrubby Saint John's wort (*Hypericum frondosum*). http://kentuckynativeplantandwildlife.blogspot.de/2014/06/plant-of-weekshrubby-saint-johns-wort.html. Retrieved on 02 October 2015.

Crockett, S.L., Robson, N.K.B., **2011**. Taxonomy and chemotaxonomy of the genus *Hypericum. Medicinal Aromatic Plant Sci. Biotech.* 5, 1-13.

Cunsolo, F., Piattelli, M., Ruberto, G., **1985**. Tetraprenyltoluquinols from the brown alga *Cystoseira jabukae. Phytochemistry* 24, 1047–1050.

Kuritzkes, D.R., **2009**. HIV-1 entry inhbitors: An overview. *Curr. Opin. HIV AIDS* 4, 82–87.

Yu, D., Suzuki, M., Xie, L., Morris-Natschke, S.L., **2003**. Recent progress in the development of coumarin derivatives as potent anti-HIV agents. *Med. Res. Rev*. 23, 322–345.

Summary

Species of the genus *Hypericum* (Hypericaceae) are used throughout the world as folk medicines. However, more than 60% of the *Hypericum* species have never been investigated chemically. This work describes the LC-MS and 1D- & 2D-NMR metabolomic profiles of 17 *Hypericum* species for extract prioritization for new compound discovery. Selected biological activities of the 17 *Hypericum* species extracts were also determined. The results from LC-MS-PCA and NMR-PCA analyses clearly indicated that *H. olympicum, H. polyphyllum, H. peplidifolium, H. roeperianum,* and *H. lanceolatum* extracts contain compounds chemically different from those well known and highly replicated/redundant within the genus *Hypericum* (i.e. from *H. perforatum*). Chemical investigation of *H. peplidifolium, H. roeperianum* and *H. lanceolatum* afforded 27 natural products (including 23 new ones) never described from the genus. This work highlights the first examples of dimeric coumarins, 6-acyl-2,2-dimethylchroman-4-one cores fused with dimethylpyran units, and prenylated furan derivatives. The structures of the isolated compounds were determined by MS, NMR, and optical methods. In addition, empetrifranzinans and selancins A and B were synthesized regioselectively. The absolute configurations of selancins, hyperselancins, and bichromonol were established by comparing calculated and experimental CD spectra. The cytotoxic, antibacterial, antifungal, anthelmintic, and anti-HIV activity of extracts and isolated compounds was evaluated. *H. roeperianum* stem bark extract exhibits significant anti-HIV activities never described for *Hypericum* species before, while extract from the leaves of the same plant shows anthelmintic activity. Bichromonol, a novel dimeric coumarin, is an example of a significantly anti-HIV-active compound isolated from *H. roeperianum* whereas the known 3-geranyl-1-(2′-methylbutanoyl)-phloroglucinol is a potent anthelmintic substance. These compounds were more active than the respective reference drugs and might therefore provide new leads against HIV (viruses) or helminths.

This thesis also presents prenylated anthraquinones and proanthocyanidins isolated for the first time from *Psorospermum densipunctatum*, a hitherto unexplored species of the family Hypericaceae. The overall results of this work suggest that: (a) metabolomic profiles combined with chemometric analyses can be used for the rapid discovery of new chemical entities; (b) *Hypericum* still is a valuable source of new bioactive natural products; and (c) prenylated compounds are important chemotaxonomic markers of the family Hypericaceae.

Zusammenfassung

Vertreter der Gattung *Hypericum* (Hypericaceae) werden weltweit in der traditionellen Medizin genutzt. Die Mehrzahl dieser Arten wurde bisher nicht phytochemisch untersucht. Die vorliegende Arbeit beschreibt Metabolitenprofiling von 17 *Hypericum*-Arten mittels LC-MS und 1D- & 2D-NMR, um Extrakte mit dem höchsten Anteil an unbekannten Naturstoffen zu identifizieren. Die biologische Aktivität der 17 *Hypericum* Arten, u.a. gegen Krebszellen, HI-Viren und Würmer, wurde ebenfalls untersucht. Die Ergebnisse der LC-MS-PCA und NMR-PCA-Analysen zeigen deutlich, dass sich Extrakte aus *H. olympicum, H. polyphyllum, H. peplidifolium, H. roeperianum* und *H. lanceolatum* in der chemischen Zusammensetzung von der bekannten Art *H. perforatum* und ähnlichen Arten unterscheiden. Die chemische Untersuchung von *H. peplidifolium, H. roeperianum* und *H. lanceolatum* lieferte 27 Verbindungen, die nie aus der Gattung *Hypericum* isoliert wurden (darunter 23 gänzlich neue Naturstoffe). Außerdem werden die ersten Beispiele für dimere Cumarine, 6-Acyl-2,2-dimethylchromen-4-on-Kerne fusioniert mit Dimethylpyran-Einheiten sowie prenylierte Furanderivate beschrieben. Die Strukturen der isolierten Verbindungen wurden durch MS, NMR und optische Methoden aufgeklärt. Zusätzlich wurden Empetrifranzinane und Selancine A und B regioselektiv synthetisiert. Die absoluten Konfigurationen von Selancinen, Hyperselancinen und Bichromonol wurden durch Vergleich von berechneten und experimentellen CD-Spektren etabliert. Die zytotoxische, antibakterielle, antimykotische, anthelmintische und anti-HIV-Aktivität von Extrakten und isolierten Verbindungen wurde evaluiert. Der Rindenextrakt von *H. roeperianum* wies signifikante anti-HIV-Aktivität auf, die noch nie für eine *Hypericum* Art beschrieben wurde, während der Extrakt aus den Blättern der gleichen Pflanzenart eine anthelminthische Aktivität zeigte. Bichromonol, ein neuartiges dimeres Cumarin aus der Rinde von *H. roeperianum*, zeigt starke anti-HIV-Aktivität, wohingegen 3-Geranyl-1-(2′-methylbutanoyl)-phloroglucinol anthelmintisch aktiv ist. Diese Verbindungen sind aktiver als die jeweiligen Referenz-Substanzen und könnten daher Ansatzpunkte für neue Wirkstoffe gegen HI-Viren oder Würmer bieten.

Darüber hinaus weist diese Arbeit erstmalig prenylierte Anthrachinone und Proanthocyanidine aus *Psorospermum densipunctatum* nach, einer bisher unerforschten Pflanzenart aus der Familie Hypericaceae. Insgesamt konnte damit gezeigt werden, dass a) die Kombination von metabolischen Profilen mit chemometrischen Analysen die schnellere Entdeckung von unbekannten Naturstoffen durch bessere Vorauswahl der geeigneten Spezies ermöglicht, b) *Hypericum* weiterhin eine wertvolle Quelle neuer bioaktiver Naturstoffe ist, und c) prenylierte Verbindungen wichtige chemotaxonomische Marker der Familie Hypericaceae darstellen.

153

M.Sc. Serge Alain Fobofou Tanemossu

Born on 09.10.1986 at Nkongsamba in Cameroon

Present address:
Weinberg 3, 06120 Halle (Saale), Germany
Tel. (office): 0049 (0) 345 5582 1313
Emails : fobofouserge@yahoo.fr/ sfobofou@ipb-halle.de

Education

2012-2015	PhD in Organic Chemistry, Leibniz Institute of Plant Biochemistry/University of Halle, Germany *Supported by the DAAD research grant for doctoral candidates and young academics and scientists*
2011-2012	German Language Studies, InterDAF am Herder-Institut der Universität Leipzig, Germany *Supported by the DAAD*
2010-2011	Doctoral School (1st year PhD), University of Dschang, Cameroon
2008-2010	Master's Degree (Distinctions) in Organic Chemistry, University of Dschang, Cameroon
2005-2008	Bachelor's Degree (with Honors) in Chemistry, University of Dschang, Cameroon. *Partly supported by the British American Tobacco Award for the National Academic Excellence*
2005	Baccalaureate (on the Top List, National Ranking) in Mathematics and Life and Earth Sciences, Government High School Nkongsamba, Cameroon

Fellowships/Awards/Distinctions/Honors

2016	Alzheimer's Drug Discovery Foundation (ADDF) Young Investigator 2016 (Miami, USA)
2012-2015	German Academic Exchange Service (DAAD) Doctoral Fellowship
2015	Lindau Nobel Laureate Meeting Foundation Fellowship
2014	A.T. Kearney Fellowship: finalist of the Falling Walls Young Innovator 2014 (Berlin, Germany)
2014, 2015, 2016	DAAD-RISE Fellowship_ Supervisor (Interns: Chelsea Harmon from MTSU, USA; Megan Wancura from Smith College, USA; Christopher Dade from the University of Missouri, USA)
2011	TWAS-IACS (The World Academy of Sciences) PhD Fellowship in Organometallic Chemistry- Declined (in competition with the DAAD)
2009, 2010, 2011	Cameroonian President's Prize for the University Academic Excellence
2006, 2007, 2008	British American Tobacco Award for the National Academic Excellence
2006	Ranked best student (1st out of approx. 700) newly registered at the Faculty of Science of the University of Dschang

Work/Research Experience

2012-present   Research (Natural Products Group), Department of Bioorganic Chemistry, Leibniz Institute of Plant Biochemistry, Germany

2009-2011   Research, Laboratory of Natural Products Chemistry, University of Dschang, Cameroon

2009-2011
- Part-time teacher of Physics and Chemistry, Government Technical High School Dschang, Dschang-Cameroon
- Assessor/Examiner of Physics and Chemistry national exams of the Cameroon Baccalaureate Board

2009   Tutor of Atomistics, Chemical Bondings, and General Organic Chemisty, University of Dschang, Cameroon

2008   Marketing and sales for the DS-MAX USA, Dschang-Cameroon

Oral communications (PhD research work)

25 April 2016   The role of natural products in drug discovery: from plant extracts to new bioactive compounds, Leibniz-Wirkstofftage, Jena, Germany

15 Oct 2015   Metabolomic profile directed isolation of bioactive compounds from *Hypericum* species, International Conference on Natural Products Utilization: from Plants to Pharmacy Shelf (ICNPU-2015), Plovdiv, Bulgaria

09 Oct 2015   Natural products from African *Hypericum* species, 50th Naturstofftreffen, Würzburg, Germany

2 July 2015   Harnessing complex matrices with NMR spectroscopy and chemometrics: strategies to generate and analyze one and two dimensional NMR metabolomics data, 65th Lindau Nobel Laureate Meeting, Nobel Laureate Prof. Kurt Würthrich's Master Class, Lindau, Germany

09 Nov 2014   Breaking the wall of infectious diseases, Falling Walls Conference/Lab, Berlin, Germany

Poster (PhD research work)

March 2016   New compounds from *Hypericum riparium*, an African St. John's wort species used against epilepsy and mental disorders. **S.A. Fobofou**, K. Franke, A. Porzel, Jürgen Schmidt, and L.A. Wessjohann. 10th Annual Drug Discovery for Neurodegeneration Conference, Miami Beach (FL), USA

Feb 2015   Metabolomics coupled with chemometrics: Powerful tool for natural products discovery. **S.A. Fobofou**, K. Franke, A. Porzel, L.A. Wessjohann. EMBO Practical Course on Metabolomics, European Bioinformatics Institute (EBI), Hinxton-Cambridge, UK

Sept 2013   *Caenorhabditis elegans* as model organism for detection of anthelmintic compounds. H. Thomsen, K. Reider, K. Franke, **S.A. Fobofou**, L. Wesjohann, J. Keiser, N. Arnold. 1st European Conference on Natural Products, DECHEMA, Frankfurt am Main, Germany

Peer-reviewed publications (PhD research work)

Fobofou, S.A.T., Franke, K., Porzel, A., Brandt, W., Wessjohann, L.A., **2016**. Tricyclic acylphloroglucinols from *Hypericum lanceolatum* and regioselective synthesis of selancins A and B. *J. Nat Prod*., published online. doi:10.1021/acs.jnatprod.5b00673.

Fobofou, S.A.T., Harmon, C.R., Lonfouo, A.H., Franke, K., Wright, S.T., Wessjohann, A.L., **2016**. Prenylated phenyl polyketides and acylphloroglucinols from *Hypericum peplidifolium*. *Phytochemistry* 124, 108-113. doi:10.1016/j.phytochem.2016.02.003.

Bitchagno, G.T.M., Tankeo, S.B., Tsopmo, A., Mpetga, J.D.S., Tchinda, A.T., **Fobofou, S.A.T**., Nkuete, A.H.L., Wessjohann, L.A., Kuete, V., Tane, P., **2016**. Ericoside, a new antibacterial biflavonoid from *Erica manii* (Ericaceae). *Fitoterapia.* 109, 206-211. doi:10.1016/j.fitote.2015.12.022.

Fobofou, S.A.T., Franke, K., Sanna, G., Porzel, A., Bullita, E., La Colla, P., Wessjohann, L.A., **2015**. Isolation and anticancer, anthelmintic, and antiviral (HIV) activity of acylphloroglucinols, and regioselective synthesis of empetrifranzinans from *Hypericum roeperianum*. *Bioorg. Med. Chem.* 23, 6327-6334. doi:10.1016/j.bmc.2015.08.028.

Fobofou, S.A.T., Franke, K., Schmidt, J., Wessjohann, L.A., **2015**. Chemical constituents of *Psorospermum densipunctatum* (Hypericaceae). *Biochem. Syst. Ecol.* 59, 174-176. doi:10.1016/j.bse.2015.01.018.

Bitchagno, G.T.M., Tankeo, S.B., Tsopmo, A., Mpetga, J.D.S., Tchinda, A.T., **Fobofou, S.A.T**., Wessjohann, L.A., Kuete, V., Tane, P., **2015**. Lemairones A and B: Two new antibacterial tetraflavonoids from the leaves of *Zanthoxylum lemairei* (Rutaceae). *Phytochem. Lett.* 14, 1-7. doi:10.1016/j.phytol.2015.08.012.

Fobofou, S.A.T., Franke, K., Arnold, N., Schmidt, J., Wabo, H.K., Tane, P., Wessjohann, L.A., **2014**. Rare biscoumarin derivatives and flavonoids from *Hypericum riparium*. *Phytochemistry* 105, 171-177. doi:10.1016/j.phytochem.2014.05.008.

Fobofou, S.A.T., Franke, K., Sanna, G., Brandt, W., Wessjohann, L.A., La Colla, P., **2016**. Bichromonol, a new anti-HIV biscoumarin with atropisomerism from the African St. John's wort species *Hypericum roeperianum*. In preparation.

Fobofou, S.A.T., Porzel, A., Franke, K., Wessjohann, L.A., **2016**. NMR and LC-MS based metabolome analyses of plant extracts for natural product class mapping and prioritization in new natural product discovery: the example of St. John's wort (*Hypericum*). In preparation.

Selected press and video releases

Ngabonzita, P. (Rwanda), Barkhuizen M. (South Africa), **Fobofou, S.** (Cameroon), Barré-Sinoussi, F. (Nobel Laureate, France), Agre, P. (Nobel laureate, USA)., **2015**. Panel discussion: the first African scientist with a Nobel Prize? (original title in German: *Der erste afrikanische Forscher mit Nobelpreis*? Published on June 30, 2015). *Stuttgarter Zeitung.* Retrieved from: http://www.stuttgarter-zeitung.de/inhalt.nobelpreistraegertagung-in-lindau-der-erste-afrikanische-forscher-mit-nobelpreis.7e455c71-e9ff-45d6-9fd5-1e9fdc9d903d.html.

ARD-alpha TV, **2015**. ARD-alpha interviewed young scientist Serge Fobofou about plants and bioactive compounds. Retrieved from: https://www.youtube.com/watch?v=Jf_MBH2D7ro.

Mitteldeutsche Zeitung of January 13, **2015**, page 20. Three minutes to present a research project: Falling Walls Lab is a challenge (original title in German: *Drei Minuten für Erklärung eines Projektes. "Falling Walls Lab" ist Herausforderung*).

Falling Walls Foundation, **2014**. Breaking the wall of infectious diseases (presentation by Serge Fobofou). Retrieved from: https://www.youtube.com/watch?v=hnF02cxz8aM.

Bild-Zeitung (Halle) of January 18, **2014**, page 10. *Forscher heilen Alzheimer mit Johanniskraut*.

Author's declaration about his contribution to publications on which the thesis is based

The present thesis is based on seven peer-reviewed and original publications (five already published and two in preparation). Some of the results were also presented and discussed at internatonal conferences and most recently the author was presented as an ADDF Young Investigator 2016.

1) **Fobofou, S.A.T.**, Porzel, A., Franke, K., Wessjohann, L.A., 2016. NMR and LC-MS based metabolome analyses of plant extracts for natural product class mapping and prioritization in new natural product discovery: the example of St. John's wort (*Hypericum*). Unpublished (in finalization for submission).

SATF designed the experiments and hypothesis, collected the *Hypericum* species to be investigated, performed the extraction and statistical analysis, interpreted the results and wrote the manuscript. AP performed NMR measurements at 600 MHz. KF (project leader) and LAW (supervisor) designed and supervised the project and revised the manuscript. All authors provided fuitful discussions on experimental setup.

2) **Fobofou, S.A.T.**, Franke, K., Porzel, A., Brandt, W., Wessjohann, L.A., 2016. Tricyclic acylphloroglucinols from *Hypericum lanceolatum* and regioselective synthesis of selancins A and B. *J. Nat Prod*. 79, 743-753.

SATF collected the plant material, performed the extraction, isolation, syntheses, anthelmintic assays, and 1D & 2D NMR measurements, elucidated the structures and wrote the manuscript. WB performed ECD spectra calculations, revised the manuscript and provided fruitful discussions. AP provided fruitful discussions and revised the manuscript. KF (project leader) and LAW (supervisor) supervised the work and revised the manuscript. All authors contributed to the determination of the absolute configuration.

3) **Fobofou, S.A.T.**, Franke, K., Sanna, G., Porzel, A., Bullita, E., La Colla, P., Wessjohann, L.A., **2015**. Isolation and anticancer, anthelmintic, and antiviral (HIV) activity of acylphloroglucinols, and regioselective synthesis of empetrifranzinans from *Hypericum roeperianum*. *Bioorg. Med. Chem*. 23, 6327-6334.

SATF collected the plant material, performed the extraction, isolation, syntheses, anthelmintic assays, and 1D & 2D NMR measurements at 400 MHz, elucidated the structures and wrote the manuscript. GS (Italy) and EB (Italy) performed antiviral and antibacterial assays and revised the manuscript. AP provided fruitful discussions and revised the manuscript. PLA (Italy) supervised GS and EB. KF (project leader) and LAW (supervisor) supervised the work and revised the manuscript. All authors were involved in writing the manuscript.

4) **<u>Fobofou, S.A.T</u>**., Franke, K., Arnold, N., Schmidt, J., Wabo, H.K., Tane, P., Wessjohann, L.A., **2014**. Rare biscoumarin derivatives and flavonoids from *Hypericum riparium. Phytochemistry* 105, 171-177.

SATF collected the plant material, performed the extraction and isolation, elucidated the structures and wrote the manuscript. JS performed HR-MS/MS^n meaurements, proposed the fragmentation pattern of biscoumarins and revised the manuscript. NA (group leader), HKW and PT helped for the realization of the project. KF (project leader) and LAW (supervisor) supervised the work and revised the manuscript. All authors provided fuitful discussions on structure elucidation or experimental setup.

5) **<u>Fobofou, S.A.T</u>**., Franke, K., Sanna, G., Brandt, W., Wessjohann, L.A., La Colla, P., **2016.** Bichromonol, a new anti HIV biscoumarin with atropisomerism from the African St. John's wort species *Hypericum roeperianum*. Unpublished (in finalization for submission).

SATF collected the plant material, performed the extraction and isolation, elucidated the structure of bichromonol and wrote the manuscript. GS (Italy) performed antiviral assays and revised the manuscript. WB performed ECD spectra calculations, revised the manuscript and provided fruitful discussions. PLA (Italy) supervised GS. KF (project leader) and LAW (supervisor) supervised the work and revised the manuscript. All authors were involved in writing the manuscript.

6) **<u>Fobofou, S.A.T</u>**., Harmon, C.R., Lonfouo, A.H., Franke, K., Wright, S.T., Wessjohann, A.L., 2016. Prenylated phenyl polyketides and acylphloroglucinols from *Hypericum peplidifolium. Phytochemistry* 124, 108-113.

SATF designed the project, trained and guided CRH, performed NMR measurements and structure elucidation and wrote the manuscript. CRH performed isolation and structure elucidation. AHL provided the plant extract. STW performed the antiviral assays and revised the manuscript. KF (project leader) and LAW (supervisor) supervised the work and revised the manuscript. All authors provided fruitful discussions (e.g. on experimental set up or structure elucidation).

7) **<u>Fobofou, S.A.T</u>**., Franke, K., Schmidt, J., Wessjohann, L.A., **2015**. Chemical constituents of *Psorospermum densipunctatum* (Hypericaceae). *Biochem. Syst. Ecol.* 59, 174-176.

SATF collected the plant material, performed the extraction and isolation, elucidated the structures and wrote the manuscript. JS performed HR-MS meaurements, provided fruitful discussions and revised the manuscript. KF (project leader) and LAW (supervisor) supervised the work and revised the manuscript. All authors were involved in writing the manuscript.

158

Certificates (Urkunden)

2016 Young Investigator

Presented by the Alzheimer's Drug Discovery Foundation

to

Serge Alain Fobofou, PhD (cand.)

at the

10th Annual Drug Discovery for Neurodegeneration Conference:
An Educational Course on Translating Research into Drugs
held March 6-8, 2016 in Miami Beach, FL

Alzheimer's
Drug Discovery
Foundation

Howard Fillit, MD
Executive Director
Chief Science Officer

March 7, 2016

LINDAU
NOBEL LAUREATE
MEETINGS

This is to certify that

Serge Alain Fobofou

has qualified in a global competition among young
scientists worldwide to participate in the

65th Lindau Nobel Laureate Meeting

Lindau, 28 June- 3 July 2015

Council for the Lindau Nobel Laureate Meetings

Countess Bettina Bernadotte
President of the Council

Prof. Burkhard Fricke
Chairman of the Selection Committee

Prof. Klas Kärre
Scientific Chairperson (Medicine)

Prof. Astrid Gräslund
Scientific Chairperson (Chemistry)

Prof. Lars Bergström
Scientific Chairperson (Physics)

Prof. Stefan Kaufmann
Scientific Chairperson (Medicine)

Prof. Wolfgang Lubitz
Scientific Chairperson (Chemistry)

Prof. Rainer Blatt
Scientific Chairperson (Physics)

160

FALLING WALLS
YOUNG INNOVATOR
OF THE YEAR 2014

SERGE ALAIN FOBOFOU TANEMOSSU

has participated as

FINALIST

in the Falling Walls Lab Berlin on November 8, 2014.

The Falling Walls Lab is an international forum, which aims at building and promoting interdisciplinary connections between young excellent academics, entrepreneurs and professionals from all fields. All participants present their research work, business model or initiative to an audience of industry experts, decision makers and scientists – in 3 minutes each. A distinguished jury awards a prize to the best presentations. The Falling Walls Lab is organised by the Falling Walls Foundation and A.T. Kearney (Founding Partner) with the support of Festo (Global Partner).

Prof. Dr. Jürgen Mlynek
Chairman of the Board of Trustees,
Falling Walls Foundation

Prof. Dr. Carl-Henrik Heldin
Chairman of the Board,
Nobel Foundation
Chairman of the Jury

Dr. Martin Sonnenschein
Managing Director Central Europe,
A.T. Kearney
Vice Chairman of the Jury

FALLING
WALLS

FALLING
WALLS
LAB 2014

Founding Partner
AT**Kearney**

Global Partner
FESTO

DAAD   Deutscher Akademischer Austausch Dienst
German Academic Exchange Service

Referat ST32 – Afrika

DAAD • Postfach 200404 • D-53 134 Bonn

Serge Alain Fobofou Tanemossu

Leibniz-Institut für Pflanzenbiochemie
Weiberg 3
06120 Halle (Saale)

Contact person: Ms. Julia Kizio
Telephone: (0228) 882- 535
Fax: (0228) 882- 9535
e-mail: kizio@daad.de
Our reference:

3. August 2015

Certificate

Confirmation is hereby given that Mr. Serge Alain Fobofou
Tanemossu born October 9th 1986 in Cameroon, is holding a
scholarship for postgraduate studies from the German Academic
Exchange Service (DAAD) with the aim to obtain a PhD in
Chemistry at the "Leibniz- Institut für Pflanzenbiochemie" in Halle
(Saale), Germany.

The scholarship covers the period from April 1st 2012 to
September 30th 2015.

Cay Etzold
Head of Section

Kennedyallee 50 D-53175 Bonn   Tel (0228) 882 0   Fax (0228) 882 444 http://www.daad.de

162

DAAD

Deutscher Akademischer Austausch Dienst
German Academic Exchange Service

Section 316 – North America, Programs for North
Americans, Project Grants

DAAD • Postfach 200404 • D-53 134 Bonn

Serge Alain Fobofou Tanemossu
Leibniz-Institut Halle (Saale)
Department of Bioorganic Chemistry
Weinberg 3
06120 Halle (Saale)

Contact partner: Michaela Gottschling
Telefon: (0228) 882-567
Fax: (0228) 882- 9-567
e-mail: gottschling@daad.de
website:www.daad.de/rise
Unser Zeichen: 316/go

Datum: 8. Oktober 2014

RISE Research Internships
in Science and Engineering

Certificate of participation for Serge Alain Fobofou Tanemossu

Dear Sir or Madam,

This is to certify that in 2014, Serge Alain Fobofou Tanemossu
participated very successfully in the DAAD's RISE scholarship program.
For a period of 12 weeks, Serge Alain Fobofou Tanemossu acted as a
supervisor for Chelsea Harmon, an undergraduate student from Middle
Tennessee State University in the US.

Since its inception in 2004, the objective of RISE has been to enable
promising students from the United States and Canada to spend the
summer in Germany for research. In 2009 the program was also opened
to students from UK. Scholarship holders are selected from a large pool
of applicants on the basis of their academic performance and personal
qualifications. Many of them report that RISE has sparked their interest in
Germany as a place to study, conduct research, and work.

The project offers are developed by German PhD students like Serge
Alain Fobofou Tanemossu. They are embedded in the hosts' PhD theses
which ensure that the cooperation with the visiting student is close and
fruitful. Additionally, the projects deal with some of today's most relevant
scientific questions and use state-of-the-art methods and technology. By
supervising an undergraduate student, the PhD students improve their
knowledge of English as well as their mentoring and leadership abilities.

We are pleased to learn that the cooperation between
Serge Alain Fobofou Tanemossu and Chelsea Harmon has been
successful and of great benefit to both. We hope that this is the beginning
of a fruitful transatlantic exchange, and we wish them continued success.

With best regards,

p.p. Michaela Gottschling

Kennedyallee 50, D-53175 Bonn, Tel. (0228) 882-0, Fax: (0228) 882-444, http://www.daad.de

163

DAAD Deutscher Akademischer Austausch Dienst
German Academic Exchange Service

Section 23 – North America, RISE Programs

DAAD • Postfach 200404 • D-53 134 Bonn

Serge Alain Fobofou Tanemossu
Leibniz Institute of Plant Biochemistry
Department of Bioorganic Chemistry
Weinberg 3
D-06120 Halle

Contact partner: Michaela Gottschling
Telefon: (0228) 882-567
Fax: (0228) 882- 9-567
e-mail: rise-germany@daad.de
website:www.daad.de/rise

Datum: 23. September 2015

Certificate of participation for Serge Alain Fobofou Tanemossu

Dear Sir or Madam,

This is to certify that in 2015, Serge Alain Fobofou Tanemossu participated very successfully in the DAAD's RISE scholarship program. For a period of up to 3 month, Serge Alain Fobofou Tanemossu acted as a supervisor for Megan Wancura, an undergraduate student from the Smith College in the USA.

Since its inception in 2004, the objective of RISE has been to enable promising students from the United States and Canada to spend the summer in Germany for research. In 2009 the program was also opened to students from UK. Scholarship holders are selected from a large pool of applicants on the basis of their academic performance and personal qualifications. Many of them report that RISE has sparked their interest in Germany as a place to study, conduct research, and work.

The project offers are developed by German PhD students like Serge Alain Fobofou Tanemossu. They are embedded in the hosts' PhD theses which ensure that the cooperation with the visiting student is close and fruitful. Additionally, the projects deal with some of today's most relevant scientific questions and use state-of-the-art methods and technology. By supervising an undergraduate student, the PhD students improve their knowledge of English as well as their mentoring and leadership abilities.

We are pleased to learn that the cooperation between Serge Alain Fobofou Tanemossu and Megan Wancura has been successful and of great benefit to both. We hope that this is the beginning of a fruitful transatlantic exchange, and we wish them continued success.

With best regards,

p.p. Michaela Gottschling

Kennedyallee 50, D-53175 Bonn, Tel. (0228) 882-0, Fax: (0228) 882-444, http://www.daad.de

Declaration

I declare that I have completed this dissertation without unauthorized help of a second party and only with the assistance acknowledged therein. I have appropriately acknowledged and referenced all text passages that are derived literally from or based on the content of published or unpublished work of other authors. The thesis is submitted to the Faculty of Natural Sciences II of the Martin-Luther University Halle-Wittenberg and has not been presented elsewhere for the purpose of gaining a doctoral degree.

Erklärung

Hiermit erkläre ich an Eides Statt, dass ich die vorliegende Arbeit selbständig und nur unter Verwendung der angegebenen Literatur und Hilfsmittel angefertigt habe. Die Dissertation wurde ausschließlich der Naturwissenschaftlichen Fakultät II der Martin-Luther-Universität Halle-Wittenberg vorgelegt und bisher an keiner anderen Hochschule oder Universität zur Erlangung des Doktorgrades eingereicht.

Serge Alain Fobofou Tanemossu